ALMA MATER STUDIORUM
UNIVERSITÀ DI BOLOGNA

DOTTORATO DI RICERCA IN

PSYCHOLOGY

Ciclo 38

Settore Concorsuale: 11/E1 - PSICOLOGIA GENERALE, PSICOBIOLOGIA E PSICOMETRIA

Settore Scientifico Disciplinare: M-PSI/02 - PSICOBIOLOGIA E PSICOLOGIA FISIOLOGICA

THE MOTOR COMPONENT OF PAIN ANTICIPATION: CORTICOSPINAL EXCITABILITY AS A CONDITIONED RESPONSE

Presentata da: Daniela Dalbagno

Coordinatore Dottorato

Mariagrazia Benassi

Supervisore

Giuseppe Di Pellegrino

Co-supervisore

Elisa Ciaramelli

Esame finale anno 2026

Table of contents

ABSTRACT

Pain is an adaptive and predictive experience, serving not only as a reaction to injury but also as a mechanism for anticipating and preventing harm. The human brain continuously generates predictions about potential bodily threats, preparing the motor system for defensive responses before nociceptive input occurs. Despite extensive evidence of sensory, affective, and cognitive modulation during pain anticipation, the motor component of this process remains poorly understood. To address this gap, the studies reported in this thesis aim to investigate how predictive learning of painful stimulation engages the motor system. Specifically, we examined how corticospinal excitability encodes the intensity, spatial location, and timing of anticipated acute pain. By combining Pavlovian conditioning with transcranial magnetic stimulation (TMS) and autonomic recordings, results revealed sensory-tuned, topographically organized in both hemispheres, and sustained motor inhibition, characterized by muscle-specific reductions in corticospinal excitability in the upper limbs that reflect the predicted features of pain.

In the first experimental chapter, we focused on whether anticipatory motor inhibition is specific to pain or generalizes to other somatosensory events. Participants learned to predict painful, non-painful tactile, or no-shock outcomes while corticospinal excitability was recorded across acquisition and reversal phases. Results showed a graded inhibition of corticospinal excitability scaled on the anticipated stimulus intensity and flexible adjustment during reversal learning, indicating that the motor system encodes sensory rather than affective features of anticipated events.

Then, we examined the spatial organization of motor anticipation. Using lateralized painful stimuli, corticospinal excitability revealed selective inhibition in muscles contralateral to the predicted site of pain, establishing a topographically organized motor representation of threat. Moreover, during reversal learning, corticospinal inhibition flexibly updated in response to changes in the spatial contingencies, showing that the motor system can adaptively reorganize its anticipatory modulation when perceptual evidence indicates a shift in pain location on the body.

We subsequently investigated the temporal dynamics of this anticipatory inhibition. By applying single-pulse TMS at multiple points during the anticipation interval, we observed sustained suppression of corticospinal excitability that persisted throughout the anticipation period and recovered only after the expected pain onset had passed. Stronger early inhibition correlated with more accurate temporal predictions, suggesting that the motor system encodes the full temporal window of threat and maintains preemptive readiness until the time of the anticipated nociceptive event. This pattern indicates that motor inhibition is not a transient response to imminent pain but a temporally extended, adaptive mechanism that ensures optimal motor control and protection throughout the period in which pain is predicted.

Finally, we investigated muscle-specific anticipatory adaptations and how the motor system updates from pain acquisition to extinction. Corticospinal excitability was recorded from the right first dorsal interosseous (FDI) and extensor carpi radialis (ECR) muscles, while painful shocks were delivered to the forearm, in proximity to ECR or in proximity to the flexor carpi radialis (FCR) in a between-subject experimental design. This design allowed us to test whether motor adaptations depend on the functional role of the recorded ECR muscle, acting as either agonist or antagonist relative to the site of anticipated pain. Across acquisition and extinction, MEPs from the FDI muscle showed consistent inhibition during pain anticipation, whereas MEPs from the ECR muscle exhibited inhibition only when shocks targeted the ECR site itself, emerging during extinction. These findings showed that anticipatory motor inhibition can be both muscle-specific and resistant to extinction, suggesting that in the absence of bottom-up sensory input, the motor system remains in a state of readiness to respond as a protective mechanism.

These results show that pain anticipation is an embodied process in which the motor system plays a predictive role. Corticospinal excitability encodes the intensity, location, and timing of predicted pain through muscle-specific inhibition that prepares the body for protective responses. This motor modulation occurs alongside global autonomic adjustments, indicating parallel recruiting of complementary systems. Together, these findings highlight how the brain integrates motor and autonomic responses to optimize anticipatory defense, while also revealing mechanisms that may contribute to maladaptive conditions when persistent or altered.

CHAPTER 1:
INTRODUCTION

Pain as prediction: integrating sensory, affective, and cognitive dimensions

A life without pain is dangerous. Indeed, pain is an essential experience in human life since it protects the body by signaling actual or potential harm, compelling us to withdraw, rest, or seek help. Pain is not a direct mirror of tissue injury, nor a mere product of nociceptive transmission. It is a multidimensional experience emerging from the interplay of sensory, emotional, cognitive, and motivational systems.

Traditionally, pain has been viewed as a straightforward indicator of physical injury, tissue damage, or some underlying organic disorder. Within this framework, the intensity of pain was assumed to directly reflect the extent of bodily harm. Such a Cartesian view of pain has been influential in both clinical practice and public understanding (De Ruddere et al., 2013). Nevertheless, empirical evidence consistently shows that the subjective experience of pain, whether acute or chronic, is only weakly related to the presence or magnitude of tissue pathology (Blasini et al., 2017; Brinjikji et al., 2015).

A central turning point in this conceptual evolution was introduced by the Neuromatrix Theory of Pain (Melzack, 2001), which proposed that pain arises from the activity of a distributed neural network that integrates sensory, affective, and cognitive information. The neuromatrix generates a characteristic neurosignature pattern influenced by genetic, experiential, and stress-related factors, reframing pain as an internally generated experience shaped by both the body and the brain. Building on this view, more recent cognitive frameworks describe pain as a predictive process, whereby the brain continuously evaluates bodily states based on prior expectations and contextual cues (Strube et al., 2023).

The International Association for the Study of Pain (IASP) provides a definition that captures this multidimensional nature, describing pain as "…an unpleasant sensory and emotional

experience associated with, or resembling that associated with, actual or potential tissue damage" (IASP, 1979). This definition marks a crucial departure from the traditional biomedical model; indeed, it recognizes pain not merely as a signal of physical harm, but as a complex, subjective, and context-dependent phenomenon that integrates both body and mind. This shift, from a purely peripheral to a centrally constructed process, has been supported by advances in cognitive neuroscience (Casey, 2023; Melzack & Casey, 1968; Raja et al., 2021; Vlaeyen & Crombez, 2020).

What is perhaps most missing in the well-accepted definition of pain are its behavioral and motivational dimensions. Typically, pain urges an individual to act, and it interrupts ongoing activities (Hodges & Smeets, 2015). These characteristics may not be unique to pain, but they are nonetheless intrinsic to the experience of pain (Mollet & Harrison, 2006; Peyron et al., 2000). Understanding pain, in fact, requires a framework that integrates its sensory, affective, cognitive, and motor dimensions. Pain is not merely an event to be felt, but a signal to be acted upon. It could be considered a process that unfolds across time, linking the past (through learning), the present (through perception), and the future (through anticipation). By examining how the brain engages the motor system during the anticipation of pain, this thesis aims to shed light on the dynamic relationship between pain and motor responses.

How pain affects behavior

From both experimental and clinical evidence emerges that pain affects behavior (Waddell & Richardson, 1992). Individuals with pain consistently exhibit altered movement patterns compared to pain-free controls (Farina et al., 2003). For instance, in low back pain, movement patterns differ widely across individuals, with variations in speed, force, range of motion, and muscle coordination observed within and outside clinical environments (Arvanitidis et al., 2021; Gizzi et al., 2019; Knechtle et al., 2021; Laird et al., 2014, 2018).

When pain occurs, motor behavior adapts primarily to protect the affected body part, but whether these adaptations are beneficial or maladaptive remains debated. During acute pain, the nervous system initiates protective responses aimed at minimizing tissue damage, such as reflex withdrawal, muscle splinting to stabilize the painful region, inhibition of painful movements, or avoidance of specific activities (Svensson, Houe, et al., 1997; Vlaeyen & Linton,

2000). In chronic pain, however, such adaptations often persist beyond the initial threat, becoming less clearly protective and potentially contributing to ongoing pain and disability (Hodges & Tucker, 2011).

Following the historical development of the concept of pain, early physiological theories described these adaptations as simple, stereotypical responses to nociceptive input. The Vicious-Cycle Theory proposed that muscle spasm induces ischemia and metabolite accumulation, further exciting nociceptors (Roland, 1986), whereas the Pain Adaptation Model posited a coordinated modulation of motor output, i.e. inhibition of the agonists and facilitation of antagonists, to reduce painful movement (Lund et al., 1991). Although some animal studies supported these spinal-level mechanisms, they fail to explain the large interindividual variability observed in complex behavioral responses (Cote & Hoeger Bement, 2010; Hodges et al., 2003; Hodges & Tucker, 2011).

Recent insights emphasize the importance of cognitive-emotional and anticipatory mechanisms in motor adaptation. Changes in motor control can emerge even when pain is only expected, suggesting a “top-down” modulation of motor output (Hollander et al., 2010; Moseley et al., 2004; Tucker et al., 2012). The Fear-Avoidance Model (Elman & Borsook, 2018; Leeuw et al., 2007) provides a cognitive-behavioral framework explaining how pain-related fear or anxiety can alter behavior. When pain is perceived as a signal of threat or harm, individuals may avoid movement to prevent injury, even when no real danger exists. This avoidance behavior, maintained by catastrophic expectations rather than the pain itself, contributes to functional limitation and disability (Zale et al., 2013). Indeed, pain-related fear has been associated with reduced range of motion, increased muscle activity, and impaired motor performance (Christe et al., 2021). The complexity of anticipatory pain-related motor adaptation also extends to changes in the behavior of motor units. Tucker et al. (2012) showed that during pain or pain anticipation, the nervous system recruits motor units differently to achieve the same force output. This altered recruitment likely reflects an uneven distribution of synaptic inputs across the motoneuron pool, driven by top-down modulation rather than by nociceptive input alone. Such adaptations in motor unit discharge properties may underpin the altered motor patterns observed during both acute and anticipatory pain conditions.

Contemporary models now recognize pain-related motor adaptation as a dynamic, multilevel process that: a) may precede or follow pain onset, b) includes diverse patterns of muscle

activation or avoidance, c) varies across individuals and tasks, and d) involves both spinal and supraspinal (cortical) mechanisms influenced by biological, psychological, and social factors (Hodges & Smeets, 2015). In acute pain, these adaptations may arise from chemical, thermal, or mechanical stimuli, with abnormal loading, leading to nociceptor activation and subsequent protective motor changes. The interplay between loading, exposure, and injury is complex, helping to explain why some individuals develop pain while others do not. The motor system, therefore, adapts rapidly (likely through an iterative process of trial and error) to achieve an optimal, although not always beneficial, protective strategy.

The neural bases of pain

The Neuromatrix Theory of Pain (Melzack, 2001) provides a valid starting point for understanding pain as a centrally constructed phenomenon rather than a mere product of peripheral nociceptive input. According to this model, pain arises from the output patterns of a widely distributed neural network that integrates perceptual, homeostatic, and behavioral responses to injury, pathology, or chronic stress, thereby underpinning the multidimensional experience of pain and its behavioral correlates.

From a neurophysiological perspective, nociceptive information ascends from the periphery through multiple parallel spinal pathways. There are two broadly different types of nociceptor ("slow burning" C-fibers and "fast sharp" A-delta fibers) (Besson & Chaouch, 1987), which feed into several ascending spinal tracts, including the spinothalamic, spinoreticular, and spinoparabrachial pathways (Craig, 2002; Treede et al., 1999). These ascending signals reach not only thalamic nuclei but also key brainstem structures, such as the periaqueductal gray (PAG) and parabrachial nucleus, both of which send projections to limbic and cortical regions (Mano & Seymour, 2015). The PAG plays a dual role: it contributes to the modulation of nociceptive transmission via descending inhibitory control and mediates affective and defensive responses to pain through its projections to the amygdala and hypothalamus (Tracey & Mantyh, 2007). Neuroimaging studies sought to distinguish the sensory and emotional dimensions of pain within distinct cortical streams, the so-called lateral (sensory) and medial (affective) pain systems (Kulkarni et al., 2005). However, this model has proven overly simplistic. Two major issues limited its validity: first, the inherently subjective nature of pain makes it difficult to neatly separate intensity (sensory) from unpleasantness (affective)

in experimental settings; second, the problem of functional multiplicity, whereby brain regions activated by pain are also engaged in a wide range of other cognitive and affective processes (Henson, 2006; Mouraux et al., 2011; Poldrack, 2006). Current models, therefore, emphasize a distributed and reciprocally connected network architecture, in which ascending and descending pathways dynamically interact from the spinal cord to the cortex (Mano & Seymour, 2015).

Positron emission tomography (PET) and functional magnetic resonance imaging (fMRI) studies showed that pain perception engages a distributed set of cortical and subcortical regions, often referred to as the Pain Matrix (Ingvar, 1999; Peyron et al., 2000; Rainville, 2002). These include the thalamus, the primary (S1) and secondary (S2) somatosensory cortices, the insula, the anterior cingulate cortex (ACC), and prefrontal regions. Together, these areas reflect the multidimensional organization of pain, encompassing sensory-discriminative, affective-motivational, and cognitive-evaluative components.

The thalamus acts as a major relay center for nociceptive information, distributing ascending inputs to both sensory and limbic regions. Bilateral thalamic activation has been reported in response to painful stimuli (Peyron et al., 2000), possibly reflecting a generalized arousal response. The somatosensory cortices (S1/S2) encode the intensity and spatial characteristics of the noxious input, forming the neural basis of the sensory-discriminative dimension of pain. In contrast, the insula and ACC are involved in the affective and motivational value of pain. Specifically, the insula serves as a hub for interoceptive processing, integrating nociceptive, thermoregulatory, and autonomic information to construct a coherent representation of the body's internal state (Rainville, 2002). The ACC plays a pivotal role in integrating the affective, attentional, and motor aspects of pain processing, contributing to the affective-motivational dimension of pain and to the allocation of attentional and behavioral resources necessary for adaptive responding. In contrast to primary sensory regions, the ACC does not encode the intensity or spatial characteristics of painful stimuli but functions as a central node, transforming sensory input into action-oriented behavior (Peyron et al., 2000; Rainville, 2002). Functional subdivisions of the ACC mediate distinct yet interacting processes. The rostral and ventral portions are preferentially engaged during affective and motivational appraisal, including pain-induced avoidance learning in animal models (Johansen et al., 2001; Koyama et al., 2000, 2001). These sectors are also implicated in autonomic and arousal components of

pain, consistent with their connectivity to limbic and hypothalamic systems. In contrast, dorsocaudal regions are more closely associated with motor control and response selection, showing overlap with areas activated during movement preparation and execution tasks (Davis et al., 1997; Kwan et al., 2000). This pattern suggests that pain-related ACC activity may simultaneously encode emotional salience and prepare motor systems for protective or withdrawal behaviors.

In addition to limbic and somatosensory areas, pain consistently engages higher-order associative cortices that contribute to the attentional and cognitive-evaluative dimensions of pain processing (Peyron et al., 2000). Increased blood flow in the posterior parietal and prefrontal cortices during noxious stimulation reflects the recruitment of attentional and working-memory networks involved in evaluating stimulus relevance and modulating behavioral responses (Peyron et al., 1999). Importantly, motor-related regions also participate in the processing of pain. The striatum, cerebellum, and supplementary motor area (SMA) show increased activation during painful experiences, suggesting a close link between nociceptive processing and motor readiness. Even the primary motor cortex (M1) has been found to exhibit pain-related changes in regional cerebral blood flow, though the functional interpretation of this effect remains debated (Baciu et al., 1999; Casey et al., 1996; Porro et al., 2002; Seifert et al., 2013; Summerfield et al., 2018; Svensson et al., 1998). Some studies propose that M1 activation reflects the preparation of defensive or withdrawal movements, while others suggest an inhibitory process aimed at restraining overt action. In either case, these findings highlight that pain engages not only sensory and affective systems but also circuits directly implicated in the control of behavior (Peyron et al., 2000).

Reflecting what happens at the muscular level, the anticipation of pain engages complex cognitive and emotional mechanisms that mirror, to some extent, those involved in pain perception itself. Anticipatory coping relies on cognitive appraisal processes that continuously adapt to one's perception of potential harm and its consequences (Ingvar, 1999). Anticipation or expectation of pain can evoke emotional and physiological responses comparable to actual pain experiences (Hsieh et al., 1999). Neuroimaging evidence confirms that anticipation recruits a network overlapping with that activated during pain, including the ACC, insula, and somatosensory cortices (S1/S2), although activity tends to shift rostrally within the ACC and insula during anticipatory states. Additional activations are observed in the ventromedial

prefrontal cortex (vmPFC) and PAG, suggesting engagement of affective and regulatory components. Interestingly, ACC and vmPFC activity decreases when pain becomes predictable, indicating that these regions encode the emotional salience and anxiety associated with uncertain aversive events rather than perceptual pain itself (Carlsson et al., 2000; Critchley et al., 2001; Ploghaus et al., 2016). This anticipatory circuitry may thus reflect a broader mechanism of expectancy and emotional regulation that generalizes beyond pain to other motivationally significant outcomes (Rainville, 2002). Furthermore, the suppression of α-oscillations recorded over the local sensorimotor region contralateral to the pain side (Babiloni et al., 2006; Peng, Huang, et al., 2019; Peng, Peng, et al., 2019) indicates the sensorimotor cortex's readiness to respond to impending pain. While anticipating an impending pain, the dorsolateral prefrontal cortex (dlPFC) exerts descending pain regulatory effects over brain regions like the cingulate cortex, thalamus, and PAG (Atlas & Wager, 2012; Lorenz et al., 2003; Seminowicz & Moayedi, 2017; Wager et al., 1881), preparing individuals for forthcoming pain and potentially enhancing their ability to modulate the pain experience. This highlights the different roles of M1 and dlPFC in pain anticipation: M1 primarily suppresses local α-oscillations while DLPFC regulates global functional connectivity to respond to impending pain.

Understanding how pain interacts with the motor system is crucial, as pain is a sensory and affective experience that shapes behavior. It alters how we plan, execute, and inhibit actions, promoting protective responses and preventing further harm. These adaptive mechanisms rely on both spinal and cortical processes, reflecting a dynamic interplay between nociceptive and motor systems. However, the motor implications of pain have received comparatively little attention, partly because they are challenging to investigate with neuroimaging methods due to movement-related confounds. A deeper understanding of how pain modulates motor excitability and how motor activity, in turn, influences pain holds important clinical implications (Wiech & Tracey, 2013). It may help clarify how maladaptive motor responses contribute to the transition from acute to chronic pain and guide the development of more effective rehabilitation and neuromodulation strategies aimed at restoring normal motor function and reducing pain.

The adaptive function of learning to anticipate pain

Why do we feel pain? Not only to respond to it, but to predict it and prevent it. Pain is a complex and adaptive experience that cannot be reduced to tissue injury itself. It acts as a learning signal in the brain, guiding the formation of pain predictions and motivating actions aimed at the prospective reduction of harm (Seymour, 2019). Indeed, pain operates within a predictive framework, where the brain continuously generates expectations about potential bodily threats and evaluates whether these predictions match sensory evidence. This predictive process reflects one of the brain's fundamental operating principles: to minimize surprise and uncertainty. When the predicted sensory outcome does not align with the actual experience, a prediction error (PE) arises, signaling the need to update internal models of the environment and the body. In the context of pain, a positive PE occurs when the experienced pain is stronger or arrives earlier than expected, whereas a negative PE emerges when pain is weaker or absent. These discrepancies serve as core teaching signals that refine future predictions and shape behavioral responses. Neuroimaging and computational studies have shown that prediction error signals are encoded in regions central to aversive learning and motivation, including the anterior insula, ACC, amygdala, and ventral striatum. Together, these structures form an integrated network that dynamically adjusts negative expectations and orchestrates appropriate defensive or avoidance actions.

This predictive perspective can be embedded within the broader Pain Perception-Action Cycle, a conceptual model describing how sensory evaluation, attention, memory, and sensorimotor integration jointly regulate pain-related behaviors (Chen & Wang, 2023). Within this cycle, pain anticipation is not a passive waiting state but an active inferential process in which the brain prepares the body for potential harm. Predictive coding theory provides a mechanistic background to understand how top-down expectations modulate pain perception and guide physiological and motor responses even before nociceptive input occurs. In this sense, the brain's aim is not merely to react to pain but to predict it, enabling rapid and energy-efficient behavioral adjustments that maximize survival (Chen & Wang, 2023; Wiech & Tracey, 2013).

To formalize these predictive dynamics, reinforcement learning models describe how prediction errors drive learning and shape future choices (Schultz et al., 1997; Sutton & Barto, 2014). In reinforcement learning, the expected value of an outcome is continuously updated

according to the mismatch between what was predicted and what was actually experienced. Although originally developed to explain reward-based behaviors, the same computational principles apply to aversive learning and pain (Seymour, 2019; Tabor et al., 2017). Within the framework of Pavlovian threat conditioning, for instance, neutral cues acquire predictive value through their association with painful stimuli, and prediction errors determine how quickly and strongly this learning occurs (Tabor & Burr, 2019). Thus, reinforcement learning provides a formal and quantitative extension of associative learning models, offering a computational lens through which to study the dynamics of pain anticipation.

The motor component of pain

As anticipated before, among the several other areas that show hemodynamic changes during pain, the presence of brain regions involved in motor function is noteworthy. The M1, SMA, lenticular and caudate nuclei, and cerebellum indeed show metabolic modifications induced by painful stimuli (Peyron et al., 2000). While the finding of pain-dependent activation of cerebral motor structures is not uncommon, only a minority of functional neuroimaging studies have ever discussed these aspects. Casey et al. (Casey et al., 1996) documented differential regional cerebral blood flow (rCBF) changes in motor areas, depending on the kind of nociceptive stimulation. More specifically, they found that cold stimulation was accompanied by a significant increase in rCBF in sensorimotor and prefrontal cortices, which were not responsive or less responsive during cutaneous phasic heat pain. The authors suggested that this different pattern may reflect differences in physical, perceived spatiotemporal and qualitative characteristics of these stimuli. These results, suggesting that different forms of noxious stimulation produce similar yet not identical patterns of increases in rCBF, were confirmed by the evidence that phasic cutaneous pain and phasic muscle pain may activate different cortical areas (Svensson, Minoshima, et al., 1997). Cutaneous pain was obtained by CO_2 laser stimulation, while muscle pain was obtained by intramuscular electrical stimulation. The S1, the lenticular nucleus and the contralateral ACC, which are cerebral regions involved in motor control, were activated only by painful muscle stimulation. Given these results, whether the metabolic changes in M1 reflect motor activation (withdrawal

reaction) or motor inhibition (movement refrain) cannot be ascertained by functional neuroimaging findings.

Indeed, although PET and fMRI studies revealed pain-related activation within M1, their indirect nature and limited temporal resolution preclude a real-time characterization of nociceptive-motor interactions. They allow for the identification of regions involved in pain processing but cannot capture the rapid dynamics through which nociceptive inputs interact with the motor system. Pain-related motor modulation, however, occurs on the scale of milliseconds, involving fast inhibitory and excitatory processes within both cortical and spinal circuits. Therefore, to understand the functional interplay between nociceptive and motor systems, neurophysiological approaches with higher temporal resolution are required.

At the neurophysiological level, several studies showed that pain modulates spinal reflexes, increasing the excitability of nociceptive withdrawal pathways in both experimental and clinical pain conditions (Cook et al., 1986; Sandrini et al., 2005; Wall & Woolf, 1985; Woolf & McMahon, 1985). The increase in regional rCBF within M1 during muscle pain is consistent with neurophysiological evidence showing altered M1 excitability following muscle nociceptor stimulation (Le Pera et al., 2001). Moreover, motor cortex stimulation can alleviate chronic pain (Canevaro & Bonicalzi, 1995; Katayama et al., 1994), suggesting a bidirectional link between nociceptive and motor circuits. Although the physiological basis of this phenomenon has not yet been fully investigated, it suggests that, since the motor cortex activity modifies pain perception, the nociceptive inputs may influence the motor cortex excitability. Therefore, pain-related changes in the motor system could occur concurrently in the spinal cord and motor cortex, and the pain-related facilitation of the spinal nociceptive reflexes might be due to modifications of the descending control from the motor cortex onto the spinal interneuronal circuits.

Corticospinal excitability in response to pain

In this thesis, single-pulse transcranial magnetic stimulation (spTMS) will be employed as the primary technique to investigate corticospinal excitability under threat of pain. Specifically, it will be used to characterize how the excitability of M1 changes during the anticipation of phasic pain, modulating the spatial, physical, and temporal characteristics of the painful

stimulation and its uncertainty. By measuring pain-related fluctuations in motor evoked potential (MEP) amplitude across different experimental contexts, the studies presented in the following chapters aim to clarify how nociceptive information interacts with motor circuits to regulate action readiness and protective behavior.

A MEP is the peripheral electromyographic response resulting from a descending volley of action potentials triggered by stimulation of M1. The amplitude and latency of MEP provide a quantitative measure of corticospinal excitability, reflecting the balance of excitatory and inhibitory influences along the corticospinal pathway. Changes in MEP amplitude, moreover, can indicate transient modulations in cortical activity, spinal motoneuron excitability, or both. The temporal precision of TMS makes it uniquely suited to study short-latency interactions between nociceptive afferents and motor output, such as those involved in pain-related motor reactions. Beyond single-pulse stimulation, TMS protocols can be adapted to probe specific intracortical mechanisms. Paired-pulse paradigms, for instance, use two consecutive magnetic pulses separated by a few milliseconds to measure intracortical inhibition (SICI) and intracortical facilitation (ICF), which are primarily mediated by GABAergic and glutamatergic circuits, respectively. These measures allow for the dissection of the inhibitory and excitatory processes within M1 that contribute to the overall modulation of corticospinal excitability under pain. Similarly, repetitive TMS (rTMS) protocols can induce lasting plastic changes in cortical excitability, providing causal evidence for the motor cortex's role in pain perception and modulation (Rokyta & Fricovà, 2012). For instance, there is evidence that high-frequency rTMS on M1 has immediate effects on modulating cortical α-oscillations during pain anticipation and nociceptive processing (X. Li et al., 2024). Therapeutically, the same stimulation has been shown to reduce pain perception in patients with intractable chronic pain, supporting a bidirectional interaction between motor and nociceptive systems (Yang & Chang, 2020).

By enabling the quantification of excitability changes at both cortical and spinal levels, TMS thus offers a unique tool to characterize the dynamic interactions between pain and motor control. Phasic or tonic nociceptive input can transiently modify the state of the corticospinal system, altering motor readiness, inhibitory control, and the recruitment of motor circuits involved in protective behaviors. Investigating these modulatory effects can reveal how the brain integrates sensory and motor information to adapt behavior under painful conditions.

In the literature, there is clear evidence of M1 modulation following phasic pain (Bank et al., 2013; Chowdhury et al., 2022). Kofler and colleagues provided proof that brief nociceptive input can dynamically modulate corticospinal excitability in a muscle-specific manner across the upper limb. In a first study, painful electrical stimuli were applied to the index finger of healthy participants, and TMS was delivered over the contralateral primary motor cortex 100 ms after the peripheral noxious pulse. MEPs were recorded from the thenar eminence, representing distal hand muscles involved in grasping, and the biceps brachii, a proximal flexor contributing to withdrawal movements. The results revealed a marked suppression of MEP amplitude in the thenar muscles and a facilitation of MEP amplitude in the biceps brachii, reflecting a rapid redistribution of motor excitability that enhances withdrawal and inhibits grasping. Importantly, the authors highlight that these changes occurred within 160 ms of the painful stimulus, before nociceptive signals could reach cortical areas, indicating that they were mediated predominantly by spinal mechanisms. Specifically, activation of Aδ afferents is thought to transiently inhibit motoneurons controlling distal grasp-related muscles while facilitating proximal withdrawal-related responses, promoting protective limb retraction (Kofler et al., 1998). Subsequently, they extended these findings by recording MEPs from thenar eminence, abductor digiti minimi, biceps brachii, and triceps brachii while applying painful and non-painful digital stimuli to digits II and V. TMS pulses were delivered at interstimulus intervals (ISIs) ranging from 40 to 160 ms following peripheral painful digital stimulation. Results showed a biphasic modulation pattern characterized by an early inhibition (maximal at 40–80 ms ISI) in distal hand muscles and in triceps brachii, followed by a later facilitation (100–160 ms) in proximal flexors (i.e., biceps brachii). This pattern paralleled the cutaneous silent period (CSP) observed in the same muscles, a spinally mediated inhibitory phenomenon driven by Aδ-fiber activation, characterized by transient motoneuron inhibition (Kofler et al., 2001). Moreover, MEPs elicited by TMS were compared with those elicited by transcranial electrical stimulation (TES) at ISI 80 ms from the thenar eminence. While both techniques can evoke motor responses, they differ in the site and mechanism of neuronal activation. Indeed, TMS provides information about both cortical and spinal contributions to motor output, whereas TES primarily indexes spinal-level modulation. Comparing the motor evoked potentials elicited by these two methods allows us to infer the anatomical level (cortical or spinal) at which pain-related modulation occurs (Farina et al., 2001; Kofler et al., 2001; Kotler et al., 1998; Le Pera et al., 2001; Romaniello et al., 2000; Valeriani et al., 1999a,

2001). The authors found that MEPs elicited by TES showed similar modulation to TMS-evoked MEPs, which further supports a spinal origin of these effects. Overall, these findings demonstrate that nociceptive input induces temporally distinct spinal and cortical motor modulations, which together serve adaptive protective functions (Kofler et al., 2001).

Similarly, Kaneko and colleagues (1998) investigated how noxious cutaneous stimulation modulates corticospinal excitability during the cutaneous silent period. Painful electrical stimuli were applied to the digital nerve of healthy participants and patients with cervical spinal pathologies, while spTMS was delivered over the contralateral M1 at interstimulus intervals (ISIs) ranging from 0 to 100 ms. MEPs were recorded from the abductor pollicis brevis to assess distal hand muscle excitability. In healthy controls, conditioning stimulation produced a clear suppression of MEP amplitude at ISIs between 40 and 80 ms, peaking at 60 ms. In patients with cervical syringomyelia, attenuation occurred in asymptomatic hands similarly to controls but was absent in hands with reduced pain sensation. These findings indicate that noxious cutaneous input can suppress spinal motor neurons while leaving cortical motor excitability largely unaffected during CSP, suggesting a predominant spinal mechanism. Clinically, assessing MEP suppression after painful nerve stimulation may provide valuable information on the integrity of pain-related neural pathways in patients with sensory deficits.

On the other hand, in the study by Valeriani and colleagues (2001), MEPs were recorded from the right biceps brachii following TMS or TES stimulation over the left M1, while painful CO_2 laser stimuli were applied to the right hand dorsum or the lateral surface of the right arm. Painful stimulation of the hand significantly reduced MEP amplitude elicited by TMS but not by TES, whereas arm stimulation produced no effect. Since TMS activates corticospinal neurons trans-synaptically and TES directly excites their axons, these results indicate that hand pain inhibits proximal motor representations at a cortical, rather than spinal, level. Then, Algoet and colleagues (2018) further explored nociceptive modulation of corticospinal excitability using TMS and CO_2 laser-induced pain. MEPs were recorded simultaneously from flexor (FDI, FCR) and extensor (ECR) muscles of both hands after laser stimulation to one hand dorsum, with variable TMS–laser intervals (50–2000 ms). The results revealed a triphasic modulation pattern: an early facilitation (~100 ms) in flexors of the stimulated hand, likely reflecting spinal nociceptive withdrawal reflex activity; a subsequent inhibition (150–400 ms)

affecting both flexors and extensors, suggesting cortical nociceptive–motor interactions; and a late facilitation (600–2000 ms) in contralateral hand muscles, potentially linked to interhemispheric or C-fibre–mediated effects. Extending this line of evidence, Barnes and colleagues (Barnes et al., 2021) examined how negative pain expectancy influences corticospinal excitability using single-pulse TMS over M1 with MEPs recorded from the first dorsal interosseous muscle. Participants received painful and non-painful heat stimuli paired with cues inducing high or low pain expectancy. Expecting pain led to reduced corticospinal excitability, increased pain perception, and heightened autonomic arousal (even when the nociceptive input was identical), suggesting that expectancy alone can inhibit the motor system similarly to real pain.

Few studies have examined the effects of tonic pain on human motor cortex excitability. Experimental studies show that tonic pain inhibits motor cortex excitability through both cutaneous and muscular pathways. Topical capsaicin, which activates C-polymodal nociceptors and produces prolonged burning pain, induces localized inhibition of MEPs from muscles beneath the painful area, coinciding with pain onset and intensity peak (Bevan & Szolcsányi, 1990; S. Farina et al., 2001; Grönroos & Pertovaara, 1993; Kenins, 1982). Unlike CO_2 laser stimulation, which activates Aδ fibers and produces widespread inhibition, capsaicin-induced C-fiber activation results in a more restricted cortical suppression, possibly enhancing vigilance to nearby phasic nociceptive events and facilitating spinal protective reflexes. Similarly, tonic muscle pain induced by hypertonic saline causes inhibition of MEPs in the affected and adjacent muscles, paralleled by a reduction in H-reflex amplitude (Le Pera et al., 2001). Thus, tonic cutaneous and muscle pain both reduce M1 excitability, where cutaneous pain may heighten alertness, while muscle pain may suppress motor actions that exacerbate pain.

Overall, the reported studies show that both phasic and tonic pain modulate corticospinal excitability through distinct spinal and cortical mechanisms. Nociceptive input produces rapid, muscle-specific changes mediated mainly at the spinal level. Prolonged or tonic pain, by contrast, induces a sustained cortical inhibition of M1 excitability. Moreover, cognitive factors such as pain anticipation or expectancy can suppress motor output even in the absence of actual nociceptive stimulation, highlighting the dynamic and bidirectional interaction between pain and motor systems.

Corticospinal excitability during pain anticipation

The motivational nature of pain links it intimately with the motor system. To protect the body, pain must translate perception into movement through a withdrawal reflex, a defensive posture, or a learned avoidance behavior. This combination of perception and action extends beyond the immediate moment of pain. Anticipating pain may also engage motor and preparatory processes, allowing the organism to predict and minimize potential harm before it occurs. From this perspective, pain and its anticipation form part of a continuous adaptive loop, in which perception, expectation, and motor readiness interact to guide behavior (Christe et al., 2021). Within the human defensive system, the importance of expectancy has been described as an adaptive behavior to predict the likelihood of aversive events. Indeed, the expectancy for a threatening event, associated with fear and anxiety, plays an important role in threat perception and risk assessment and modulates defensive responses. Thus, physiological motor responses to aversive stimuli may depend not only on the objective magnitude of the stimulus itself but also on the subjective expectation of the related risk. Nonetheless, the role of expectancy for threatening stimuli in modulating motor defensive responses has not been fully understood.

In the literature, few studies have investigated the role of motor corticospinal excitability in the anticipation of pain. Dubé and Mercier (2011) examined whether pain and its anticipation modulate corticospinal excitability using single-pulse TMS applied over the left M1. MEPs were recorded from the right first dorsal interosseous and abductor digiti minimi muscles while participants received thermal stimuli to the right hand under five conditions: neutral, heat, pain, expected heat, and expected pain. Results showed a significant reduction of MEP amplitudes during painful stimulation, indicating pain-related corticospinal inhibition, whereas no modulation occurred during non-painful or expectancy conditions. These findings suggest that actual nociceptive input, but not pain expectation, suppresses motor cortex excitability. The authors argued that the lack of corticospinal inhibition during expected pain likely reflects the moderate intensity of the painful stimuli used. Indeed, the intensity of the painful stimulus was not individualized but fixed for all participants, leading to variability in perceived pain across subjects. Although no correlation was found between pain ratings and the degree of corticospinal inhibition, the use of a single pain intensity per participant

prevents conclusions about whether stronger pain perception within an individual would produce greater inhibition. Therefore, while the results indicate that motor inhibition is not directly dependent on subjective pain perception, the relationship between pain intensity and corticospinal excitability remained uncertain.

Investigating the relationship between motor preparation and painful stimulations, Neige and colleagues (2018) studied how movement-related pain anticipation influences motor behavior and corticospinal excitability during movement preparation. Healthy participants performed elbow flexion and extension movements while painful laser stimuli were delivered to the lateral epicondyle and paired with one specific movement direction. During the action preparation phase, spTMS was applied over the left M1, and MEPs were recorded from the biceps brachii. Results showed opposite modulations of corticospinal excitability depending on the muscle's functional role, specifically, inhibition when the biceps acted as the agonist for the painful movement (i.e., flexion) and facilitation when it was the antagonist (i.e., extension), consistent with the Pain-Adaptation Model (Lund et al., 1991). Behaviorally, movements associated with pain exhibited longer reaction times but faster execution speeds, suggesting a "get it over and done with" motor strategy when movement-related pain cannot be avoided (Neige et al., 2018; Starita et al., 2022).

Furthermore, Fossataro and colleagues (2018) showed that corticospinal excitability can be modulated by the mere expectation of pain when the anticipated stimulus is sufficiently salient. They employed a Pavlovian conditioning paradigm in which neutral visual and auditory cues were paired with painful electrical shocks delivered to the right fifth digit. SpTMS was applied over the left M1, and MEPs were recorded from distal hand muscles, specifically the abductor pollicis brevis and abductor digiti minimi. The TMS pulse was delivered 50 ms after shock onset in paired trials, or at the corresponding time in unpaired trials, to capture maximal corticospinal modulation (according to a previous study by Urban et al., 2004). In participants receiving painful shocks, MEP amplitudes were significantly reduced both when shocks were actually delivered and when shocks were only expected, demonstrating that pain anticipation alone can elicit corticospinal inhibition. No modulation was observed in the non-painful control group, confirming the specificity of the effect to pain expectancy rather than general anticipation. Additionally, higher trait anxiety was associated with stronger MEP suppression during expected pain, suggesting that individual anxiety levels influence preparatory defensive

motor responses. These results indicate that anticipation of salient pain engages the motor system in a proactive, adaptive manner, preparing the body for potential harm even in the absence of actual nociceptive input. Later, Fossataro and colleagues (2020) also investigated whether voluntary actions modulate defensive motor responses to painful stimuli. Using spTMS over the left M1, MEPs were recorded from the abductor pollicis brevis and first dorsal interosseous muscles while high-intensity transcutaneous electrical shocks were delivered to the right fifth digit. Shocks were either self-generated via the participant's button press or other-generated by an experimenter. TMS pulses were applied 50 ms after the electrical stimulus, maximizing pain-dependent corticospinal inhibition. Results confirmed that painful stimuli reduce MEP amplitude in both conditions. Crucially, inhibition was attenuated for self-generated shocks compared to other-generated ones, paralleling behavioral reports of lower perceived pain. These findings suggest an agent-dependent modulation, likely mediated by predictive motor mechanisms; it means that efference copies of voluntary actions allow the nervous system to anticipate and down-regulate defensive responses to self-generated aversive stimuli, possibly via top-down control over the reticular formation through the PAG. This mechanism may serve an adaptive function, enhancing sensitivity to unpredictable or externally generated threats while reducing responses to foreseeable self-generated events.

The most recent work, from Betti and colleagues (2024), showed through two experiments that the anticipation of pain can modulate corticospinal excitability in a topographically specific manner. In the first experiment, painful electrocutaneous stimuli were delivered to either forearm while single-pulse TMS was applied over the left M1, 60 ms before the potential onset of pain, to elicit MEPs from the right first dorsal interosseous (FDI) and extensor carpi radialis (ECR) muscles. Visual cues signaled potential pain to the right or left forearm, while a third control stimulus was never paired with pain. When participants anticipated a shock to the right forearm, MEP amplitudes were significantly suppressed in both FDI and ECR, indicating a lateralized reduction in corticospinal excitability of the threatened arm. Anticipation of pain to the left forearm, however, produced no motor inhibition, showing that this modulation was specific to the threatened upper limb. In the second experiment, the noxious stimulation site was shifted from the forearm to the hand. Here, MEP amplitudes suppression was limited to the FDI, with no significant modulations in ECR, suggesting that inhibition was specific to the muscle group closest to the expected pain

location. Importantly, autonomic responses, recorded through skin conductance responses during cue presentation, were enhanced for all the cues anticipating pain, regardless of the side of pain, confirming that the observed motor suppression could not be explained by generalized arousal. Furthermore, the magnitude of corticospinal inhibition was positively correlated with individual anxiety traits, indicating that people with higher trait anxiety exhibited stronger motor suppression during pain anticipation. Together, these findings show that the motor system adaptively downregulates excitability in a topographically selective manner according to the predicted location of pain, potentially reflecting a preparatory mechanism that prevents movement of threatened body parts (Emadi Andani et al., 2025).

Overall, the evidence points to a close link between the motor system and the anticipation of pain, suggesting that corticospinal excitability can be modulated in a specific and context-dependent manner. Nevertheless, whether and how pain shapes motor learning by tuning the system in anticipation of future painful events remains unclear. In particular, little is known about how the corticospinal tract modulates in relation to the characteristics of the predicted painful stimulus and whether these changes reflect a conditioned response to pain anticipation. Investigating these mechanisms is important, as they likely represent adaptive strategies that prepare the body for potential harm. A better understanding of this process could shed light on how the motor system integrates sensory, cognitive, and motivational information to support flexible and protective behavior.

The Pavlovian conditioning paradigm to study pain anticipation

During Pavlovian conditioning, a neutral stimulus regularly precedes a biologically salient stimulus, named unconditioned stimulus (US), that elicits an unconditioned response (UR). Through repeated CS-US pairings, the value of the neutral stimulus changes from a neutral event that can easily be dismissed to a salient cue with behavioral and motivational significance. This will also induce a shift in the response toward the neutral stimulus. Responses that were initially observed after the US (unconditioned response) can then, to some extent, be observed already during the presence of the neutral stimulus, which will now

be referred to as conditioned stimulus (CS) and the response as conditioned response (CR) (Lonsdorf et al., 2017; Wiech & Tracey, 2013).

The strength of the unconditioned response may vary, and individuals who report pain to be highly threatening also show stronger conditioned pain responses (Crombez et al., 1998). Innate and hardwired behavioral responses to biologically significant events, such as pain, are swiftly learned in anticipation of these events, enabling an effective preparation for and efficient response to these events in their natural environment (Vlaeyen & Crombez, 2020). Thus, the pain conditioning paradigm offers a powerful approach to studying how the brain transforms nociceptive experience into prediction, expectation, and action. It provides a conceptual bridge between acute pain perception and the maladaptive patterns that sustain chronic pain, framing pain not merely as a passive sensory event but as a dynamic learning signal that guides behavior to minimize harm (Seymour, 2019; Vlaeyen & Crombez, 2020).

In the literature, Pavlovian threat conditioning in humans is often investigated through autonomic arousal, which subserves defensive behaviors (e.g., flight, fight or freeze) (LeDoux, 2014; Lonsdorf et al., 2017). Several studies have shown that the autonomic nervous system exhibits multiple conditioned responses in terms of increased skin conductance (Boucsein et al., 2012), heart rate (Castegnetti et al., 2016), pupil size (Korn et al., 2016; Leuchs et al., 2017; Reinhard & Lachnit, 2002), and respiratory amplitude (Castegnetti et al., 2017; Van Diest et al., 2009). The expression of conditioned responses is largely controlled by the amygdala, as sensory information from the conditioned stimulus and unconditioned stimulus is integrated in the lateral nucleus of the amygdala, which projects to the central amygdala, which in turn projects to the hypothalamus and thereby influences the sympathetic nervous system (Knight et al., 2005; J. E. LeDoux, 2014; Wood et al., 2014). During extinction learning, conditioned responses appear to be suppressed through projections from the medial prefrontal cortex to the amygdala (Cho et al., 2013). Among autonomic indices, the skin conductance response (SCR) is the most widely used measure of conditioned arousal (Lonsdorf et al., 2017; Mertens & Engelhard, 2020). It reflects a phasic change in electrodermal activity following a stimulus and serves as a reliable marker of associative learning. During acquisition, pairing a CS with a noxious US elicits increased SCRs to the CS, whereas during extinction, repeated presentations of the CS without the US typically lead to a decline in this response (Jentsch et al., 2020). Moreover, SCR has proven sensitive to reversal learning, indexing the flexibility of threat

updating when CS–US contingencies are reversed (Schiller et al., 2008). The integration of measures from the autonomic and the motor systems provides a unified framework for examining how learning signals, prediction errors, and expectations interact to shape the neural and behavioral dynamics of pain anticipation. Investigating motor excitability through the lens of predictive processing links associative learning to action readiness, elucidating the mechanisms through which adaptive anticipatory responses may transform into maladaptive patterns of pain behavior.

Starting from this perspective, the studies included in this thesis took inspiration from the work by Betti and colleagues (2024), who first demonstrated that pain anticipation modulates corticospinal excitability, revealing a lateralized motor inhibition contralateral to the predicted pain site. Expanding on these findings, we investigated how this anticipatory inhibition is specifically tuned to pain, how it is organized somatotopically across both hemispheres, how early it emerges relative to the expected pain timing, and how it behaves during reversal and extinction of learned contingencies. To these aims, we recorded autonomic and motor measures, combining SCRs as a psychophysiological control measure of conditioning and MEPs elicited through single-pulse transcranial magnetic stimulation (spTMS). This multimodal approach allowed us to capture complementary aspects of pain anticipation, taking into account the technical differences between the two measures, which refer to two different systems. In fact, while SCR reflects autonomic arousal developing over a temporal window of 0.5–4.5 seconds after CS onset (Boucsein et al., 2012), corticospinal excitability is measured on a millisecond scale (Betti et al., 2022; Granovsky et al., 2019; Spampinato et al., 2023), providing a temporally precise index of the motor system's readiness. Consequently, each experimental setup was specifically optimized to account for these different temporal dynamics, ensuring the most accurate assessment of both autonomic and motor anticipatory processes.

CHAPTER 2:

PAINFUL OUTCOMES DRIVE HUMAN PAVLOVIAN CONDITIONING

Unconditioned stimulus affective value is considered a primary driver in determining *if*, *how quickly*, and *how strongly* a previously neutral cue becomes predictive of threat. This foundational assumption underpins countless experimental designs in threat (or fear) conditioning research, as well as being a central assumption of classic reinforcement learning models (Mackintosh, 1975; Pearce & Hall, 1980; Rescorla & Wagner, 1972). In addition, it is critical for understanding both normal adaptive threat learning and the development of anxiety- and trauma-related disorders, as well as pathological pain-related disorders (e.g., Beckers et al., 2023; Foa et al., 1989). Indeed, rodent studies consistently show that unconditioned stimuli (USs) that have higher affective value, often operationalized as outcome aversiveness, yield more robust conditioned threat responses (Bolles et al., 1981; Morris & Bouton, 2006; J. C. Smith & Sclafani, 2002; M. C. Smith, 1968). Specifically, manipulations of shock intensity revealed that the rate and magnitude of conditioning increase with higher shock intensities (Annau & Kamin, 1961). While weak intensities elicit minimal defensive behavior (Baldi et al., 2004; Phillips & LeDoux, 1992), defensive responses intensify at moderate and high shock intensities (Baldi et al., 2004; Laxmi et al., 2003; Luyten et al., 2011).

In contrast to the wealth of animal research, relatively few studies have explored how outcome affective value modulates conditioned responses in humans (Pool et al., 2019, 2023). Based on animal findings and established theoretical models, a consistent relationship between outcome aversiveness and the strength of conditioned responses is expected. However, existing human data remains limited and shows inconsistent results. In particular, despite the centrality of outcome intensity in animal models, surprisingly little is known about how anticipatory autonomic activity scales with unconditioned stimulus intensity in humans.

Beyond autonomic markers, the cortical motor system offers another promising window into how the brain prepares for aversive events of different intensities. Given that motor readiness is critical for adaptive defensive behavior, probing corticospinal excitability may reveal how

the motor system contributes to anticipatory threat processing. In line with the overarching aim of this thesis, our primary interest was to investigate whether the intensity of the anticipated outcome modulates cortical motor excitability. Nevertheless, given that skin conductance responses (SCRs) represent the standard autonomic index in human threat conditioning research, and that systematic evidence on their modulation by US intensity is lacking, we conducted a first study focused specifically on SCRs (experiment 1). Building on these findings, we then examined whether comparable modulation by outcome intensity occurs at the level of the cortical motor system, by analyzing motor evoked potentials (experiment 2).

EXPERIMENT 1[1]

THEORETICAL BACKGROUND

While some studies observed greater conditioned skin conductance responses (SCRs) with high-intensity aversive outcomes (Ney et al., 2023; Ouyang & Dunsmoor, 2024; Willems & Vervliet, 2021), others found that also low-intensity aversive or even non-aversive outcomes can elicit conditioned SCRs (Dunsmoor, Kroes, et al., 2017; Hamm & Vaitl, 1996; Lipp et al., 1994). Thus, a systematic investigation into the role of outcome aversiveness in the acquisition of conditioned responses is warranted, particularly given that those previous studies relied on between-subject designs or paradigms optimized for the study of generalization, rather than direct and within-individual comparisons of aversiveness. This also appears to be of timely relevance, considering recent proposals for moving fear conditioning research online (McGregor et al., 2022; Ney et al., 2023), posing the challenge of ensuring that truly intense and aversive unconditioned stimuli (USs) with a high affective value are delivered in a remote setting (Stussi & Coppin, 2024).

The impact of the outcome affective value also pertains to mathematical models of associative learning, which are often used to model physiological responses. The Rescorla-Wagner model

[1] Reference: Dalbagno D., Stussi Y., Pool E.R., Betti S., Garofalo S., Sander D., di Pellegrino G., Starita F. (under review). The role of outcome affective value in driving human Pavlovian learning. *Journal of Experimental Psychology: Animal Learning and Cognition*.

(Rescorla & Wagner, 1972), one of the most influential models of associative learning, attributes a central role to the concept of outcome value in its learning rule. According to this model, the outcome value is integrated into the computation of prediction errors and determines the maximal associative strength supported by the unconditioned stimulus (Rescorla & Wagner, 1972). Moreover, the Rescorla-Wagner model includes a learning rate associated with the US, reflecting its salience or intensity, which modulates the extent to which prediction errors are integrated into the updating of the associative strength. While they emphasize the role of outcome value more indirectly, the Rescorla-Wagner (1975) and Pearce-Hall (1980) models also posit that the US intensity or salience contributes to modulating the associability of the conditioned stimulus and how prediction errors are integrated into the computation of associative strength.

Despite the key influence these models assign to the outcome affective value, studies implementing these classical reinforcement learning models often do not consider or estimate parameters related to the US. For instance, the learning rate associated with the US is generally not distinguished from the learning rate associated with the conditioned stimulus, as these two parameters are typically not identifiable when they are estimated concurrently due to their multiplicative nature. More importantly, outcome value is often factored into the model as a fixed value (e.g., 0 or 1), thus assuming a uniform sensitivity to the outcomes across individuals and outcome types. Whereas this assumption may be warranted or convenient depending on the study design and aims, it may poorly reflect how the outcome affective value shapes Pavlovian conditioning in humans. To address this, free parameters that modulate outcome value can be modeled, allowing for interindividual variability in outcome sensitivity (e.g. Aylward et al., 2019; Niv et al., 2015). Under this approach, the outcome sensitivity directly modulates the value of the outcome, differently across individuals, so reflecting individual differences. In addition to modulating the outcome value, the outcome aversiveness could impact the speed of conditioning, analogous to what is found for conditioned stimuli. Indeed, the intensity of conditioned stimuli has been positively related to the learning rate (Bower, 1994; Downing, 1968; McLaren & Mackintosh, 2002). For example, threat-relevant conditioned stimuli are characterized by a faster and more persistent acquisition of conditioned responses than fear-irrelevant stimuli (Öhman & Mineka, 2001; Stussi, 2025; Stussi et al., 2021). However, while the relationship between learning rate and

the affective value of conditioned stimuli has been extensively studied, how outcome sensitivity influences learning trajectories remains open for investigation in humans, even though it is one of the strongest assumptions of Pavlovian conditioning.

In the present work, we used a within-subject design that enabled a direct comparison of the conditioned response magnitude to outcomes having different affective values during a Pavlovian threat conditioning task. In line with animal studies, we operationalized the outcome affective value in terms of aversiveness. We used electric shocks as USs and manipulated their intensity, such that they were perceived as either tactile (non-aversive) or painful (aversive). The tactile and painful outcomes were delivered through the same electrodes, allowing for controlled comparisons of their associative impact, and were associated with distinct conditioned stimuli. A third conditioned stimulus that predicted the absence of shock was also used as a control stimulus. We examined the relationship between outcome aversiveness and SCRs in the intervals preceding and following the outcome delivery, to test whether aversive outcomes elicit greater unconditioned and conditioned responses than non-aversive ones. Interestingly, recent work has shown that omissions of USs with a higher expected aversiveness (manipulated through their intensity) give rise to larger SCRs than omissions of USs with a lower expected aversiveness (Willems & Vervliet, 2021), suggesting that the prediction error generated by the omission of an expected aversive stimulus in itself depends on the stimulus' anticipated aversiveness (Spratling, 2012). Hence, in our analyses, we distinguished the post-outcome interval responses into reinforced and non-reinforced trials to separately assess SCRs to the expected outcome delivery and the SCRs to the unexpected omission of the outcome (i.e., the prediction error generated by the shock's omission).

We hypothesized that the unexpected omission of an aversive outcome would elicit a greater SCR than the omission of a non-aversive outcome. Using reinforcement learning algorithms (see to Kangas et al., 2024, for a similar approach), we further aimed to model the mechanisms by which the outcome aversiveness may give rise to heightened conditioned and unconditioned affective responses. Specifically, we compared whether a reinforcement learning model that incorporates free parameters capturing outcome sensitivity would outperform a model without such parameters. Moreover, we expected that the painful outcome would be associated with a higher outcome sensitivity than the tactile outcome,

leading to the computation of larger prediction errors driving Pavlovian conditioning and thereby resulting in increased conditioned and unconditioned defensive responding.

METHODS

Participants

Twenty healthy adult volunteers (13 female, aged between 19 and 28 years: M = 23, SD = 2.74) participated in the experiment and were included in the data analysis. All participants were right-handed, as assessed by the Edinburgh Handedness Inventory (Oldfield, 1971), with normal or corrected-to-normal visual acuity. Participants had no current neurological or psychiatric diagnosis, or chronic medical condition, nor were they currently suffering from any pain or taking any analgesic medication. The study followed the American Psychological Association Ethical Principles of Psychologists and Code of Conduct and the Declaration of Helsinki and was approved by the Bioethics Committee of the University of Bologna (protocol number 224364). All participants were naïve to the purposes of the experiment and gave their written informed consent for their participation.

A sensitivity power analysis was conducted using MorePower (Campbell & Thompson, 2012) to estimate the smallest effect size (η^2_p) that could be detected with the available sample size. The analysis was based on a one-way repeated-measures ANOVA with one within-subjects factor consisting of three levels, an alpha level of .05, and assumed sphericity. Given the sample size of 20, the study had 80% power to detect a η^2_p of 0.22, 90% power to detect a η^2_p of 0.27, and 95% power to detect a η^2_p of 0.31. These results reflect the minimum effect sizes that the design could detect with adequate power.

Procedure

Participants were tested individually in a single experimental session lasting approximately one hour. They were comfortably seated in a silent room in front of a computer screen (size: 43 inches; resolution: 1920 × 1080 pixels; refresh rate: 60 Hz), at ~80 cm viewing distance. Written informed consent was acquired. Then, the intensity of the tactile and painful electrotactile stimulations was calibrated. The Pavlovian threat conditioning task followed,

and explicit learning was assessed afterwards. Finally, participants were debriefed about the experimental hypotheses at the end of the whole experiment. A PC running the OpenSesame software (Mathôt et al., 2012), connected through a NI USB-6281 device (National Instruments, Austin, TX) to a BIOPAC MP-150 System (Goleta, CA) and two Digitimer Stimulators (Model DS7A, Digitimer Ltd., UK), controlled the flow of the experimental task, stimulations' delivery and data recording.

Tactile and painful shocks calibration. The tactile and painful shocks used as USs consisted of a 2-ms electrocutaneous stimulation generated by a Digitimer Stimulator (Model DS7A, Digitimer Ltd., UK) and delivered through pre-gelled Ag/AgCl snapped electrodes (Friendship Medical, SEAg-S-15000/15x20) attached to the right participants' wrist. Two stimulators were connected in parallel to allow stimulation through the same electrodes using two different shock intensities, as instructed by the developer's application notes. The shock intensities were calibrated for each participant as follows. First, to tailor the intensity of the tactile stimulation, the experimenter set the shock intensity using an ascending staircase procedure (Cornsweet, 1962; Klein, 2001), starting from 0 mA and increasing in steps of 0.1 mA to a level perceived by the participant as clearly detectable but not at all unpleasant. Then, to find the intensity of the painful stimulation, the shock intensity was further increased in steps of 0.5 mA to reach the pain tolerance level (i.e., the maximum pain tolerable). This procedure was repeated twice, and the mean was calculated to obtain the final values of the tactile (*M*=1.53 mA, *SD*=0.53) and painful (*M*=69.44 mA, *SD*=27.36) shocks. Stimuli did not exceed individual tolerance limits, in line with the International Association for the Study of Pain (IASP) guidelines (Charlton, 1995).

Experimental task. Participants completed a Pavlovian threat conditioning task (Mathôt et al., 2012), during which they learned the association between three visual stimuli and their respective outcomes. The three visual stimuli were filled colored circles (64 pixels diameter, blue #5698D4, pink #C760CA, or yellow #F4E634), representing the three different conditioned stimuli (CSs). In detail, the CS+touch was associated with the tactile outcome, the CS+pain was associated with the painful outcome and the CS- was never associated with any shock.

In each experimental trial (Figure 2.1), a CS appeared on the left or the right of the computer screen on a black background for 6000 ms, which then resulted in the delivery of shock in the

case of a CS+ reinforced trial. The inter-trial interval (ITI) was jittered between 12-14 s. Each CS was presented 12 times, for a total of 36 trials. For each CS+, the shock occurred in 8 trials (i.e., 66% reinforcement rate). The first three trials and the last three trials consisted of the presentation of a CS-, a reinforced CS+touch, and a reinforced CS+pain, in random order. The remaining trials proceeded in pseudo-random order with no more than two consecutive CSs of the same type in a row. Color assignment to each CS was counterbalanced among participants.

Before starting the task, participants were instructed as follows: “You will see a colored circle appearing on the screen. Sometimes, the circle may deliver a shock. Your task is to understand with which color the circle gives you the shock”. In addition, they were instructed to observe the screen throughout the task while keeping their hands and arms relaxed, without executing any motor response. Importantly, participants were not informed about the existence of two distinct stimulation conditions (tactile and painful) in order to avoid biasing their perception or expectations during the task.

At the end of the task, explicit learning was assessed by having participants rate the pleasantness of each CS and the CS-US contingency on a series of 11-point Likert scales (ranging from 0 to 10). The following two questions were answered regarding each CS, presented in random order: i) “When I saw this circle, the feeling I had was” (pleasantness rating; ranging from 0=’unpleasant’ to 10=’pleasant’); ii) “This circle gave me the shock” (contingency rating; from 0=’never’ to 10=’always’). Moreover, a question on the CS-US intensity contingency was assessed on an 11-point Likert scale. The following question was answered for each CS: “The shock associated with this circle was” (from 0=’not at all painful’ to 10=’extremely painful’).

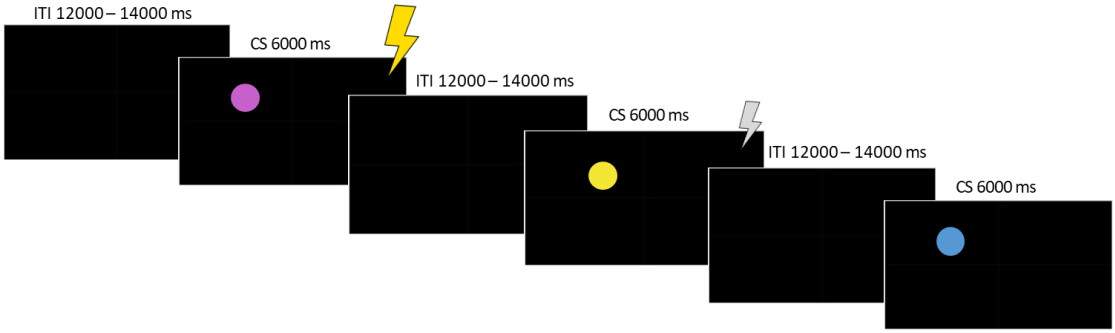

Figure 2.1. Illustration of the task structure. Three types of conditioned stimuli (CSs), presented for 6000 ms each, were used: a CS+touch associated with the tactile outcome, a CS+pain associated with the painful outcome, and a CS- never paired with any outcome. Outcomes were delivered at the CS offset.

Measured variables

Skin conductance response (SCR). Electrodermal activity was recorded continuously at 1250 Hz, with a 10 Hz low-pass filter, from pre-gelled snap electrodes (BIOPAC EL501) placed on the hypothenar eminence of the palmar surface of the left hand, connected to a BIOPAC MP-150 System (Goleta, CA, USA). Continuous electrodermal activity was epoched from the time of CSs appearance to 18 seconds later to examine the change of skin conductance response during the presentation of the CS and following the CS offset in reinforced and non-reinforced trials. To obtain the change value, the raw electrodermal values in the epoch were corrected by subtracting the value of the electrodermal response at time 0 seconds from the epoch data. To obtain trough-to-peak SCR values to analyze differences in average conditioned SCR between CSs, the digitalized signal was processed using Autonomate 2.8 (Green et al., 2014a) to obtain trough-to-peak SCR values. A SCR was considered valid if the trough-to-peak deflection started between 0.5–6 seconds following the CS onset or the CS offset (depending on the interval analyzed: during CS presentation or after the CS offset, respectively), lasted for a maximum of 5 seconds, and was greater than 0.02 µS. Trials that did not meet these criteria were scored as zero and remained in the analysis (see, e.g., Betti et al., 2024; Delgado et al., 2009; Dunsmoor et al., 2017; Golkar et al., 2013; Jiang et al., 2021; Starita et al., 2019, 2022; Starita, Pirazzini, et al., 2023; Storm et al., 2001; Stussi et al., 2018). To reduce the impact of individual differences in skin conductance response, within-participant z-scoring was performed on the raw SCRs (Boucsein et al., 2012; Lykken & Venables, 1971). Finally, we used

the SCR's cumulative sums of z-scores as an overall quantification of the accumulated information regarding the predictive value of the CSs and responses to the different outcomes during threat conditioning.

Explicit ratings. Participants' explicit ratings of CS pleasantness, CS-US contingency, and CS-US intensity contingency for each CS were used in statistical analyses to compare responses between CSs.

Computational modeling

Reinforcement learning models (see, e.g., Li et al., 2011; Pearce & Hall, 1980; Rescorla & Wagner, 1972) were applied to examine how outcome aversiveness influences threat conditioning at an algorithmic level. Specifically, we tested whether and how the outcome aversiveness impacts learning parameters modulating the computation and integration of prediction errors during Pavlovian conditioning on a trial-by-trial basis.

Model space. The candidate models included (1) a version of the Rescorla-Wagner model (Rescorla & Wagner, 1972) that does not account for outcome sensitivity, (2) a version of the Rescorla-Wagner model (e.g. Niv et al., 2012; Stussi et al., 2018, 2021) incorporating different outcome sensitivities as a function of the US, (3) the hybrid model combining the Pearce-Hall associability mechanism with the Rescorla-Wagner model (e.g., Le Pelley, 2004; Homan et al., 2019; J. Li et al., 2011; Pearce & Hall, 1980; Zhang et al., 2016), and (4) a modified version of the hybrid model that incorporates different outcome sensitivities as a function of the US (see Starita et al., 2023; Stussi et al., 2018, 2021, for a similar modeling approach). We included the hybrid model because it has been shown to sometimes provide a better fit for SCR data in human threat conditioning procedures than the Rescorla-Wagner model (e.g., Homan et al., 2019; Li et al., 2011; Zhang et al., 2016; but see, e.g., Starita et al., 2023; Stussi, 2025).

Rescorla-Wagner model. The Rescorla-Wagner model (Rescorla & Wagner, 1972) is a standard model of Pavlovian conditioning. According to this model, learning occurs when events deviate from expectations and acts to update future expectations (Niv & Schoenbaum, 2008). It postulates that associative learning is directly driven by the difference between the predicted and the actual outcome, thereby formalizing the notion of prediction error. Formally, the Rescorla-Wagner model states that the predictive value (or associative strength) V at trial t + 1 of a given CS j is updated based on the sum of the current expected value V_j at

trial t and the prediction error ($\delta(t)$) between the expected value V_j and the outcome O at trial t (i.e., $O(t)$-$V_j(t)$), weighted by a constant learning rate α:

$$V_j(t+1) = V_j(t) + \alpha \times \delta(t)$$

where the learning rate α is a free parameter within the range [0, 1]. In this implementation of the Rescorla-Wagner model, if the tactile or painful outcome was delivered on the current trial t, O(t) = 1, else O(t) = 0.

Rescorla-Wagner model with varying outcome sensitivities. To account for the fact that the outcome affective value influences Pavlovian conditioning, we tested a version of the Rescorla-Wagner model that models a different outcome sensitivity for the tactile and painful outcomes. This approach, rather than using fixed a priori values for the tactile and painful outcomes, allowed the model to capture individual differences in the affective value of the outcomes. Thus, in this model, a participant has an expectation ($V_j(t)$) of the average outcome aversiveness that they might receive on a given trial through a prediction error $\delta(t)$, which represents the difference $\delta(t) = \lambda \times O(t) - V_j(t)$ (i.e., the discrepancy between the obtained outcome $\lambda \times O(t)$ and expected $V_j(t)$ value), where λ is a free parameter within the range [0, 1] modeling the outcome sensitivity. In other words, the outcome sensitivity modulates the extent to which the outcome is weighted into the computation of the prediction error. This prediction error is then utilized to adjust future expectations, according to the classical Rescorla-Wagner formula.

Hybrid model. The hybrid model (Le Pelley, 2004; J. Li et al., 2011) combines the Rescorla-Wagner (1975) and Pearce-Hall (1980) models. It assumes that associative learning is driven by prediction errors while incorporating the Pearce-Hall associability mechanism. Associability acts as a dynamic learning rate that modulates how prediction errors are weighted into updating the CS expected value. The associability of a given CS is updated on a trial-by-trial basis based on absolute past prediction errors. More precisely, associability increases when the CS does not reliably predict the outcome, while it decreases when the CS reliably predicts the outcome. In the hybrid model, the expected value ($V_j(t)$) and associability ($\kappa_j(t)$) of a given CS j are updated as follows:

$$V_j(t+1) = V_j(t) + \kappa_j(t) \times \alpha \times \delta(t)$$

$$\kappa_j(t+1) = \gamma \times |\delta(t)| + (1-\gamma) \times \kappa_j(t)$$

where the initial associability $\kappa_j(0)$, the static learning rate α, and the associability weight γ are free parameters within the range [0, 1]. In this implementation of the hybrid model, if the tactile or painful outcome was delivered on the current trial t, O(t) = 1, else O(t) = 0.

Hybrid model with varying outcome sensitivities. A modified version of the hybrid model was considered by incorporating the outcome sensitivity as an additional free parameter λ within the range [0, 1]. As in the Rescorla-Wagner model including this parameter, the outcome sensitivity influences the weighting of the outcome in the computation of the prediction error (i.e., $\delta(t) = \lambda \times O(t) - V_j(t)$), which is used to update the CS expected value and its associability following the learning rules of the hybrid model described above.

Model and parameter fitting. The reinforcement learning models were fitted to the trial-by-trial z-scored SCR in response to all the CSs. The variants of the Rescorla-Wagner model were fitted by mapping the trial-by-trial z-scored SCR onto the trial-by-trial timeseries of expected values $V_j(t)$. The variants of the hybrid model were fitted by mapping the trial-by-trial z-scored SCR onto (a) the trial-by-trial timeseries of expected values $V_j(t)$, (b) the trial-by-trial timeseries of associabilities $\kappa_j(t)$, or (c) the combination of both expected values and associabilities (e.g., Homan et al., 2019; Li et al., 2011; Starita et al., 2023; Stussi, 2025; Zhang et al., 2016). Because participants were expected to receive electric shocks at the beginning of the Pavlovian threat conditioning task based on the shock calibration procedure and the instructions, we set each initial CS expected value $V_j(0)$ to 0.5.

The free parameters were estimated using maximum a posteriori estimation, which consists of finding the set of parameters maximizing the likelihood of each participant's trial-by-trial z-scored SCRs to the CSs given the model constrained by a regularizing prior (Gershman, 2016; see the "Computational modeling details" paragraph). We used the mfit toolbox (Gershman, 2016; https://github.com/sjgershm/mfit) in MATLAB to estimate the free parameters. We modeled and extracted separate learning rates, initial associability, and associability weights for each CS, as well as separate outcome sensitivities for each shock intensity (as in Wu et al., 2017).

Model comparison. Model comparison was performed using the Bayesian information criterion (BIC; Schwarz, 2007; see also Starita et al., 2023; Stussi et al., 2018, 2021; Zhang et al., 2016). The BIC provides a quantitative measure of the goodness of fit of the models, while considering penalizing model complexity. We computed the mean BIC value for each model across participants. The model associated with the lowest mean BIC value was selected as the best-fitting model. We then compared the learning parameters extracted from this model.

In addition, a model and parameter recovery analysis (Correa et al., 2018; Palminteri et al., 2017; Wilson & Collins, 2019) was conducted to confirm that the models considered were identifiable and that their parameters can be reliably recovered (see "Computational modeling details" paragraph).

Statistical analyses

Data distributions were visually inspected for normality, and data analyses were performed with JASP software (version 0.16.3; Love et al., 2019). Repeated-measures analyses of variance (rmANOVA) were performed to investigate differences between more than two conditions, followed by Bonferroni-corrected post-hoc comparisons, wherever appropriate, while paired t-tests were used to investigate differences between two conditions. Moreover, a linear mixed-effects model was used to examine the relationship between prediction error (δ), derived from the Rescorla-Wagner model, and SCRs following the shock omission in non-reinforced trials. Partial eta-squared (η^2_p) was computed as estimates of effect sizes for the ANOVAs' main effects and interactions, while Cohen's d for the t-tests (Lakens, 2013). A statistical significance threshold of $p<.05$ was adopted.

In addition, a set of cluster-based permutation tests (through the *permutest* MATLAB function) was conducted to test differences in average electrodermal activity modulation throughout the 6s of CS presentation and 12s post CS offset, with the null hypothesis that differences in electrodermal activity among the CSs were due to random variation. Thus, an *F* test was conducted, which detected cluster formation with a threshold corresponding to a p-value <0.05 (as in Sassenhagen & Draschkow, 2019).

All data, analysis code, and research materials are available at the link: *https://osf.io/kszft/*.

RESULTS

Explicit ratings

CS pleasantness. A rmANOVA was performed with CS type (CS-, CS+touch, CS+pain) as a within-subject factor on the CS pleasantness ratings. The main effect of CS type emerged ($F_{(2,38)}$=27.00, p<.001, η^2_p=0.587, 90% η²CI [0.466, 0.680]). Bonferroni-corrected post-hoc comparisons showed that participants rated the CS+pain (M=2.20, SD=1.80) as less pleasant than both the CS+touch (M=6.40, SD=1.93, p<.001) and the CS- (M=6.90, SD=2.79, p<0.001), whereas ratings for CS+touch and CS- did not differ (p>.99).

CS-US contingency. A rmANOVA was performed with CS type (CS-, CS+touch, CS+pain) as a within-subject factor. The main effect of CS type was statistically significant ($F_{(2,38)}$=46.60, p<.001, η^2_p=0.710, 90% η²CI [0.600, 0.786]). Bonferroni-corrected post-hoc comparisons showed that participants rated the CS+touch (M=5.55, SD=2.67) and the CS+pain (M=7.15, SD=2.08) as more associated with the shock than the CS- (M=0.40, SD=1.57; p<.001), whereas ratings for CS+touch and CS+pain did not statistically differ (p=.100).

CS-US intensity. A rmANOVA was performed with CS type (CS-, CS+touch, CS+pain) as a within-subject factor. There was a main effect of CS type ($F_{(2,38)}$=371.00, p<.001, η^2_p=0.951, 90% η²CI [0.925, 0.966]). Bonferroni-corrected post-hoc comparisons showed that participants rated the outcome associated with the CS+pain (M=7.30, SD=1.13) as more intense than the outcome associated with the CS+touch (M=0.80, SD=1.36, p<.001), and than the CS- (M=0, SD=0, p<.001), whereas ratings for CS+touch and CS- did not differ statistically significantly (p=.050, uncorrected p=.017).

These results indicate the successful learning of associations at an explicit level.

Continuous electrodermal activity

Figure 2.2 represents the change in electrodermal activity during the 6s of CS presentation and 12s post CS offset, averaged across participants and each CS. For each CS+, reinforced (Figure 2.2.A) and non-reinforced (Figure 2.2.B) trials are presented in separate plots, while the same CS- responses are represented in both plots. A non-parametric cluster-based permutation analysis was performed to test the effect of conditions (p<.05). For reinforced

trials, the contrast between the CS- and CS+touch revealed a cluster in the observed data beginning at approximately 9926 ms and continuing until the end of the analyzed interval ($p<.001$). The contrast between the CS- and CS+pain identified a cluster starting at approximately 3306 ms and continuing to the end of the interval ($p<.001$). Finally, the contrast between the CS+touch and CS+pain showed a cluster beginning at approximately 4128 ms and continuing until the end of the interval ($p<.001$). In non-reinforced trials, the contrast between the CS- and CS+pain identified a cluster starting at approximately 3393 ms and continuing to the end of the interval ($p<.001$). However, no significant clusters were detected in the comparisons between CS+touch and CS+pain or CS– and CS+touch.

Overall, in reinforced trials, statistically significant differences emerged across all CS conditions, with CS+pain eliciting the strongest electrodermal response both during anticipation and following the painful outcome. In contrast, the CS+touch condition showed increased electrodermal activity relative to CS− only after the tactile outcome was delivered, but not during its anticipation. In non-reinforced trials, a similar response pattern was observed for CS+pain, indicating that the pain-associated CS continued to evoke a differential response even in the absence of the painful shock, suggesting the persistence of threat-related processing, such as a prediction error effect following shock omission (Spoormaker et al., 2011, 2012; Vervliet et al., 2017; Willems & Vervliet, 2021). In contrast, no differences emerged between CS+touch and CS− in the absence of a tactile outcome.

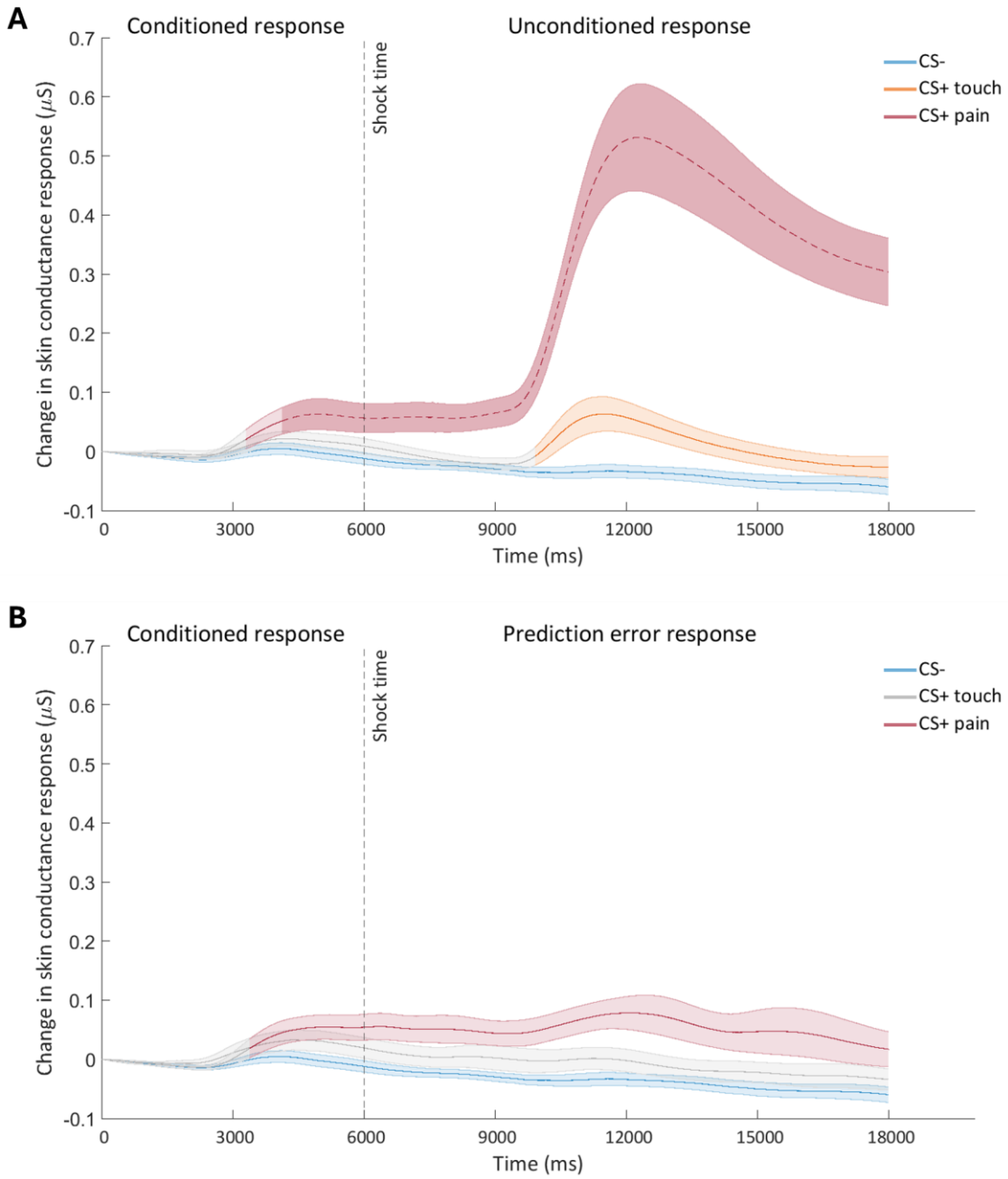

Figure 2.2. Representation of the change in electrodermal activity during the 6s of CS presentation and 12s post CS offset, averaged across participants and each CS. (**A**) represents reinforced trials and (**B**) non-reinforced trials. The colored portions of the lines indicate the clusters in which the SCR following the CS+touch (yellow) or CS+pain (violet) differ from the SCR following the CS- (blue); note that where the lines remain gray, no differences with the CS- emerged. The dashed line superimposed on the graph highlights the interval in which the SCR following the CS+pain differs from the SCR following the CS+touch.

SCR amplitude post CS offset

Average response. Similarly to the analysis on continuous electrodermal activity, we analyzed the average SCR amplitude for reinforced and non-reinforced trials separately. First, we conducted a rmANOVA with the factor outcome (no-outcome, tactile, painful) on SCR amplitude, including all CS- trials and only reinforced trials for the CS+touch and CS+pain (Figure 2.3.A). A main effect emerged ($F_{(2,38)}$=51.20, p<.001, η^2_p=0.729, 90% η^2CI [0.625, 0.799]). Bonferroni-corrected post-hoc comparisons indicated that the SCR amplitude was statistically significantly higher in response to the painful outcome (M=1.01, SD=0.60) compared to both the tactile outcome (M=-0.13, SD=0.27; p<.001) and the no-outcome condition (M=-0.46, SD=0.27; p<.001) trials, and statistically significantly higher for the tactile outcome compared to the no-outcome trials (p=.005). These results suggest that the painful outcome elicits a greater SCR than the tactile outcome. Furthermore, the outcome delivery, whether painful or tactile, induced a higher SCR than the absence of an outcome.

The same rmANOVA was also conducted including only non-reinforced trials for the CS+touch and CS+pain, and again all CS- trials (Figure 2.3.B). A main effect emerged ($F_{(2,38)}$=5.73, p=.007, η^2_p=0.232, 90% η^2CI [0.063, 0.403]). Bonferroni-corrected post-hoc comparisons indicated that the SCR amplitude was statistically significantly higher in response to the omission of a painful outcome (M=-0.04, SD=0.40) compared to the no-outcome trials (M=-0.46, SD=0.27; p=.008), but not to the tactile outcome (M=-0.35, SD=0.52; p=0.184). Also, tactile and no-outcome conditions did not statistically differ from each other (p=.940). These results suggest that even when no painful outcome was delivered, a higher SCR amplitude was elicited after the painful outcome omission compared to the no-outcome condition.

SCR amplitude during CS presentation

Average response. We conducted a rmANOVA with the factor CS type (CS-, CS+touch, CS+pain) to examine whether anticipating outcomes of varying intensities or no outcome influenced the SCR amplitude (Figure 2.3.C). A main effect emerged ($F_{(2,38)}$=17.10, p<.001, η^2_p=0.474, 90% η^2CI [0.300, 0.609]). Post-hoc comparisons indicated that the SCR amplitude was statistically significantly higher in response to the CS+pain (M=0.36, SD=0.35) compared to both in response to the CS+touch (M=-0.15, SD=0.23; p=.002) and the CS- (M=-0.21, SD=0.22; p<.001),

which did not statistically differ from each other (p>.99). These findings suggest that the SCR amplitude increased specifically when anticipating a painful, but not a tactile, outcome.

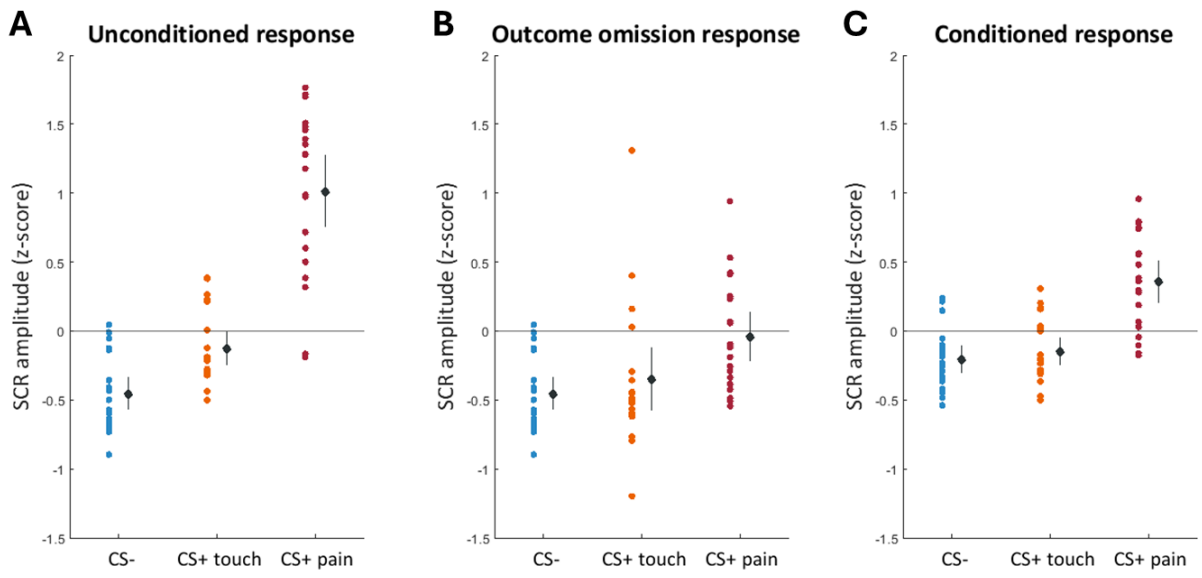

Figure 2.3. Representation of skin conductance response (SCR) of participants for CS- (blue), CS+touch (yellow), and CS+pain (violet). (**A**) represents the unconditioned SCR post CS offset, (**B**) represents the outcome omission SCR post CS offset, and (**C**) represents the conditioned SCR during CS presentation. Black dots represent means, and vertical bars represent their standard error.

Model comparison

Model comparison using the BIC identified the Rescorla-Wagner model with varying outcome sensitivities as the best-fitting model. This model was associated with a lower mean BIC value than the version of the Rescorla-Wagner model that does not include an outcome sensitivity parameter and the variants of the hybrid model (see Table 2.1). Therefore, we extracted and compared the learning rates and the outcome sensitivities from this model.

Table 2.1. Mean BIC value and number of estimated parameters for each model

Model	Mean BIC	Number of estimated parameters
RW(*V*)	117.85	6 (3 free + 3 regression parameters)

$RW_S(V)$	117.34	8 (5 free + 3 regression parameters)
Hybrid(V)	131.39	10 (7 free + 3 regression parameters)
Hybrid(α)	122.52	10 (7 free + 3 regression parameters)
Hybrid(α+V)	122.40	11 (7 free + 4 regression parameters)
$Hybrid_S(V)$	131.09	12 (9 free + 3 regression parameters)
$Hybrid_S(\alpha)$	126.81	12 (9 free + 3 regression parameters)
$Hybrid_S(\alpha+V)$	119.72	13 (9 free + 4 regression parameters)

Note. RW = Rescorla-Wagner model, V = predictive values, α = associabilities, s = model with varying outcome sensitivities

Estimated learning rates and outcome sensitivities

To assess differences in learning rate (α) estimates as a function of CS-US intensity association, a rmANOVA was performed with CS type (CS-, CS+touch, CS+pain) as a within-subject factor (Figure 2.4.A). No main effect emerged ($F_{(2,38)}$=0.82, p=.450, η^2_p=0.041, 90% η²CI [0.000, 0.170]), revealing no statistically significant difference in learning rates between the CS- (M=0.41, SD=0.34), CS+touch (M=0.49, SD=0.29), and CS+pain (M=0.38, SD=0.31).

To assess the effects of the outcome intensity (tactile, painful) at the computational level, a two-tailed paired t-test was performed on the outcome sensitivity (λ) estimates (Figure 2.4.B). This analysis showed a higher outcome sensitivity for the painful (M=0.46, SD=0.32) compared to the tactile (M=0.22, SD=0.22) outcome ($t_{(19)}$=3.45, p=.003, Cohen's d=0.771, 95% dCI [0.238,1.304]).

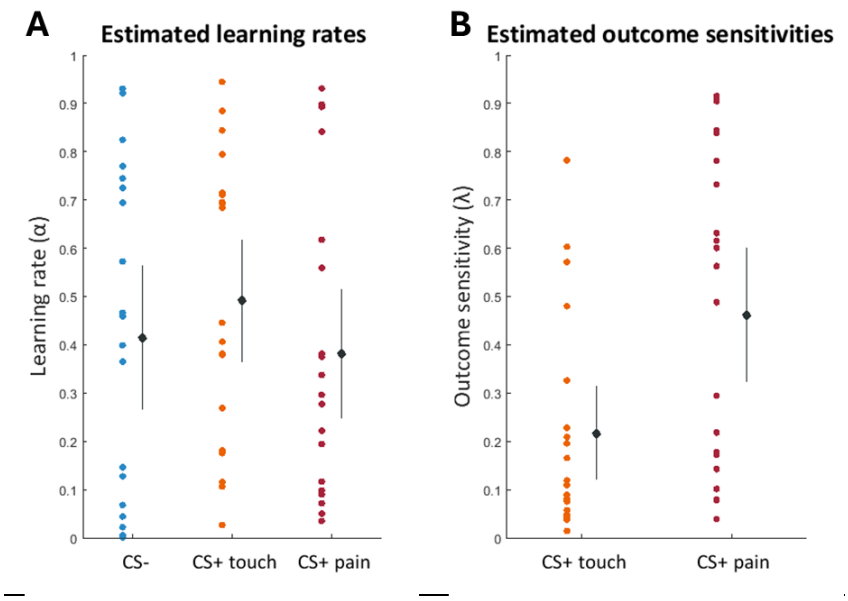

Figure 2.4. Estimated learning rate (**A**) and outcome sensitivity (**B**) parameters of participants for CS- (blue), CS+touch (yellow), and CS+pain (violet). Black dots represent means, and vertical bars represent their standard error.

Computational parameters predict autonomic and affective responses

To test whether trial-by-trial learning signals predicted autonomic responses to outcome expectancy, we examined the relationship between prediction error (δ) timeseries derived from the Rescorla-Wagner model with varying outcome sensitivities, and SCR following the expected time of the outcome on non-reinforced trials. A linear mixed-effects model with random slopes was conducted as follows:

SCR ~ 1 + δ + (δ | id_participant)

The analysis revealed that the prediction error timeseries predicted the SCR to the outcome omission ($F_{(1,\ 34.31)}$=6.87, p=.013, η^2_p=0.167, 90% η^2CI [0.033, 0.359]), indicating that larger prediction errors were associated with stronger skin conductance response after the CS+pain offset when no outcome was delivered (Figure 2.5.A). This finding supports the idea that expectancy violation, as encoded by the prediction error signal, drives physiological arousal even in the absence of reinforcement (Spoormaker et al., 2011, 2012; Vervliet et al., 2017; Willems & Vervliet, 2021). In particular, the increase in SCR following the painful outcome omission could be considered a psychophysiological correlate of the prediction error.

In addition, we conducted exploratory analyses to investigate the role of individual differences in outcome sensitivity (λ) in shaping subjective affective responses. These analyses are intended to better understand how computational parameters relate to inter-individual variability in learning and emotional processing. The λ parameter of the painful outcome was found to negatively correlate with the explicit ratings of CS+pain pleasantness ($r_{(18)}$=-0.531, p=.016), indicating that greater outcome sensitivity to the painful outcome was associated with lower pleasantness attributed to the corresponding CS (Figure 2.5.B).

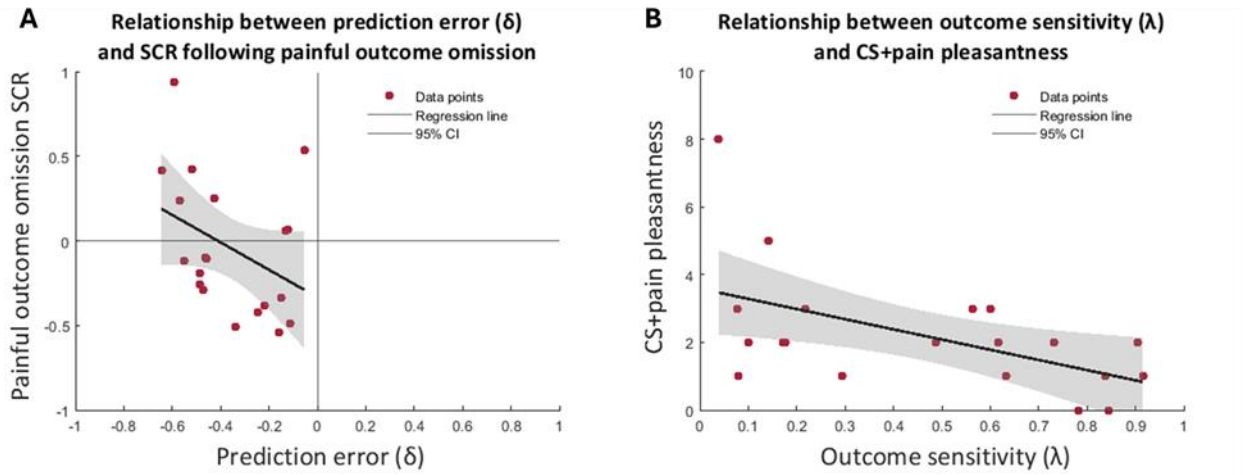

Figure 2.5. Panel (**A**) represents the relationship between the prediction error (δ) and the skin conductance response after the CS+pain offset when no outcome was delivered. Panel (**B**) represents the negative correlation between the outcome sensitivity (λ) of the painful outcome and the explicit ratings of CS+pain pleasantness.

COMPUTATIONAL MODELING DETAILS

Model and parameter fitting

We fitted and optimized the free parameters of the reinforcement learning models using maximum a posteriori estimation. All the free parameters were constrained with a weak ß(1.2, 1.2) prior distribution that slightly favors value in the middle of the parameter range (see, e.g., Niv et al., 2012; Stussi, 2025). To avoid local optima, we used 50 random initializations to compute maximum likelihood estimates for each parameter.

The loglikelihood of each trial's z-scored skin conductance response (SCR) $LL_{SCR(t)}$ was modeled as a Gaussian distribution around a mean determined by the scaled expected value V*(t)*, the scaled associability $\kappa(t)$, or the scaled combination of both expected value and associability computed by the model plus a constant term β_0, and a variance parameter σ (J. Li et al., 2011; Zhang et al., 2016), as follows:

1) $LL_{SCR(t)} \sim N(\beta_0 + \beta_1 \cdot V(t) \cdot x(t), \sigma), or$
2) $LL_{SCR(t)} \sim N(\beta_0 + \beta_1 \cdot \alpha(t) \cdot x(t), \sigma)$, or
3) $LL_{SCR(t)} \sim N(\beta_0 + \beta_1 \cdot V(t) \cdot x(t) + \beta_2 \cdot \alpha(t) \cdot x(t), \sigma)$

These are equivalent to linear regressions from (1) the expected value timeseries, (2) the associability timeseries, or (3) the combination of both, to the z-scored SCRs. We used the trial-by-trial timeseries of expected values V*(t)* to estimate the free parameters for the Rescorla-Wagner model variants. For the hybrid model variants, the free parameters were estimated separately for each possible combination based on the trial-by-trial timeseries of values V*(t)*, the trial-by-trial timeseries of associabilities $\kappa(t)$, or the combination of both expected values and associabilities (see Li et al., 2011; Zhang et al., 2016).

Model and parameter recovery

We performed a model recovery and a parameter recovery analysis to ensure that the models can be correctly identified, and the parameters recovered, respectively (see Palminteri et al., 2017; Wilson & Collins, 2019). We ran 20 simulations that each generated model predictions for 20 synthetic participants with each of the models considered in the model space (see Correa et al., 2018, for a similar approach). All parameters were randomly sampled from a ß(1.2, 1.2) distribution for each simulation. The structure and properties of the task were identical to the 20 instances that participants experienced during the experiment. The models were fitted to the simulated data to (a) verify whether the model that generated the data was identified as the best-fitting model according to BIC across simulation (i.e., associated with the lowest averaged mean BIC) and at the individual simulation level (i.e., associated with the lowest mean BIC for each simulation), and (b) estimate the free parameters to assess whether the recovered parameter values were tightly correlated with the simulated parameters. For the hybrid model variants, the free parameters were estimated based on the combination of both values and associability timeseries.

The model recovery analysis (Figure 2.6) confirmed that all the models were correctly identified in all simulations. Linear regressions between the simulated and estimated parameters showed that the regression intercepts ($ß_0$ values) were equal or close to 0 (all $ß_0$s = [-0.002, 0.002]) and the regressions slopes ($ß_1$ values) were equal or close to 1 (all $ß_1$s > 0.99, all *p*s < .001) for all models. These results indicate that the free parameters were virtually perfectly recovered for each model considered. At the individual simulation level, the averaged Pearson correlations between the simulated and estimated parameters across synthetic participants were equal or close to 1 for all the models (all averaged *r*s > .99, all averaged R^2 > .99). We did not observe large cross-correlations across estimated parameters (all averaged R^2 < .09). Parameter recovery and averaged Pearson correlations between the simulated and estimated parameters for the Rescorla-Wagner model with varying outcome sensitivities are depicted in Figure 2.7.A,B.

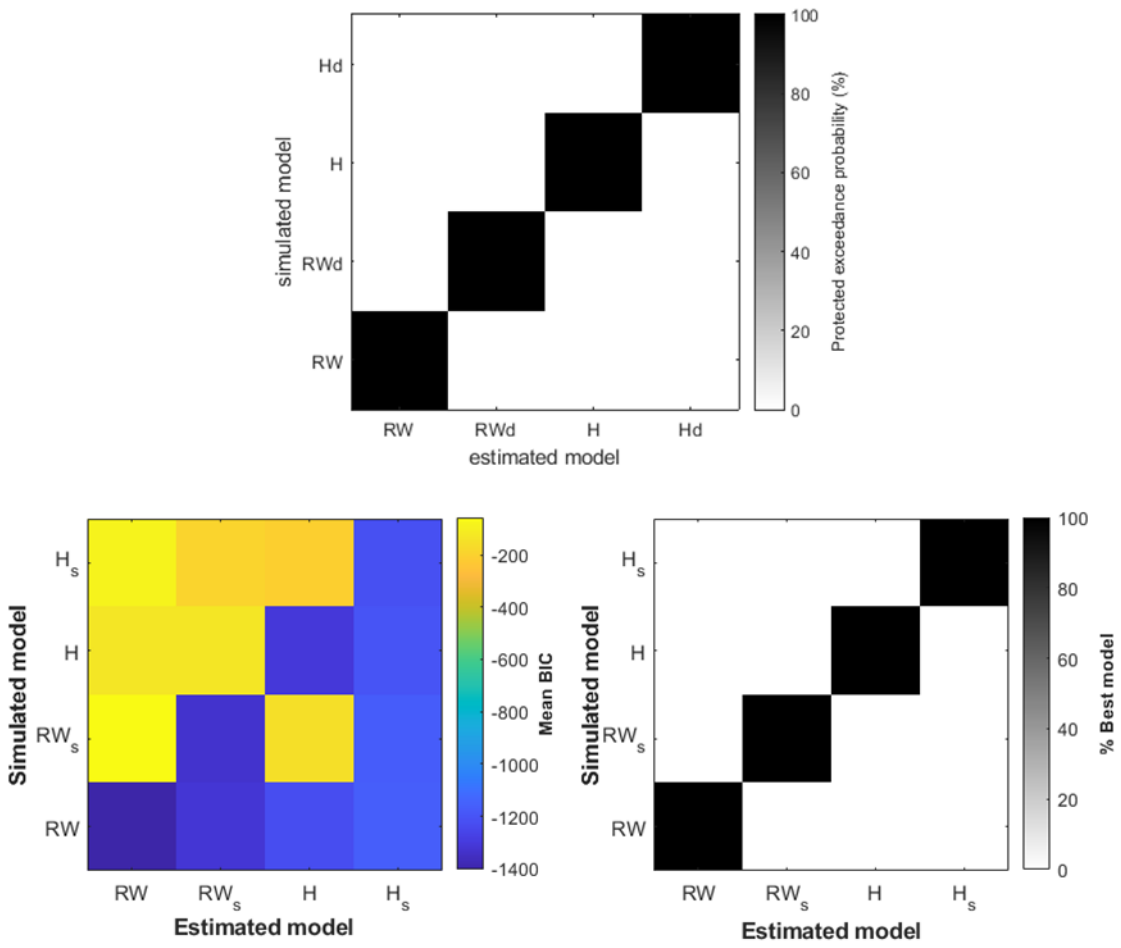

Figure 4.6. Model recovery analysis. Data from 20 synthetic participants were simulated with each of the models considered. Bayesian information criterion was used to identify the model that fitted best to the simulated data. This procedure was repeated 20 times. The model used to simulate the data was associated with the lower mean BIC averaged across simulation for each model (left panel) and all models were correctly identified in all simulations (right panel).

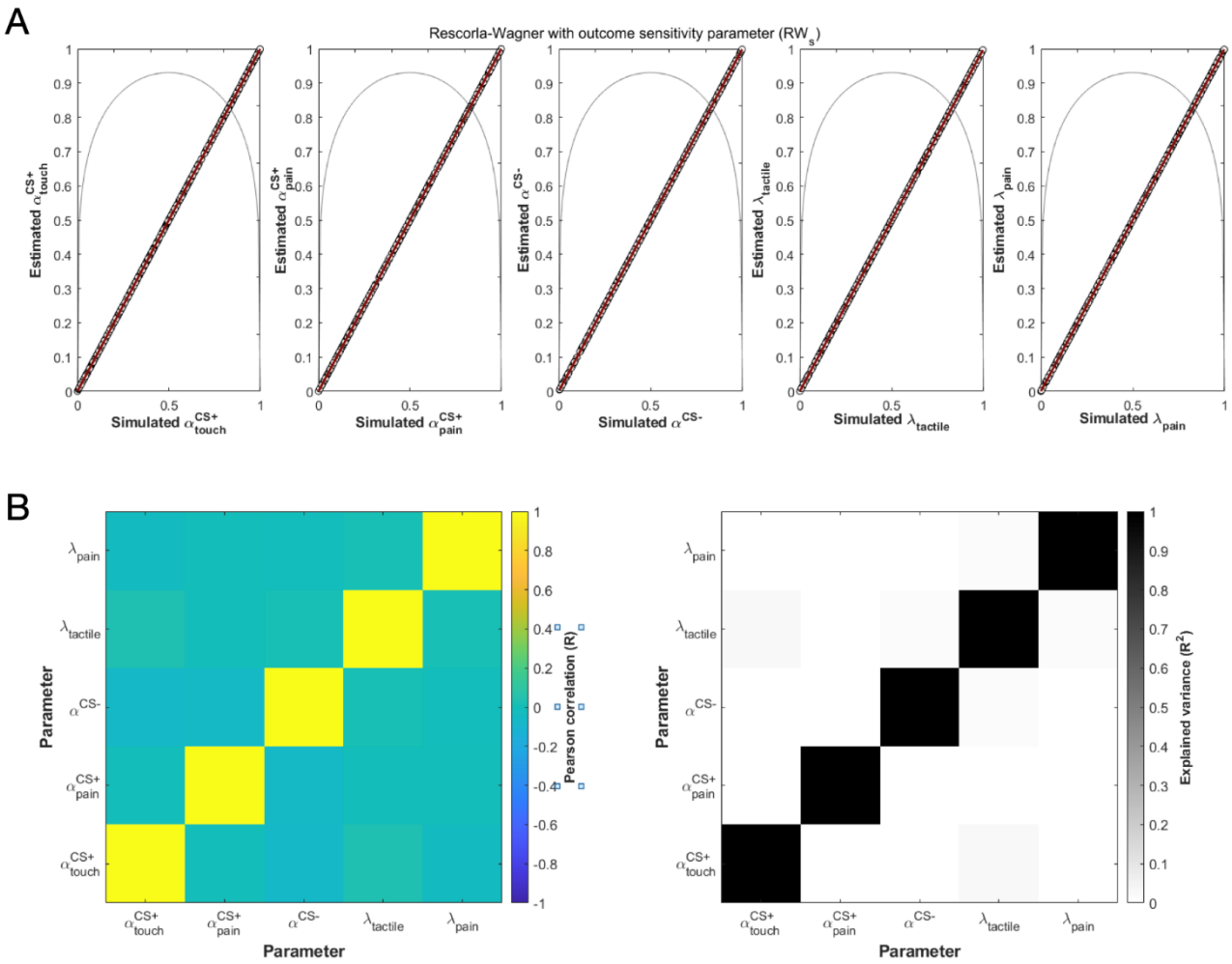

Figure 4.7. Parameter recovery analysis for the Rescorla-Wagner model with varying outcome sensitivities. (A) Data from 400 synthetic participants (20 simulations ´ 20 individuals) were simulated with the model. The five free parameters per participant (3 learning rates and 2 outcome sensitivities) were then regressed against the true parameters used for simulating the data. The regression results show perfect identifiability (β_0s = 0, β_1s = 1, all ps < .001) . Each dot represents a synthetic participant. The red lines represent the best linear fits, and the shaded gray areas their 95% confidence intervals. The gray densities represent the probability distribution used to sample the parameters. (B) Confusion matrices representing the Pearson correlations (left) and explained variances (right) between parameters at the individual simulation level. The parameters were estimated over 20-participant simulations and averaged over the 20 simulations. The diagonals represent the correlations between the simulated and estimated parameters. The off-diagonals represent the cross-correlations between estimated parameters.

DISCUSSION

The present study tested how the aversiveness of unconditioned stimuli influences the acquisition of conditioned threat responses and whether this influence was reflected by distinct estimated learning rates or outcome sensitivities at the algorithmic level. During a Pavlovian threat conditioning task, participants learned to anticipate either a tactile, a painful, or a no-shock outcome. We found that both the painful (i.e., aversive) and tactile (i.e., non-aversive) outcomes elicited an unconditioned skin conductance response (SCR), albeit greater for the painful than the tactile outcome. In contrast, conditioned SCRs were selectively observed in anticipation of the painful outcome but not the tactile outcome, along with an increase in SCR when the anticipated painful outcome was omitted, reflecting a prediction-error-related SCR. Reinforcement learning models also revealed that the sensitivity to the painful outcome was greater than that to the tactile outcome. The sensitivity to the painful outcome was furthermore related to prediction-error-related SCRs and to the explicit pleasantness ratings of its associated conditioned stimulus. These findings highlight the critical role of the individual's sensitivity to the affective value of the outcome in driving human threat conditioning.

At the end of the task, the explicit ratings of the conditioned stimuli showed that participants evaluated the CS+pain as less pleasant compared to the other CSs and attributed a higher intensity to the painful than the tactile (and absence of) outcome. In addition, participants correctly rated the CS+pain and the CS+touch as more often associated with the painful and tactile outcome, respectively, than the CS-. Thus, participants demonstrated successful differential threat conditioning at the explicit, declarative level.

Crucially, the analysis of the SCRs following the time of the outcome delivery (as in Inoue et al., 2020) showed that both the tactile and painful outcomes elicited unconditioned responses in reinforced trials. Specifically, the painful outcome elicited a greater unconditioned response than the tactile outcome, which in turn produced a higher unconditioned response than the no-outcome condition. This finding confirmed the assumption of our study that aversive and non-aversive unconditioned stimuli led to distinct psychophysiological responses (Treister et al., 2012; Tursky, 1974). These results suggest that variations in outcome aversiveness,

manipulated through shock intensity, shape the acquisition of conditioned responses during Pavlovian threat conditioning.

In contrast to the SCRs after the outcome delivery in reinforced trials, in non-reinforced trials, a SCR emerged only to the omission of the painful outcome. This suggests that, during acquisition, only the unexpected omission of an aversive outcome elicited a robust SCR, consistent with a response driven by prediction errors. This is in line with findings showing that SCRs increase when an expected aversive stimulus is omitted (Spoormaker et al., 2011, 2012; Stemerding et al., 2022; although see Bach & Friston, 2012), and possibly scaling proportionally at increasing intensities (Spratling, 2012; Willems & Vervliet, 2021). Our results extend these findings by formally demonstrating that SCRs elicited by the outcome omission are driven by prediction error signals and correlate with the magnitude of the prediction error.

Similarly, the analysis on the conditioned SCRs showed an increase only in anticipation of the painful outcome, but not the tactile one. Considering this result together with the results regarding the explicit ratings, they suggest that awareness of the CS-outcome association may not be sufficient to produce conditioned autonomic responses, but rather this may be more reflected by ratings of the outcome intensity and CS (un)pleasantness. Although participants demonstrated explicit knowledge of the CS–US contingencies across conditions, only the CS+pain was rated as less pleasant, and only the painful outcome was evaluated as more intense and accompanied by a robust anticipatory SCR. Whereas previous studies (e.g., Hamm & Vaitl, 1996; Li et al., 2025) have emphasized the importance of contingency awareness in eliciting differential SCRs, our results suggest that SCRs may be driven not only by contingency awareness but also by the affective value of the anticipated outcome, or by an interaction between these factors.

The results concerning the parameter estimates of the outcome sensitivity derived from reinforcement learning models confirmed that participants' SCRs reflected a higher aversiveness attribution to the painful than the tactile outcome. This difference influenced both the magnitude of prediction errors and the values assigned to different conditioned stimuli. This is coherent with our manipulation of outcome aversiveness and aligns with fundamental principles of classical conditioning and reinforcement learning, which propose that motivationally relevant outcomes are necessary to produce conditioning, operating

through prediction errors as key determinants of associative strength (Nasser & Delamater, 2016; Pearce & Hall, 1980; Rescorla & Wagner, 1972; Wagner, 1981).

Interestingly, the model-estimated outcome sensitivity attributed to the painful outcome positively correlated with both the increase in SCRs when the painful outcome was omitted and the explicit ratings of the CS+pain (un)pleasantness. The first correlation corroborates the interpretation that the SCR increase following the painful outcome omission was likely driven by a prediction error signal, with the magnitude of the prediction error predicting the SCR magnitude in response to the omitted painful outcome. This relationship indicates that greater expectancy violations were associated with heightened physiological arousal in the absence of reinforcement. These results suggest that the affective value participants attribute to the aversive outcome, as captured by the outcome sensitivity parameter, shapes the magnitude of prediction errors generated during threat acquisition, which in turn is a primary driver of learning (as in Wu et al., 2017). Moreover, the negative correlation between the estimated outcome sensitivity and the explicit pleasantness rating of the CS+pain points to a link between the affective value assigned to the outcome and the explicit evaluation of the conditioned stimulus, highlighting how the affective value of the outcome influences conditioned stimuli evaluation in Pavlovian threat conditioning.

In contrast to the outcome sensitivity estimates, the learning rates did not statistically differ between the conditioned stimuli associated with the painful and tactile outcomes. This null finding suggests that a conditioned stimulus associated with an aversive outcome might not benefit from accelerated learning relative to a conditioned stimulus paired with a non-aversive outcome. This could be due to the fact that we manipulated the outcome aversiveness rather than the conditioned stimulus features. Indeed, while the learning rate parameter reflects the speed with which the value of the CS is updated via the integration of prediction errors, the outcome sensitivity parameter captures the affective value individuals attribute to the outcome and its subsequent influence on prediction errors. The fact that the Rescorla-Wagner model incorporating an outcome sensitivity parameter provided the best fit to our data likely reflects its capacity to model learning as a function of both stable learning rates across conditions and individual differences in outcome valuation, as captured by the outcome sensitivity parameter. This allowed the model to account for a similar integration of prediction errors into the updating of the conditioned stimulus value across conditions while

also incorporating variations in the affective value attributed to the outcome, all while relying on the minimal number of free parameters necessary to explain the data.

To conclude, our findings indicate that the affective value attributed to the outcome modulates both autonomic and explicit responses during Pavlovian threat conditioning. Specifically, the sensitivity to the outcome enhanced unconditioned and prediction-error-related SCRs, which in turn drove the acquisition of anticipatory conditioned SCRs. Moreover, a negative correlation emerged between the outcome sensitivity and the explicit pleasantness attributed to the CS associated with the painful outcome. By combining psychophysiological, computational, and self-report measures, our results provide a mechanistic account of how internal representations of aversive outcomes influence emotional learning in humans. Crucially, our results also emphasize the methodological importance of employing sufficiently intense and appropriate stimuli, such as a painful outcome, to capture the nuanced dynamics of threat conditioning (as highlighted by Stussi & Coppin, 2024) when aiming to study either healthy or pathological emotional learning processes.

EXPERIMENT 2

THEORETICAL BACKGROUND

Anticipating potential threats while ignoring innocuous events is critical for survival. For example, upcoming painful stimuli pose a threat to bodily integrity, whereas tactile stimulation, although salient, does not. Accurately predicting whether an upcoming event is dangerous allows organisms to deploy defensive resources efficiently: overreacting to innocuous cues wastes energy, while underreacting to real threats can be deadly. Yet how the nervous system learns to differentially anticipate threatening events (e.g. pain) from other non-threatening events (e.g. touch) remains poorly understood.

Pain is not only a sensory experience but also carries an affective-motivational component that drives protective behavior (Casey, 2023; Melzack & Casey, 1968; Raja et al., 2021). Thus, pain processing is not only about detecting noxious input, but also about its emotional impact

and behavioral significance (Casey, 2023; Melzack & Casey, 1968).Neuroanatomical and physiological evidence (Kohoutová et al., 2022; Kulkarni et al., 2005; Mano & Seymour, 2015; A. Xu et al., 2020; X. Xu et al., 1997) shows that distinct but interacting circuits mediate the sensory and affective components of pain (Tan & Kuner, 2021) that are coactivated by painful inputs, engaging limbic and hypothalamic circuits (Kohoutová et al., 2022; Kulkarni et al., 2005; LeDoux, 2014; MacLean, 1949; Mano & Seymour, 2015; A. Xu et al., 2020; X. Xu et al., 1997) alongside somatosensory areas. This evidence suggests that affect is not added on top of the sensory experience but is intrinsic to the pain experience (Auvray et al., 2010). Importantly, both the sensory and affective-motivational dimensions are already engaged during the anticipation of pain (Carlsson et al., 2006; Porro et al., 2002). In this view, pain anticipation is not just about preparing for what it will physically require (sensorimotor component) but also for how bad it will feel (affective, motivational component).

Learning to anticipate threatening stimuli mobilizes both the autonomic and motor systems (Lonsdorf et al., 2017). Human Pavlovian threat conditioning studies have shown that the autonomic nervous system exhibits multiple conditioned responses in terms of increased skin conductance (Boucsein et al., 2012), heart rate (Castegnetti et al., 2016), pupil size (Korn et al., 2016; Leuchs et al., 2017; Reinhard & Lachnit, 2002), and respiratory amplitude (Castegnetti et al., 2017; Van Diest et al., 2009). Also, the motor system shows conditioning of defensive reflexes (e.g., fear potentiated startle), changes in motor preparation (as assessed through reaction times) (Krypotos et al., 2015, 2015; Pittig et al., 2020), as well as in action execution (Karos et al., 2017; Neige et al., 2018; Starita et al., 2022). Interestingly, autonomic and motor responses have been proposed to anticipate partially distinct aspects of anticipated outcomes, with the motor system encoding the sensory and perceptual features of anticipated outcomes, while autonomic system tracking affective value, being tightly related to the response of the amygdala (Pool et al., 2019, 2023; Zhang et al., 2016). Consistent with this, we have shown that reductions in corticospinal excitability specifically encode the location and timing of expected pain during threat conditioning, such information are not captured by skin conductance response, which reflected a non-specific increase in arousal (Betti et al., 2024).

Despite this evidence, it remains unclear how the autonomic and motor systems learn to differentially anticipate threatening painful stimuli versus non-threatening but perceptible

somatosensory stimuli (i.e. tactile stimuli). Animal research has shown that stronger threats elicit more robust conditioned responses (Bolles et al., 1981; Morris & Bouton, 2006; J. C. Smith & Sclafani, 2002; M. C. Smith, 1968). Indeed, manipulations of shock intensity consistently show that both the rate and magnitude of conditioned responses increase with stronger shocks (Annau & Kamin, 1961), whereas low-intensity shocks elicit minimal responses (Baldi et al., 2004; Phillips & LeDoux, 1992). Yet in humans, such evidence is lacking because most threat conditioning studies contrast the anticipation of aversive stimuli with their absence (Pool et al., 2019, 2023), leaving open the question of how innocuous events such as touch are represented within learning systems.

To address this, the present study used a Pavlovian threat conditioning task in which participants learned to anticipate painful shocks, tactile stimulation, or no shocks, while skin conductance responses (SCRs) and motor evoked potentials (MEPs) were simultaneously recorded to track autonomic and motor system activity throughout learning. The task included an acquisition phase, to test initial learning, and a reversal phase, to test how both systems adapt when previously learned predictions are updated, specifically when cues that once predicted pain came to predict touch, and vice versa. Indeed, adaptive behavior depends not only on forming accurate threat predictions but also on flexibly updating them when environmental contingencies change. Failing to recognize that a previously threatening stimulus has become safe can be costly, and the persistence of outdated threat responses is a hallmark of anxiety-related disorders (Duits et al., 2015). By combining measures of autonomic arousal and motor excitability within this study, we aim to clarify how these psychophysiological systems learn to differentially anticipate threatening from non-threatening events, and how they flexibly adjust to changing contingencies. We expected that both autonomic and motor systems would show robust conditioned responses in anticipation of pain compared to shock absence, in line with the wealth of previous literature. Crucially, given the idea that the autonomic system may track the affective value of impending stimuli, we further expected the response of the autonomic system to be more closely tuned to the painful outcome, producing the largest increases for pain anticipation compared to touch or shock absence. In contrast, given that the motor system may primarily encode the sensory features of the anticipated outcome, its response may show less sensitivity to the aversive

value of the painful stimulus, but rather show a more graded response as anticipated shock intensity increases from shock absence to touch to pain.

METHODS

Participants

Thirty healthy adult volunteers participated in the experiment; two of them were excluded due to technical problems during data recording, so twenty-eight participants were included in the data analysis (14 females, 14 males, aged between 19 and 39 years: mean (M) = 24, standard deviation (SD) = 3.85). The sample size was calculated through a power analysis conducted with MorePower 6.0.4 (Campbell & Thompson, 2012) with the following parameters: Analysis: ANOVA; Design factors: repeated measures 2 (Phases: acquisition, reversal) x 3 (CS: CS+early, CS+late, CS-); Effect of interest: 3x2; Alpha: 0.05; Power: 0.8 (partial eta = 0.17, Cohen's f = 0.45). The effect size was based on the effect size found in our previous study (Betti et al., 2024).

All participants were right-handed, as assessed by the Edinburgh Handedness Inventory (Oldfield, 1971), with normal or corrected-to-normal visual acuity. They were all screened for TMS exclusion criteria to exclude any history of head trauma or head surgery, seizures, and family history of epilepsy, implanted hardware, medications, and neurological and medical illnesses according to safety guidelines (Rossi et al., 2009, 2021). Also, participants self-reported to have no current neurological, or psychiatric diagnosis or chronic medical condition, as well as no recent history of trauma affecting the upper limbs, nor were they currently suffering from any pain or taking any analgesic medication. The study followed the American Psychological Association Ethical Principles of Psychologists and Code of Conduct and the Declaration of Helsinki and was approved by the Bioethics Committee of the University of Bologna (protocol number 224364). All participants gave their written informed consent for their participation.

Experimental task and stimuli

Pavlovian threat conditioning and reversal task. Participants completed a Pavlovian threat conditioning and reversal task (Mathôt et al., 2012), composed of an acquisition and a reversal phase with identical trial structure (Figure 2.8). During each phase, they learned the association between three visual stimuli and their respective outcomes. The three visual stimuli were filled colored circles (64 pixels diameter, blue #5698D4, pink #C760CA, or yellow #F4E634), representing the three different conditioned stimuli (CSs); color assignment to each CS was counterbalanced among participants. Two of them were CSs+ associated with the delivery of a shock (either tactile or painful) to the right forearm, while the other was a CS- never associated with shock. In each experimental trial, one of the CSs appeared in the center of a computer screen on a black background for 4560ms. The inter-trial interval (ITI) was jittered between 8000-9000ms, and before the beginning of each trial, a white fixation cross was presented for 1s in the center of the screen. In each trial, single-pulse TMS (spTMS) was delivered 4500 ms after the CS onset to probe corticospinal excitability and elicit an MEP.

Each CS was presented 20 times, for a total of 60 trials. For each CS+, the shock occurred in 14 trials (i.e., 70% reinforcement rate) at the CS offset. Crucially, the two CSs+ differed in the intensity of the associated shock, i.e. the CS+touch was associated to the tactile shock, while the CS+pain was associated to the painful shock. The first three trials consisted of the presentation of a CS-, a reinforced CS+touch, and a reinforced CS+pain, in random order, while the remaining trials proceeded in pseudo-random order with no more than two consecutive CSs of the same type. In the reversal phase, the CS+touch of the acquisition phase became the CS+pain associated with the painful shock, while the CS+pain of the acquisition phase became the CS+touch associated with the tactile shock; the CS- served as a control stimulus in both phases never paired with a shock (Figure 2.8).

Before starting the task, participants were instructed as follows: “You will see a colored circle appearing on the screen. Sometimes, the circle may deliver a shock. Your task is to understand with which color the circle gives you the shock”. In addition, they were instructed to observe the screen throughout the task while keeping their hands and arms relaxed, without executing any motor response.

At the end of both acquisition and reversal phases, explicit learning was assessed by having participants rate the valence and arousal of each CS, and the CS-shock contingency on a series of 11-point Likert scales (ranging from 0 to 10). The following three questions were answered regarding each CS, presented in random order: i) "When I saw this circle, the feeling I had was" (Valence rating; ranging from 0='unpleasant' to 10='pleasant'); ii) "When I saw this circle, the feeling I had was" (Arousal rating; ranging from 0='not activated at all' to 10='extremely activated'); iii) "This circle gave me the shock" (Contingency rating; from 0='never' to 10='always'). Additionally, the following question on US intensity was aswered on an 11-point Likert scale, with each US delivered immediately before the question appearance: "The stimulation I perceived was" (from 0='no stimulation' to 10=' intolerable', including the following anchors: 2='tactile', 5='unpleasant', 8='painful').

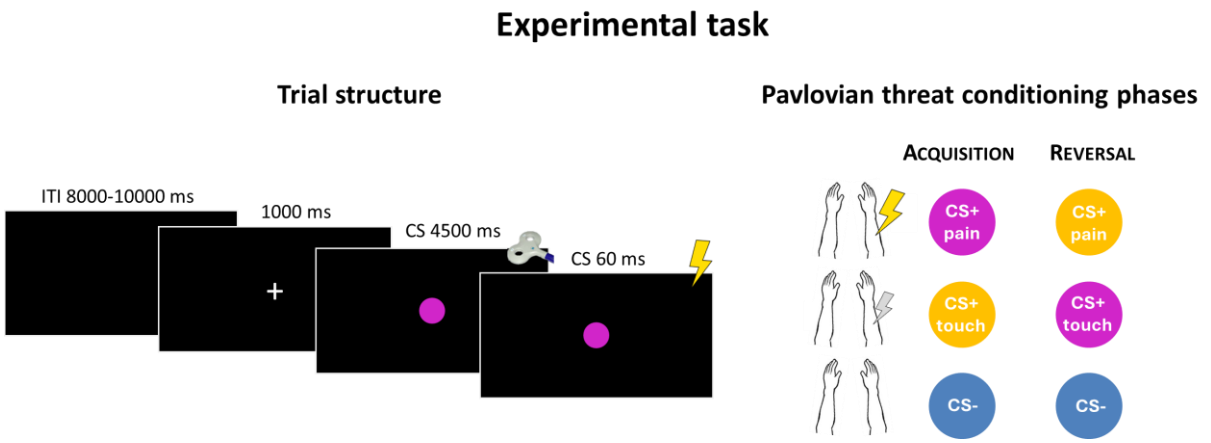

Figure 2.8. Illustration of the experimental task. On the left, the trial structure is represented. Three types of conditioned stimuli (CSs), presented for 4560 ms each, were used: a CS+touch associated with the tactile outcome, a CS+pain associated with the painful outcome, and a CS- never paired with any outcome. In each trial spTMS was delivered 4500 ms after the CS onset. Outcomes were delivered at the CS offset. On the right, the Pavlovian threat conditioning phases are represented. Three types of CSs were used: a CS+pain associated with the painful shock on the right arm, a CS+touch associated with the painful shock on the right arm, and a CS- never paired with any outcome. In the reversal phase, the CS+touch of the acquisition phase became the CS+pain associated with the painful shock and vice versa, while the CS- was never paired with a shock in both phases.

Stimulations and recordings

The experimental setup for the Pavlovian threat conditioning task (Figure 2.9) included the delivery of tactile and painful electrotactile stimulations (shocks) over the participant's right forearm (Betti et al., 2024). In each trial, electrodermal activity was recorded continuously to assess autonomic system activity. Additionally, electromyography was recorded continuously from the first dorsal interosseus (FDI) muscle of the right hand, while spTMS pulses were delivered over the left primary motor cortex (M1) to probe corticospinal excitability and evoke MEPs as described below.

Tactile and painful shocks calibration. The tactile and painful shocks consisted of a 2ms electro-cutaneous stimulation generated by a Digitimer Stimulator (Model DS7A, Digitimer Ltd., UK) and delivered through pre-gelled Ag/AgCl snapped electrodes (Friendship Medical, SEAg-S-15000/15x20) attached to the participants' right extensor carpi radialis (ECR) muscle. Two stimulators were connected in parallel to allow stimulation through the same electrodes using two different shock intensities, as instructed by the developer's application notes. The shock intensities were calibrated for each participant as follows. First, to tailor the intensity of the tactile stimulation, the experimenter set the shock intensity using an ascending staircase procedure (Cornsweet, 1962; Klein, 2001), starting from 0 mA in steps of 0.1 mA to a level perceived by the participant as clearly detectable but not at all unpleasant. Then, to determine the intensity of the painful stimulation, the shock intensity was further increased in steps of 0.5 mA to reach the pain tolerance level (i.e., the maximum tolerable pain). This procedure was repeated twice, and the mean was calculated to obtain the final values of the tactile (M=1.25 mA, SD=0.40) and painful (M=63.82 mA, SD=25.05) shocks. Stimuli did not exceed individual tolerance limits, in line with the International Association for the Study of Pain (IASP) guidelines (Charlton, 1995).

Electrodermal activity. Electrodermal activity was recorded continuously at 1250 Hz, with a 10 Hz low-pass filter, from pre-gelled snap electrodes (BIOPAC EL503) placed on the hypothenar eminence of the palmar surface of the left hand, connected to a BIOPAC MP-150 System (Goleta, CA, USA) and fed into AcqKnowledge. Given that skin conductance responses (SCRs) primarily reflect general autonomic arousal rather than effector-specific preparatory processes, recording from the hand contralateral to the threatened one does not compromise the validity of the measure. Indeed, previous evidence shows that autonomic responses

assessed through SCRs do not differentiate the laterality of predicted or delivered pain, displaying comparable conditioning to cues associated with left or right stimulation (e.g., Betti et al., 2024; Zhang et al., 2016). Therefore, recording SCR from the contralateral hand provides a robust and valid index of conditioned autonomic arousal (Lonsdorf et al., 2017).

Electromyography recording. Surface EMG activity was recorded from the FDI muscle of the participant's right hand at 5000 Hz, with a 5 kHz lowpass filter, through a pair of Ag/AgCl electrodes (BIOPAC EL501) placed in a belly-tendon montage connected to an EMG100C module of the BIOPAC MP-150 System (Goleta, CA). After skin preparation, a small amount of isotonic hyposaturated conductant gel (Lectron III Gel, NEUROSPEC) was added to the electrodes, which were placed and fixed on the target positions. The active electrode was placed over the muscle belly, determined by palpation during maximum voluntary contraction, while the reference and ground electrodes were placed over the proximal interphalangeal juncture and the radial styloid process.

Transcranial magnetic stimulation (TMS). Single-pulse TMS (spTMS) was administered using a 70 mm figure-of-eight coil connected to a Magstim Rapid2 stimulator (Magstim Co., Whitland, UK). Pulses were delivered to the left primary motor cortex (M1) of the participant, in correspondence with the FDI muscle representation. The coil was placed on the head at a 45-degree angle relative to the interhemispheric fissure, with the handle pointing laterally and caudally (Brasil-Neto et al., 1992; Mills et al., 1992). Then, to find the FDI muscle representation, the best position for the coil on the scalp at which the lower stimulation intensity elicits the largest MEP, i.e. optimal scalp position, was determined by moving the coil in approximately 0.5 cm steps around the presumed hand motor area. The position was then marked on a tight-fitting cap worn by the participants, ensuring a correct coil placement throughout the experiment. For each participant, the resting motor threshold (rMT) was then determined by finding the lowest stimulation intensity inducing MEPs with at least ≥ 50 mV peak-to-peak amplitude in a relaxed muscle in 5 out of 10 trials (Rossini et al., 1994). During the experiment, the intensity of TMS stimulation was set at 120% of the individual rMT to ensure a stable and reliable recording of cortical output while accounting for interindividual differences in cortical excitability (Di Lazzaro et al., 2004; Rothwell, 1997), in accordance with established safety and methodological guidelines for non-invasive brain stimulation (Rossini et al., 2015). The rMT ranged from 61 to 100% (M=75.07%, SD=11.10) of the maximum

stimulator output. Corticospinal excitability was probed by delivering single pulse TMS 4500 ms after CS onset (see Figure 4.8), 60 ms before the time of the shock in reinforced trials.

To exclude any non-specific, long-lasting changes in basal corticospinal excitability that could be related to the TMS, the task, or the shocks per se, baseline corticospinal excitability was probed at the beginning and the end of the experimental session. This was done by delivering 15 single TMS pulses and acquiring MEPs while participants passively observed a fixation cross on the screen. An inter-pulse interval of at least 5000ms was adopted, thereby avoiding changes in corticospinal excitability due to repeated TMS pulses (R. Chen et al., 1997). No difference emerged when comparing MEPs recorded during the initial (M=0.898, SD=0.585) and final (M=1.038, SD=0.779) baseline phases ($t_{(27)}$=-1.886, p=.070).

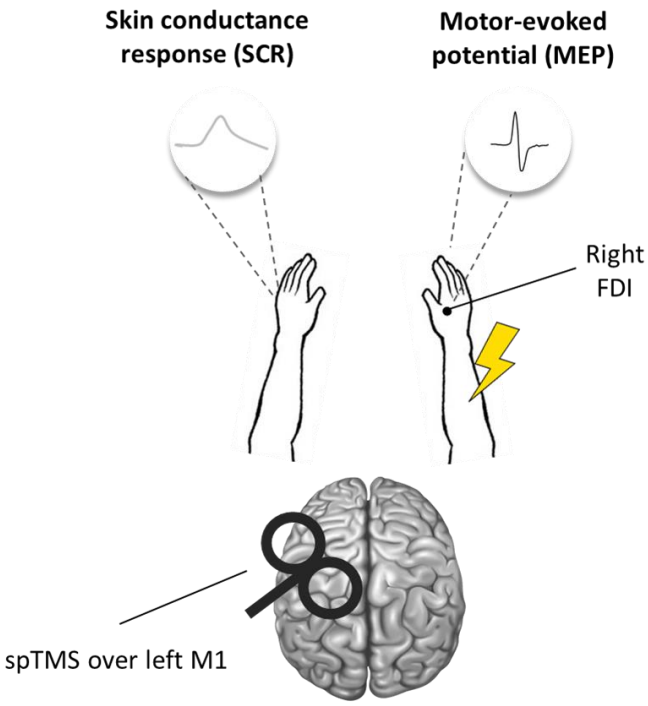

Figure 2.9. Stimulations and recordings for the Pavlovian threat conditioning task. The shock was delivered at the right extensor carpi radialis muscle, and spTMS was delivered over the left M1 to record MEP from the right FDI of participants. SCR was recorded from the palm of the left hand of participants.

Dependent variables

Skin conductance response (SCR). To obtain trough-to-peak SCR values to analyze differences in average conditioned SCR between CSs, the digitalized signal was processed using Autonomate 2.8 (Green et al., 2014). A SCR was considered valid if the trough-to-peak deflection started between 0.5–4.5 seconds following the CS onset, lasted for a maximum of 5 seconds, and was greater than 0.02 μS; trials that did not meet these criteria were scored as zero and retained for further analysis (Storm et al., 2001). To reduce the impact of individual differences in skin conductance response, within-participant z-scoring was performed on the raw SCRs using the average and standard deviation calculated across all CSs, separately for each participant and each phase (Boucsein et al., 2012; Lykken & Venables, 1971). Z-scored SCR amplitudes were then averaged for each CS and used for statistical analyses.

Corticospinal excitability. The EMG signal was preprocessed offline in MATLAB using custom made scripts. First, epochs from the time of the TMS pulse to 60 ms after it were extracted from the continuous data for MEP identification and analysis, and epochs from –100 ms to the time of the TMS pulse were extracted to identify any muscular preactivation, before TMS delivery. For each epoch, the min and max MATLAB functions were then used to determine the minimum and maximum peak in the EMG signal. The signal was then visually inspected to ensure the correctness of the automatic procedure. Muscular preactivations were defined as trials in which peaks of EMG activity in the 100 ms window preceding the TMS pulse exceeded 2 SD from the mean background EMG activity. MEPs preceded by such preactivation were discarded to prevent contamination of the MEP measurements (a total of 2.5% of MEPs in acquisition phase and 2.62% in reversal phase were excluded). This enabled the exclusion of any influence of participants' movement or muscle contraction on MEPs. For the remaining trials, individual peak-to peak MEP amplitudes (mV) were calculated and considered as a proxy for corticospinal excitability during threat acquisition and reversal. Then, MEPs' whose amplitude exceeded ± 2 SD of the mean amplitude for each experimental condition were excluded as outliers (CS-: 0.38%, CS+touch: 0.54%, CS+pain: 0.54% in total in acquisition phase; CS- and CS+pain: 0%, CS+touch: 0.36% in total in reversal phase). To control interindividual variability in MEP amplitudes, the raw MEP amplitudes were z-transformed using the average and standard deviation calculated across all CSs, separately for each participant and each

phase. Z-scored MEP amplitudes were then averaged for each CS and used for statistical analyses.

Explicit ratings. Participants' explicit ratings of CSs valence, CSs arousal, CSs-shock contingency for each CS, and US intensity for each US were used in statistical analyses to compare responses between CSs and USs.

Procedure

Participants were tested individually in a single experimental session lasting approximately two hours. They were comfortably seated in a silent room in front of a computer screen (size: 43 inches; resolution: 1920 × 1080 pixels; refresh rate: 60 Hz), at ~80 cm viewing distance. The shock intensities were calibrated, and baseline corticospinal excitability was measured. The Pavlovian threat acquisition and reversal phases followed; after each phase explicit learning was assessed. Finally, baseline corticospinal excitability was measured again. Participants were debriefed about the experimental hypotheses at the end of the whole experiment. A PC running the OpenSesame software (Mathôt et al., 2012) connected through a NI USB-6281 device (National Instruments, Austin, TX) to a BIOPAC MP-150 System (Goleta, CA), a Digitimer Stimulator (Model DS7A, Digitimer Ltd., UK), and Magstim Rapid2 stimulator (Magstim Co., Whitland, UK) controlled the f low of the experimental tasks, stimulations delivery and data recording.

Statistical analyses

Analyses were performed with JASP 0.16.3 (JASP Team, 2022). Repeated-measures ANOVA (rmANOVA) were used to investigate differences between more than 2 conditions, while paired t-tests were used to investigate differences between two conditions. For SCR, MEP, and explicit ratings data, the analysis considered CS (CS-, CS+touch, CS+pain) and Phase (acquisition , reversal) as within-subject factors. Polynomial and Helmert planned contrasts were adopted to test for differences among CSs (i.e., CS- vs. CS+touch, CS- vs. CS+pain, CS+touch vs. CS+pain) over phases (i.e., acquisition vs. reversal) conditions. Degrees of freedom and p-values were Greenhouse–Geisser corrected whenever a violation of the sphericity assumption occurred. Partial eta- squared (η^2_p) was computed as an estimate of

effect sizes for the rmANOVAs' main effects and interactions. A statistical significance threshold of $p<0.05$ was adopted for all analyses.

RESULTS

Explicit ratings

US intensity. The 2 (Phase: acquisition, reversal) x 2 (US: tactile, pain) rmANOVA on US intensity explicit rating showed a significant main effect of the US ($F_{(2,26)}=487.500$, $p<.001$, $n^2_p=0.949$), indicating that participants rated the painful US (M=7.327, SD=1.611) as more intense than the tactile US (M=1.482, SD=0.831), regardless of the phase. No other significant effect emerged (all $p\geq.187$).

CS valence. The 2 (Phase: acquisition, reversal) x 3 (CS: CS-, CS+touch, CS+pain) rmANOVA on CS valence showed a main effect of the CS ($F_{(1.58,42.66)}=60.247$, $p<.001$, $n^2_p=0.691$). Participants rated the CS+pain (M=2.357, SD=2.349) as less pleasant than the CS+touch (M=6.500, SD=2.571; $p<.001$), while no significant difference emerged between CS+touch and CS- (M=7.679, SD=2.729; $p=.073$). No other significant effect emerged (all $p\geq.546$).

CS-shock contingency. The 2 (Phase: acquisition, reversal) x 3 (CS: CS-, CS+touch, CS+pain) rmANOVA on CS-shock contingency showed a significant main effect of the CS ($F_{(1.30,34.97)}=88.251$, $p<.001$, $n^2_p=0.766$). Participants rated the CS+pain (M=7.786, SD=1.235) as more often associated with the shock compared to the CS+touch (M=5.339, SD=3.111; $p<.001$), which in turn was rated as more often associated with the shock than the CS- (M=0.625, SD=1.534; $p<.001$). No other significant effect emerged (all $p\geq.223$).

CS arousal. The 2 (Phase: acquisition, reversal) x 3 (CS: CS-, CS+touch, CS+pain) rmANOVA on CSs' arousal rating showed a significant Phase*CS interaction ($F_{(2,54)}=3.609$, $p=.034$, $n^2_p=0.118$). After both the acquisition and reversal phases, participants rated the CS+pain (acquisition: M=8.500, SD=1.319; reversal: M=8.929, SD=0.979) as more arousing than the CS+touch (acquisition: M=3.214, SD=2.025, $p<.001$; reversal: M=3.857, SD=2.155, $p<.001$), which in turn was more arousing than the CS- (acquisition: M=1.107, SD=1.729, $p<.001$; reversal: M=0.679, SD=1.188, $p<.001$). However, planned comparisons indicated that the

CS+touch was rated as more arousing after the reversal phase compared to the acquisition phase (p=.031), whereas no phase-related differences emerged for the CS+pain or CS- (all p≥.147).

Skin conductance response

A 2 (Phase: acquisition, reversal) x 3 (CS: CS-, CS+touch, CS+pain) rmANOVA and polynomial planned contrasts were performed to analyze differences in SCR as a function of CS type and phase. A significant Phase*CS interaction emerged ($F_{(1.60,35.20)}$=7.765, p=.003, n^2_p=0.261; Figure 2.10.A).

Polynomial contrasts conducted separately for the two phases revealed distinct trends in acquisition and reversal. In the acquisition phase, SCR showed a parabolic trend, with both the linear (p<.001) and quadratic (p=.006) trends being significant. SCR increased slightly from CS- (M =-0.204, SD=0.217) to CS+touch (M=-0.152, SD=0.159) followed by a steeper increase from CS+touch to CS+pain (M=0.356, SD=0.346). Indeed, repeated planned contrasts also showed that CS+pain significantly differed from CS+touch (p<.001), while CS- and CS+touch did not (p=.276). This pattern indicated that SCR peaked in the presence of CS+pain.

In contrast, in the reversal phase, only the linear trend was significant (p<.001), indicating a more gradual increase in SCR across CS- (M=-0.134, SD=0.197), CS+touch (M=-0.031, SD=0.190) and CS+pain (M=0.165, SD=0.308). This linear trend was reflected in an increase in SCR to CS+touch and a decrease in SCR to CS+pain from acquisition to reversal, such that CS+touch and CS+pain became more similar. Indeed, planned repeated contrasts showed that CS+pain and CS+touch did not differ significantly (p=.054), while CS- and CS+touch became significantly different (p=.042). Thus, the pronounced differences between the anticipation of touch versus pain observed during acquisition were attenuated during reversal, reflecting the influence of the learning established during acquisition over reversal.

Corticospinal excitability

A 2 (Phase: acquisition, reversal) x 3 (CS: CS-, CS+touch, CS+pain) rmANOVA and polynomial planned contrasts were performed to analyze differences in MEP amplitudes. A significant main effect of the CS emerged ($F_{(1.42,38.35)}$=6.000, p=.011, n^2_p=0.182; Figure 2.10.B). No other effect was significant (all p≥.328).

Polynomial contrasts showed a significant linear trend (p<.001), indicating a linear decrease in MEP amplitudes across CS- (M=0.124, SD=0.236), CS+touch (M=-0.012, SD=0.203) and CS+pain (M=-0.110, SD=0.282), regardless of the phase. Additionally, repeated planned contrasts showed that CS+pain did not differ significantly from CS+touch (p=.163), while CS- differed significantly from CS+touch (p=.005).

In contrast to SCR, which peaked with the CS+pain, these results suggest that CSE was modulated by the anticipated shock intensity, with higher intensities leading to increasingly reduced MEP amplitude. This occurred independently of the experimental phase, suggesting greater flexibility of the motor system in updating previously learned stimulus-outcome associations.

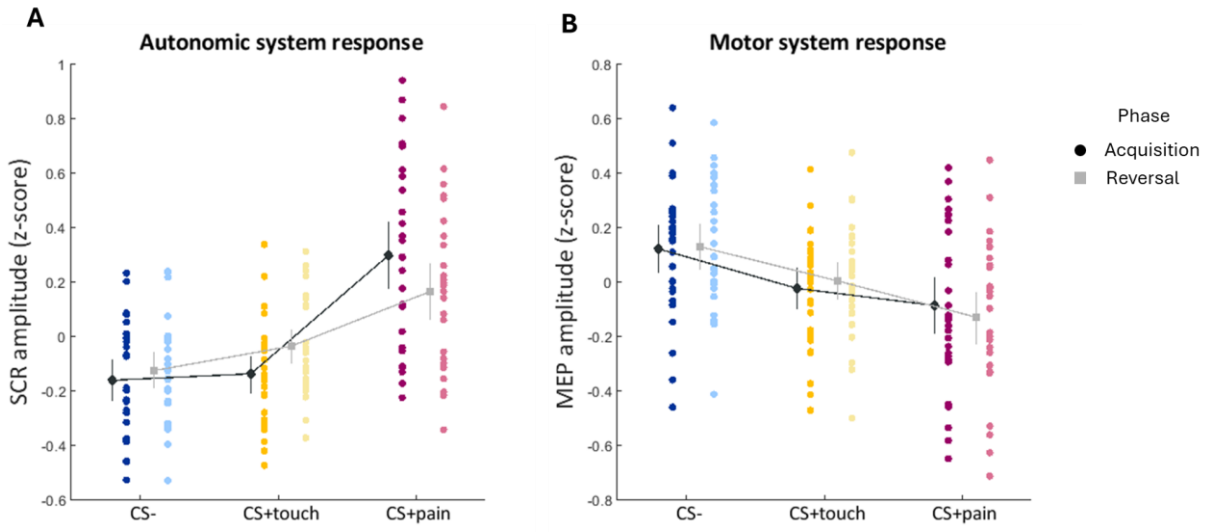

Figure 2.10. (**A**) Skin conductance responses (SCRs) of participants as a function of CS type and experimental phase, showing the quadratic trend of SCR increase during acquisition and the linear trend during reversal. (**B**) Motor evoked potentials (MEPs) of participants as a function of CS type and experimental phase, showing the linear trend of MEP reduction during both acquisition and reversal phases. Colored dots indicate single subjects' values in each experimental condition. Black dots and grey squares represent means, and vertical bars represent their standard error.

DISCUSSION

This study investigated how the autonomic and motor systems learn to differentially anticipate threatening painful stimuli and non-threatening tactile stimuli, and how they flexibly update their responses when stimuli contingencies change. To this end, SCRs and MEPs were recorded in a Pavlovian threat conditioning task that included an acquisition and a reversal phase to test the extent to which these systems track the affective-motivational versus sensory-discriminative dimensions of anticipated outcomes. Results showed a functional dissociation between the two systems. Both autonomic and motor responses scaled with the intensity of the predicted outcome, with painful stimuli eliciting stronger anticipatory responses than tactile ones and shock absence. However, the autonomic system was more closely tuned to the affective threat value of the predicted outcome, showing a response profile that peaked in anticipation of pain, with markedly weaker responses in anticipation of touch and shock absence. This tuning effect was attenuated during reversal, suggesting that autonomic responses were influenced by previously acquired learning and showed limited flexibility in updating. In contrast, the motor system showed a linear decrease of corticospinal excitability from shock absence to touch to pain anticipation, independent of the acquisition phase, indicating a more flexible response primarily driven by the sensory properties of the anticipated stimulus rather than its threat value.

The selective tuning of SCR on pain anticipation supports the idea that the autonomic system tracks the affective–motivational (threat) value of predicted outcomes (in line with Dalbagno et al., under review; Pool et al., 2019, 2023; Zhang et al., 2016). During acquisition, SCRs peaked in anticipation of pain compared to touch or shock absence, which elicited similarly low responses. Notably, this tuning on pain anticipation was attenuated during reversal, where the anticipatory response to pain and touch no longer differed from each other, reflecting both a decrease in responses to pain anticipation and an increase in responses to touch anticipation. The absence of significant differences during reversal suggests that autonomic responses may be more susceptible to the persistence of previously acquired learning and show limited flexibility in updating. Thus, while acquisition revealed a selective affective tuning, reversal highlighted the persistence of previously learned affective value on current responses. In the context of threat conditioning, such limited flexibility in response

updating of threat representations by the autonomic system may confer an adaptive advantage, as incorrectly identifying a safe stimulus as a dangerous stimulus is far less costly than the alternative. Nevertheless, this rigidity could contribute to the persistence of fear memories and pain responses, underlying the development of anxiety and pain disorders, even when the threat has resolved (Duits et al., 2015).

In contrast to the autonomic system, MEP results indicated that corticospinal excitability scaled linearly with the predicted intensity of outcomes, regardless of their threat value. During both acquisition and reversal, corticospinal inhibition increased progressively from shock absence to touch to pain anticipation, without showing the peak-like response pattern observed for SCRs. This response profile suggests that the motor system is primarily driven by the sensory–discriminative properties of anticipated outcomes rather than their affective–motivational value. Additionally, the consistency of this linear modulation across phases suggests that the response of the motor system is less affected by previous learning and more closely related to the current predictions of the sensory characteristics of the outcome. This aligns with the idea that corticospinal inhibition reflects anticipatory adjustments to expected sensorimotor demands rather than affective threat value.

Together, our findings highlight that complementary but functionally distinct learning systems learn to discriminate threat from safety. The autonomic system, reflected in SCRs, appears specialized to signal the affective–motivational significance of impending events, generating an affectively tuned response that prioritizes potential threats over innocuous stimulation, with limited flexibility in updating previously learned threat value. This may be adaptive to prioritize responding to the most urgent dangers, but at the cost of reduced flexibility when contingencies change. In contrast, the motor system encodes a graded, sensory-driven representation of the expected events, adjusting action readiness proportionally to stimulus intensity rather than its learned threat value (Betti et al., 2024). Such a representation may support flexible action preparation even when the affective meaning of cues changes. These functional differences highlight how different systems contribute to adaptive behavior: the autonomic system signals general motivational salience, preparing the organism for potential threat, whereas the motor system encodes detailed sensory predictions, guiding precise defensive actions. This distinction may also provide a framework for understanding maladaptive responses in both fear learning and chronic pain. Specifically, excessive

autonomic sensitivity to anticipated pain could contribute to hypervigilance and heightened affective responses in pain disorders, while altered motor encoding could affect adaptive defensive or protective actions.

CHAPTER 3:

LEARNING TO PREDICT PAIN LOCATION ON THE BODY

EXPERIMENT 3[2]

THEORETICAL BACKGROUND

The pain system is not only reactive but inherently predictive, enabling organisms to anticipate potential injury and prepare adaptive responses. To support adaptive behavior, it must predict not only the occurrence of pain (i.e., threat value) but also its specific features, such as bodily location (Seymour, 2019; Seymour & Dolan, 2013). Within this predictive coding framework, pain operates as a learning signal that drives the acquisition and updating of predictions about impending painful inputs, thereby promoting preemptive defensive responses aimed at reducing the risk of future injury (Song et al., 2021; Tabor & Burr, 2019).

Crucially, for the pain system to support adaptive responses, it must not only predict whether a painful stimulus will occur, i.e., threat versus safety discrimination, to support a general state of threat preparedness, but also its specific features, such as its location on the body, to select the appropriate actions that minimize harm (Cisek, 2021; Zhang et al., 2016). Yet, how the nervous system acquires, maintains, and updates such multiple, concurrent predictions about impending painful stimuli, such as both their potential occurrence and spatial attributes, remains poorly understood.

Previous studies have shown that learning to predict pain engages a distributed network of brain regions (Mano & Seymour, 2015; Tan & Kuner, 2021), alongside the autonomic nervous system (Colloca et al., 2006; Lang et al., 2000; Willer, 1975). Within this context, the skin conductance response (SCR) has been consistently shown to increase during pain anticipation, regardless of the pain's bodily location (Ojala & Bach, 2020; Zhang et al., 2016), thus reflecting

[2] Reference: Di Gregorio F.*, Betti S.*, Dalbagno D.*, Mannari V., di Pellegrino G., Starita F. (under review). Predictive encoding of pain location in the motor system indexed by somatomotor alpha and corticospinal excitability. *NeuroImage*.

a signal of general threat preparedness. More recently, corticospinal excitability has also been shown to decrease during pain anticipation contralaterally to the expected pain location (Betti et al., 2024), suggesting the encoding of spatial features of the pain, alongside threat. Together, these findings identify candidate neural and autonomic markers of pain predictions. However, it remains unclear how these markers differentially represent the general threat value of predicted pain versus its specific bodily location, and how they interact to support a unified anticipatory state of pain.

To address these questions, we adopted a multimodal approach that employed a combination of double-coil transcranial magnetic stimulation (TMS) and electrodermal activity (EDA) recordings to track the dynamic process by which the nervous system learns to predict limb-specific pain and updates such predictions following the reversal of pain-related spatial contingencies. In detail, a Pavlovian threat conditioning protocol was adopted in which, during acquisition, two different visual stimuli (e.g., colored dots) predicted pain either to the left (e.g., left conditioned stimulus, CS+L) or right (CS+R) arm, representing the threat conditions. Then, during reversal, the associations between the CS+ and the side of pain delivery were switched (i.e., reversal of the spatial pain contingencies). Another visual stimulus (CS-) never predicted pain and represented the within-subject safety control condition. Thus, our paradigm not only allowed us to examine how the nervous system acquires predictions about the spatial location of impending pain but also extended previous work by testing corticospinal excitability in both hemispheres. Indeed, while previous findings demonstrated contralateral inhibition during pain anticipation testing only in the dominant (left) hemisphere of right-handed participants (Betti et al., 2024), it remained unclear whether this effect generalizes to the non-dominant side. Moreover, by including a reversal phase, in which the spatial contingencies of pain were switched, we were able to directly probe the flexibility of these motor adaptations as the nervous system updates previously learned associations.

Based on previous literature, our investigation focused on changes in corticospinal excitability and skin conductance response to test whether they reflect the acquisition and updating of pain-related spatial features and their interaction. Given previous evidence and the lateralized and highly modular organization of sensorimotor circuits, with each module adapting distinct sensory inputs to motor outputs (Levine et al., 2012), we hypothesized that corticospinal inhibition would specifically encode the spatial properties of expected pain, thus mapping its

anticipated location on the body. In contrast, we hypothesized that the SCR would exhibit a more generalized threat response, without spatial specificity.

METHODS

Participants

Twenty-nine healthy volunteers (17 women, aged between 19 and 43 years, mean age 25.62 ± 6.1 years) participated in the experiment. All participants were right-handed, as assessed by the Edinburgh Handedness Inventory (Oldfield, 1971) and had normal or corrected-to-normal visual acuity. Based on self-report screening questionnaires, they had no contraindication to TMS stimulation (Rossi et al., 2021) nor neurological, psychiatric, or chronic medical condition. One participant was excluded from the final sample because of technical problems that occurred during data collection. The study was conducted in accordance with the Declaration of Helsinki and approved by the bioethics committee of the University of Bologna (protocol number 0290289). All participants were naïve to the purposes of the experiment and gave written informed consent to participate in the study.

Experimental task

Pavlovian threat acquisition and reversal task. The Pavlovian threat conditioning task included an acquisition and a reversal block. Stimuli and trial structure are illustrated in Figure 3.1. The stimuli consisted of three dots (64 pixels diameter) colored blue, pink or yellow (hex code: #5698D4, #C760CA and #F4E634, respectively). During acquisition, participants learned to identify two colored dots as dangerous (e.g. pink and yellow), representing the conditioned stimuli (i.e. CS+), such that their presentation terminated with an aversive shock (i.e. unconditioned stimulus, US) in 70% of the trials, delivered to participants' left (CS+L) or right (CS+R) forearm. During the reversal phase, the spatial contingencies of the CS+ and US were switched. For example, if during acquisition the pink dot was designated as CS+L and the yellow dot as CS+R, then in the reversal phase, the pink dot became CS+R, while the yellow dot became CS+L. A third dot (e.g., blue) served as a within-subject control stimulus (CS-), never being paired with shock at any point during the task.

On each trial, the CS appeared at the center of the computer screen for 4500 ms. Afterwards, two TMS pulses were administered for MEP registration over the left and right primary motor cortices, using a double-coil approach (Derosiere et al., 2020) such that two suprathreshold pulses were delivered within the same trial, using a 1-ms inter-pulse interval to induce the concurrent depolarization of both corticospinal pathways. In this way, independent MEPs were elicited bilaterally (Grandjean et al., 2018). Then, 60 ms after the double-coil TMS pulses, CS presentation was terminated, and, in designated CS+ trials, it co-terminated with a 2 ms shock. Thus, corticospinal excitability (CSE) was probed on each trial during CS presentation, before shock administration, to obtain a neurophysiological measure of shock prediction in the motor system. An inter-trial interval (ITI) of 8000-10000 ms followed, before the beginning of the next trial. The first three acquisition and reversal trials included the presentation of all CSs (CS+L, CS+R, CS-) in random order; with all CSs+ trials being reinforced with the shock. The remaining trials proceeded in pseudo-random order with no more than two consecutive CSs of the same type in a row. The three CSs were presented during the acquisition and reversal blocks for a total of 20 repetitions each (thus, 60 trials per block in total. Color assignment to each CS was counterbalanced among participants. A break between the acquisition and reversal blocks was given to participants to reduce fatigue.

At the end of the acquisition and reversal blocks, explicit learning was assessed by having participants rate the valence of each CS and the CS-shock contingency on a series of 11-point Likert scales (ranging from 0 to 10). The following two questions were answered regarding each CS, which was presented in random order: i) “The feeling I had when the circle was this color was” (Valence rating; ranging from 0=‘unpleasant’ to 10=‘pleasant’); ii) “ When the circle was this color, it gave me a shock on my left/right arm” (Contingency rating; from 0=‘never’ to 10=‘always’).

Participants were instructed to observe the screen and try to predict which color would give them the shock, while keeping their hands and arms relaxed, without executing any motor response. No information was provided regarding the specific color-shock contingencies and participants learned them through experience. A PC running the OpenSesame software (Mathôt et al., 2012), connected through a NI USB-6281 device (National Instruments, Austin, TX) to a BIOPAC MP-150 System (Goleta, CA), controlled the flow of the task.

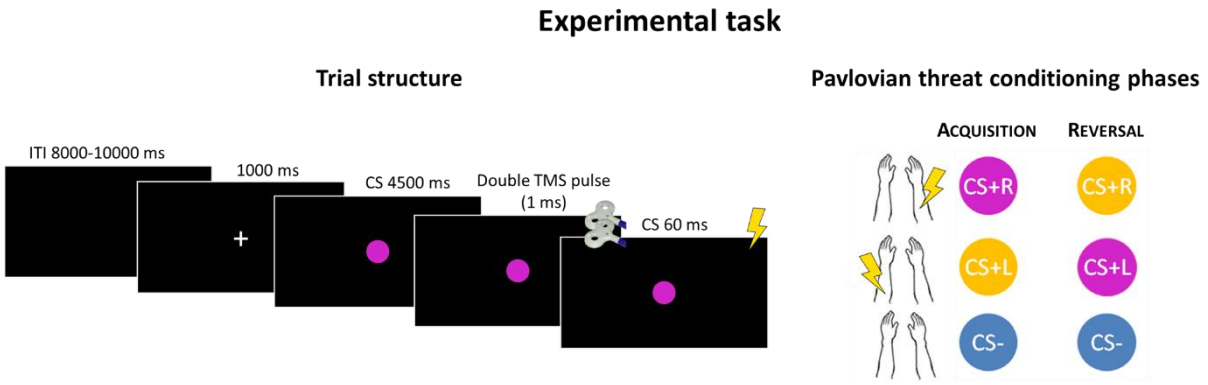

Figure 3.1. Illustration of the experimental task. On the left, the trial structure is represented. Conditioned stimuli (CSs) were presented for 4500 ms on the screen, then the double coil transcranial magnetic stimulation (TMS) was delivered on the left and right primary motor cortices, with 1 ms between the two pulses, to collect motor evoked potentials (MEPs) from the right and left FDI muscles. Skin conductance response (SCR) was continuously recorded from the palms of the left and right hands. Outcomes were delivered at the CS offset. On the right, the Pavlovian threat conditioning phases are represented. Three types of CSs were used: a CS+left associated with the painful shock on the left arm, a CS+right associated with the painful shock on the right arm, and a CS- never paired with any outcome.

Experimental procedures and psychophysiological recordings

Participants were tested individually in a single experimental session lasting approximately three hours. Participants were comfortably seated in a silent room in front of a computer screen (size: 43 inches; resolution: 1920 × 1080 pixels; refresh rate: 60 Hz), at a 57 cm viewing distance, and informed consent was collected. Then, EMG, EDA and shock electrodes were attached to the participants, and shock intensity was calibrated. After this, coil position and TMS stimulation intensity were determined, and baseline corticospinal excitability was measured. The Pavlovian threat conditioning task was then completed. Finally, baseline corticospinal excitability (CSE) was measured again to assess any basal change in CSE.

Painful electrotactile stimulation. The painful stimulation involved a 2 ms electrotactile shock generated by a Digitimer Stimulator (Model DS7A, Digitimer Ltd., UK) and delivered to the participants' left or right forearm, proximal to the extensor carpi radialis (ECR) muscle (see Figure 3.2), through pre-gelled Ag/AgCl electrodes (Friendship Medical, SEAg-S-15000/15x20). The shock intensity was calibrated using an ascending staircase procedure (Cornsweet, 1962; Klein, 2001). In detail, for each participant, the shock was set to a level deemed at the threshold between highly unpleasant and painful, such that participants would rather not

experience it if they knew it was coming, starting from 0 mA and increasing in 5 mA steps. When the participant reported that the shock intensity level was reached, they rated the shock on a Likert scale from 0 (no sensation) to 10 (intolerably painful). If a score of 8 was reported, that intensity was maintained for the experiment. If a lower score was reported, participants were asked if they were comfortable with increased intensity until reaching a score of 8 (see Betti et al., 2024). Stimuli did not exceed individual tolerance limits, in line with the International Association for the Study of Pain (IASP) guidelines (Charlton, 1995). This procedure resulted in a shock intensity of (mean±SD) 57.77±29.51 mA and 58.47±30.33 mA and a rating of 7.71±1.31 and 7.62±1.12 for the left and right forearm, respectively.

Double-coil transcranial magnetic stimulation. Double-coil TMS pulses were administered using two small 50 mm figure-of-eight coils, each connected to a Magstim monophasic stimulator (i.e., the coils stimulating the left and right hemispheres were connected to a Bistim2 and a 2002 magnetic stimulator, respectively; Magstim Co., Whitland, UK). On each experimental trial, two consecutive pulses (1 ms delay, see Derosiere et al., 2020; Grandjean et al., 2018) were delivered to the left and right primary motor cortex (M1) of the participant 60ms before CSs offset, in correspondence with the target muscle representations. This procedure enables the simultaneous assessment of bilateral changes in corticospinal excitability (Derosiere et al., 2020). Small coils were used so that they could be simultaneously placed on the M1 of each hemisphere (see Figure 3.2). The hemisphere receiving the first pulse was counterbalanced, so that in half of the trials it was the left and in the remaining half the right hemisphere.

For each M1, the optimal scalp position (OSP), that is the best position for the coil on the scalp at which the lower intensity of stimulation elicits the largest MEP in the target muscle, was determined by moving the coil in approximately 0.5 cm steps around the presumed hand motor area. Once found, the OSP for each hemisphere was then marked, ensuring correct coil placement throughout the experiment. For each participant, the resting motor threshold (rMT) was then determined by finding, in each hemisphere, the lowest stimulation intensity inducing MEPs with at least ≥ 50 mV peak-to-peak amplitude in a relaxed muscle in 5 out of 10 trials (Rossini et al., 1994). During the experiment, the intensity of TMS stimulation was set at 120% of the individual rMT to ensure a stable and reliable recording of cortical output while accounting for interindividual differences in cortical excitability (Di Lazzaro et al., 2004;

Rothwell, 1997), in accordance with established safety and methodological guidelines for non-invasive brain stimulation (Rossini et al., 2015). The rMT ranged from 45 to 92% (mean = 62.5%, SD = 9.8) of the maximum stimulator output for the left hemisphere and from 40 to 85% (mean = 57.6%, SD = 9.8) for the right hemisphere. The left- and right-hand MEPs recorded during the experiment were then preprocessed and analyzed as described in the statistical analysis section.

Before the beginning and at the end of the conditioning task, double-coil TMS stimulation was used to measure baseline corticospinal excitability by acquiring 15 MEPs (inter-pulse interval 9-10 s) while participants passively observed a fixation cross on a screen to exclude any non-specific, long-lasting changes in basal corticospinal excitability. No difference emerged when comparing MEPs recorded during the initial (left FDI: M=1.053, 95% confidence interval (CI) [0.83 1.28]; right FDI: M=1.096, CI [0.770 1.422]) and final (left FDI: M=1.198, 95% CI [0.99 1.41]; right FDI: M=1.148, 95% CI [0.86 1.44]) baseline phases (left FDI: t28=-1.913, p=0.07; right FDI: t28=-0.554, p=0.58;).

Electromyography recording. Surface EMG activity was recorded simultaneously from both hands for the left and right first dorsal interosseous (FDI) muscle, through two pairs of Ag/AgCl electrodes (BIOPAC EL501) placed in a belly-tendon montage connected to an EMG100C module of the BIOPAC MP-150 System (Goleta, CA). After skin preparation, a small amount of isotonic hyposaturated conductant gel (Lectron III Gel, NEUROSPEC) was added to the electrodes, which were placed and fixed on the target positions. The active electrode was placed over the muscle belly, determined by palpation during maximum voluntary contraction, the reference was placed over the proximal interphalangeal juncture and the ground electrode placed over the radial styloid process.

Electrodermal activity recording. Electrodermal activity was recorded at 5000 Hz, with a 10 Hz lowpass filter, from two pairs of Ag/AgCl electrodes (TSD203; BIOPAC Systems) filled with isotonic hyposaturated conductant gel (GEL101 model; BIOPAC System), attached to the hypothenar eminence of participants' left and right hands (see Figure 3.2), and connected to two EDA100C modules of the BIOPAC MP-150 System (Goleta, CA).

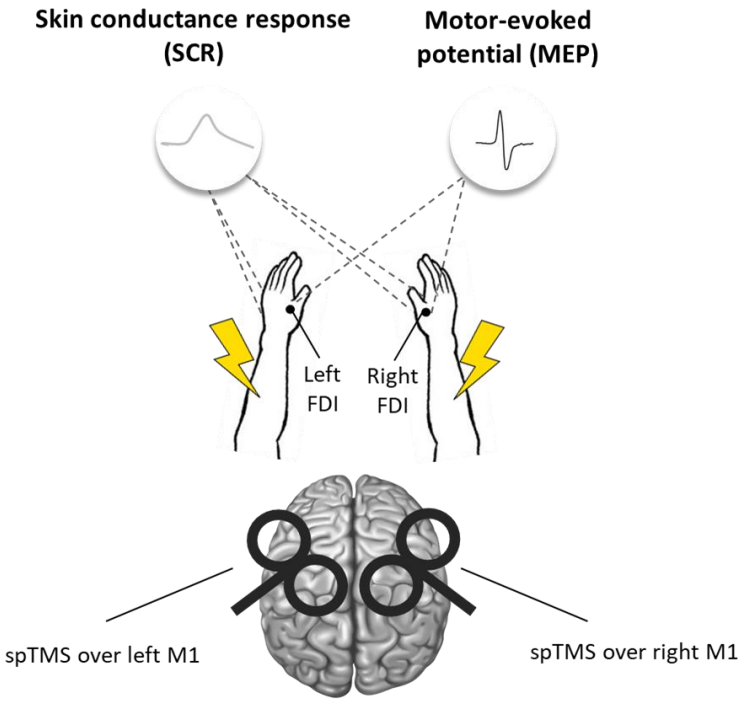

Figure 3.2. Stimulations and recordings for the Pavlovian threat conditioning task. The shock was delivered at the right and left extensor carpi radialis muscle, depending on the CS+ presented. SpTMS was delivered over the left and right M1 (with 1 ms in between) to record MEP from the right and left FDI of participants. SCR was recorded from the palms of both hands of participants.

Dependent variables and measures

Conditioned corticospinal response. EMG data were preprocessed offline in MATLAB using custom-made scripts. First, for MEP identification and analysis, epochs from the time of the TMS pulse to 60 ms after it were extracted from the continuous data, and epochs from –100 ms to the time of the TMS pulse were extracted to identify any muscular preactivation, before TMS delivery. For each epoch, the min and max MATLAB functions were then used to identify the minimum and maximum peaks in the EMG signal. The signal was then visually inspected to ensure the correctness of the automatic procedure. Muscular preactivations were defined as trials in which peaks of EMG activity in the 100 ms window preceding the TMS pulse exceeded 2 SD from the mean background EMG activity. MEPs preceded by such preactivation were discarded to prevent contamination of the MEP measurements (for the Acquisition and the Reversal phase, a total of 5% and 4.7% and 5.3% and 5.2% of MEPs were excluded for left and right FDI, respectively). For the remaining trials, individual peak-to-peak MEP amplitudes (mV) for the FDI muscle were calculated and considered as a proxy for corticospinal excitability

during threat learning. Then, MEPs' whose amplitude exceeded ± 2 SD of the mean amplitude for each experimental condition were excluded as outliers (Acquisition, CS-: 4.3% and 2.8%; CS+L: 4.0% and 3.3%; CS+R: 3.8% and 4.5%; Reversal, CS-: 4.5% and 4.1%; CS+L: 3.3% and 5.2%; CS+R: 4.1% and 3.6%, for left and right FDI, respectively). To control interindividual variability in MEP amplitudes, the raw MEP amplitudes were z-transformed using the average and standard deviation calculated on all CS conditions, separately for each participant and each muscle.

Conditioned skin conductance response. Skin conductance response (SCR) was assessed as it represents the most widely assessed conditioned response, with extensive literature showing that it increases for the CS+ presentation as compared to CS- (Lonsdorf et al., 2017). The digitalized electrodermal activity signal was processed using Autonomate 2.8 (Green et al., 2014) running in MATLAB (The Mathworks) to obtain trough-to-peak SCR values. The digitalized signal was down-sampled at 625 Hz, a SCR was considered valid if the trough-to-peak response occurred between 500 to 4500 ms following CS onset, lasted for a maximum of 5000 ms, and was greater than 0.02 µS. Raw SCR data were z-transformed and values exceeded ± 2 SD of the sample mean were excluded as outliers (Acquisition: CS-: 3.3% and 4.1%; CS+L: 4.7% and 4.3%; CS+R: 5.3% and 5.0%; Reversal: CS-: CS-: 2.6% and 2.9%; CS+L: 4.3% and 3.6%; CS+R: 4.5% and 5.2%; for the left and right hand, respectively).

Explicit ratings. Participants' explicit ratings of CSs valence and CSs-shock contingency for each CS were used in statistical analyses to compare responses between CSs after both the acquisition and the reversal block.

Statistical analyses

All the analyses were performed with JASP 0.16.3 (JASP Team, 2022). Repeated-measures analyses of variance (RM ANOVA) were used to investigate differences between more than two conditions, followed by planned contrasts in case of significant main effects or interactions. Degrees of freedom and p-values were Greenhouse–Geisser corrected; whenever a violation of the sphericity assumption occurred, corrected p-values will be reported alongside uncorrected degrees of freedom. Partial eta-squared (η^2_p) was computed as an estimate of effect sizes for the ANOVAs' main effects and interaction. A statistical significance threshold of $p < 0.05$ was adopted for all analyses.

RESULTS

Explicit ratings

CS-US contingency. The 3 (CS: CS-, CS+L, CS+R) *2 (Block: Acquisition, Reversal) *2 (Side: left, right) rmANOVA on the CS-US contingency ratings showed a significant CS*Side interaction effect ($F_{(1.23,34.56)}$=598.295, p<.001, $\eta 2_p$=.955), meaning that the CS+left was associated with the shock delivered on the left (M=7.741, SD=1.628) but not the right (M=0.517, SD=1.636; p<.001) arm, the CS+right was associated with the shock delivered on the right (M=8.034, SD=1.184) but not the left (M=0.500, SD=1.668; p<.001) arm, more than CS- (left: M=0.596, SD=1.731; right: M=0.500, SD=1.592; all p<.001), independently on the phase.

CS valence. The 3 (CS: CS-, CS+L, CS+R) *2 (Block: Acquisition, Reversal) rmANOVA on the CSs valence ratings showed a significant main effect of the factor CS ($F_{(1.23,34.52)}$=58.783, p<.001, $\eta 2_p$=.667), meaning that the CS- (M=2.362, SD=1.935) was rated as more pleasant than the CS+left (M=6.448, SD=2.226; p<.001) and the CS+right (M=2.431, SD=2.303; p<.001), independently on the phase, while no difference emerged between the CSs+ (p=.874). Moreover, a significant main effect of the factor Phase ($F_{(1,28)}$=4.723, p=.038, η^2_p=.144), revealing that ratings in the acquisition phase (M=4.046, SD=2.921) were higher compared to ratings in the reversal phase (M=3.448, SD=2.819).

Conditioned skin conductance response

The 3 (CS: CS-, CS+L, CS+R) *2 (Phase: Acquisition, Reversal) *2 (Hand: right, left) rmANOVA on SCRs revealed a main effect of CS ($F_{(2, 44)}$=4.046, p=.024, η^2p=0.155; Figure 3.3.A). Planned contrasts showed greater responses for CS+left (M=0.029, SD=0.184) and for the CS+right (M=0.060, SD=0.190) compared to the CS- (M=-0.090, SD=0.209; p=.046 and p=.009 respectively), while responses to CS+L and CS+R did not differ (p=.504), independent of block or hand. No other significant effects emerged (all p>.248). These results indicate that SCR reflected the prediction of pain occurrence but was not sensitive to the lateralized location of the stimulus or to changes in spatial contingencies during reversal.

Conditioned corticospinal response

The 3 (CS: CS-, CS+L, CS+R) *2 (Phase: Acquisition, Reversal) *2 (Hand: right, left) rmANOVA on MEPs showed a significant main effect of CS ($F_{(1.46, 40.96)}$=10.08, p<.001, η^2_p=0.265; Figure 3.3.B), with greater corticospinal inhibition (i.e., reduced MEPs amplitude) for CS+ compared to CS-, independently of the phase and the hand. Crucially, the CS*Hand interaction was also significant ($F_{(1.6, 44.5)}$=21.18, p<.001, η^2p=0.43), with a greater MEPs amplitude reduction of left FDI in presence of the CS+left (M=-0.220, SD=0.252) compared to the CS+right (M=0.091, SD=0.235; p<.001) and the CS- (M=0.121, SD=0.259; p<.001) which did not differ (p=.682), and a greater MEPs amplitude reduction of right FDI in presence of the CS+right (M=-0.165, SD=0.292) compared to the CS+left (M=-0.017, SD=0.224; p<.001) which in turn was greater than the CS- (M=0.173, SD=0.312; p=.008), independent of acquisition or reversal phase. No other significant effects emerged (all p>.185). Thus, corticospinal inhibition reflected pain prediction, tuned to the expected location on the body.

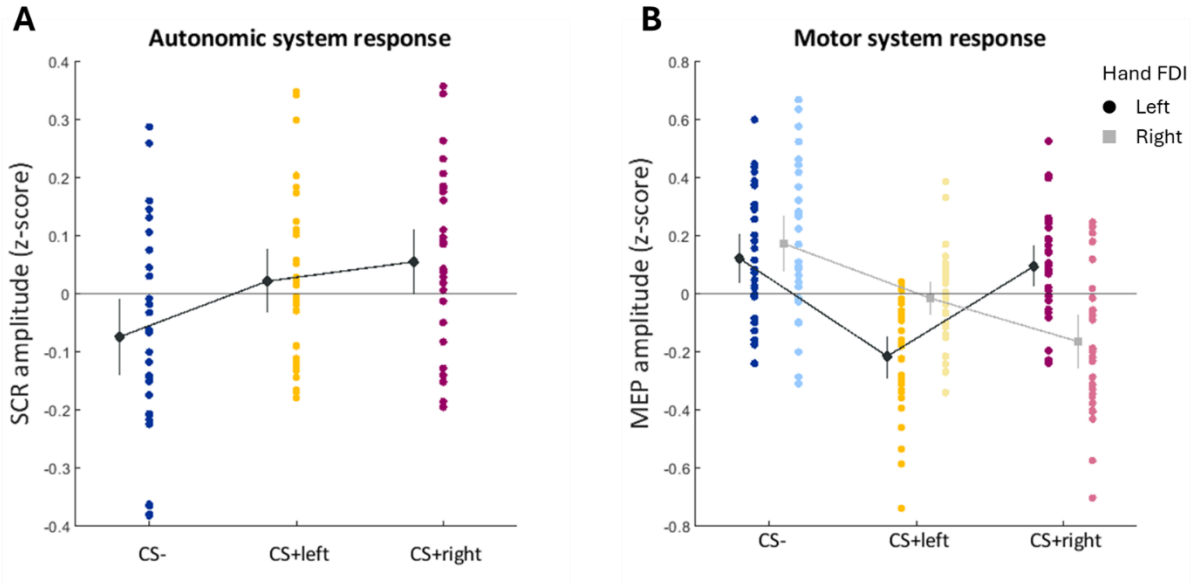

Figure 3.3. (**A**) Skin conductance responses (SCRs) of participants as a function of CS type, showing the SCR increase in the presence of the CSs+ compared to the CS-. (**B**) Motor evoked potentials (MEPs) of participants as a function of CS type and hand laterality, showing the reduction of MEP amplitude of left FDI in the presence of the CS+left, and the reduction of MEP amplitude of right FDI in the presence of the CS+right. Black dots and grey squares represent means, and vertical bars represent their standard error.

DISCUSSION

This study investigated the neural mechanisms underlying pain prediction, focusing on how the brain learns and updates expectations about the spatial location of pain on the body. Using a Pavlovian threat conditioning paradigm with lateralized pain stimuli, we combined skin conductance and corticospinal excitability to examine autonomic and motor system contributions to pain anticipation. Our findings revealed dissociable yet complementary systems for pain anticipation in the human nervous system. While SCRs, reflecting sympathetic activation, encoded the general threat value of impending pain, corticospinal excitability was spatially tuned, selectively tracking the body location where pain was expected. This dissociation highlights the coexistence of a general threat preparedness system and a spatially specific predictive system supporting motor readiness.

First, we found that skin conductance responses (SCRs), reflecting autonomic nervous system activity, reliably encoded the impending occurrence of pain, as shown by their increased amplitude during anticipation. This result is consistent with previous research (Betti et al., 2024; Lonsdorf et al., 2017; Zhang et al., 2016) and confirms the effectiveness of our paradigm in eliciting anticipatory responses. However, SCRs did not differentiate between pain locations on the body or adapt to changes in spatial pain contingencies during reversal. While previous literature has demonstrated the sensitivity of SCRs to changes in the motivational significance of stimuli, for instance, when formerly threatening cues become safety cues (i.e., CS+ to CS- reversal), our study presented a unique scenario. Here, both CSs+ remained aversive during reversal but differed only in predicted pain location, and SCRs showed no corresponding modulation. This suggests that while SCRs predict the motivational, general threat value of impending stimuli, they do not represent their specific spatial characteristics. These findings align with prior work (Zhang et al., 2016), reinforcing the view that autonomic nervous system activity primarily reflects a general state of preparedness to the impending threat, rather than encoding its detailed sensory features.

In contrast to the general autonomic response, corticospinal excitability showed precise spatial tuning during pain anticipation. Specifically, corticospinal inhibition occurred in the hemisphere contralateral to the predicted pain location, directly reflecting the side of the body where pain was expected. These results advance prior research (Betti et al., 2024;

Starita, Pirazzini, et al., 2023), confirming the role of this neural marker in pain anticipation not only in the dominant hemisphere but in both hemispheres with a specific accuracy. In our experimental task, where participants could not avoid the pain, the reduction of corticospinal excitability may be functional to prevent movements that could aggravate the impending pain. Our findings extend previous neuroimaging and electrophysiological work demonstrating motor area engagement in the anticipation of painful events (Fullana et al., 2016; Pirazzini et al., 2023; Starita, Pirazzini, et al., 2023a; Wen et al., 2024; Zhang et al., 2016). Crucially, the present results suggest that this anticipatory activity reflects the formation of a fine-grained, somatotopically organized motor representation of expected pain, which emerges even in the absence of any overt motor requirement.

The different modulation of SCRs and corticospinal excitability supports the view that Pavlovian threat conditioning engages multiple systems, each responsible for distinct classes of conditioned responses. Some responses (also known as consummatory responses) are outcome-specific, encoding the sensory properties of the expected event, such as its bodily location, while others are more general, encoding only its motivational value, such as its aversive quality (Dickinson & Balleine, 2002; Pool et al., 2019; Rangel et al., 2008; Zhang et al., 2016). In this regard, our results corroborate the preparatory nature of SCRs, which were not sensitive to shock laterality. Crucially, they also advance the understanding of consummatory responses, extending their neural correlates (Zhang et al., 2016) to the cortical motor system. Corticospinal inhibition was side-congruent to the expected shock and tuned to its position on the hand or forearm. The somatotopic-like modulation of the conditioned corticospinal inhibition suggests that consummatory responses encode a significantly more detailed representation of the sensory properties of the outcome than previously known in humans.

The findings of this study have significant implications for understanding pain processing in both healthy and pathological states. By identifying corticospinal excitability as a neural marker of pain-related spatial features, our work opens the way to a deeper understanding of the neural basis of pain localization. This knowledge could inform therapeutic approaches for maladaptive pain responses, particularly in chronic pain conditions where the flexibility of predictive models may be compromised. Future research is warranted to explore how individual differences in pain sensitivity or anxiety influence these neural markers of pain anticipation. Importantly, investigating how these dynamic mechanisms are altered in clinical

populations could provide further insight into the neurobiological underpinnings of chronic pain and identify potential targets for intervention.

In conclusion, the present study advances the understanding of pain processing, providing evidence for the predictive nature of the pain system and highlighting its capacity for flexible learning in an ever-changing environment. Our results show that the pain system not only predicts the imminent occurrence of pain but also its specific features, such as its location on the body. This is achieved through parallel predictive signals from both the autonomic and central nervous systems. The autonomic system contributes to a general state of threat anticipation, predicting the possibility of injury. In contrast, the corticospinal system supports predictions of specific spatial features of the expected pain.

CHAPTER 4:

LEARNING THE TIME OF PAIN IN THE HUMAN MOTOR SYSTEM

EXPERIMENTS 4 AND 5[3]

THEORETICAL BACKGROUND

Despite the intimate relationship between pain and motor processes (Seymour & Mancini, 2020), current models of pain still suggest that pain-related motor responses follow pain perception, which is itself triggered by painful stimulation (Chen & Wang, 2023). In fact, we have recently shown that pain-related motor changes can precede a pain percept. Specifically, as healthy humans learn that visual stimuli predict the occurrence of painful shocks, the mere threat of pain, cued by the presence of the visual stimuli, is sufficient to reduce corticospinal excitability, immediately before (i.e. 60ms) shock occurrence (Betti et al., 2024). Nevertheless, the functional role of such corticospinal inhibition during pain anticipation remains unexplored.

Importantly, as organisms learn which stimuli in the environment predict pain, they also learn about the timing of that pain (Kirkpatrick & Balsam, 2016; Nasser & Delamater, 2016). Indeed, the capacity to accurately time defensive responses is crucial for survival. In this regard, the motor cortex is known for its role in event and interval timing and temporal learning, being engaged not only in time perception but also in timed behavior (Coull & Nobre, 2008; Halsband et al., 1993; Lucchetti et al., 2005; Merchant & Yarrow, 2016; Roux et al., 2003). Considering this evidence, here, we test whether the motor system learns the time of pain and thus, whether the inhibition of the motor system under threat of pain (Betti et al., 2024) is bound to the time of pain occurrence.

[3] Reference: Dalbagno D., Betti S., Garofalo S., Mannari V., di Pellegrino G., Starita F. (2025). Learning the time of pain in the human motor system. *PAIN*. DOI: 10.1097/j.pain.0000000000003730.

To this end, we conducted two experiments: the first aimed at testing our main hypotheses, and the second designed to exclude any effects of task structure that could have confounded the results of the first experiment. In both experiments, we applied single-pulse TMS (spTMS) over the primary motor cortex (M1), during a Pavlovian threat conditioning task in which we manipulated the temporal imminence of pain (Betti et al., 2025; Fanselow et al., 1988; Mobbs et al., 2020). Thus, corticospinal excitability was probed while participants learned that initially neutral visual stimuli predicted pain early, i.e. conditioned stimulus early (CS+early) or later, i.e. conditioned stimulus late (CS+late), after their appearance (see Figure 5.1). Such manipulation enabled us to test corticospinal excitability at three critical timepoints during the threat of pain, marked by CS+ presentation (see Figure 5.1). In detail, two timepoints occurred during the pain anticipation interval, namely at the time long before and immediately before pain, and one timepoint occurred long after the time of pain had passed. Note that, in both experiments, we expected to replicate the reduction in corticospinal excitability immediately before pain occurrence during CS+late presentation, in line with our previous findings (Betti et al., 2024). Notably, in that study corticospinal excitability was probed at a late time window after CS+ onset, i.e. >4000 ms. However, to ensure survival, motor reactivity should be tightly coupled with visual processing (LeDoux & Daw, 2018) and thus we also expected a reduction in corticospinal excitability immediately before pain occurrence for the CS+early, i.e. <1700 ms.

Crucially, we formulated three a-priori hypotheses about the modulations of motor system excitability during the task (see Figure 5.1), inspired by the different brain activity patterns found to be associated with processing time (Tallot & Doyère, 2020). The first hypothesis (H1) the *phasic inhibition hypothesis*, posits that the motor system specifically encodes the precise timing of the painful event. Under this hypothesis, the reduction in corticospinal excitability is observable exclusively immediately before the time of pain occurrence, but not long before or after it. The second hypothesis (H2), the *sustained inhibition throughout pain anticipation hypothesis*, posits that the motor system encodes the time interval elapsed between threat appearance and pain occurrence, discriminating the interval before from that after the time of pain. Under this hypothesis, the reduction in corticospinal excitability starts at threat appearance and is maintained until the time of pain (i.e. immediately before the expected pain for the CS+early and both long and immediately before pain for the CS+late), but recovers

once the time of pain has passed (i.e. long after pain for CS+early). The third hypothesis (H3), the *sustained inhibition throughout threat of pain hypothesis*, posits that the motor system encodes only the presence of a threat, without encoding the time of pain associated with that threat. Under this hypothesis, the reduction in corticospinal excitability occurs throughout the presentation of the threat (i.e. for both CS+early and CS+late), regardless of the actual time of pain.

Pain processing occurs under the influence of cognitive, affective, and dispositional factors (Khera & Rangasamy, 2021; Tyng et al., 2017). Nevertheless, the relationship between these factors and neurophysiological responses remains poorly understood. Thus, in both experiments, participants also performed a time interval reproduction task, after completing the Pavlovian threat conditioning task, to measure their subjective estimate of the time interval between the CSs+ appearance and shock occurrence. Crucially, such subjective estimates were used to explore their correlations with the changes in corticospinal excitability, assessed during threat conditioning. Understanding the psychophysiological mechanisms underlying pain is essential to advance our knowledge of pain processes in both healthy individuals and those with pain-related disorders. Indeed, pain perception may not only be the result of the pain itself but also of maladaptive predictions about it (Vlaeyen & Linton, 2000).

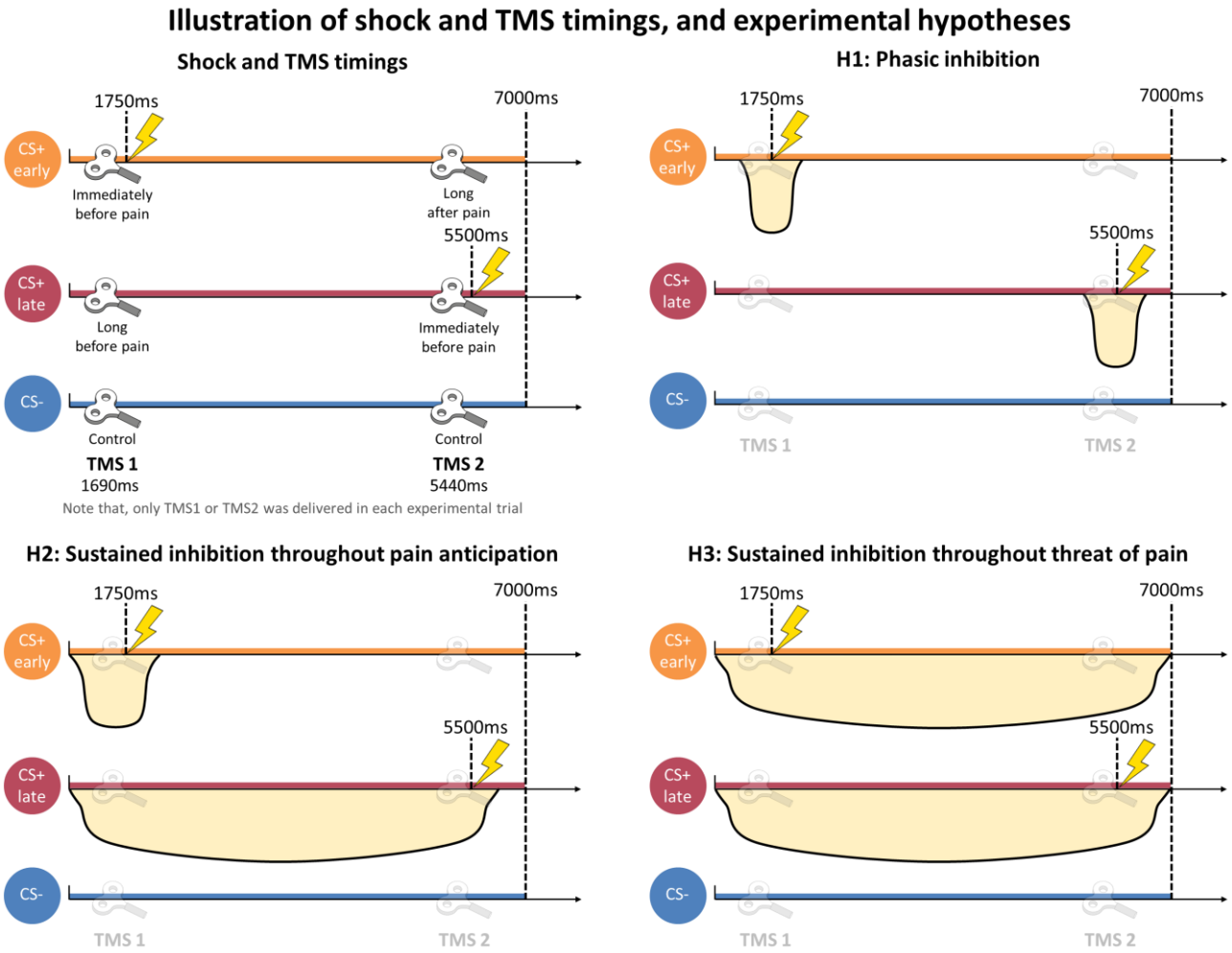

Figure 5.1. Illustration of shock and TMS timings, and experimental hypotheses. Shock and TMS timings. Timings of electrotactile shocks and TMS pulses used in the Pavlovian threat conditioning task during the presentation of each conditioned stimulus (CS) are represented. Experimental hypotheses. Graphical representation of the three experimental hypotheses regarding corticospinal excitability under threat of pain. H1: phasic inhibition hypothesis; H2: sustained inhibition throughout pain anticipation hypothesis; H3: Sustained inhibition throughout threat of pain hypothesis. The yellow curved dips indicate when the reduction in corticospinal excitability is expected under each hypothesis.

METHODS

Experiment 4

Participants

A total of thirty healthy adult volunteers participated in the experiment. Two of them were excluded from data analysis due to a difference in baseline amplitude of MEPs recorded before and after the conditioning task (see ”Transcranial magnetic stimulation” section below)

which could have compromised the integrity of the results of the conditioning task (although additional analyses confirmed that their exclusion did not affect the overall findings). Thus, data from twenty-eight participants (14 female, aged between 19 and 29 years: mean (M) = 25, standard deviation (SD) = 2.973) were included in the data analysis. The sample size was calculated through a power analysis conducted with MorePower 6.0.4 (Campbell & Thompson, 2012) with the following parameters: Analysis: ANOVA; Design factors: repeated measures 3 (CS: CS+early, CS+late, CS-) x 2 (Timing TMS: early, late); Effect of interest: 3x2; Alpha: 0.05; Power: 0.8 (partial eta = 0.17, Cohen's f = 0.45). The effect size was based on the effect size found in our previous study (Betti et al., 2024). All participants were right-handed, as assessed by the Edinburgh Handedness Inventory (Oldfield, 1971), with normal or corrected-to-normal visual acuity. They were all screened for TMS exclusion criteria to exclude any history of head trauma or head surgery, seizures, family history of epilepsy, implanted hardware, medications, and neurological and medical illnesses, according to safety guidelines (Rossi et al., 2009, 2021). Also, participants had no current neurological or psychiatric diagnosis or chronic medical condition, as well as no recent history of trauma affecting the upper limbs, nor were they currently suffering from any pain or taking any analgesic medication. The study followed the American Psychological Association Ethical Principles of Psychologists and Code of Conduct and the Declaration of Helsinki and was approved by the Bioethics Committee of the University of Bologna (protocol number 224364). All participants were naïve to the purposes of the experiment and gave their written informed consent for their participation.

Experimental task

Pavlovian threat conditioning task. Participants completed a Pavlovian threat conditioning task (Mathôt et al., 2012), during which they learned the association between three visual stimuli and their respective outcomes (Figure 5.2). The three visual stimuli were filled colored circles (64 pixels diameter, blue #5698D4, pink #C760CA, or yellow #F4E634), representing the three different conditioned stimuli (CSs). Two of them were CSs+ associated with the delivery of an electrotactile shock to the right forearm, while the other was a CS- never associated with shock.

In each experimental trial, one of the CSs appeared in the center of a computer screen on a black background for 7000 ms. Crucially, the two CSs+ differed in the timing of shock delivery, specifically, for the CS+early the shock occurred 1750 ms after CS onset, while for the CS+late the shock occurred 5500 ms after CS onset. The inter-trial interval (ITI) was jittered between 8-9 s, and before the beginning of each trial, a white fixation cross was presented for 1 s in the center of the screen. Each CS was presented 46 times, for a total of 138 trials. For each CS+, the shock occurred in 28 trials (i.e., 61% reinforcement rate). Having a partial reinforcement enabled us to verify that the modulations of corticospinal excitability were bound to the time of shock, rather than to its occurrence (or non-occurrence), as highlighted in the results. The first three trials consisted of the presentation of a CS-, a reinforced CS+early, and a reinforced CS+late, in random order, while the TMS pulse was never delivered to facilitate the understanding of the CS-shock contingency. The remaining trials proceeded in pseudo-random order with no more than two consecutive CSs of the same type in a row. The task was divided into two blocks, with a one-minute break between blocks to reduce participants' fatigue. Color assignment to each CS was counterbalanced among participants.

Before beginning the task, participants were instructed as follows: "You will see a colored circle appearing on the screen. Sometimes, the circle may deliver a shock on your arm. Your task is to understand with which color and when the circle gives you the shock". Note that no information was provided regarding the shock-time-CS contingency, and participants had to learn this through experience. In addition, they were instructed to observe the screen throughout the task while keeping their hands and arms relaxed, without executing any motor response. During the task, corticospinal excitability was probed during CS presentation by delivering single pulse TMS, as detailed in the transcranial magnetic stimulation section below.

At the end of the task, explicit learning was assessed by having participants rate the valence and arousal of each CS and the CS-shock contingency on a series of 11-point Likert scales (ranging from 0 to 10). The following three questions were answered regarding each CS, presented in random order: i) "When I saw this circle, the feeling I had was" (Valence rating; ranging from 0='unpleasant' to 10='pleasant'); ii) "Seeing this circle was" (Arousal rating; ranging from 0='not activating at all' to 10='extremely activating'); iii) "This circle gave me the shock" (Contingency rating; from 0='never' to 10='always'). This task was pre-registered at *https://osf.io/z26a4*.

Time interval reproduction task. To assess learning of the timing of shock delivery for each CS+, participants performed an interval reproduction task, in which they reproduced the time elapsed between the CS+ appearance and shock occurrence (Figure 5.2). Thus, in each trial, a CS+ appeared in the center of the screen until the participant pressed the space bar on the computer keyboard, to indicate their subjective estimation of the time of shock occurrence and end CS+ presentation. Spacebar pressing was required only to end the presentation of the CS+, while the CS+ appearance was computer-generated (a similar approach to (Mioni et al., 2014)). Each CS+ was presented for 5 trials, in random order followed by a jittered 8-9 s ITI (steps of 500 ms), then a 1 s fixation cross was presented in the center of the screen before the next CS+ appearance. No shock was delivered during this task.

Given the novelty of the paradigm, and the fact that delivering the TMS pulse during CS presentation prevented the artifact-free recording of psychophysiological measures typical of conditioning paradigms (e.g., skin conductance response (Lonsdorf et al., 2017), we conducted a preliminary validation experiment to ensure the suitability of the task in inducing a well-established conditioned response in participants and learning of CS-US time intervals. In particular, skin conductance response was assessed as a reliable and validated measure of conditioning (Bauer et al., 2022; Lonsdorf et al., 2017), as well as explicit ratings. The results of this validation experiment are reported in the “Task validation experiment” paragraph below. Briefly, they support the validity of our paradigm in inducing the acquisition of threat conditioning, showing an increase in skin conductance response (SCR) during the presentation of both CS+early and CS+late, as compared to CS-.

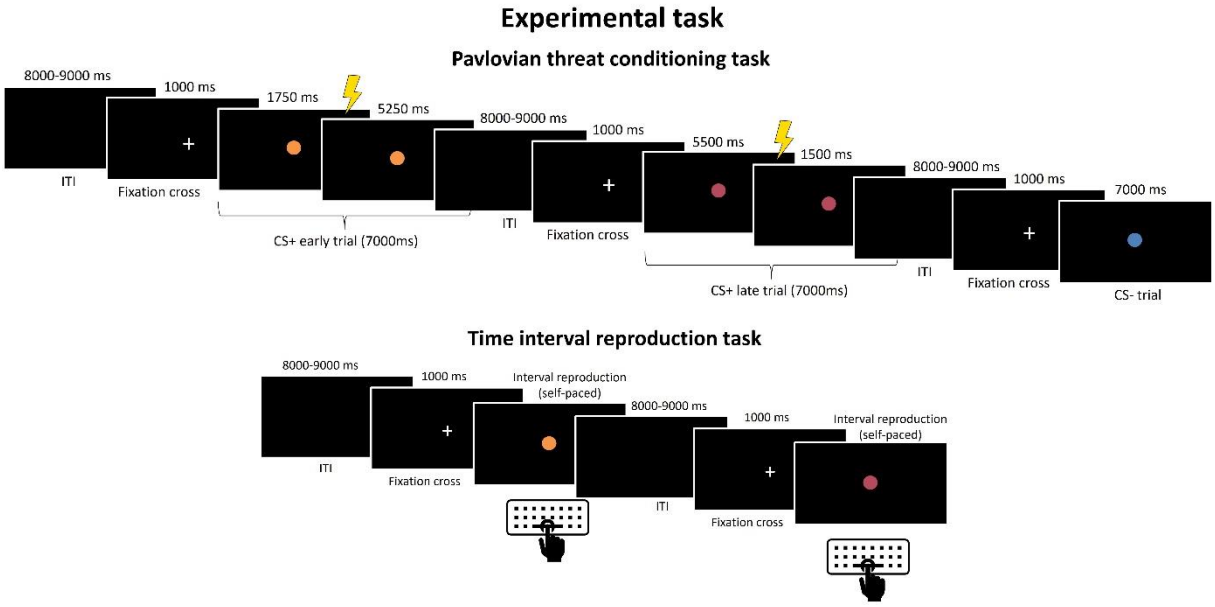

Figure 5.2. Experimental task. Pavlovian threat conditioning task. The trial structure is represented. Three types of CS, presented for 7000 ms each one, were used: a CS+early associated with shock delivered 1750 ms after stimulus onset (60 ms after TMS 1), a CS+late which was associated with shock delivered 5500 ms after stimulus onset (60 ms after TMS 2), and a CS- never paired with shock. Time interval reproduction task. A CS+ appeared until participants pressed the keyboard space bar, indicating their time estimate of shock occurrence and ending the CS+ reproduction.

Stimulations and recordings for the Pavlovian threat conditioning task

The experimental setup for the Pavlovian threat conditioning task (Figure 5.3) included the delivery of painful electrotactile stimulations (shocks) over the participant's right forearm. Additionally, in each trial, TMS pulses were delivered over the left primary motor cortex (M1), while electromyography was recorded continuously from the first dorsal interosseus (FDI) muscle of the right hand.

Painful electrotactile stimulation. The painful stimulation consisted of a 2 ms electrotactile shock generated by a Digitimer Stimulator (Model DS7A, Digitimer Ltd., UK) and delivered to the participant's right forearm proximal to the extensor carpi radial muscle, through pre-gelled Ag/AgCl snapped electrodes (Friendship Medical, SEAg-S-15000/15x20). The shock intensity (M=55.00 mA, SD=7.07) was calibrated for each participant to a level deemed "at the threshold between highly unpleasant and painful, to the point that if they knew it was coming, they would prefer not to experience it" using an ascending staircase procedure (Cornsweet, 1962; Klein, 2001). When the participant reported that the stimulation intensity level was

reached, they rated the shock on a scale ranging from 0 (no sensation) to 10 *(*untolerable pain), aiming for a rating of 8, both before (M=7.889, SD=0.424) and after the conditioning task (M=7.417, SD=1.248) to confirm the maintenance of the aversive value of the shock (Bayesian paired sample t-test BF_{10}=1.189; err%=0.022). Stimuli did not exceed individual tolerance limits, in line with the International Association for the Study of Pain (IASP) guidelines (Charlton, 1995).

Transcranial magnetic stimulation (TMS). Single-pulse TMS was administered using a 70 mm figure-of-eight coil connected to a Magstim Magstim Rapid^2 stimulator (Magstim Co., Whitland, UK). Pulses were delivered to the left primary motor cortex (M1) of the participant, in correspondence with the FDI muscle representation. The coil was placed on the head at a 45-degree angle relative to the interhemispheric fissure, with the handle pointing laterally and caudally (Brasil-Neto et al., 1992; Mills et al., 1992). Then, to find the FDI muscle representation, the best position for the coil on the scalp at which the lower stimulation intensity elicits the largest MEP, i.e. optimal scalp position, was determined by moving the coil in approximately 0.5 cm steps around the presumed hand motor area. The position was then marked on a tight-fitting cap worn by the participants, ensuring a correct coil placement throughout the experiment. For each participant, the resting motor threshold (rMT) was then determined by finding the lowest stimulation intensity inducing MEPs with at least ≥ 50 mV peak-to-peak amplitude in a relaxed muscle in 5 out of 10 trials (Rossini et al., 1994). During the experiment, the intensity of TMS stimulation was set at 120% of the individual rMT to ensure a stable and reliable recording of cortical output while accounting for interindividual differences in cortical excitability (Di Lazzaro et al., 2004; Rothwell, 1997), in accordance with established safety and methodological guidelines for non-invasive brain stimulation (Rossini et al., 2015). The rMT ranged from 56 to 83% (mean=71.25%, SD=11.148) of the maximum stimulator output.

Corticospinal excitability was probed by delivering single pulse TMS 1690 ms (i.e. TMS 1) or 5440 ms (i.e. TMS 2) after CS onset (see Figure 5.1). The timing of the TMS pulse was selected to probe corticospinal excitability at specific moments relative to the time of shock. Specifically, corticospinal excitability was probed immediately before the time of shock (i.e., 60 ms before) when TMS 1 was delivered during CS+early trials and when TMS 2 was delivered during CS+late trials. At the same time, these timings also enabled us to probe corticospinal

excitability long before (i.e., 3810 ms) and long after (i.e., 3790 ms) the time of shock, corresponding to TMS 1 in CS+late trials and TMS 2 in CS+early trials, respectively. The same TMS 1 and TMS 2 timings were applied in CS- trials as a control comparison. Also, the timing of TMS 2 ensured that 3750 ms had passed since the shock delivered in CS+early reinforced trials, ruling out the possibility that any observed changes in corticospinal excitability were due to the shock itself. Indeed, previous studies have shown that modulations of corticospinal excitability in response to painful electrotactile (Clouston et al., 1995; Fossataro et al., 2020; Kofler et al., 2001a; Neige et al., 2022; Tamburin et al., 2001; Urban et al., 2004) or laser stimulation (Algoet et al., 2018; Dubé & Mercier, 2011b; Valeriani et al., 1999b, 2001) typically last no longer than 2000 ms. Importantly, only a single TMS pulse was delivered per CS trial, to exclude a modulation of corticospinal excitability due to the delivery of repetitive TMS pulses, rather than due to threat conditioning (R. Chen et al., 1997; Julkunen et al., 2012). Finally, to ensure that the occurrence of a TMS pulse could not be predicted during conditioning, for each CS, only 40 out of 46 trials had a TMS pulse. In particular, for each CS+, TMS 1 occurred in 20 trials (12 reinforced and 8 non-reinforced), while it did not occur in 3 trials (2 reinforced, 1 non-reinforced); the same happened for TMS 2. To exclude any non-specific, long-lasting changes in basal corticospinal excitability that could be related to the TMS, the task, or the shocks per se, and thus affecting the results, baseline corticospinal excitability was probed at the beginning and the end of the experimental session. This was done by delivering 15 single TMS pulses and acquiring MEPs while participants passively observed a fixation cross on the screen. An inter-pulse interval of at least 5000 ms was adopted, thereby avoiding changes in corticospinal excitability due to repeated TMS pulses (R. Chen et al., 1997). No difference emerged when comparing MEPs recorded during the initial (M=1.244, 95% credible interval (CI) [0.942, 1.576]) and final (M=1.383, 95% CI [1.035, 1.705]) baseline phases (BF_{10}=0.594; err%=0.027).

Electromyography recording. Surface EMG activity was recorded from the FDI muscle of the participant's right hand at 5000 Hz, with a 5 kHz lowpass filter, through a pair of Ag/AgCl electrodes (BIOPAC EL501) placed in a belly-tendon montage connected to an EMG100C module of the BIOPAC MP-150 System (Goleta, CA). After skin preparation, a small amount of isotonic hyposaturated conductant gel (Lectron III Gel, NEUROSPEC) was added to the electrodes, which were placed and fixed on the target positions. The active electrode was

placed over the muscle belly, determined by palpation during maximum voluntary contraction, while the reference and ground electrodes were placed over the proximal interphalangeal juncture and the radial styloid process.

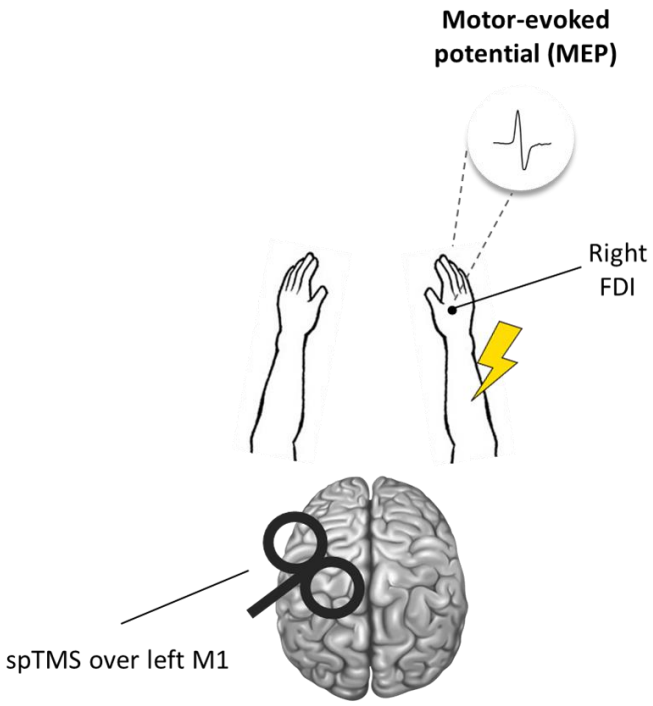

Figure 5.3. Stimulations and recordings for the Pavlovian threat conditioning task. The shock was delivered at the right extensor carpi radialis muscle, and spTMS was delivered over the left M1 to record MEP from the right FDI of participants.

Procedure

Participants were tested individually in a single experimental session lasting approximately two hours. They were comfortably seated in a silent room in front of a computer screen (size: 43 inches; resolution: 1920 × 1080 pixels; refresh rate: 60 Hz), at ~80 cm viewing distance. Then, before Pavlovian threat conditioning, the shock intensity was calibrated. Then, baseline corticospinal excitability was measured. The Pavlovian threat conditioning task followed, after which explicit learning was assessed and the time interval reproduction task performed. Finally, baseline corticospinal excitability was measured again. Participants were debriefed about the experimental hypotheses at the end of the whole experiment. A PC running the OpenSesame software (Mathôt et al., 2012) connected through a NI USB-6281 device (National Instruments, Austin, TX) to a BIOPAC MP-150 System (Goleta, CA), a Digitimer

Stimulator (Model DS7A, Digitimer Ltd., UK), and Magstim Rapid^2 stimulator (Magstim Co., Whitland, UK) controlled the flow of the experimental tasks, stimulations delivery and data recording.

Dependent variables

Threat conditioned corticospinal response. EMG data were preprocessed offline in MATLAB using custom-made scripts. First, epochs from the time of the TMS pulse to 60 ms after it were extracted from the continuous data for MEP identification and analysis, and epochs from –100 ms to the time of the TMS pulse were extracted to identify any muscular preactivation, before TMS delivery. For each epoch, the min and max MATLAB functions were then used to determine the minimum and maximum peak in the EMG signal. The signal was then visually inspected to ensure the correctness of the automatic procedure. Muscular preactivations were defined as trials in which peaks of EMG activity in the 100 ms window preceding the TMS pulse exceeded 2 SD from the mean background EMG activity. MEPs preceded by such preactivation were discarded to prevent contamination of the MEP measurements (a total of 5.57% of MEPs were excluded). This enabled the exclusion of any influence of participants' movement or movement that may have been evoked by shock delivery to influence MEPs recorded on the next trial. For the remaining trials, individual peak-to-peak MEP amplitudes (mV) were calculated and considered as a proxy for corticospinal excitability during threat conditioning. Then, MEPs' whose amplitude exceeded ± 2 SD of the mean amplitude for each experimental condition were excluded as outliers (CS+early: 4.38%; CS+late: 3.66%; CS-: 4.02%). To control for interindividual variability in MEP amplitudes, the raw MEP amplitudes were z-transformed using the average and standard deviation calculated across all CSs, separately for each participant. Z-scored MEP amplitudes were then averaged for each CS and used for statistical analyses.

Time interval reproduced. For each CS+, raw participants' response times for each trial (extracted in ms) were averaged and used for statistical analyses.

Explicit acquisition of threat conditioning. Participants' explicit ratings of valence, arousal and CS-US contingency for each CS were used in statistical analyses to compare responses between CSs.

Statistical analyses

Threat conditioned corticospinal response. Given our three a-priori hypotheses on the corticospinal response during threat of pain (Figure 5.1), a Bayesian model comparison approach, namely Bayesian informative hypothesis testing (Garofalo et al., 2022, 2023; Gu et al., 2014; Hoijtink et al., 2016a), was chosen for statistical analysis. This approach enables us to quantify how much more likely the data are under a given hypothesis as compared to the other experimental hypotheses tested (Garofalo et al., 2023; Hoijtink, Mulder, et al., 2019). Bayesian Informative hypothesis can be seen as an extension of rmANOVA, allowing for specification and testing structured hypotheses about relationships between means, rather than solely assessing overall differences, as done by classically defined alternative hypotheses. Indeed, research hypotheses in psychological and cognitive sciences often extend beyond the classical null and alternative framework. Each model expressed a specific hypothesis that could be defined in terms of equality and/or inequality constraints among the parameters (Béland et al., 2012; Garofalo et al., 2022; Gu et al., 2018; Hoijtink et al., 2016b; Hoijtink, Mulder, et al., 2019; Kluytmans et al., 2012). The prior distribution in our models is assumed to be equal among the hypotheses, this means that we manipulated the alternative hypotheses tested in each model, but not the associated prior distribution. For each hypothesis, the posterior model probability (PMP) was calculated via the Bayes theorem and expressed with a value between 0 and 1. This value can be interpreted as the relative amount of support for each hypothesis given the data and the set of competing hypotheses included, namely, the unconstrained hypothesis (Hu), which is a hypothesis representing all possible sets of relationships between the parameters without constraints, and the complement hypothesis (Hc), which is a model that contains any set of restrictions between the parameters except the one represented by the hypothesis (Garofalo et al., 2023; Hoijtink, Mulder, et al., 2019). The posterior model probability associated with each hypothesis is, by default, calculated in three ways, that is relative to: all other hypotheses tested (PMPa); all other hypotheses tested plus the unconstrained hypothesis Hu (PMPb); and all other hypotheses tested plus the complement hypothesis Hc (PMPc). The model with the highest PMP reflects the hypothesis that best describes the observed data (i.e., the hypothesis with the highest relative probability) (Garofalo et al., 2023; Hoijtink, Gu, et al., 2019). The Bayes factor matrix was also calculated to show the Bayes factor deriving from the ratio between the marginal

likelihoods of all possible pairs of hypotheses tested (Garofalo et al., 2023; Hoijtink, Gu, et al., 2019). To perform these analyses, the "bain" package (Garofalo et al., 2023; Gu et al., 2019) was implemented in R software (v4.2.1) (*R Core Team (2022) R A Language and Environment for Statistical Computing. R Foundation for Statistical Computing, Vienna. - References - Scientific Research Publishing*, n.d.) and RStudio (v2022.07.2 Build 576).

Specifically, we formulated three a-priori hypotheses to describe the dynamics of motor system excitability under threat of pain, which were tested against each other using Bayesian informative hypotheses testing (Figure 5.1).

(1) **H1: Phasic inhibition hypothesis.** Motor inhibition is selectively tuned to the time of pain occurrence. Thus, the reduction in corticospinal excitability is observed exclusively immediately before the time of shock (CS+early_TMS 1 and CS+late_TMS 2) but not long before (CS+late_TMS 1) or after (CS+early_TMS 2) it, or during CS- presentation (CS-_TMS 1 and CS-_TMS 2). This hypothesis can formally be represented as follows:

H1: (CS+late_TMS 1 = CS-_TMS 1) > CS+early_TMS 1
&
CS+late_TMS 1 > CS+late_TMS 2
&
(CS+early_TMS 2 = CS-_TMS 2) > CS+late_TMS 2

(2) **H2: Sustained inhibition throughout pain anticipation hypothesis.** Motor inhibition starts at the appearance of the CS+, persists throughout the time preceding pain occurrence, and then recovers once it has passed. Thus, in this case, the reduction in corticospinal excitability is already observed long before the time of shock (CS+late_TMS 1), as well as immediately before it (CS+early_TMS 1 and CS+late_TMS 2), but not long after it (CS+early_TMS 2), or during CS- presentation (CS-_TMS 1 and CS-_TMS 2). This hypothesis can formally be represented as follows:

H2: (CS+late_TMS 1 = CS+early_TMS 1) < CS-_TMS 1
&
CS+late_TMS 1 = CS+late_TMS 2
&
(CS+early_TMS 2 = CS-_TMS 2) > CS+late_TMS 2

(3) **H3: Sustained inhibition throughout threat of pain hypothesis.** Motor inhibition persists during the entire time of CS+ presentation, regardless of the actual time of pain. The rationale is that as learning progresses, the CS+ acquires the same aversive value as the painful shock outcome. Thus, in this case, the reduction in corticospinal excitability is observed as long as a CS+ is present on the screen regardless of the time of shock occurrence, namely at CS+early_TMS 1, CS+early_TMS 2, CS+late_TMS 2 and CS+late_TMS 1, but not during CS- presentation (CS-_TMS 1 and CS-_TMS 2). This hypothesis can formally be represented as follows:

H3: CS+early_TMS 1 = CS+early_TMS 2
&
(CS+early_TMS 1 = CS+late_TMS 1) < CS-_TMS 1
&
(CS+early_TMS 2 = CS+late_TMS 2) < CS-_TMS 2

Finally, we included a fourth hypothesis, representing the null hypothesis, assuming no differences amongst all conditions.

(4) **H0: Null hypothesis**. No significant differences exist among the different CS conditions or across different TMS timings.

H0: CS+early_TMS 1 = CS+late_TMS 1 = CS-_TMS 1
&
CS+early_TMS 1 = CS+early_TMS 2
&
CS+late_TMS 1 = CS+late_TMS 2
&
CS-_TMS 1 = CS-_TMS 2

Then, to confirm that changes in corticospinal excitability were driven by the time of shock, rather than shock occurrence per se, a Bayesian paired sample t-test was conducted comparing the amplitude of averaged MEPs recorded long after the time of pain (TMS 2) for reinforced and non-reinforced CS+early trials. The Bayes Factor (BF_{10}) is reported as the probability of the data under the alternative hypothesis (H_1) over the null hypothesis (H_0), along with its estimated proportional error (err%) (Andraszewicz et al., 2014; Kruschke, 2021).

Time interval reproduced. To test differences in the time interval reproduced for each CS+, Bayesian paired sample t-test and Bayesian analyses of variance (ANOVA) were respectively

used. The Bayes Factor (BF_{10}) is reported as the probability of the data under the alternative hypothesis (H_1) over the null hypothesis (H_0), along with its estimated proportional error (err%) (Andraszewicz et al., 2014; Kruschke, 2021).

Explicit acquisition of threat conditioning. Bayesian repeated measures analyses of variance (rmANOVA) and post-hoc comparisons were performed to test differences in valence, arousal and shock contingency ratings between CSs. The Bayes Factor (BF_{10}) is reported as the probability of the data under the alternative hypothesis (H_1) over the null hypothesis (H_0), along with its estimated proportional error (err%) (Andraszewicz et al., 2014; Kruschke, 2021).

All data, analysis code, and research materials will be made available to other researchers in a timely manner upon request.

Experiment 5

Given the results of experiment 4, we questioned whether the inhibition observed long before the time of pain for the CS+late (i.e., at TMS 1) indeed represented the dynamic of the motor system's response under threat of pain, or if this inhibition was driven by the structure of the threat conditioning task, where both CS+early and CS+late were presented in the same experimental block. Specifically, we considered whether the shock delivered 1750 ms after CS+early onset may have established a temporal association that generalized to the CS+late. If this were the case, the observed reduction in corticospinal excitability long before the time of pain during the CS+late presentation should be interpreted as a threat-conditioned response generalization (Cooper et al., 2022; Dunsmoor, Otto, et al., 2017; Dunsmoor & Paz, 2015; Starita et al., 2019) due to the presence of CS+early, rather than as a sustained inhibition of the motor system under threat of pain. Thus, experiment 5 was conducted to disambiguate between these two interpretations of the results.

A new group of participants completed a Pavlovian threat conditioning task. This included the same experimental conditions as experiment 4, with the key difference that CS+early and CS+late were conditioned in separate blocks. Specifically, one half of the participants experienced first a threat conditioning block with CS+early and CS-, and then a conditioning

block with CS+late and a different CS-. The other half had the order of the conditioning blocks reversed. The time interval reproduction task was also completed, as in experiment 4, but at the end of each conditioning block.

Participants

Twenty-eight healthy right-handed volunteers (16 women, aged between 18 and 30 years: M=22, SD=1.71 years) with the same characteristics as those participating in experiment 4 were tested. No participant who took part in experiment 4 was recruited for experiment 5, to prevent any effect of having previously participated in a similar threat conditioning experiment from influencing the results of experiment 5.

Experimental tasks

Pavlovian threat conditioning task. We modified the conditioning task described in experiment 4 such that CS+early and CS+late were conditioned in two separate blocks, which we will refer to as Block early and Block late, respectively. Each block included a different CS+ (early or late) and a different CS-, as control stimulus. Thus, the conditioning task included a total of four different CSs, which were circles (64 pixels diameter) colored blue (#5698D4), pink (#C760CA), green (#51D968) or yellow (#F4E634). Importantly, within each block the trial structure and timings, number of trials for each CS, and types and number of TMS pulses for each CS were the same as for experiment 4. The order of the blocks and the color assigned to each CS were counterbalanced among participants.

Time interval reproduction task. At the end of each block of the threat conditioning task, participants performed the interval reproduction task, structured as in experiment 4, with the exception that it included only the CS+ presented in that block.

Stimulation and recordings

We used the same parameters of experiment 4 to set up the experimental stimulations and recordings.

Painful electrotactile stimulation. The shock intensity (M=75.54 mA, SD=22.34) was calibrated for each participant as in experiment 4. Participants rated the unpleasantness of the shock on a scale ranging from 0 to 10, from “no sensation” to “untolerable pain”, both before (M=7.46,

SD=1.32) and at the end of the experiment (M=7.00 SD=1.49) to confirm the maintenance of the aversive value of the shock (Bayesian paired sample t-test BF_{10}=1.993; err%=1.439e-6).

Transcranial magnetic stimulation (TMS). The resting motor threshold ranged from 57 to 83% (M=71.18%, SD=8.99) of the maximum stimulator output.

Electromyography recording. As in experiment 4, trials in which peaks of EMG activity in the 100 ms window preceding the TMS pulse exceeded 2 SD from the mean background EMG activity were discarded to prevent contamination of the MEP measurements (a total of 6.54% of MEPs were excluded). In addition, values that exceeded ± 2 SD of the mean amplitude for each CS condition were excluded as outliers (in Block early CS+early: 3.57%, CS-: 3.39%; in Block late CS+late: 4.02%, CS-: 3.84%). MEP data recorded from one participant were excluded due to technical issues during the registration.

As in experiment 4, no differences emerged when comparing MEPs recorded during the initial (M=0.958, 95% (CI) [0.730, 1.254]) and final (M=0.951, 95% (CI) [0.716, 1.159]) baseline phases (BF_{10}=0.27; err%=0.031). This indicates that TMS, the task, or the shocks per se did not induce any generalized, long-lasting changes in motor excitability during the experiment.

Procedure

The experimental procedure followed was the same as described in experiment 4.

Dependent variables

Data regarding threat conditioned corticospinal response, explicit acquisition of threat conditioning and time interval reproduced were recorded and preprocessed as in experiment 4.

Statistical analysis

Threat conditioned corticospinal response. Bayesian informative hypotheses were used to test if the pattern of results observed in experiment 4 would be replicated also in experiment 5. More specifically, we conceptually retained the same three hypotheses of experiment 4 but adapted them to the experimental conditions of experiment 5. In this case, CS-early refers to the CS- presented in the block together with the CS+early, and CS-late refers to the CS-

presented in the block together with the CS+late. We then proceeded to test the three hypotheses against each other as previously described for experiment 4.

(1) **H1: Phasic inhibition hypothesis.** Motor inhibition is selectively tuned to the time of pain occurrence. Thus, the reduction in corticospinal excitability is observed exclusively immediately before the time of shock (CS+early_TMS 1 and CS+late_TMS 2) but not long after (CS+early_TMS 2) or before (CS+late_TMS 1) it, or during CS- presentation (CS-early_TMS 1, CS-early_TMS 2, CS-late_TMS 1 and CS-late_TMS 2). This hypothesis can formally be represented as follows:

H1: CS+early_TMS 1 < CS-early_TMS 1
&
CS+early_TMS 2 = CS-early_TMS 2
&
CS+late_TMS 1 = CS-late_TMS 1
&
CS+late_TMS 1 > CS+late_TMS 2
&
CS+late_TMS 2 < CS-late_TMS 2

(2) **H2: Sustained inhibition throughout pain anticipation hypothesis.** Motor inhibition persists throughout the time preceding pain occurrence and recovers once this has passed. Thus, the reduction in corticospinal excitability is already observed long before the time of shock (CS+late_TMS 1), as well as immediately before it (CS+early_TMS 1 and CS+late_TMS 2), but not long after it (CS+early_TMS 2), or during CS- presentation (CS-early_TMS 1 and CS-early_TMS 2, CS-late_TMS 1 and CS-late_TMS 2). This hypothesis can formally be represented as follows:

H2: CS+early_TMS 1 < CS-early_TMS 1
&
CS+early_TMS 2 = CS-early_TMS 2
&
(CS+late_TMS 1 = CS+late_TMS 2) < (CS-late_TMS 1 = CS-late_TMS 2)

(3) **H3: Sustained inhibition throughout threat of pain hypothesis.** Motor inhibition persists during the entire time of CS+ presentation, regardless of the actual timing of pain. Thus,

in this case, the reduction in corticospinal excitability is observed as long as a CS+ is presented on the screen, namely at CS+early_TMS 1, CS+early_TMS 2, CS+late_TMS 1 and CS+late_TMS 2, but not during CS- presentation (CS-early_TMS 1, CS-early_TMS 2, CS-late_TMS 1 and CS-late_TMS 2). This hypothesis can formally be represented as follows:

H3: (CS+early_TMS 1 = CS+early_TMS 2) < (CS-early_TMS 1 = CS-early_TMS 2)
&
(CS+late_TMS 1 = CS+late_TMS 2) < (CS-late_TMS 1 = CS-late_TMS 2)

Finally, we included a fourth hypothesis, representing the null hypothesis, assuming no differences amongst all conditions.

(4) **H0: Null hypothesis**. No significant differences exist among the different CS conditions or across different TMS timings.

H0: CS+early_TMS 1 = CS+early_TMS 2 = CS-early_TMS 1 = CS-early_TMS 2
&
CS+late_TMS 1 = CS+late_TMS 2 = CS-late_TMS 1 = CS-late_TMS 2

Then, to confirm that changes in corticospinal excitability were driven by the time of shock, rather than shock occurrence per se, a Bayesian paired sample t-test was conducted comparing the amplitude of averaged MEPs recorded long after the time of pain (TMS 2) for reinforced and non-reinforced CS+early trials.

Time interval reproduced. The statistical analysis conducted on reproduced time intervals was performed using the same Bayesian inferential approach as in experiment 4.

Explicit acquisition of threat conditioning. Bayesian paired sample t-tests were performed to test differences in valence, arousal and shock contingency ratings between CSs, separately for the Block CS+early and Block CS+late.

RESULTS

Experiment 4

Threat conditioned corticospinal response

Posterior model probabilities were used to test our three main experimental hypotheses. They showed that H2 was associated with the highest probability, relative to the other experimental or null hypotheses (Table 5.1; Figure 5.7); thus, indicating this as the strongest hypothesis both when excluding (PMPa) or including (PMPb) the unconstrained hypothesis (Hu) and when including the complementary hypothesis (Hc, see PMPc). In line with this, H2 also presented the highest Bayes Factor relative to Hc and Hu (see BFc and BFu in Table 5.1, respectively). Additionally, as reported in the Bayes factor matrix in Table 5.2, the direct comparison between how likely the data are under each pair of informative hypotheses showed that the support in the data is larger for H2 than for H1, H3, and H0 (BF_{21}=7.998, BF_{23}=5.709, and H_{20}=1383.171). Overall, these results offer convergent support for H2, i.e. the sustained inhibition throughout pain anticipation hypothesis, which indicates a reduction in corticospinal excitability that starts long before the time of shock, is maintained also immediately before the time of shock, and finally recovers once the time of shock has passed.

To confirm that the recovery of corticospinal excitability is bound to the time of shock, rather than to the delivery of the shock we conducted a Bayesian paired sample t-test on MEPs recorded at TMS 2 for the CS+early for shocked vs. non-shocked trials. Indeed, no differences emerged between shocked (M=0.040, 95% credible interval (CI) [-0.095, 0.183]) and non-shocked CS+early trials (M=0.059, 95% (CI) [-0.114, 0.282]; BF_{10}=0.215; err%=0.031), confirming that the recovery in corticospinal excitability after the time of shock for CS+early was driven shock timing, rather than shock occurrence.

Figure 5.4 shows a descriptive representation of the data, illustrating that, relative to the CS- (TMS 1: M=0.079, 95% CI [-0.047, 0.206]; TMS 2: M=0.153, 95% CI [0.018, 0.284]) a reduction in corticospinal excitability can be observed in presence of the CS+early immediately before (M=-0.108, 95% CI [-0.212, 0.006]) but not long after (M=0.048, 95% CI [-0.072, 0.179]) the time of pain, while with the CS+late this occurs both long (M=-0.109, 95% CI [-0.197, -0.027]) and immediately (M=-0.063, 95% CI [-0.177, 0.062]) before the time of pain.

Table 5.1. Model comparison via Bayesian informative hypothesis testing

	Fit	Com	BFu	BFc	PMPa	PMPb	PMPc
H1	0.177	0.100	1.763	1.927	0.096	0.091	0.092
H2	3.772	0.267	14.105	14.105	0.769	0.729	0.732
H3	0.700	0.283	2.470	2.470	0.135	0.128	0.128
H0	0.921	90.328	0.010	0.010	0.001	0.001	0.001
Hu						0.052	
Hc	0.823	0.900	0.915				0.047

Note. Fit, data fitting index; Com, complexity of the hypotheses; BFu, Bayes Factors of the hypothesis in the row vs. the unconstrained hypothesis (Hu) and complement hypothesis (Hc); BFc, Bayes Factors of the hypothesis in the row vs. the complement hypothesis (Hc); PMPa, posterior model probability excluding the unconstrained hypothesis; PMPb, posterior model probability including the unconstrained hypothesis; PMPc, posterior model probability including the complement hypothesis.

Table 5.2. Bayes factor matrix

	H1	H2	H3	H0
H1	1	0.125	0.714	172.933
H2	7.998	1	5.709	1383.171
H3	1.401	0.175	1	242.264
H0	0.006	0.001	0.004	1

Note. BFs deriving from the ratio between the marginal likelihoods of all possible pairs of hypotheses tested are represented.

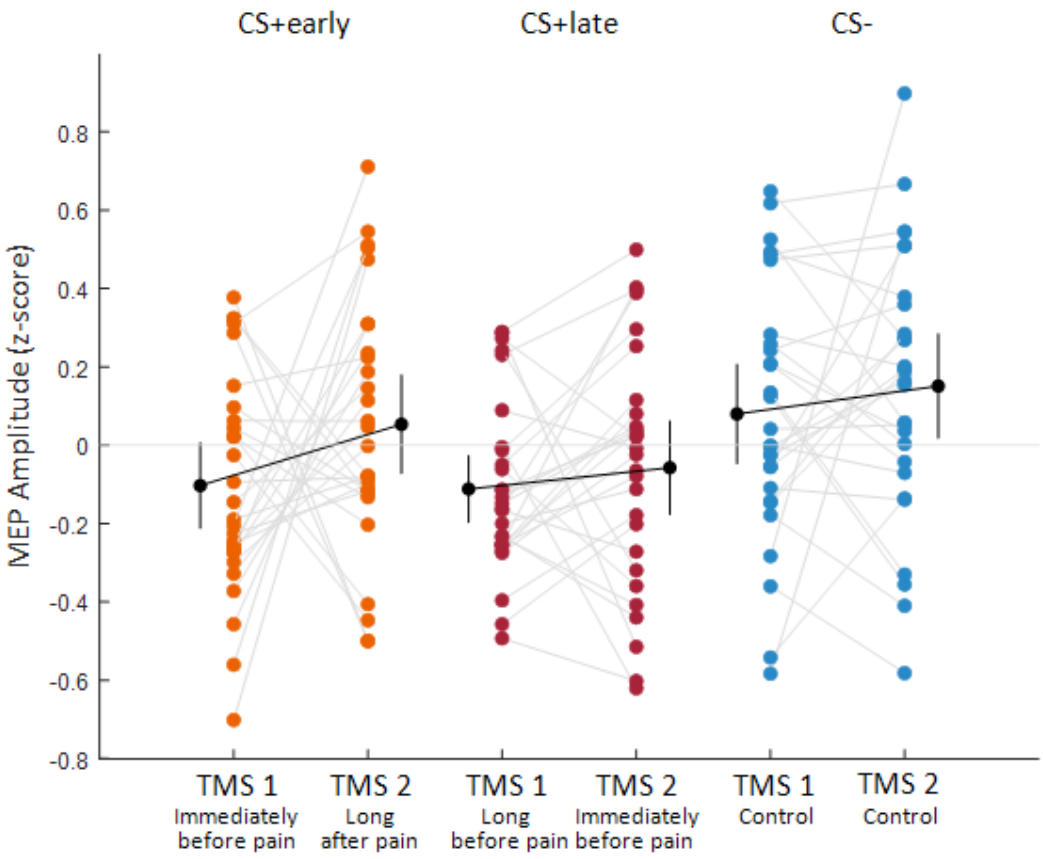

Figure 5.4. The plot shows individual participants' data (colored dots), group means (black dots), and 95 % credible intervals (vertical black lines) of MEP amplitudes (z-scored) for CS+early (orange), CS+late (red), and CS- (blue), as a function of the time of TMS delivery, i.e. TMS 1 or TMS 2. Each paired set of observations is connected by a gray line.

Time interval reproduced

A Bayesian paired sample t-test comparing the mean time intervals reproduced for the CS+early and CS+late showed that participants reproduced a shorter interval for CS+early than CS+late (CS+early: M=2029.150, 95% CI [1655.234, 2403.066], CS+late: M=4314.221, 95% CI [3715.333, 4913.110]; BF_{10}=193448.875, err%=2.730e-10), meaning that participants learned to discriminate the time of shock between the two CSs+ (Figure 5.5). Additionally, a Bayesian paired sample t-test comparing the difference between the mean reproduced time interval and the actual time of the shock for CS+early (1750 ms – mean reproduced time for CS+early) and CS+late (5500 ms – mean reproduced time for CS+late) revealed that this difference was smaller for CS+early than for CS+late (CS+early: M=-279.150, 95% CI [-653.066, 94.766]; CS+late: M=1185.779, 95% CI [586.890, 1784.667]; BF_{10}=349.609, err%=2.046e-8), indicating

that participants were more accurate in reproducing the time interval for the shock early. Finally, a Bayesian paired sample t-test comparing the standard deviation of time intervals reproduced for the CS+early and CS+late showed lower variability for the CS+early than CS+late (CS+early: M=354.073, 95% CI [265.787, 442.358], CS+late: M=495.835, 95% CI [397.040, 594.630]; BF_{10}=10.814, err%=4.992e-8), meaning that participants exhibited greater variability in reproducing the time interval for the shock late. Additionally, a Bayesian paired sample t-test comparing the difference between the actual time of shock and the mean reproduced time interval for CS+early (1750 ms – mean reproduced time for CS+early) and CS+late (5500 ms – mean reproduced time for CS+late) revealed that this difference was smaller for CS+early than for CS+late (CS+early: M=-279.150, 95% CI [-653.066, 94.766]; CS+late: M=1185.779, 95% CI [586.890, 1784.667]; BF_{10}=349.609, err%=2.046e-8), indicating that participants were more accurate in reproducing the time interval for the early shock. Finally, a Bayesian paired sample t-test comparing the standard deviation of time intervals reproduced for the CS+early and CS+late showed lower variability for the CS+early than CS+late (CS+early: M=354.073, 95% CI [265.787, 442.358], CS+late: M=495.835, 95% CI [397.040, 594.630]; BF_{10}=10.814, err%=4.992e-8), meaning that participants exhibited greater variability in reproducing the time interval for the late than the early shock.

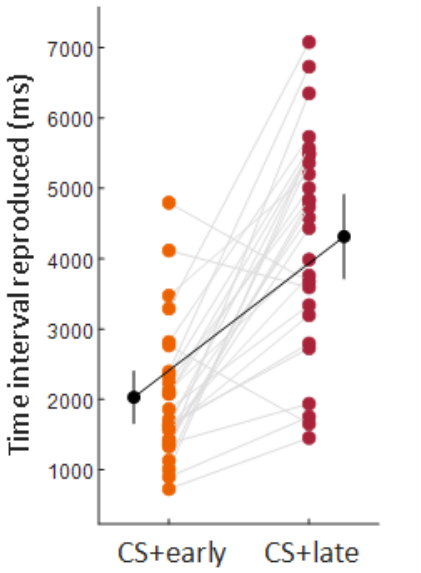

Figure 5.5. The plot shows individual participants' data (colored dots), group means (black dots), and 95 % credible intervals (vertical black lines) of the time interval reproduced (ms) for CS+early (orange) and CS+late (red). Each paired set of observations is connected by a gray line.

Explicit acquisition of threat conditioning

Three Bayesian rmANOVA and post-hoc comparisons were performed with CS (CS+early, CS+late, CS-) as a within-subject factor to analyze CSs valence, CSs arousal, and shock contingency ratings. A main effect of CS emerged for valence (BF_{10}=8.683e+18, err%=2.522), arousal (BF_{10}=3.216e+30, err%=3.310) and contingency (BF_{10}=6.815e+40, err%=1.507). Participants rated the CS+early (M=2.929, 95% CI [2.294, 3.135]) and the CS+late (M=2.714, 95% CI [1.758, 3.1]) as less pleasant than the CS- (M=6.536, 95% CI [6.356, 7.787]; BF_{10}=3.043e+9; err%=1.821e-12; BF_{10}=2.136e+8; err%=7.017e-12, respectively), whereas ratings for CS+early and CS+late did not differ (BF_{10}=0.326, err%=0.03). Moreover, participants rated the CS+early (M=7.429, 95% CI [7.028, 7.829]) and the CS+late (M=8.071, 95% CI [7.524, 8.619]) as more arousing compared to the CS- (M=1.143, 95% CI [0.486, 1.8]; BF_{10}=2.010e+12, err%=3.106e-14; BF_{10}=7.388e+11, err%=7.722e-14, respectively), whereas ratings for CS+early and CS+late did not differ relevantly (BF_{10}=1.121, err%=0.023). Regarding the CS-US contingency rating, participants attributed greater contingency to the CS+early (M=7.464, 95% CI [7.023, 7.906]) and CS+late (M=7.214, 95% CI [6.829, 7.6]) than the CS- (M=0.357, 95% CI [-0.055, 0.769]; BF_{10}=4.888e+15, err%=4.419e-19; BF_{10}=3.406e+15, err%=4.726e-19, respectively), whereas ratings for CS+early and CS+late did not differ (BF_{10}=0.356, err%=0.030).

Interim discussion

Experiment 5 showed that the Pavlovian conditioning task we designed was suitable to induce conditioning in participants. Indeed, participants rated the CS+early and the CS+late as less pleasant, more arousing, and more often associated with pain compared to the CS-, confirming the acquisition of conditioned explicit responses. Additionally, the results of the time reproduction task showed that participants discriminated between the timing of pain occurrence associated with the CS+early and the CS+late, reproducing a shorter interval for CS+early than CS+late.

Crucially, the results also confirmed that changes in corticospinal excitability under the threat of pain reflect the timing of expected pain. Specifically, the sustained inhibition throughout

pain anticipation hypothesis (H2) had the greatest support, indicating that the motor system encodes the interval between the onset of a threat and the time of pain occurrence.

Nevertheless, we questioned whether the inhibition observed long before the time of pain for the CS+late (i.e., at TMS 1) indeed represented the dynamic of the motor system's response under threat of pain, or if this inhibition was driven by the structure of the threat conditioning task, where both CS+early and CS+late were presented in the same experimental block. Specifically, we considered whether the shock delivered 1750 ms after CS+early onset may have established a temporal association that generalized to the CS+late. If this were the case, the observed reduction in corticospinal excitability long before the time of pain during the CS+late presentation should be interpreted as a threat-conditioned response generalization (Cooper et al., 2022; Dunsmoor, Otto, et al., 2017; Dunsmoor & Paz, 2015; Starita et al., 2019) due to the presence of CS+early, rather than as a sustained inhibition of the motor system under threat of pain. Thus, experiment 5 was conducted to disambiguate between these two interpretations of the results.

Experiment 5

Threat conditioned corticospinal response

Similarly, to experiment 4, posterior model probabilities were used to test our three main experimental hypotheses. They showed that H2 was associated with the highest probability, relative to the other experimental or null hypotheses (Table 5.3; Figure 5.7); thus, indicating this as the strongest hypothesis both when excluding (PMPa) or including (PMPb) the unconstrained hypothesis (Hu) and when including the complementary hypothesis (Hc, see PMPc). In line with this, H2 also presented the highest Bayes Factor relative to Hc and Hu (see BFc and BFu in Table 5.3, respectively). Additionally, as reported in the Bayes factor matrix in Table 5.4, the direct comparison between how likely the data are under each pair of informative hypotheses showed that the support in the data is larger for H2 than for H1, H3, and H0 (BF_{21}=25.199, BF_{23}=1177.134, and BF_{20}=1.561e+13). Overall, these results confirm the support for H2, i.e. the sustained inhibition throughout pain anticipation hypothesis, which indicates a reduction in corticospinal excitability that starts long before the time of shock, is

then found also immediately before the time of shock, and finally recovers once the time of shock has passed, excluding carryover or generalization effect of the timing of pain for CS+early onto the CS+late.

Then, the Bayesian paired sample t-test on MEPs recorded at TMS 2 for the CS+early for shocked vs. non-shocked trials confirmed, as in experiment 4, that the changes in corticospinal excitability were driven by the time of shock, rather than shock occurrence per se, as no differences emerged between shocked (M=0.228, 95% CI [0.048, 0.444]) and non-shocked trials (M=0.121, 95% CI [-0.017, 0.270]; BF_{10}=0.343; err%=0.030).

In Figure 5.6, a descriptive representation of the results is shown. In the Block early, we found a corticospinal excitability reduction in the presence of the CS+early immediately before (M=-0.229, 95% CI [-0.407, -0.107]) but not long after (M=0.184, 95% CI [0.051, 0.333]) pain, nor in the presence of the CS- in both the control TMS stimulation timepoints (TMS 1: M=-0.068, 95% CI [-0.154, 0.018]; TMS 2: M=0.108, 95% CI [0.031, 0.199]). In the Block late, we found a corticospinal excitability reduction in the presence of the CS+late both long (TMS1: M=-0.094, 95% CI [-0.221, 0.011]) and immediately (TMS2: M=-0.176, 95% CI [-0.279, -0.046]) before pain, while corticospinal excitability was not reduced in the presence of the CS- in both the control TMS stimulation timepoints (TMS 1: M=0.094, 95% CI [-0.006, 0.187]; TMS 2: M=0.170, 95% CI [0.069, 0.263]).

Table 5.3. Model comparison via Bayesian informative hypothesis testing

	Fit	Com	BF.u	BF.c	PMPa	PMPb	PMPc
H1	0.547	1.15	0.476	0.476	0.031	0.029	0.029
H2	3.095	0.239	12.955	12.955	0.846	0.794	0.795
H3	0.00	0.027	0.012	0.012	0.001	0.001	0.001
H0	0.000	363.691	0.000	0.000	0.000	0.000	0.000
Hu						0.064	
Hc	1.000	0.973	1.028				0.066

Note. Fit, data fitting index; Com, complexity of the hypotheses; BFu, Bayes Factors of the hypothesis in the row vs. the unconstrained hypothesis (Hu) and complement hypothesis (Hc); BFc, Bayes Factors of the hypothesis in the row vs. the complement hypothesis (Hc); PMPa, posterior model probability

excluding the unconstrained hypothesis; PMPb, posterior model probability including the unconstrained hypothesis; PMPc, posterior model probability including the complement hypothesis

Table 5.4. Bayes factor matrix

	H1	H2	H3	H0
H1	1	0.040	46.713	6.196e+11
H2	25.199	1	1177.134	1.561e+13
H3	0.021	0.001	1	1.326e+10
H0	0.000	0.000	0.000	1

Note. BFs deriving from the ratio between the marginal likelihoods of all possible pairs of hypotheses tested are represented.

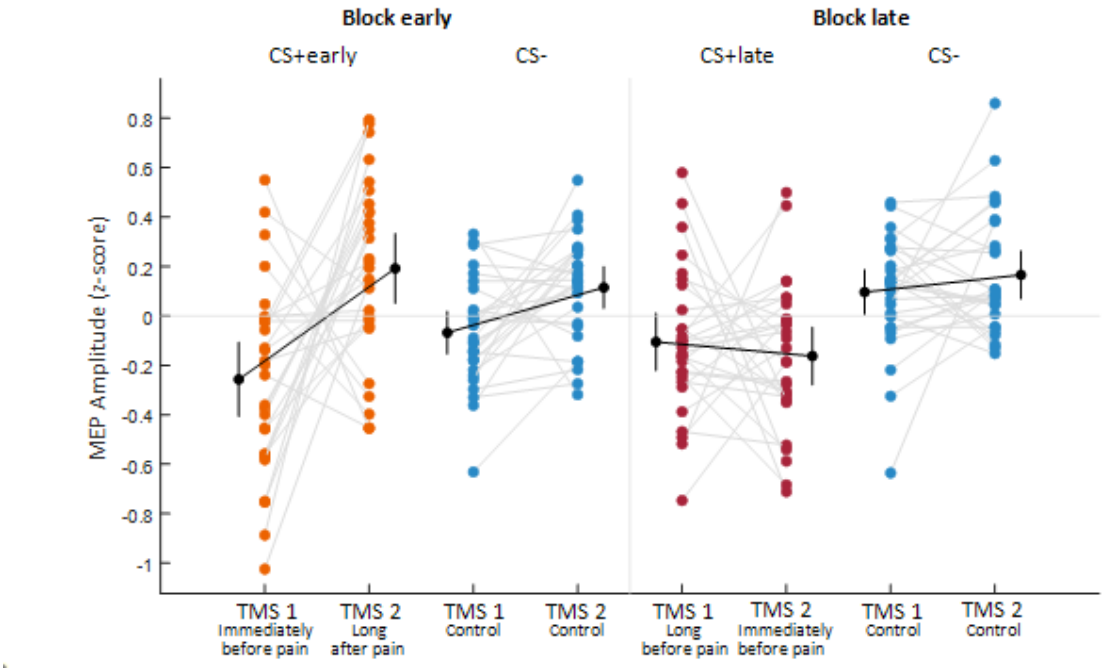

Figure 5.6. The plot shows individual participants' data (colored dots), group means (black dots) and 95 % confidence intervals (vertical black lines) of MEP amplitudes (z-scored) for CS+early (orange), CS+late (red) and CS- (blue), as a function of TMS delivery, i.e. TMS 1 or TMS 2, in Block early and Block late. Each paired set of observations is connected by a gray line.

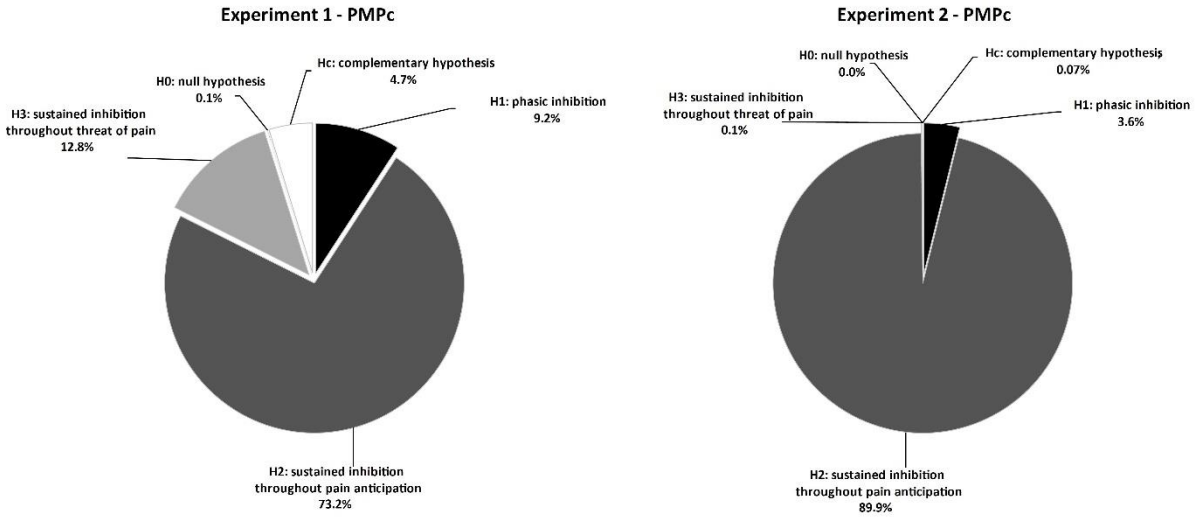

Figure 5.7. Bayesian informative hypothesis testing. The pie charts represent the posterior model probabilities associated with the four models (H1, H2, H3, and H0) when including the complementary (Hc) hypothesis. Results of experiment 4 (left panel) and experiment 5 (right panel) are represented.

Time interval reproduced

A Bayesian paired sample t-test comparing the mean time intervals reproduced for the CS+early and CS+late showed that participants reproduced a shorter interval for CS+early than CS+late (CS+early: M=2006.707, 95% CI [1461.269, 2552.146], CS+late: M=4705.171, 95% CI [4055.134, 5355.209]; BF_{10}=38394.492; err%=2.089e-10), meaning that participants learned to discriminate the time of shock between the two CSs+ (Figure 5.8). Additionally, a Bayesian paired sample t-test comparing the difference between the actual time of shock and the mean reproduced time interval for CS+early (1750 ms – mean reproduced time for CS+early) and CS+late (5500 ms – mean reproduced time for CS+late) revealed that this difference was smaller for CS+early than for CS+late (CS+early: M=-256.707, 95% CI [-802.146, 288.731]; CS+late: M=794.829, 95% CI [144.791, 1444.866]; BF_{10}=3.133, err%=7.432e-7), indicating that participants were more accurate in reproducing the time interval for the early shock. Finally, a Bayesian paired sample t-test comparing the standard deviation of time intervals reproduced for the CS+early and CS+late showed no difference in variability for the CS+early than CS+late (CS+early: M=747.337, 95% CI [264.338, 1230.335], CS+late: M=1148.444, 95% CI [558.291, 1738.596]; BF_{10}=0.357, err%=0.030); differently from experiment 4, participants exhibited similar variability in reproducing the time interval for the early and late shocks.

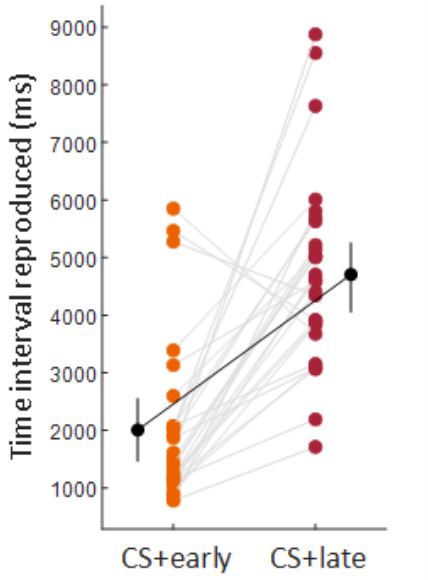

Figure 5.8. The plot shows individual participants' data (colored dots), group means (black dots), and 95 % credible intervals (vertical black lines) of the time interval reproduced (ms) for CS+early (orange) and CS+late (red). Each paired set of observations is connected by a gray line.

Explicit acquisition of threat conditioning

Three Bayesian paired sample t-tests were performed comparing CS- and CS+ on valence, arousal and shock contingency ratings, for both the Block early and Block late. After being conditioned to the CS+early, participants rated the CS+early as less pleasant (M=2.607, 95% CI [1.98, 3.235]) and more arousing (M=7.929, 95% CI [7.381, 8.476]), than the CS- (valence: M=6.286, 95% CI [5.379, 7.193]; BF_{10}=26179.312, err%=4.886e-10; arousal: M=1.536, 95% CI [0.864, 2.207]; BF_{10}=2.721e+11, err%=1.279e-13). Regarding the CS-shock contingency, participants expected to receive the shock more in the presence of the CS+early (M=7.036, 95% CI [6.582, 7.489]) than the CS-early (M=0.071, 95% CI [-0.075, 0.218]; BF_{10}=3.667e+19, err%=3.767e-21). Similarly, after participants were conditioned to the CS+late, they rated the CS+late as less pleasant (M=3.286, 95% CI [2.391, 4.180]) and more arousing (M=7.893, 95% CI [7.302, 8.484]), than the CS- (valence: M=6.429, 95% CI [5.537, 7.321]; BF_{10}=106.247, err%=1.276e-4; arousal: M=1.464, 95% CI [0.81, 2.119]; BF_{10}=6.972e+10, err%=1.098e-13), and expected more the shock in presence of the CS+late (M=7.286, 95% CI [6.869, 7.692]) than the CS-late (M=0.286, 95% CI [-0.23, 0.801]); BF_{10}=2.029e+16, err%=3.745e-18).

Interim discussion

The results of experiment 5 conceptually replicated those of experiment 4, further confirming that changes in corticospinal excitability under the threat of pain reflect the timing of expected pain and that the motor system encodes the interval between the onset of a threat and the time of pain occurrence, demonstrating sustained inhibition during the pain anticipation period.

Given the similarity of experiment 4 and 5 results, we then combined the data of the two experiments to explore, on a larger dataset, two sets of correlations. The first set tested the correlations between corticospinal excitability recorded at different timepoints during the CS+ presentation. The second set tested the correlations between corticospinal excitability and the time intervals elapsed between CS+ appearance and shock occurrence that were reproduced by participants.

Correlations combining data from experiments 4 and 5

Given the similarity of experiment 4 and 5 results, we then combined the data of the two experiments to explore, on a larger dataset, two sets of correlations. The first set tested the correlations between corticospinal excitability recorded at different timepoints during the CS+ presentation. The second set tested the correlations between corticospinal excitability and the time intervals elapsed between CS+ appearance and shock occurrence that were reproduced by participants.

Bayesian Pearson's correlations were conducted to assess two sets of correlation, as described below. For all correlations, Cook's distance (MATLAB package: influence.ME; function: influence; the output of the function influence was used in the function: cooks.distance) was used to estimate the impact of individual data points on the model outcome. Observations with Cook's distance larger than three times the mean Cook's distance were considered as outliers and excluded from the correlation (Trujillo-Ortiz, 2005). JASP 0.16 (Love et al., 2019) software was used to obtain Bayes factors.

Correlations between MEPs recorded at TMS 1 and TMS 2

These correlations tested the relation, across all participants, between the average MEP amplitudes recorded at TMS 1 and TMS 2, separately for CS+early and CS+late. For CS+early, given the MEPs reduction at TMS 1 as compared to TMS 2 (Figure 5.4 and Figure 5.6), a negative correlation was expected. Cook's distance analysis resulted in excluding three data points for the CS+early correlation (one from experiment 4 and two from experiment 5) and six data points for the CS+late correlation (three from experiment 4 and three from experiment 5). In Figure 5.9, the results are shown. A negative correlation for the CS+early (n=53, r=-0.647, BF_{10}=102204.427) emerged, indicating that the lower the corticospinal excitability immediately before the time of shock, the higher the corticospinal excitability long after the time of shock. In contrast, no correlation emerged between corticospinal excitability probed at TMS 1 and TMS 2 for the CS+late (n=50, r=-0.033, BF_{10}=0.182).

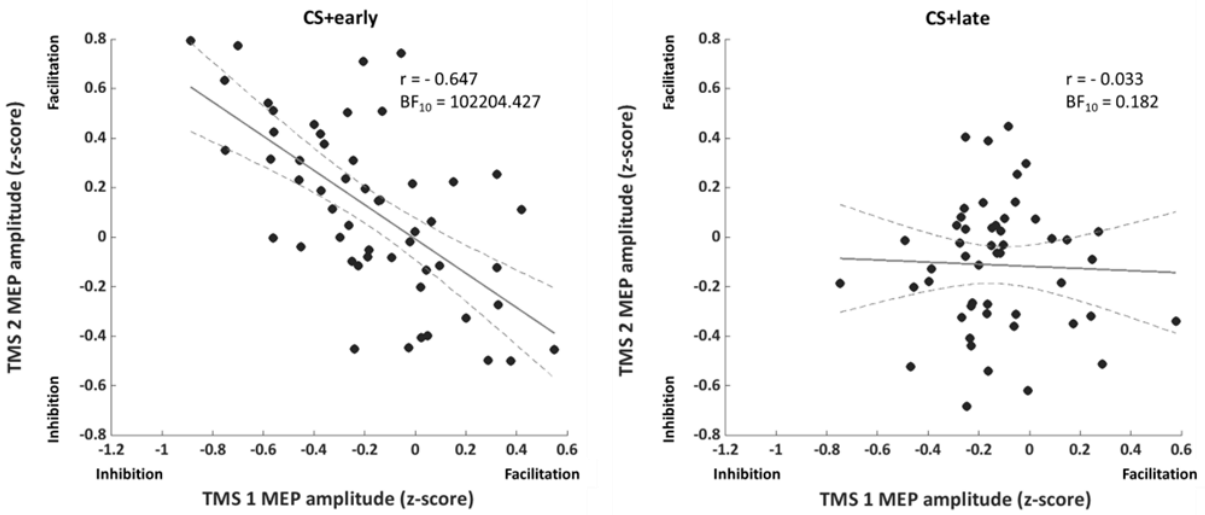

Figure 5.9. Correlations between MEPs recorded at TMS 1 and TMS 2. Dots represent single subject values, dotted lines represent 95% confidence intervals.

Correlations between MEPs and time reproduction

These correlations tested the relation, across all participants, between motor system excitability and participants' ability to accurately reproduce the interval between CS+ onset and shock occurrence. To this end, for each participant, an interval reproduction error was calculated by subtracting the time interval reproduced from the actual time of shock

occurrence for the CS+early (1750 ms - reproduced time) and CS+late (5500 ms - reproduced time). Thus, a negative value indicated that participants delayed the time of shock, while a positive value indicated that participants anticipated the time of shock. The reproduction error was then correlated with MEPs amplitude at TMS 1 and TMS 2, for CS+early and CS+late. For CS+early, Cook's distance analysis (Trujillo-Ortiz, 2005) resulted in excluding four data points (one from experiment 4 and three from experiment 5), both for the correlation with TMS 1 and TMS 2. No correlation was found between reproduction error and MEP at TMS 1 ($n=52$, $r=0.055$, $BF_{10}=0.186$) or at TMS 2 ($n=52$, $r=-0.137$, $BF_{10}=0.274$, Figure 5.10). For CS+late, Cook's distance analysis (Trujillo-Ortiz, 2005) resulted in excluding three data points (all from experiment 5) for the correlation that included MEPs at TMS 1 and four data points (one from experiment 4 and three from experiment 5) for the correlation that included MEPS at TMS 2. A negative correlation was found between reproduction error and MEP at TMS 1 ($n=53$, $r=-0.385$, $BF_{10}=8.761$, Figure 5.10). Thus, lower corticospinal excitability long before the time of the shock was associated with greater anticipation in participants' timing of the shock. No correlation was found between reproduction error and MEP at TMS 2 ($n=52$, $r=0.129$, $BF_{10}=0.427$, Figure 5.10).

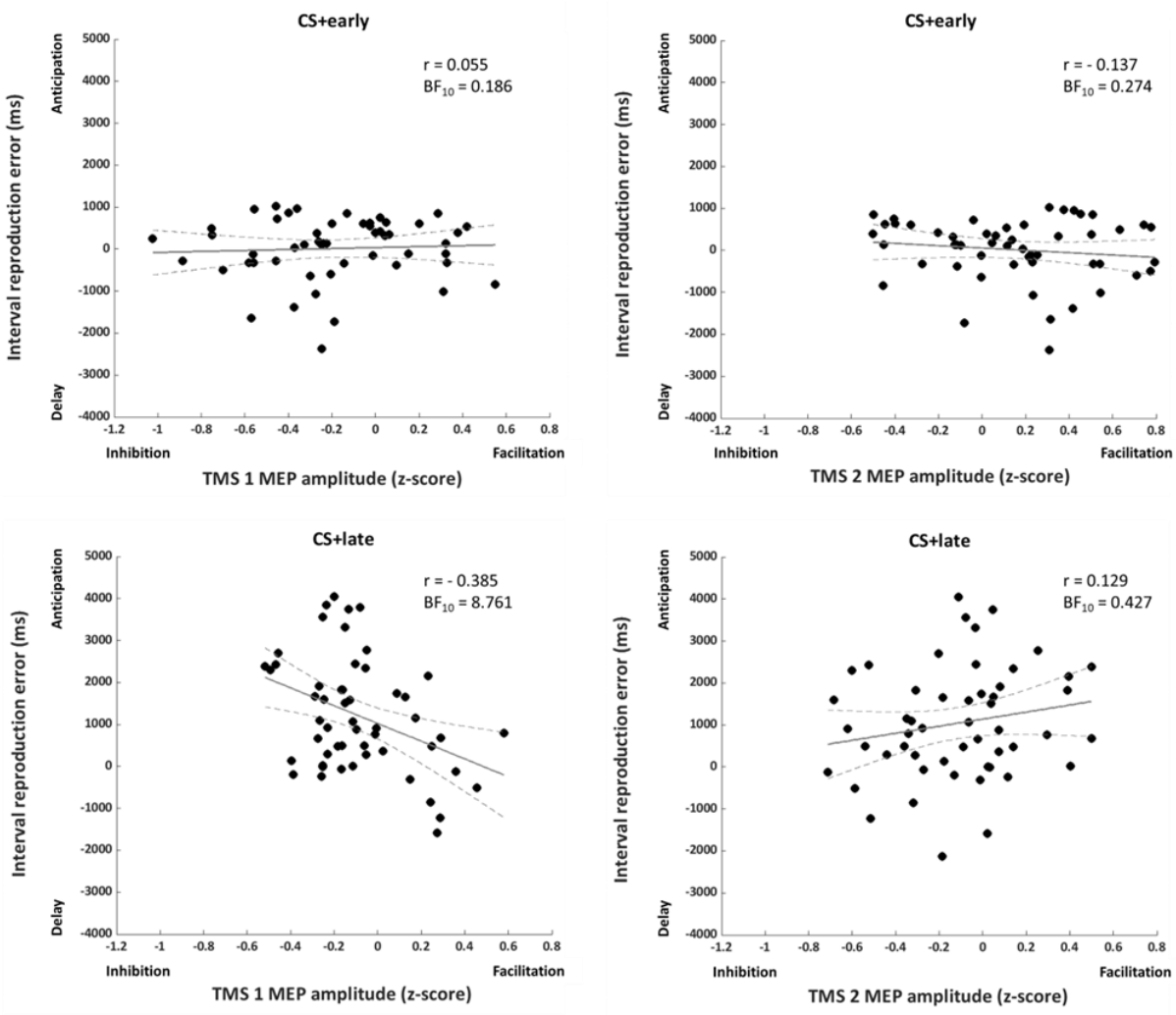

Figure 5.10. Correlations between MEPs and time interval reproduction error. Dots represent single subject values, dotted lines represent 95% confidence intervals.

DISCUSSION

The current study investigated, across two experiments, whether the motor system learns the time of pain by testing whether the inhibition of the motor system, previously found under threat of pain (Betti et al., 2024), is bound to the time of pain occurrence. To this end, corticospinal excitability was probed by administering single-pulse transcranial magnetic stimulation (spTMS) over the left primary motor cortex, during a Pavlovian threat conditioning task in which the temporal imminence of pain (Fanselow et al., 1988; Mobbs et al., 2020) was manipulated. Thus, as participants learned that neutral visual stimuli predicted pain early (CS+early) or later (CS+late) after their appearance, motor evoked potentials (MEPs) were

elicited by spTMS at three critical timepoints during visual stimuli presentation. Two timepoints occurred during the pain anticipation interval, namely long and immediately before the time of pain, and one occurred long after the time of pain. We had three a priori hypotheses regarding the modulation of corticospinal excitability. The first two hypotheses both posited that the motor system encodes the time of pain, but they differed in what aspect is encoded, namely, the precise time of pain or the interval between threat (CS+) onset and pain occurrence. In contrast, the third hypothesis posited that the motor system encodes the presence of a threat, but not the timing of pain. Bayesian informative hypothesis testing was used to test these hypotheses against each other and quantify how much more likely the data are under a given hypothesis as compared to the others (Garofalo et al., 2023; Hoijtink et al., 2019). Finally, correlational analyses explored the relationship between the changes in corticospinal excitability under threat of pain, and the subjective estimates of the time elapsed between threat onset and pain occurrence.

Our findings provide robust evidence that changes in corticospinal excitability acquired during threat conditioning are tied to the expected time of pain. Three key results support this conclusion. First, Bayesian hypothesis testing showed the strongest support for the hypothesis of sustained motor inhibition during pain anticipation. Indeed, in both experiments 1 and 2, corticospinal excitability was reduced long and immediately before the time of pain, recovering only once the time of pain had passed. This dynamic of corticospinal excitability indicates that the motor system differentiates the period leading up to pain from the period afterward, encoding the interval between the onset of a threat and the expected time of pain occurrence through a sustained inhibition. Second, corticospinal excitability appeared to recover long after the time of pain had passed, regardless of whether pain was actually administered. This time-bound recovery, even in trials without a painful shock, reinforces the interpretation that the motor system's response is linked to pain timing rather than the actual occurrence of pain. Correlation analyses further indicated that stronger inhibition during pain anticipation was associated with a more pronounced recovery after the anticipated pain time. Third, correlations between corticospinal excitability and participants' subjective estimates of the interval elapsed from threat onset to pain occurrence revealed that stronger motor inhibition long before the time of pain was associated with greater distortion of pain timing, shifting subjective perception toward greater temporal anticipation of the actual time of pain.

In detail, during the pain anticipation interval, corticospinal excitability was reduced immediately before pain occurrence during CS+late presentation, replicating our previous finding (Betti et al., 2024) showing that Pavlovian conditioning induces conditioned corticospinal inhibition measurable several seconds (>4000ms) after CS+ onset. Here, we extend this finding, demonstrating that a similar reduction in corticospinal excitability also occurs immediately before pain in the CS+early condition, which has a much shorter pain anticipation interval (1690 ms). This result indicates that a brief anticipation interval is sufficient to reduce corticospinal excitability, suggesting that the learned threat value of a visual stimulus rapidly modulates motor system excitability. This is in line with the literature on intrinsic emotional stimuli (Borgomaneri et al., 2024; Schutter et al., 2008), corroborating the tight coupling between visual processing and motor reactivity, particularly for stimuli that are motivationally relevant for survival (LeDoux & Daw, 2018). Critically, a reduction in corticospinal excitability was also observed long before the time of pain during CS+late presentation, suggesting an early recruitment of the motor system during the pain anticipation period, already several seconds before pain is imminent. Importantly, replicating such result in experiment 5 ruled out the possibility that such reduction of corticospinal excitability was due to a generalization effect of the pain-related temporal association established with the CS+early (Cooper et al., 2022; Dunsmoor, Otto, et al., 2017; Dunsmoor & Paz, 2015; Starita et al., 2019). Instead, it enabled us to confirm the early recruitment of the motor system as a physiological response under threat of pain. Notably, a negative correlation emerged between corticospinal excitability long before the time of pain and participants' accuracy in reproducing the time interval between CS+late onset and pain occurrence. Specifically, stronger motor inhibition long before the time of pain was associated with greater distortion of pain timing, with participants reproducing pain occurrence earlier than it actually did. Overall, these findings indicate rapid recruitment of the motor system during pain anticipation, which occurs not only when the time of pain is imminent, but already long before that, soon after a threat of pain appears in the environment. In addition, they may suggest a role for the motor cortex in mediating the transformation of physical time into subjective time, when under threat.

Our results also showed the recovery of corticospinal excitability once the time of pain has passed. Indeed, corticospinal excitability was reduced specifically during pain anticipation, and

not during CS- presentation or long after painful stimulation for CS+early. Importantly, the recovery observed once the time of pain had passed occurred even when no shock was delivered during CS+early presentation. This result corroborates the interpretation that the motor system encodes the expected time of pain, rather than just actual pain occurrence. Additionally, a negative correlation emerged between corticospinal excitability probed immediately before and long after the time of pain for the CS+early, indicating that a stronger reduction in corticospinal excitability during pain anticipation was associated with more pronounced recovery afterwards. These results further highlight the clear discrimination in the motor system of the intervals pre- and post-pain, which aligns its excitability state with the expected time of pain. The recovery of motor excitability after the time of pain may be a marker of motor readiness for defensive action implementation. Additionally, such recovery could represent a physiological marker of psychological relief, typically experienced when an expected negative event is omitted or terminated (Deutsch et al., 2015). Relief of aversive states, including pain, has previously been assessed by showing attenuation of startle (Andreatta et al., 2010, 2012; Mohammadi et al., 2014; Mohammadi & Fendt, 2015; Uzuneser & Fendt, 2020) and increase in skin conductance response (Vervliet et al., 2017; Willems & Vervliet, 2021). Here, we extend these findings by providing evidence of relief through changes in motor system excitability. Notably, our data suggest that this relief effect may be more pronounced following stronger anticipatory responses to pain.

The spatiotemporal proximity or urgency of expected pain critically determines which actions might be effective and how much time is available to choose among them (Fanselow et al., 1988; Mobbs et al., 2020). Temporal imminence thus plays a central role in shaping the type, vigor, and timing of defensive responses (Kirkpatrick & Balsam, 2016; Nasser & Delamater, 2016). Our findings suggest that the motor system participates in pain anticipation across the temporal imminence continuum, being rapidly recruited when a threat for pain appears, until the expected time of pain occurrence. This is consistent with the role of the cortical motor system in event and action timing (Coull & Nobre, 1998; Halsband et al., 1993; Lucchetti et al., 2005; Roux et al., 2003). Under threat of pain, the observed reduction in corticospinal excitability during pain anticipation may support the enactment of defensive responses. Anticipation of aversive events often triggers a threat-monitoring state marked by motor inhibition (e.g., freezing), serving to enhance threat perception and action preparation

(Fanselow, 1994; Hagenaars et al., 2014; Lang & Bradley, 2010; Löw et al., 2015) and prevent temporally inappropriate reactions (Duque et al., 2010; Duque & Ivry, 2009; Touge et al., 1998; Van Elswijk et al., 2007). Such an inhibitory state may be regulated by the prefrontal cortex (Martin-Fernandez et al., 2023; Narayanan et al., 2006; Narayanan & Laubach, 2006), and removed at the expected time of pain, to enable the execution of defensive response. Notably, motor inhibition was observed already several seconds prior to the actual time of pain occurrence, possibly indicating a pain prediction system that prioritizes preemptive motor inhibition over temporal precision. In uncertain environments, premature motor inhibition may facilitate the body's preparation for defense, albeit at the expense of temporal accuracy. Indeed, individuals who exhibited greater inhibition, long before the time of pain, also distorted the time of pain more, anticipating it. Thus, excessive reliance on such preemptive inhibition may mobilize defensive response preparation and create an anticipated (and potentially exaggerated) sense of a pain that may never occur.

In conclusion, our study provides robust evidence that the cortical motor system encodes the time of pain, modulating corticospinal excitability in alignment with learned pain timing and discriminating the pre- and post-pain time intervals. Specifically, the motor system shows a sustained inhibition during pain anticipation, reducing corticospinal excitability from the appearance of a threat in the environment until the time of pain occurrence, and then recovering it once the time of pain has passed. Notably, greater motor inhibition long before the time of pain is associated with greater temporal anticipation of the actual time of pain, positioning this inhibition as a potential physiological marker of individual differences in learned temporal pain predictions. This dynamic modulation of the motor system’s excitability under threat of pain may be crucial to support the enactment of temporally precise defensive responses. Crucially, the modulations here found are not bound to the actual experience of pain, but rather to its expectancy, and are, thus, implemented as soon as individuals anticipate the possibility of pain occurring or reoccurring, even in the absence of current pain or injury. Clinically, our findings should be considered, as chronic or maladaptive motor inhibition may counteract pain management interventions, particularly those aimed at restoring normal motor function. Future research may build upon these findings to explore the implications for therapeutic strategies aimed at mitigating pain responses through targeted modulation of motor system activity.

TASK VALIDATION EXPERIMENT

We conducted a preliminary experiment to test whether the experimental design used in experiments 4 and 5 was able to produce conditioning, measured through skin conductance responses (Lonsdorf et al., 2017). Participants completed a Pavlovian threat conditioning task, during which they learned the association between three visual stimuli and their respective outcomes. The three visual stimuli were filled colored circles (64 pixels diameter, blue #5698D4, pink #C760CA, or yellow #F4E634), representing three different conditioned stimuli. Two of them were conditioned stimuli (CS+) associated with the delivery of an electrotactile shock to the right arm, representing the unconditioned stimulus (US), while the other stimulus (CS-) was never associated with shock. The procedure and statistical analysis follow what is described in Experiment 4. Unlike the main experiment, TMS pulses were not delivered to the participant's scalp, but the TMS noise was still presented and was produced using an intensity of 66% of the maximum stimulator output as the average value that emerged in a previous study (Betti et al., 2024). This choice was intended to minimize differences with the experimental procedure adopted in the main study.

METHODS

Participants

Eleven healthy right-handed volunteers (7 women, aged between 18 and 30 years, M=24, SD=3.51 years) with the same characteristics as those participating in experiments 1 and 2 were tested.

Dependent variables

Skin conductance response (SCR). Galvanic skin conductance was recorded at 5000 Hz (gain switch set to 10, low-pass to 10 Hz), from pre-gelled snap electrodes (BIOPAC EL501) placed on the hypothenar eminence of the palmar surface of the left hand, connected to an EDA100C module of BIOPAC MP-150 System (Goleta, CA). The digitalized electrodermal activity signal was processed using Autonomate 2.8 (Green et al., 2014) running in MATLAB (The Mathworks) to obtain trough-to-peak SCR values. The digitalized signal was down-sampled at 625 Hz, an

SCR was considered valid if the trough-to-peak response occurred between 500 to 5440 ms following the stimulus onset, lasted for a maximum of 5000 ms, and was greater than 0.02 µS. Raw SCR data were z-transformed, and values exceeded ± 2 SD of the sample mean were excluded as outliers. The raw SCR data were z-transformed separately for each participant to control for interindividual variability in SCR.

Time interval reproduced. The reproduced time intervals were recorded and preprocessed as in experiments 1 and 2.

Explicit acquisition of threat conditioning. Explicit ratings of threat conditioning were recorded and preprocessed as in experiments 1 and 2.

RESULTS

Skin conductance response (SCR)

Only no-shock trials were included in the analysis to remove the impact that shocks administered during the CS+ presentation produced on SCR. The Bayesian rmANOVA was performed with CS (CS-, CS+early, CS+late) as a within-subject factor to analyze SCR data. A main effect of CS emerged (BF_{10}=97.691). Post-hoc comparisons highlighted that SCR was significantly higher for both CS+early (mean (M) = -0.219, 95% credible interval (CI) [-0.368, -0.069]) and CS+late (M=-0.317, 95% CI [-0.418, -0.217]) than CS- (M=-0.513, 95% CI [-0.593, -0.432]; BF_{10}=12.008; err%=5.405e-6; BF_{10}=11.500; err%=4.941e-6, respectively), but did not differ between CSs+ (BF_{10}=0.660; err%=0.017; Figure 5.11).

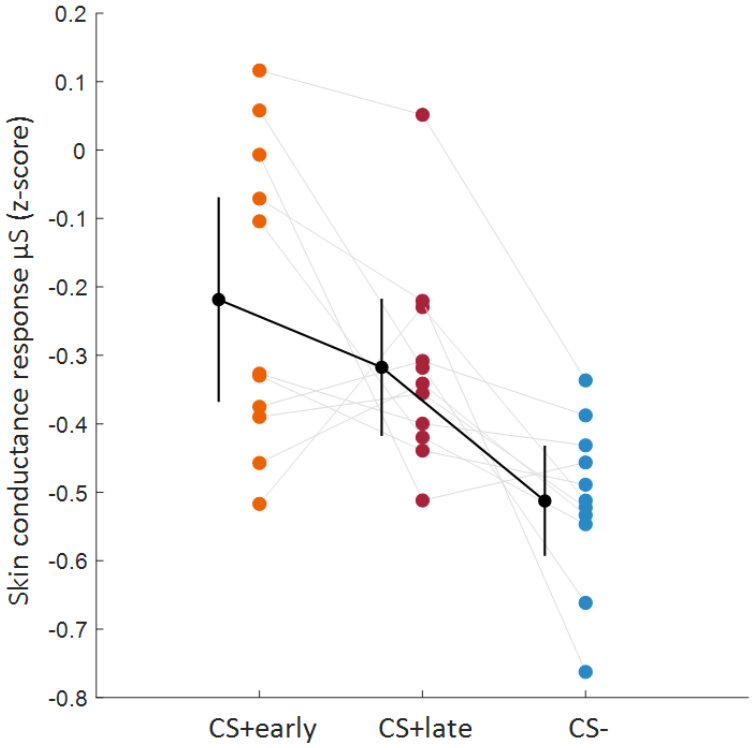

Figure 5.11. The plot shows individual participants' data (colored dots), group means (black dots), and 95 % credible intervals (vertical black lines) of SCR (µS) for CS+early, CS+late, and CS-. Each paired set of observations is connected by a gray line.

Time interval reproduced

A Bayesian paired t-test was performed to compare the mean of interval reproduced for the CS+early (M=2448.364, 95% CI [1274.488, 3622.239]) and CS+late (M=4148.218, 95% CI [2946.770, 5349.666]). We observed a difference in CSs (BF_{10}=20.558; err%=6.956e-7), meaning that participants learned the interval between the CSs+ onset and the shock delivery (Figure 5.12).

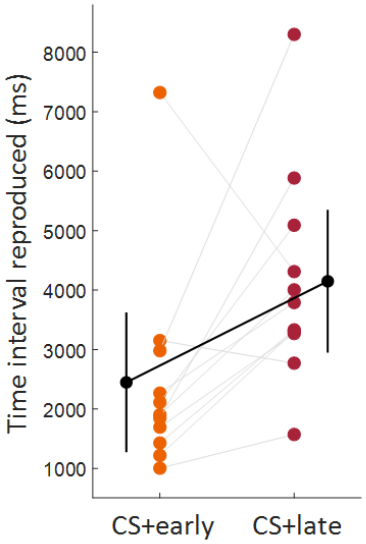

Figure 5.12. The plot shows individual participants' data (colored dots), group means (black dots), and 95 % credible intervals (vertical black lines) of the time interval reproduced (ms) for CS+early and CS+late. Each paired set of observations is connected by a gray line.

Explicit acquisition of threat conditioning

Three Bayesian rmANOVA and post-hoc comparisons were performed with CS (CS+early, CS+late, CS-) as a within-subject factor to analyze stimuli valence, shock expectancy and shock contingency ratings. Participants rated the CS- (M=7.455, 95% CI [6.203, 8.706]) as more pleasant than the CS+early and CS+late (BF_{10}=10096.182; err%=1.444e-8; BF_{10}=8425.968; err%=6.182e-8, respectively), whereas ratings for CS+early (M=2.36, 95% CI [1.269, 3.458]) and CS+late (M=1.45, 95% CI [0.487, 2.422]) did not differ (BF_{10}=0.685; err%=0.017). Moreover, participants rated as less arousing the CS- (M=0.818, 95% CI [0.093, 1.543]) compared to the CS+early and the CS+late (BF_{10}=5.162e+6; err%=1.230e-8; BF_{10}=1.013e+6; err%=9.375e-9, respectively), whereas ratings for CS+early (M=7.909, 95% CI [7.438, 8.380]) and CS+late (M=8.273, 95% CI [7.318, 9.227]) did not differ (BF_{10}=0.390; err%=0.009). Regarding the CS-US contingency, participants rated the contingency lower in the presence of the CS- (M=0, 95% CI [0, 0]) than the CS+early and CS+late (BF_{10}=1.444e+6; err%=4.915e-8; BF_{10}=266990.211; err%=2.604e-9, respectively), whereas ratings for CS+early (M=7.273, 95% CI [6.367, 8.179]) and CS+late (M=6.818, 95% CI [5.785, 7.851]) did not differ (BF_{10}=0.555; err%=0.014).

DISCUSSION

The results of this task validation experiment confirm that the experimental design used in Experiments 4 and 5 was effective in producing Pavlovian threat conditioning. Skin conductance responses differentiated between the CS+ and CS-, demonstrating successful acquisition of conditioned autonomic responses. In addition, the reproduced time intervals indicate that participants learned the temporal relationship between CS onset and shock delivery, consistent with temporal expectancy effects reported in previous conditioning studies. Explicit ratings further supported successful conditioning, with CS+ stimuli evaluated as more unpleasant, more arousing, and more strongly associated with the US than the CS-. Together, these converging measures validate the conditioning procedure and confirm that the presence of TMS noise does not disrupt threat learning. Importantly, SCRs were only collected in this preliminary experiment, as the delivery of TMS pulses during CS presentation in the main experiments could interfere with electrodermal recordings. This validation step, therefore provides a crucial methodological basis for the subsequent studies, ensuring that the absence of SCR in Experiments 1 and 2 does not limit the interpretation of conditioning effects observed at the cortical motor level.

CHAPTER 5:
PERSISTENT, MUSCLE-SPECIFIC CORTICOSPINAL INHIBITION REFLECTS ANTICIPATORY MOTOR ADAPTATION TO PAIN

EXPERIMENT 6

THEORETICAL BACKGROUND

Although muscle activity adapts in response to pain, the variability of these adaptations led to the idea that no single mechanism or outcome underlies this process. Adaptation of movement in the presence of pain, or even in anticipation of pain, is thought to serve a protective function. Several theories have been formulated over the years that bear on the relationship between pain and muscle activity. The two major theories are the Vicious Cycle Theory and the Pain Adaptation Model.

According to the Vicious Cycle Theory (Roland, 1986), pain arising from factors like abnormal posture, movement, or stress induces reflexive muscle hyperactivity, which promotes spasm or fatigue and, in turn, aggravates pain and dysfunction, perpetuating the cycle. Despite being more of a conceptual hypothesis than a mechanistic model, this theory obtained considerable clinical influence due to its simplicity and inspired strategies aimed at breaking the cycle in various pain conditions (Johansson & Sojka, 1991; Mense S., 1993; Stohler, 1999). In contrast, the Pain Adaptation Model (Lund et al., 1991) assumes that pain itself does not originate from muscle hyperactivity but rather acts through brainstem or spinal motor circuits to alter muscle activity. Specifically, the model posits that, in response to pain, agonist muscles decrease their activity, while antagonist muscles increase their activity, leading to smaller and slower movements (Farina et al., 2005; Graven-Nielsen et al., 1997, 2002; Martin et al., 2008; Svensson et al., 1997). These coordinated changes serve as a protective reflex, limiting the range and velocity of movement and thereby reducing the risk of further injury and pain. This model has been further expanded to highlight that pain results in a new recruitment strategy

for motor units influenced by the multidimensional (i.e., biological and psychosocial) components of the pain experience (Peck et al., 2008). Finally, more recently, the new theory of motor adaptation to pain (Hodges & Tucker, 2011) emphasized that the nervous system does not rely on a single stereotypical response. Instead, it selects from a repertoire of strategies, including increased, decreased, or redistributed activity, depending on the context, with the common goal of protection from actual or anticipated harm (Salomoni & Graven-Nielsen, 2012; Shanahan et al., 2015). This view shifts the focus from rigid, uniform patterns to a more flexible and individualized set of adaptations. Yet, most models have focused on motor responses during pain itself rather than on how such protective adaptations may arise before pain occurs.

Understanding motor adaptations to pain anticipation requires the identification of psychophysiological markers that capture protective behavioral adjustments before movement occurs (F. Li & Jackson, 2022). Previous studies show that corticospinal excitability is typically reduced in the presence (Algoet et al., 2018; Bank et al., 2013; Barnes et al., 2021; Chowdhury et al., 2022; Le Pera et al., 2001; Urban et al., 2004; Valeriani et al., 1999b) or during the anticipation (Betti et al., 2024; Dalbagno et al., 2025; Fossataro et al., 2018) of a painful stimulation, consistent with the notion that inhibiting motor output may protect the body from further harm.

The Pavlovian threat conditioning paradigm, in which neutral cues are paired with painful stimuli, has proven to be a powerful tool to study pain anticipation (Biggs et al., 2020). Most studies, however, examined motor adaptation only during the acquisition phase (Betti et al., 2024; Dalbagno et al., 2025; Fossataro et al., 2018), and even within this phase, the classical predictions of pain adaptation models (Hodges & Tucker, 2011; Lund et al., 1991; Peck et al., 2008) have rarely been tested in terms of corticospinal excitability. This leaves open the question of how well these models account for anticipatory motor adjustments at the level of the corticospinal pathway, and how this response evolves when threat contingencies change, such as during extinction (Lonsdorf et al., 2017). Exploring the dynamics of corticospinal modulation across these phases can therefore shed light on the flexibility and persistence of motor adaptations to anticipated pain. Indeed, although there is impressive body of knowledge on the acquisition and extinction of autonomic arousal, it may not generalize to all

conditioned fear responses, particularly more voluntary responses or evaluative responses (Armstrong et al., 2022; Beckers et al., 2013; Sevenster et al., 2012; van Meurs et al., 2014).

Taken together, these considerations highlight the need to investigate whether agonist and antagonist muscles adopt distinct motor strategies in anticipation of pain, in line with classical adaptation models, and how corticospinal excitability changes across acquisition and extinction phases, reflecting the flexibility and persistence of these anticipatory protective adaptations.

Here, we investigated anticipatory motor adaptations to pain using a Pavlovian threat conditioning task, in which neutral visual cues predicted brief painful shocks to the right forearm. Corticospinal excitability was recorded from the FDI and the ECR muscles of participants' right arm. To examine how muscles function in the roles of agonist or antagonist influences these adaptations, half of the participants received the painful shock in proximity to the ECR muscle, making it the agonist, while the other half received the painful shock in proximity to the FCR, making the ECR an antagonist. Single-pulse TMS was applied across acquisition and extinction phases to capture dynamic changes in corticospinal excitability. This approach allowed us to assess whether agonist and antagonist muscles adopt distinct motor strategies during pain anticipation and how these strategies evolve across different phases of threat learning. Because participants remained at rest, the terms agonist and antagonist are used here in a functional sense, referring to the muscle's role relative to the site of potential threat. When the painful stimulation was delivered near the ECR, this muscle was considered the agonist (directly threatened effector). In contrast, when stimulation targeted the FCR, the ECR served as the antagonist (functionally opposite to the threatened structure). This manipulation enabled us to test whether corticospinal adaptations follow the agonist–antagonist pattern predicted by pain adaptation models, even in the absence of overt movement

METHODS

Participants

Forty-four healthy volunteers participated in the experiment (22 women, aged between 19 and 36 years, M = 23.59, SD = 3.51 years). The sample size was calculated through a power analysis conducted with MorePower 6.0.4 (Campbell & Thompson, 2012) with the following parameters: Analysis: ANOVA; Design factors: repeated measures 2 (Phases: acquisition, extinction) *2(CS: CS-, CS+) *Muscle shocked (between subject factor with 2 levels); Effect of interest: 2*2; Alpha: 0.05; Power: 0.8 (partial eta = 0.15, Cohen f = 0.42). The effect size was based on the effect size found in our previous study (Betti et al., 2024). All participants were right-handed, as assessed by the Edinburgh Handedness Inventory (Oldfield, 1971) with normal or corrected-to-normal visual acuity. They were all screened for TMS exclusion criteria, to exclude any history of head trauma or head surgery, seizures, family history of epilepsy, implanted hardware, medications, neurological and medical illnesses, according to safety guidelines (Rossi et al., 2009, 2021) as well as any current neurological, psychiatric, and medical conditions. In addition, they had no recent history of trauma affecting the upper limbs, nor were they currently suffering from any pain or taking any analgesic medication. The study followed the American Psychological Association Ethical Principles of Psychologists and Code of Conduct and the Declaration of Helsinki and was approved by the Bioethics Committee of the University of Bologna (protocol number 224364). All participants were naive to the experiment's purpose and provided their written informed consent for participation.

Procedure

Painful shock calibration. The painful shock consisted of a 2 ms electro-cutaneous stimulation generated by a Digitimer Stimulator (Model DS7A, Digitimer Ltd., UK) and delivered through pre-gelled Ag/AgCl snapped electrodes (Friendship Medical, SEAg-S-15000/15x20) attached to participants' right forearm in proximity of the ECR muscle for half of the sample and in proximity of the FCR muscle for the other half. The shock intensity was calibrated for each participant as following the same procedure as the previously described experiments. First, to tailor the intensity of the tactile stimulation, the experimenter set the shock intensity using an ascending staircase procedure (Cornsweet, 1962; Klein, 2001), starting from 0 mA in steps

of 0.1 mA to a level perceived by the participant as clearly detectable but not at all unpleasant. Then, to find the intensity of the painful stimulation, the shock intensity was further increased in steps of 0.5 mA to reach the pain tolerance level (i.e., the maximum tolerable pain). This procedure was repeated twice, and the mean was calculated to obtain the final value of the painful shock used during the experiment (shock on ECR group: M=61.62 mA, SD=23.12; shock on FCR group: M=69.97 mA, SD=30.31). Stimuli did not exceed individual tolerance limits, in line with the International Association for the Study of Pain (IASP) guidelines (Charlton, 1995).

Pavlovian threat conditioning task. Participants completed a Pavlovian threat conditioning task (Mathôt et al., 2012), composed of an acquisition and an extinction (see Figure 6.1); the task was performed continuously without pauses between phases (Haaker et al., 2014). During the acquisition, they learned the association between two visual stimuli and their respective outcomes. The two visual stimuli were filled colored circles (64 pixels diameter, green #51D968 or pink #C760CA), representing the two different conditioned stimuli (CSs); color assignment to each CS was counterbalanced among participants. One of them was CS+ associated with the delivery of the electrotactile shock to the right forearm, while the other was a CS- never associated with shock. In each experimental trial, one of the CSs appeared in the center of a computer screen on a black background for 4560ms. The inter-trial interval (ITI) was jittered between 8000-9000ms, and before the beginning of each trial, a white fixation cross was presented for 1 s in the center of the screen. In each trial, single-pulse TMS (spTMS) was delivered 4500 ms after the CS onset to record the MEP amplitude. Each CS was presented 20 times, for a total of 40 trials. For the CS+, the shock occurred in 12 trials (i.e., 60% reinforcement rate) at the CS offset. The first four trials consisted of two presentations of each CS, where only one of the CSs+ was reinforced, while the remaining trials proceeded in pseudo-random order with no more than two consecutive CSs of the same type in a row. The subsequent extinction phase had the same structure as the acquisition phase, but no shocks were delivered.

Before starting the task, participants were instructed as follows: “You will see a colored circle appearing on the screen. Sometimes, the circle may deliver a shock. Your task is to understand with which color the circle gives you the shock”. In addition, they were instructed to observe the screen throughout the task while keeping their hands and arms relaxed, without executing any motor response.

At the end of the task, explicit learning was assessed by having participants rate the valence and arousal associated with each CS and the CS-shock contingency on a series of 11-point Likert scales (ranging from 0 to 10). The following three questions were answered regarding each CS, presented in random order: i) “When I saw this circle, the feeling I had was” (Valence rating; ranging from 0=‘unpleasant’ to 10=‘pleasant’); ii) “When I saw this circle, the feeling I had was” (Arousal rating; ranging from 0=‘not activated at all’ to 10=‘extremely activated’); iii) “This circle gave me the shock” (Contingency rating; from 0=‘never’ to 10=‘always’).

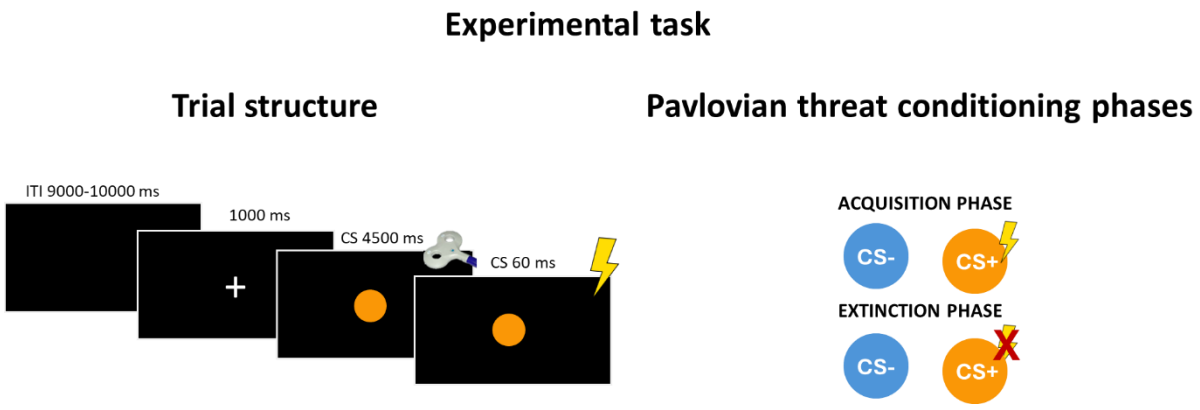

Figure 6.1. Illustration of the experimental task. On the left, the trial structure is represented. Conditioned stimuli (CSs) were presented on the screen for 4500 ms, then double coil spTMS was delivered to the left M1 to collect MEPs from the right FDI muscle. The painful outcome was delivered at the CS+ offset in acquisition phase. On the right, the Pavlovian threat conditioning phases are represented. Two types of CSs were used: a CS+ associated with the painful shock on the right arm during acquisition (60% reinforcement rate) and a CS- never paired with any outcome. During the extinction phase, no shock was delivered.

Stimulation and recordings

The experimental setup (see Figure 6.2) for the Pavlovian threat conditioning task involved the delivery of painful electrotactile stimulation (shocks) to the participant's right forearm. Additionally, in each trial, electromyography was recorded continuously from the first dorsal interosseus (FDI), and the extensor carpi radialis (ECR) muscles of the right arm, while spTMS pulses were delivered over the left primary motor cortex (M1) (Betti et al., 2024).

Electrodermal activity. Electrodermal activity was recorded continuously at 1250 Hz, with a 10 Hz low-pass filter, from pre-gelled snap electrodes (BIOPAC EL501) placed on the hypothenar

eminence of the palmar surface of the left hand, connected to a BIOPAC MP-150 System (Goleta, CA, USA).

Electromyography recording. Surface EMG activity was recorded from the FDI muscle of the participant's right hand at 5000 Hz, with a 5 kHz lowpass filter, through a pair of Ag/AgCl electrodes (BIOPAC EL501) placed in a belly-tendon montage connected to an EMG100C module of the BIOPAC MP-150 System (Goleta, CA). After skin preparation, a small amount of isotonic hyposaturated conductant gel (Lectron III Gel, NEUROSPEC) was added to the electrodes, which were placed and fixed on the target positions. The active electrode was placed over the muscle belly, determined by palpation during maximum voluntary contraction, while the reference and ground electrodes were placed over the proximal interphalangeal juncture and the radial styloid process for the FDI muscle, and over the ulnar styloid process and the lateral epicondyle for the ECR muscle.

Transcranial magnetic stimulation (TMS). Single-pulse TMS was administered using a 70-mm figure-of-eight coil connected to a Magstim Rapid2 stimulator (Magstim Co, Whitland, United Kingdom). Standard procedures of the MEP literature (see Betti et al., 2022; Groppa et al., 2012; Rossini et al., 1994) were used for the TMS application. Pulses were delivered to the left M1 of the participant, in correspondence with the target muscle representation. The coil was placed on the head at a 45-degree angle relative to the interhemispheric fissure, with the handle pointing laterally and caudally (Hallett, 2007; Mills et al., 1992). The optimal scalp position, which is the best position for the coil on the scalp at which the lower intensity of stimulation elicits the largest MEP of both the right hand FDI and the right forearm ECR muscles, was determined by moving the coil in approximately 0.5-cm steps around the presumed hand motor area. Once found, the optimal scalp position was then marked on a tight-fitting cap worn by the participants, ensuring correct coil placement throughout the experiment. For each participant, the resting motor threshold (rMT) was then determined by finding the lowest stimulation intensity inducing MEPs with at least ≥ 50 mV peak-to-peak amplitude in a relaxed muscle in 5 out of 10 trials (Rossini et al., 1994) in both the FDI and ECR muscles at the same time. Although the figure-of-eight coil provides relatively high spatial resolution, the cortical representations of intrinsic hand muscles (FDI) and forearm muscles (ECR) within the primary motor cortex are adjacent and partially overlapping (Schieber, 2001). As a result, a single optimal scalp position can reliably evoke MEPs in both muscles (as in Betti

et al., 2024). Importantly, the optimal position on the scalp was indeed defined functionally, based on the coil position that elicited stable and reproducible MEPs in both target muscles (Rossini et al., 2015). During the experiment, the intensity of TMS stimulation was then set at 120% of the individual rMT to ensure a stable and reliable recording of cortical output while accounting for interindividual differences in cortical excitability (Di Lazzaro et al., 2004; Rothwell, 1997), in accordance with established safety and methodological guidelines for non-invasive brain stimulation (Rossini et al., 2015). The rMT ranged from 59% to 93% (mean=76%, SD=11.17) of the maximum stimulator output. Motor evoked potentials recorded during the experiment were then preprocessed and analyzed as described in the dependent variables section.

To exclude any non-specific, long-lasting changes in basal corticospinal excitability that could be related to the TMS, the task, or the shocks per se, and thus affecting the results, baseline corticospinal excitability was probed at the beginning and the end of the experimental session. This was done by delivering 15 single TMS pulses and acquiring MEPs while participants passively observed a fixation cross on the screen. An inter-pulse interval of at least 5000 ms was adopted, thereby avoiding changes in corticospinal excitability due to repeated TMS pulses (Chen et al., 1997). No difference emerged when comparing MEPs recorded during the initial (FDI: M=1.112, SD=0.776; ECR: M=0.914, SD=0.468) and final (FDI: M=1.199, SD=0.710; ECR: M=0.965, SD=0.508) baseline phases (FDI: $t_{(39)}$=-1.480, p=.147; ECR: $t_{(39)}$=-1.150, p=.257); note that 3 participants have been excluded from the baseline analysis because of recording issues.

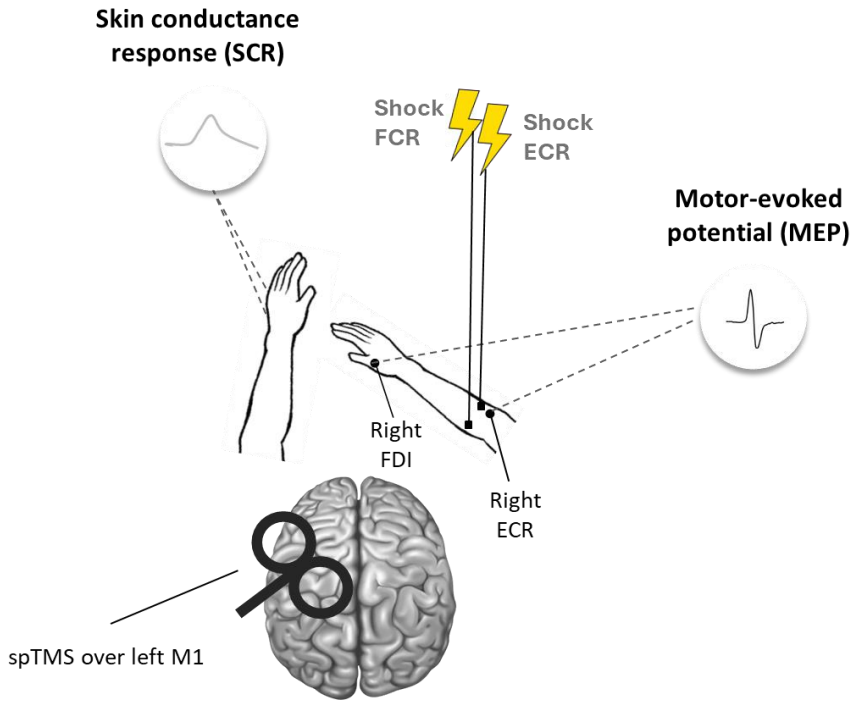

Figure 6.2. Stimulations and recordings for the Pavlovian threat conditioning task. The shock was delivered to the ECR muscle in half of the sample and to the FCR muscle in the other half. SpTMS was delivered over the left M1 to elicit MEP from the right FDI and ECR muscles of participants. SCR was recorded from the palm of the left hand of participants.

Dependent variables

Skin conductance response. To obtain trough-to-peak SCR values to analyze differences in average conditioned SCR between CSs, the digitalized signal was processed using Autonomate 2.8 (Green et al., 2014) to obtain trough-to-peak SCR values. A SCR was considered valid if the trough-to-peak deflection started between 0.5–4.5 seconds following the CS onset, lasted for a maximum of 5 seconds, and was greater than 0.02 μS; trials that did not meet these criteria were scored as zero and retained for further analysis (Storm et al., 2001). To control interindividual variability in SCR amplitudes, the raw SCR amplitudes were z-transformed using the average and standard deviation calculated across all CSs, separately for each participant (Boucsein et al., 2012; Lykken & Venables, 1971). Z-scored SCR amplitudes were then averaged for each CS and used for statistical analyses. One participant has been excluded from the analysis due to a technical problem during the signal recording.

Corticospinal excitability response. EMG data recorded from FDI and ECR were preprocessed offline in MATLAB using custom-made scripts. First, epochs from the time of the TMS pulse to 60 ms after it were extracted from the continuous data for MEP identification and analysis, and epochs from –100 ms to the time of the TMS pulse were extracted to identify any muscular preactivation, before TMS delivery. For each epoch, the min and max MATLAB functions were then used to determine the minimum and maximum peaks in the EMG signal. The signal was then visually inspected to ensure the correctness of the automatic procedure. Muscular preactivations were defined as trials in which peaks of EMG activity in the 100 ms window preceding the TMS pulse exceeded 2 SD from the mean background EMG activity. MEPs preceded by such preactivation were discarded to prevent contamination of the MEP measurements (a total of 6.90% of MEPs for FDI and 6.78% for ECR were excluded). This enabled the exclusion of any influence of participants' movement or movement that may have been evoked by shock delivery to influence MEPs recorded on the next trial. For the remaining trials, individual peak-to-peak MEP amplitudes (mV) were calculated and considered as a proxy for corticospinal excitability during threat conditioning. Then, MEPs whose amplitude exceeded ± 2 SD of the mean amplitude for each experimental condition were excluded as outliers (0% MEP excluded for all two muscles). To control interindividual variability in MEP amplitudes, the raw MEP amplitudes were z-transformed using the average and standard deviation calculated across all CSs, separately for each participant. Z-scored MEP amplitudes were then averaged for each CS and used for statistical analyses. One participant has been excluded from the analysis due to a technical problem during the signal recording.

Explicit ratings. Participants' explicit ratings of CSs valence, CSs arousal, CSs-shock contingency for each CS were used in statistical analyses to compare responses between CSs.

Statistical analysis

Analyses were performed with JASP 0.16.3 (Love et al., 2019). Repeated-measures ANOVA (rmANOVA) were used to investigate differences between more than 2 conditions, while paired t-tests were used to investigate differences between two conditions. The CS type and the Experimental phases were the within-subject factors, while the Muscle shocked was the between-subject factor. Planned contrasts were adopted to test differences among CSs due to learning in the acquisition and extinction phases. Degrees of freedom and p-values were Greenhouse–Geisser corrected whenever a violation of the sphericity assumption occurred.

To test for any basal change in CSE during the experiment, the raw MEPs acquired during the initial and final baseline blocks were compared through paired t-tests. Partial eta- squared (η^2_p) was computed as an estimate of effect sizes for the ANOVAs' main effects and interactions, while Cohen's d was used for the t-tests (Lakens, 2013). A statistical significance threshold of p<.05 was adopted for all analyses.

RESULTS

Explicit ratings

CS valence. The 2 (CS: CS-, CS+) × 2 Muscle shocked rmANOVA showed the main effect of CS ($F_{(1,41)}$=11.35, p=.002, η^2_p=0.21). Participants rated the CS+ (M=3.59, SD=2.20) as less pleasant than the CS- (M=5.39, SD=2.19), independently of the muscle which received the painful shock.

CS arousal. The 2 (CS: CS-, CS+) × 2 Muscle shocked rmANOVA showed the main effect of CS ($F_{(1,42)}$=83.05, p<.001, η^2_p=0.67). Participants rated the CS+ (M=7.25, SD=1.91) as more arousing than the CS- (M=2.82, SD=2.38), independently of the muscle which received the painful shock.

CS-shock contingency. The 2 (CS: CS-, CS+) × Muscle shocked rmANOVA showed the main effect of CS ($F_{(1,42)}$=133.54, p<.001, η^2_p=0.76). Participants rated the CS+ (M=5.50, SD=1.62) as more often associated with the shock than the CS- (M=0.61, SD=2.07), independently of the muscle which received the painful shock.

Conditioned skin conductance response

A 2 Phase (acquisition, extinction) × 2 CS (CS-, CS+) × 2 Muscle shocked (FCR, ECR) rmANOVA was conducted. A significant Phase × CS interaction effect emerged ($F_{(1,41)}$=19.698, p<.001, η^2_p =0.325; Figure 6.3.A). Planned contrasts revealed that, regardless of the muscle receiving the painful shock, during acquisition SCR was greater for the CS+ (M=0.538, SD=0.399) compared to the CS− (M=−0.146, SD=0.248, p<.001). Despite the overall reduction in SCRs in the extinction phase, responses remained greater for the CS+ (M=−0.027, SD=0.305) than the CS− (M=−0.234, SD=0.167, p=.003). Importantly, both CS+ and CS− responses significantly

decreased from acquisition to extinction (all p<.001), with the reduction being more pronounced for the CS+, as also reflected in the descriptive means. These results indicate that the difference between CS+ and CS− observed at the beginning of extinction likely reflects the associative learning established in the acquisition phase, even though both responses declined.

To further test this interpretation, we repeated the same 2 Phase (acquisition, extinction) × 2 CS (CS-, CS+) × 2 Muscle shocked (FCR, ECR) rmANOVA considering only the second half of trials, when the conditioned response to the CS+ was expected to be fully acquired at the end of acquisition and fully extinguished at the end of extinction. Again, a significant Phase × CS interaction effect emerged ($F_{(1,41)}$=23.168, p<.001, η^2_p =0.361; Figure 6.3.B). Planned contrast showed that, independently of the muscle which received the painful shock, during acquisition, SCR was greater for the CS+ (M=0.337, SD=0.485) than the CS- (M=-0.233, SD=0.158, p<.001); moreover, SCR to the CS+ significantly decreased from acquisition to extinction (p<.001). No other significant difference across conditions emerged (all p≥.162). These results indicate that participants showed successful autonomic discrimination between CS+ and CS− during acquisition, and this discrimination diminished during extinction.

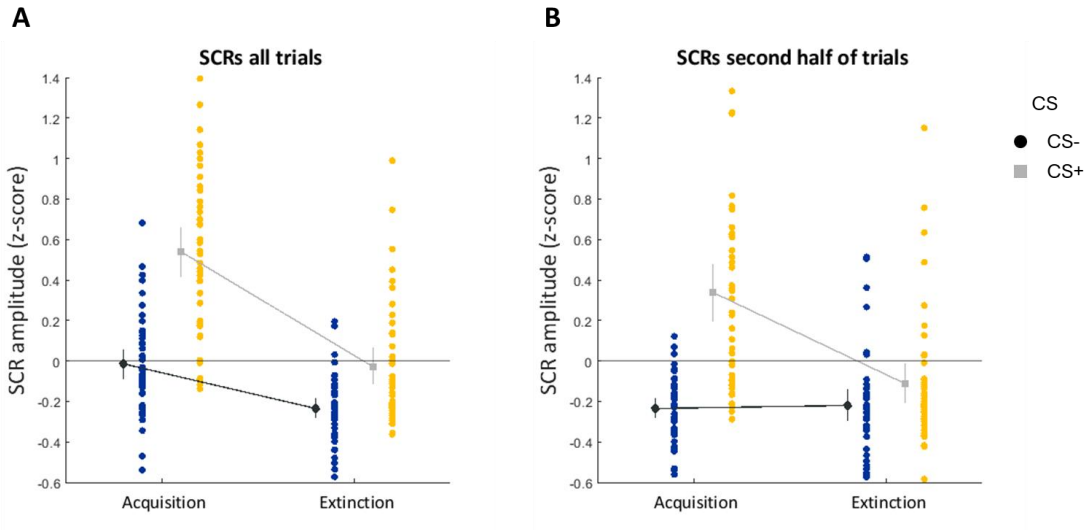

Figure 6.3. Skin conductance responses (SCRs) of participants, including all the trials (**A**) or only the second half of trials (**B**), during the presentation of the CS- (blue dots, black lines) and CS+ (yellow dots and grey lines) in acquisition and extinction phases. Black dots and grey squares represent means, and vertical bars represent their standard error.

Conditioned corticospinal response

A 2 (Phase: acquisition, extinction) × 2 (CS: CS−, CS+) × Muscle shocked rmANOVA on FDI MEP amplitudes was performed. The main effect of CS emerged ($F_{(1,41)}$=15.860, p<.001, η^2_p=0.279), meaning that the MEP amplitude for the CS+ (M=-0.185, SD=0.383) was smaller than for the CS- (M=0.027, SD=0.348), regardless of the phase and the muscle which received the painful shock. Moreover, a significant Phase × CS interaction effect emerged ($F_{(1,41)}$=5.630, p=.022, η^2_p =0.121; Figure 6.4.A). Planned contrasts revealed that both in the acquisition and extinction phases, MEP amplitude was smaller for the CS+ (acquisition: M=-0.207, SD=0.465; extinction: M=-0.164, SD=0.282) compared to the CS- (acquisition: M=-0.070, SD=0.355, p=.033; extinction: M=0.125, SD=0.315, p<.001); in addition, MEP amplitude was smaller for the CS- in acquisition compared to extinction (p=.020), while no difference emerged for the CS+ across phases (p=.581).

A 2 (Phase: acquisition, extinction) × 2 (CS: CS−, CS+) × Muscle shocked rmANOVA on ECR MEP amplitudes was performed. The main effect of CS emerged ($F_{(1,41)}$=6.067, p=.018, η^2_p=0.129), meaning that the MEP amplitude for the CS+ (M=-0.123, SD=0.422) was smaller than for the CS- (M=0.040, SD=0.346), regardless of the phase and the muscle which received the painful shock. Moreover, the Phase × CS × Muscle shocked interaction effect emerged ($F_{(1,41)}$=6.626, p=.014, η^2_p=0.259; Figure 6.4.B). Planned contrasts showed that when the shock was delivered to the ECR muscle, no difference between CS+ and CS- emerged during acquisition in MEP amplitudes (CS+: M=−0.123, SD=0.574; CS−: M=0.043, SD=0.369; p=.925). However, during extinction MEP amplitudes were smaller for CS+ (M=−0.210, SD=0.286) compared to CS− (M=0.076, SD=0.289; p<.001). In contrast, when the shock was delivered to the FCR muscle, no significant difference between CS+ and CS- emerged among phases (all p>.093). These results indicate that corticospinal inhibition was selectively tuned to the muscle associated with the predicted shock during extinction, while no modulation occurred in the non-threatened muscle.

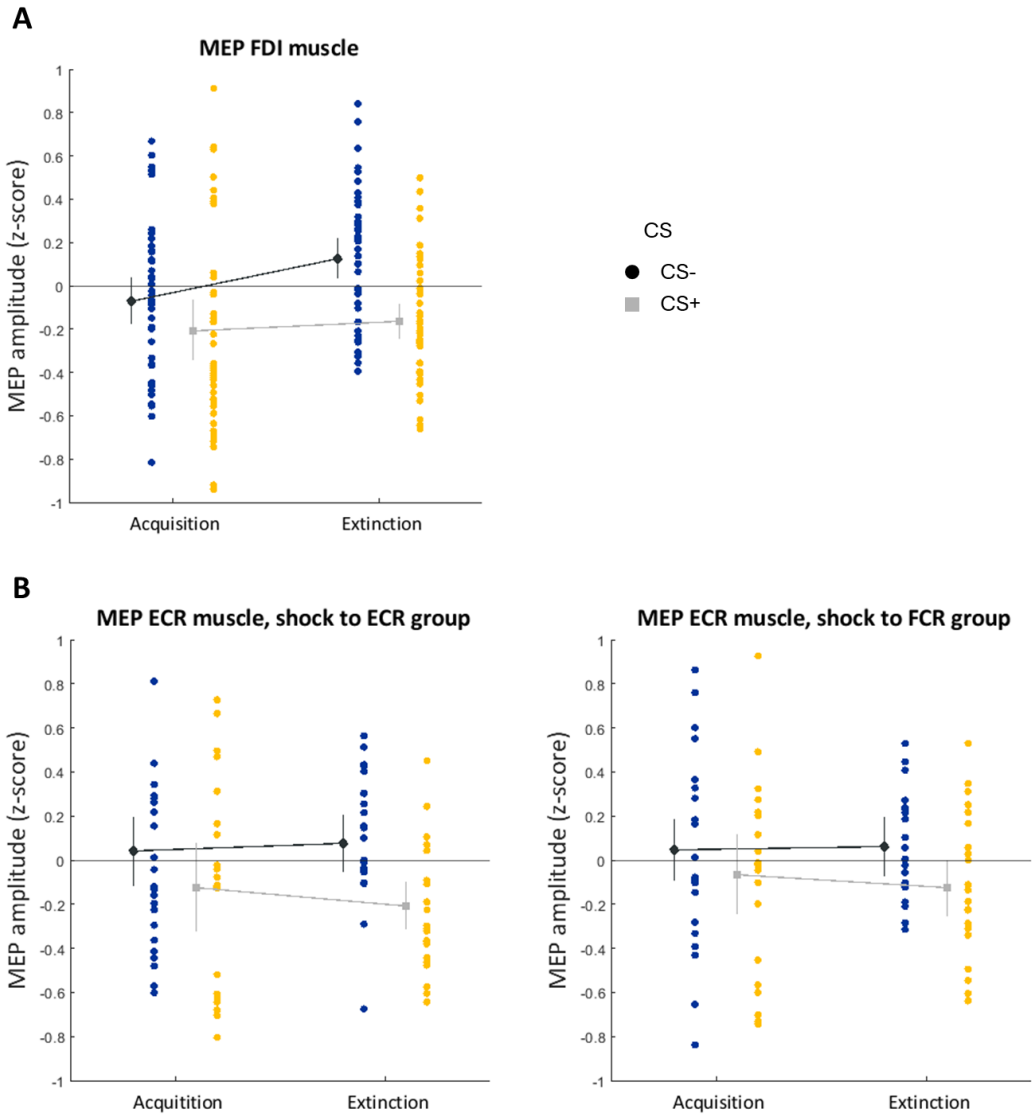

Figure 6.4. Motor evoked potentials (MEPs) amplitudes of participants from the FDI muscle (**A**), the ECR muscle when the shock was delivered to the ECR muscle and the ECR muscle when the shock was delivered to the FCR muscle (**B**), during the presentation of the CS- (blue dots, black lines) and CS+ (yellow dots and grey lines) in acquisition and extinction phases. Black dots and grey squares represent means, and vertical bars represent their standard error.

DISCUSSION

In this work, we investigated anticipatory motor adaptations to pain using a Pavlovian threat conditioning paradigm. Corticospinal excitability was measured from both the right FDI and ECR muscles, while painful shocks were delivered to the right forearm, localized in proximity to the ECR muscle for half of the participants and in proximity to the FCR muscle for the other

half. This between-subjects manipulation allowed us to examine how muscle-specific adaptations depend on the agonist or antagonist role of the pain-targeted muscle. By assessing responses across acquisition and extinction phases, we were able to test the flexibility of these motor adaptations across changing threat contingencies.

Our results confirmed successful threat learning, as evidenced by both explicit ratings and autonomic responses. Participants rated the CS+ as less pleasant, more arousing, and more often associated with the shock than the CS−. SCRs further indicated that autonomic responses to the CS+ were initially greater than those to the CS− and showed flexibility across the extinction phases. Although a residual response persisted during the first extinction phase, reflecting the carryover of prior learning, the difference between CS+ and CS− diminished in the second half of the phase, consistent with effective extinction. Importantly, these autonomic effects were independent of which muscle received the painful shock, suggesting that SCR reflects a generalized learned threat response rather than a muscle-specific effect (Betti et al., 2024; Dickinson & Balleine, 2002; Pool et al., 2019; Zhang et al., 2016).

In contrast, corticospinal excitability results provided more nuanced, muscle-specific insights. MEPs recorded from the FDI showed a reduction in the MEP amplitude for the CS+ compared to the CS-, regardless of the site of the painful shock, during the acquisition phase. Interestingly, the discrimination between CS+ and CS- persisted in the extinction phases. Differently, MEPs recorded from the ECR muscle revealed a selective, site-dependent effect. When the shock was delivered on the ECR, making it the functionally agonist muscle relative to the threatened site, we observed a reduction of MEP amplitude for CS+ compared to CS−; however, this effect emerged only during the extinction phases, not during acquisition. Conversely, when the painful shock was delivered to the FCR, thereby rendering ECR the functional antagonist muscle relative to the threatened site, no significant CS-dependent modulation of MEPs was observed across any phase.

The resistance of corticospinal excitability to extinction parallels findings from other domains of threat conditioning. For instance, Armstrong and colleagues (2022) demonstrated that conditioned vigilance responses, indexed by sustained gaze bias toward threat cues, can persist after extinction, even when autonomic and subjective fear responses diminished. The authors interpreted this as reflecting an adaptive, energy-efficient mechanism for maintaining environmental monitoring in the context of uncertain threat. Similarly, the maintained

corticospinal inhibition observed in our study may reflect an analog motor response of such vigilance, serving a preparatory state that biases the motor system toward caution even when immediate danger is no longer signaled. This interpretation challenges predictive coding models of pain (Seymour & Mancini, 2020; Song et al., 2021; Tabor et al., 2017; Tabor & Burr, 2019), which proposes that the nervous system continuously updates and maintains priors about potential harm to optimize protective behavior. The omission of an expected shock should generate a negative prediction error, leading to the suppression of the threat prediction and thus facilitating extinction. The fact that this modulation did not occur suggests that the motor system may update differently from other systems involved in threat learning. While the autonomic system rapidly adjusted to the new contingencies, showing a decrease in anticipatory arousal, the motor system appeared less flexible. This difference may arise because the autonomic response is mainly guided by the affective significance of the anticipated event, while the motor system appears to be tuned more to perceptual and sensorimotor cues. In this context, the mere absence of the aversive event may not provide a reliable cue for the motor system to update its prediction.

From this perspective, motor inhibition may persist longer because revising established action priors requires recalibrating not only sensory predictions about pain but also the motor affordances that define which actions are safe to perform. These motor priors tend to update conservatively, maintaining a bias toward bodily protection until sufficient evidence of safety accumulates. Even when a threat is no longer consciously expected, as in extinction when the autonomic system shows the extinction of the conditioned response (Lonsdorf et al., 2017; Mertens & Engelhard, 2020), the motor system may retain a conservative, somatotopically specific inhibition pattern, reflecting an embodied form of vigilance. This persistent inhibition likely represents the maintenance of action priors about potential harm as an adaptive mechanism under uncertainty that ensures bodily protection (Körding & Wolpert, 2004; Sugiyama et al., 2024). However, when such conservative states fail to resolve, they may foster maladaptive patterns of movement inhibition that contribute to the maintenance of chronic pain.

At the muscle-specific level, our findings further support the notion of differentiated motor strategies depending on the functional role of the muscle. When the shock was delivered on the ECR, making it the agonist muscle relative to the threatened site, corticospinal inhibition

for CS+ relative to CS− emerged selectively during the extinction phases. This delayed modulation may reflect the slower updating of motor responses compared with autonomic reactions, even in the absence of immediate aversive feedback. Conversely, when the ECR served as the functionally antagonist muscle (i.e., the shock was delivered to the FCR), no modulation of MEPs was observed, consistent with the predictions of classical models such as the Pain Adaptation Model (Lund et al., 1991), in which agonist and antagonist muscles show opposing adjustments to protect threatened structures. Moreover, although both FDI and ECR were not directly targeted by the painful stimulation when the shock was delivered to the FCR, their differential modulation likely reflects their distinct functional roles within the motor system rather than a simple threatened versus non-threatened distinction. The FDI, as an intrinsic hand muscle, is critically involved in fine motor control and object manipulation and may therefore be particularly sensitive to generalized anticipatory states during threat learning, even when the predicted pain is located elsewhere. In contrast, modulation of the ECR appears to be more tightly linked to its functional relevance with respect to the anticipated site of pain, emerging selectively when the muscle contributes to protecting or stabilizing the threatened body part. Together, these results support the view of the motor system inhibition during pain anticipation as topographically organized (Betti et al., 2024), engaging inhibitory strategies that depend on both the spatial localization of the predicted pain and the functional role of the effector.

From a broader perspective, these findings refine current theoretical models of pain-related motor adaptation. While the Pain Adaptation Model originally emphasized stereotyped reductions in agonist and increases in antagonist activity as reflexive responses to pain, our results, in line with the framework of Hodges and Tucker (2011), suggest that such adaptations can occur even in the anticipatory phase before actual nociceptive input and may persist beyond the extinction of autonomic or explicit conditioned threat responses. This persistence may serve an adaptive purpose, maintaining a conservative motor state that minimizes the risk of re-injury or renewed pain. However, when these inhibitory adaptations become entrenched and fail to resolve, they may contribute to maladaptive movement patterns characteristic of chronic pain conditions.

In conclusion, our results show that while autonomic markers such as SCR reflect transient and flexible learning of threat contingencies, corticospinal excitability captures a more

persistent component of pain anticipation that resists extinction. This maintained inhibition may represent a protective response representing a form of learned vigilance that optimizes safety, but, when excessive or prolonged, could underline the rigidity of motor behavior observed in chronic pain.

While these results support differentiated motor strategies between agonist and antagonist muscles, some methodological limitations should be acknowledged. In our experimental design, corticospinal excitability was recorded only from the ECR and FDI muscles, preventing us from demonstrating a true double dissociation to conclusively test the predictions of the Pain Adaptation Model (Lund et al., 1991). For instance, to confirm reciprocal modulation between agonist and antagonist muscles, it would be necessary to record both from the ECR and FCR when the painful stimulation is applied to the ECR site (Suzuki et al., 2012). Moreover, as specified in the introduction, the terms “agonist” and “antagonist” were used in a functional sense based on the location of the painful stimulation rather than on actual movement dynamics, since participants remained at rest throughout the task. Although this operationalization captures the muscle’s functional relation to the predicted threat, it does not perfectly reflect the physiological definition of agonist–antagonist pairs, which is determined by the action performed (Suzuki et al., 2012). These constraints should be considered when interpreting the muscle-specific findings.

CHAPTER 6:
GENERAL DISCUSSION

The specific and protective motor component of pain anticipation

Pain is a complex and adaptive experience that extends beyond the mere tissue injury. As previously described in the introduction, it arises from the dynamic interplay between sensory, affective, cognitive, and motivational processes, integrating body and brain to serve protection and survival. The Neuromatrix Theory (Melzack, 2001) represented a remarkable shift, describing pain as the output of a distributed neural network that integrates perceptual, homeostatic, and behavioral responses to injury, pathology, or chronic stress, thereby underpinning the multidimensional experience of pain and its behavioral correlates. Predictive and cognitive models further refine this view, framing pain as an inferential process through which the brain anticipates and interprets bodily states rather than passively reacting to nociceptive input (Strube et al., 2023).

From this perspective of predictive coding, pain is not only perceived but also anticipated, driving behavioral adaptations that are protective but can become maladaptive under certain conditions (Hodges & Tucker, 2011). Motor adaptations to pain reflect hierarchical interactions between spinal and cortical systems. Early theoretical models of pain and motor interaction emphasized spinal reflexes and reciprocal inhibition between agonist and antagonist muscles (Lund et al., 1991; Roland, 1986). More recent evidence, instead, highlights how cognitive and emotional factors influence motor output even without nociceptive input (Hodges & Smeets, 2015; Hollander et al., 2010; Moseley et al., 2004; Tucker et al., 2012). Consequently, pain functions both as a sensory event and a motivational signal oriented to organize behavior to minimize harm.

At the neural level, pain engages a distributed network, named the Pain Matrix, including sensory-discriminative regions (S1, S2, thalamus), affective-motivational areas (insula, anterior cingulate cortex), and cognitive-evaluative regions (prefrontal cortex) (Ingvar, 1999;

Peyron et al., 2000; Rainville, 2002). Importantly, this network extends to motor-related areas such as M1, SMA, basal ganglia, and cerebellum (Baciu et al., 1999; Casey et al., 1996; Peyron et al., 2000; Porro et al., 2002; Seifert et al., 2013; Summerfield et al., 2018; Svensson et al., 1998), highlighting the intrinsic link between nociception and action. Indeed, there is evidence that acute painful inputs transiently modulate corticospinal excitability in a muscle-specific manner, suppressing activity in distal muscles while facilitating proximal withdrawal movements (Kofler et al., 1998, 2001). Sustained pain shifts the balance toward cortical inhibition, reflecting protective immobilization (Le Pera et al., 2001; Farina et al., 2001). These temporally distinct modulations illustrate pain's dual role in immediate defense and longer-term protection. Interestingly, similar inhibitory patterns emerge even before pain occurs. There is evidence of preparatory reductions in corticospinal excitability of muscles associated with the predicted pain site on the body (Carlsson et al., 2000; Fossataro et al., 2018). This anticipatory inhibition likely represents a proactive mechanism to prevent unnecessary movement of the threatened body part while mobilizing defensive readiness. Thus, corticospinal excitability serves as a dynamic marker bridging nociceptive processing and motor control.

Considering this theoretical background, the present thesis employed Pavlovian threat conditioning combined with spTMS to examine how anticipation of phasic pain modulates corticospinal excitability. This paradigm provides a robust framework to study how neutral cues acquire aversive value by association with pain, capturing the transition from nociceptive experience to expectation. Indeed, repeated associations between a cue and a painful stimulation enable the study of the predictive processes, assessing anticipatory responses in the motor systems during cue presentation (Seymour, 2019; Vlaeyen & Crombez, 2020; Wiech & Tracey, 2013). Thus, through a set of studies, we progressively explored how the motor system adapts during pain anticipation. Each study addressed a distinct aspect of this anticipatory mechanism, revealing a motor system that learns and predictively modulates its excitability, taking into account the motivational, spatial and temporal features of the anticipated pain.

The first experimental question aimed to investigate whether the anticipatory motor inhibition is specific to pain or generalizes to other somatosensory events. To address this question, we examined how the conditioned corticospinal excitability differentiates between

anticipated painful and non-painful tactile outcomes. Participants learned to anticipate either a painful, tactile, or no-shock outcome while corticospinal excitability was recorded during acquisition and reversal phases. Corticospinal excitability showed a scaled inhibition tuned to the intensity of the anticipated somatosensory event, sensitive to the reversal phase, indicating a flexible encoding of sensory intensity rather than affective value (Pool et al., 2019; Zhang et al., 2016).

The second experimental question aimed to deeply investigate the spatial organization of anticipatory motor inhibition. Using lateralized painful stimuli, corticospinal excitability was recorded across acquisition and reversal conditioning phases. In contrast, corticospinal excitability showed spatially tuned inhibition, contralateral to the predicted pain side, determining a topographically organized representation of expected pain (Betti et al., 2024). This lateralized inhibition likely prevents movements that could exacerbate anticipated pain, revealing a spatially precise motor pathway encoding sensory expectations. This finding is consistent with neuroimaging evidence showing contralateral activation of somatosensory and insular cortices during painful stimulation (Coghill et al., 2001), suggesting that lateralization is not restricted to cortical sensory processing but also emerges at the motor output level.

Another experimental manipulation we performed aimed to investigate the temporal pattern of anticipatory motor inhibition, addressing whether corticospinal excitability modulation occurs only immediately before the expected pain or is sustained throughout the entire anticipation period (Tallot & Doyère, 2020). In the previous studies, TMS was applied 60 ms before the potential pain onset, capturing a narrow temporal window of preparatory processing. To investigate the dynamics during the entire anticipation period of pain anticipation, spTMS was applied over the left primary motor cortex at different time points during the presentation of cues predicting an early or late painful outcome. Specifically, MEPs were elicited at three key time points: immediately before, long before, and long after the time of pain. Results revealed a sustained motor inhibition throughout the anticipation interval, which recovered only after the expected pain time, even when no shock was delivered. Furthermore, early inhibition strength correlated with both the degree of post-expected-time recovery and individual distortions in temporal anticipation, suggesting that participants with stronger early suppression anticipated the timing of the threat more

precisely. These findings indicate that the motor system does not merely react to imminent pain but encodes the entire temporal window of predicted threat. The sustained inhibition likely reflects a preemptive, adaptive mechanism that maintains defensive readiness during the full anticipation period, ensuring that the motor system is optimally prepared to minimize harm throughout the threat interval (Coull & Nobre, 1998; Halsband et al., 1993; Lucchetti et al., 2005; Roux et al., 2003).

Finally, we tested muscle-specific anticipatory adaptations, investigating whether and how the motor system updates across the transition from pain acquisition to extinction. Corticospinal excitability was recorded from both the right FDI and ECR muscles, while painful shocks were delivered to the right forearm, localized in proximity to the ECR muscle for half of the participants and in proximity to the FCR muscle for the other half. This between-subjects manipulation allowed us to examine how muscle-specific adaptations depend on the agonist or antagonist functional role of the targeted muscle. By assessing responses across acquisition and extinction phases, we were able to test the flexibility of these motor adaptations across changing threat contingencies. Corticospinal excitability results showed muscle-specific modulations. While FDI MEPs decreased for CS+ compared to CS− during acquisition and persisted through extinction, ECR MEPs showed site-dependent inhibition emerging during extinction only when shocks targeted ECR, consistent with the Pain Adaptation Model (Lund et al., 1991). These persistent motor adaptations resemble vigilance mechanisms (Armstrong et al., 2022) and align with predictive coding models of pain (Seymour & Mancini, 2020; Song et al., 2021; Tabor et al., 2017; Tabor & Burr, 2019), suggesting context-dependent motor inhibition supports safety but may contribute to maladaptive chronic pain patterns.

Together, these studies depict the motor system as an active component of the pain anticipation network. Corticospinal excitability encodes predicted intensity, spatial location, temporal expectancy, and learned relevance of pain. By integrating Pavlovian conditioning with TMS measures, this work proves that motor inhibition under threat is dynamic, context-sensitive, and enduring, integrating sensory, motivational, and temporal dimensions to optimize defensive behavior. Although the motor system is characterized by a certain degree of flexibility, this flexibility was not uniform across all forms of learning. Indeed, corticospinal excitability dynamically adapted to changes in contingencies only when perceptual evidence supported the update, as observed during the reversal phase. In that context, modulation in

the motor system successfully tracked the newly learned associations, shifting its pattern of inhibition according to the sensory characteristics of the predicted outcomes. This flexibility suggests that the motor system can rapidly reorganize its anticipatory state when the environment provides reliable sensory information, indicating, for instance, that the threat location or somatosensory properties have changed. In contrast, in the context of extinction, where cues were no longer paired with pain but the somatosensory context remained the same, corticospinal inhibition persisted despite the absence of reinforcement.

Contrasting corticospinal specificity with autonomic preparedness

While each study targeted specific features of pain anticipation in the motor system, a broader pattern emerges when comparing autonomic and motor indices across experiments. The autonomic and motor systems appear to operate as complementary components of a unified predictive process, each tuned to distinct aspects of the same anticipated painful stimulation. Specifically, corticospinal excitability provided access to the sensory–discriminative and action-oriented dimension, revealing how the nervous system translates threat prediction into spatially, temporally, and functionally precise motor adjustments. In contrast, skin conductance responses captured the affective-motivational dimension of pain prediction, reflecting the organism's general preparedness and emotional arousal toward potential harm.

Evidence from the first experiment, which focused exclusively on autonomic responses, further supports this view. Participants learned to anticipate either a painful, tactile, or no-shock outcome while SCRs were recorded. Both painful and tactile outcomes elicited unconditioned SCRs, but larger for pain, confirming that both outcomes were suitable to determine psychophysiological responses (Treister et al., 2012; Tursky, 1974). Crucially, conditioned SCRs emerged only in anticipation of pain and increased when expected pain was omitted, reflecting prediction-error-driven responses (Spoormaker et al., 2011, 2012; Stemerding et al., 2022). Computational modeling analyses on conditioned SCRs (Pearce & Hall, 1980; Rescorla & Wagner, 1972) revealed that painful outcomes were implicitly modulated by a greater outcome sensitivity to painful than to tactile stimulations (Nasser & Delamater, 2016; Wu et al., 2017), linking affective valuation of the outcome with both physiological and explicit measures. These findings show that autonomic conditioning

depends on the affective tuning of the system to the salience of anticipated outcomes, intrinsic to painful but not tactile outcomes.

Across the full set of experiments, evidence pointed to a dual predictive system comprising a general autonomic pathway encoding motivational salience and a spatially precise motor pathway encoding sensory expectations. The motor system exhibited lateralized, muscle-specific corticospinal inhibition, likely preventing movements that could exacerbate anticipated pain. In contrast, SCRs increased during pain anticipation, reflecting the affective valuation of the expected somatosensory outcomes (Hall & Rodríguez, 2017; Poulos et al., 1979), and indicating generalized threat learning independent of the site of painful stimulation (Betti et al., 2024; Dickinson & Balleine, 1990; Pool et al., 2019; Zhang et al., 2016). This subdivision of labor echoes contemporary frameworks of defensive control (J. LeDoux & Daw, 2018; Pool et al., 2019), suggesting that while the motor system orchestrates targeted inhibition and action readiness to minimize potential injury, the autonomic system ensures global vigilance and mobilization of energy resources.

Importantly, both systems are shaped by associative learning, exhibiting conditioned responses during pain anticipation, but differ in their flexibility. The motor system showed a stable inhibitory response, suggesting that motor predictions were not updated when no explicit perceptual signal indicated that the threat had ceased. This pattern reveals a selective flexibility, for which the motor system updates its internal model in response to bottom-up sensory changes (for instance, with reversal learning) but resists revision when only top-down inference or contextual learning would require it (for instance, during extinction). Such behavior may reflect a conservative strategy aimed at minimizing the cost of premature disinhibition in uncertain environments, maintaining motor caution until the absence of threat is perceptually confirmed. Differently, the autonomic system responds rapidly to changes in stimulus salience but tends to habituate once the threat value decreases, leading to a faster extinction of conditioned responses. This selective adaptability mirrors predictive coding accounts of learning, in which both autonomic and motor systems may compute prediction errors, but rely on different types of information to update their internal models. While the motor system predominantly uses sensory-discriminative evidence to update motor priors (Friston, 2010), ensuring an optimal trade-off between flexibility and safety in the control of defensive behavior, the autonomic system is more sensitive to affective-motivational

information (Nasser & Delamater, 2016; Pearce & Hall, 1980; Rescorla & Wagner, 1972; Wagner, 1981).

An important open question concerns whether similar autonomic and motor anticipatory responses would also emerge under conditions of more implicit learning, in which attention is not explicitly directed toward the predictive relationship between the conditioned stimulus and the outcome. In the present experiments, participants were informed that specific cues could be associated with an upcoming stimulation, thereby encouraging attentional engagement with the CS–US contingency. However, in everyday life, associative learning about potentially harmful events often occurs incidentally, without explicit monitoring of predictive cues. Future studies could therefore examine whether anticipatory autonomic and corticospinal effects are preserved when task demands shift attention away from the CS, for instance, by engaging participants in a task focused on the sensory or evaluative processing of the US itself. Such designs would help to clarify the ecological relevance of our findings.

A functional interpretation of anticipatory corticospinal inhibition

The observed patterns of corticospinal inhibition lead to important implications for understanding the functional role of the motor system in pain anticipation. The muscle-specific modulation is not consistent with a freezing or tonic immobility interpretation. Indeed, these two mechanisms are typically global, reflecting a general arousal, thus affecting the whole body rather than a specific cluster of muscles, and are primarily associated with autonomic responses to threat, such as heart rate deceleration, startle potentiation, and activation of the PAG and anterior insula (Roelofs, 2017; Wendt et al., 2017). Such responses are largely driven by the affective-motivational characteristics of anticipated threat, reflecting an overall state of orienting and general preparation.

In contrast, anticipatory corticospinal inhibition, which is expressed in muscles according to their functional role, is tuned to the predicted location and timing of the painful stimulus, exhibiting lateralized, topographically and temporally organized responses. This pattern suggests a functional role serving as a targeted protective mechanism, limiting movements that could worsen anticipated pain while preserving the capacity to act when necessary. The selectivity of this mechanism may also reflect the inevitable nature of the anticipated pain in

our paradigm, whereby the optimal strategy is not to avoid the threat entirely but to prevent exacerbating harm through precise motor control.

Interestingly, the coexistence of selective corticospinal inhibition and global autonomic responses during pain anticipation may reflect the engagement of complementary but partially independent systems, each tuned to distinct features of the predicted threat. While autonomic measures index a global affective-motivational state, the motor system appears to prepare targeted, muscle-specific adaptations even in the absence of actual nociceptive input. These changes in corticospinal excitability likely reflect a proactive adjustment of motor activity, allowing selective inhibition or preparation of specific movements depending on the predicted location and timing of pain. In this way, the motor system is activated to prevent actions that could exacerbate the anticipated injury, while the autonomic system supports a more global state of alert and readiness across the body. From this perspective, both systems may operate in parallel, monitoring different aspects of threat and producing coordinated anticipatory responses. While the autonomic system conveys the overall salience and motivational value of the threat, the motor system encodes spatial, temporal, and action-specific information to optimize protective behavior. This interpretation suggests that the brain integrates multiple streams of information to generate the most adaptive anticipatory response, combining preparatory motor inhibition with global autonomic adjustments. An open question, yet, concerns how the motor system would behave when an active response to avoid or mitigate the threat is possible, as this could engage different preparatory processes within the corticospinal excitability.

The dynamics of corticospinal inhibition observed in our experiments raise questions about the anatomical level at which these anticipatory modulations occur, since TMS reflects both cortical and spinal contributions to motor output. This issue has been examined in studies measuring corticospinal excitability after painful stimulation, where MEPs evoked by TMS and TES were compared to disentangle cortical and spinal components (Farina et al., 2001; Kofler et al., 2001; Kotler et al., 1998; Le Pera et al., 2001; Romaniello et al., 2000; Valeriani et al., 1999a, 2001). In our paradigm, however, corticospinal excitability was measured during pain anticipation, before any peripheral nociceptive input. Under these conditions, spinal reflex circuits are unlikely to contribute, suggesting that the observed inhibition predominantly reflects cortical modulation (Wallwork et al., 2017). Nevertheless, an issue could be that

residual spinal effects might occur as a sequential consequence of nociceptive stimulation delivered in the previous trial. Still, the inter-trial interval employed in our studies was sufficiently long to allow the corticospinal tract to return to baseline excitability following painful stimulation, minimizing the likelihood of such carry-over effects (Hassanzahraee et al., 2019; Julkunen et al., 2012). This aspect is further supported by our findings showing that the inhibitory effect on corticospinal excitability was no longer present long after the time of pain (i.e., 3790 ms), indicating a full recovery of baseline excitability between trials. Future studies combining cortical and spinal measures could provide further insight into the relative contributions of these circuits, particularly when comparing anticipatory and post-pain motor responses.

Clinical implications

Pain is an all-encompassing behavioral phenomenon**.** As Sullivan (2008) argued, what distinguishes individuals with and without pain is not simply how they feel, but how they act. People in pain alter their facial expressions, gestures, and posture. Concretely, they restrict or avoid movement, slow down their gait, and often disengage from activities perceived as potentially harmful. These observable behavioral adaptations are not epiphenomena but integral components of the pain system itself. Understanding pain anticipation as a predictive behavioral system has profound clinical implications.

Acute pain, by its very nature, is adaptive: it signals injury, mobilizes attention, and coordinates protective behaviors that facilitate healing. Motor inhibition during pain anticipation, as shown across our studies, likely serves this adaptive function, preventing movements that could exacerbate injury and maintaining readiness for defensive action. However, when pain persists beyond the expected healing period, the same anticipatory mechanisms that once promoted survival can become maladaptive. In chronic pain, anticipatory inhibition may no longer reflect a transient protective state but a learned, persistent motor strategy maintained by altered cortical excitability and predictive error processing. Such maladaptive inhibition could underlie the motor stiffness, guarded movement, and functional disuse commonly observed in chronic pain patients (Hodges & Tucker, 2011). The transition from adaptive to maladaptive pain can thus be interpreted as a

failure in updating predictive models: the brain continues to anticipate pain even in the absence of actual threat.

From a neurophysiological perspective, the sustained inhibition of corticospinal excitability during pain anticipation provides a potential mechanistic substrate for these maladaptive states. Whether this inhibition is adaptive or maladaptive depends on its energetic cost and functional relevance. When the anticipatory inhibition is less costly than the potential reaction required if a threat occurs unexpectedly, it remains adaptive, serving as an efficient preparatory mechanism. Conversely, if this inhibitory state is chronically engaged in the absence of threat, it becomes maladaptive, consuming resources and constraining movement without conferring protection. The same principle applies to extinction: when perceptual evidence indicating safety fails to downregulate inhibition, the system remains locked in a defensive state, maintaining maladaptive readiness.

Predictive coding theories of pain (Seymour & Mancini, 2020; Tabor & Burr, 2019) provide a complementary explanation. When prediction errors fail to update due to persistent threat expectations or distorted sensory precision, cortical inhibitory states may become chronically maintained, fostering both the experience and anticipation of pain even in the absence of nociceptive input. This may explain why chronic pain often persists independently of peripheral pathology (Derbyshire et al., 2004; Eisenberger et al., 2003; Raij et al., 2005). The flexible modulation of corticospinal excitability observed during reversal phases, when the brain successfully updates predictions in response to changing contingencies, contrasts with its persistence during extinction, where learned inhibitory states resist devaluation. Notably, the motor response begins well before the expected onset of pain, and this early, persistent inhibition may contribute to maladaptive anticipation, sustaining defensive motor patterns and potentially underlying mechanisms of pain chronification. This context-dependent pattern suggests that cortical inhibitory mechanisms are flexible when perceptual evidence for change is available but rigid when such evidence is lacking, possibly reflecting a safety bias that prioritizes protection over efficiency. Clinically, this dual property is significant: flexibility supports recovery and adaptation, whereas rigidity may promote the persistence of protective behaviors and maladaptive motor inhibition in chronic pain syndromes.

Integrating our TMS findings into this framework suggests that chronic pain may be sustained by maladaptive plasticity within cortical motor circuits that continue to encode pain

anticipation and threat despite the absence of nociceptive input. These insights highlight the need to target the anticipatory component of pain, and not only its sensory or affective dimensions, in therapeutic interventions. By addressing the cortical inhibitory processes that encode persistent threat predictions, clinicians may help patients not only feel less pain but also restore fluid, confident movement.

Recognizing the motor system's active role in pain processing opens new therapeutic ways. Interventions aimed at modulating cortical excitability, such as repetitive TMS (rTMS), transcranial direct current stimulation (tDCS) (Lefaucheur et al., 2020), or motor imagery training, could help recalibrate sensorimotor integration and reduce maladaptive inhibition. Similarly, behavioral treatments such as graded exposure or motor retraining programs can provide safe sensory evidence that contradicts threat expectations, thereby determining flexible motor responses. From a predictive coding perspective, these approaches may help reduce top-down inhibitory biases by facilitating the extinction of erroneous pain predictions.

Furthermore, the interplay between autonomic and motor systems, highlighted in our studies, may hold diagnostic relevance. While autonomic responses encode the affective–motivational salience of threat, the motor system encodes its sensory-specific and temporal features. An imbalance between these systems (e.g., heightened autonomic arousal coupled with rigid motor inhibition) may represent a physiological marker of vulnerability to chronic pain or anxiety-related disorders. Multimodal physiological measures could thus serve as objective biomarkers for identifying individuals at risk of maladaptive pain anticipation.

In conclusion, understanding pain as a predictive, embodied phenomenon bridges sensory, emotional, and behavioral domains. The studies presented in this thesis demonstrate that the motor system is not a passive recipient of nociceptive information but an active participant in pain prediction and anticipation. When functioning adaptively, it prepares the body for protection and recovery; when dysregulated, it sustains maladaptive patterns that perpetuate chronic pain and disability.

Acknowledgments

When I pause to reflect on the many thoughts, uncertainties, and choices that shape a journey, I come to realize that every success and failure, every moment of ease and exhaustion, every tear of joy or sorrow becomes an essential piece in learning to value oneself. I am deeply grateful to all those who have been part, even in a small way, of the path I have taken over the past years.

I am especially thankful to Giuseppe di Pellegrino and Francesca Starita for their guidance and teachings, to Mirta Fiorio and Luisa Sartori for carefully revising my thesis, to all the colleagues who contributed to my motivation, and to all the students who supported the data collection.

A special dedication goes to my wonderful family, where no endeavor is ever considered impossible.

BIBLIOGRAPHY

Algoet, M., Duque, J., Iannetti, G. D., & Mouraux, A. (2018). Temporal Profile and Limb-specificity of Phasic Pain-Evoked Changes in Motor Excitability. *Neuroscience*, *386*, 240–255. https://doi.org/10.1016/j.neuroscience.2018.06.039

Andraszewicz, S., Scheibehenne, B., Rieskamp, J., Grasman, R., Verhagen, J., & Wagenmakers, E. J. (2014). An Introduction to Bayesian Hypothesis Testing for Management Research: *Https://Doi.Org/10.1177/0149206314560412*, *41*(2), 521–543. https://doi.org/10.1177/0149206314560412

Andreatta, M., Fendt, M., Mühlberger, A., Wieser, M. J., Imobersteg, S., Yarali, A., Gerber, B., & Pauli, P. (2012). Onset and offset of aversive events establish distinct memories requiring fear and reward networks. *Learning and Memory*, *19*(11), 518–526. https://doi.org/10.1101/lm.026864.112

Andreatta, M., Mühlberger, A., Yarali, A., Gerber, B., & Pauli, P. (2010). A rift between implicit and explicit conditioned valence in human pain relief learning. *Proceedings of the Royal Society B: Biological Sciences*, *277*(1692), 2411–2416. https://doi.org/10.1098/rspb.2010.0103

Annau, Z., & Kamin, L. J. (1961). The conditioned emotional response as a function of intensity of the US. *Journal of Comparative and Physiological Psychology*, *54*(4), 428–432. https://doi.org/10.1037/h0042199

Armstrong, T., Engel, M., & Dalmaijer, E. S. (2022). Vigilance: A novel conditioned fear response that resists extinction. *Biological Psychology*, *174*(February), 108401. https://doi.org/10.1016/j.biopsycho.2022.108401

Arvanitidis, M., Falla, D., Sanderson, A., & Martinez-Valdes, E. (2021). Does pain influence force steadiness? A protocol for a systematic review. *BMJ Open*, *11*(1), 1–8. https://doi.org/10.1136/bmjopen-2020-042525

Atlas, L. Y., & Wager, T. D. (2012). How expectations shape pain. *Neuroscience Letters*, *520*(2), 140–148. https://doi.org/10.1016/j.neulet.2012.03.039

Auvray, M., Myin, E., & Spence, C. (2010). The sensory-discriminative and affective-motivational aspects of pain. *Neuroscience and Biobehavioral Reviews*, *34*(2), 214–223. https://doi.org/10.1016/j.neubiorev.2008.07.008

Aylward, J., Valton, V., Ahn, W. Y., Bond, R. L., Dayan, P., Roiser, J. P., & Robinson, O. J. (2019). Altered learning under uncertainty in unmedicated mood and anxiety disorders. *Nature Human Behaviour*, *3*(10), 1116–1123. https://doi.org/10.1038/s41562-019-0628-0

Babiloni, C., Brancucci, A., Percio, C. Del, Capotosto, P., Arendt-Nielsen, L., Chen, A. C. N., & Rossini, P. M. (2006). Anticipatory electroencephalography alpha rhythm predicts subjective perception of pain intensity. *The Journal of Pain*, *7*(10), 709–717. https://doi.org/10.1016/J.JPAIN.2006.03.005

Bach, D. R., & Friston, K. J. (2012). No evidence for a negative prediction error signal in peripheral indicators of sympathetic arousal. *NeuroImage*, *59*(2), 883–884. https://doi.org/10.1016/j.neuroimage.2011.08.091

Baciu, M. V., Bonaz, B. L., Papillon, E., Bost, R. A., Le Bas, J. F., Fournet, J., & Segebarth, C. M. (1999). Central processing of rectal pain: A functional MR imaging study. *American Journal of Neuroradiology*, *20*(10), 1920–1924.

Baldi, E., Lorenzini, C. A., & Bucherelli, C. (2004). Footshock intensity and generalization in contextual and auditory-cued fear conditioning in the rat. *Neurobiology of Learning and Memory*, *81*(3), 162–166. https://doi.org/10.1016/j.nlm.2004.02.004

Bank, P. J. M., Peper, C. E., Marinus, J., Beek, P. J., & Van Hilten, J. J. (2013). Motor consequences of experimentally induced limb pain: A systematic review. *European Journal of Pain (United Kingdom)*, *17*(2), 145–157. https://doi.org/10.1002/j.1532-2149.2012.00186.x

Barnes, K., McNair, N. A., Harris, J. A., Sharpe, L., & Colagiuri, B. (2021). In anticipation of pain: expectancy modulates corticospinal excitability, autonomic response, and pain perception. *Pain*, *162*(8), 2287–2296. https://doi.org/10.1097/j.pain.0000000000002222

Bauer, E. A., Wilson, K. A., & MacNamara, A. (2022). Cognitive and Affective Psychophysiology. In *Comprehensive Clinical Psychology, Second Edition* (Second Edi, Vol. 3). Elsevier. https://doi.org/10.1016/B978-0-12-818697-8.00013-3

Beckers, T., Krypotos, A. M., Boddez, Y., Effting, M., & Kindt, M. (2013). What's wrong with fear conditioning? *Biological Psychology*, *92*(1), 90–96. https://doi.org/10.1016/J.BIOPSYCHO.2011.12.015

Béland, S., Klugkist, I., Raîche, G., & Magis, D. (2012). A short introduction into Bayesian evaluation of informative hypotheses as an alternative to exploratory comparisons of multiple group means. *Tutorials in Quantitative Methods for Psychology*, *8*(2), 122–126. https://doi.org/10.20982/tqmp.08.2.p122

Besson, J.-M., & Chaouch, A. (1987). Peripheral and Spinal Mechanisms of Nociception. *Physiological Reviews*, *67*(1), 67–186.

Betti, S., Badioli, M., Dalbagno, D., Garofalo, S., di Pellegrino, G., & Starita, F. (2024). Topographically selective motor inhibition under threat of pain. *Pain*, 1–12.

Betti, S., Capizzi, M., & Mioni, G. (2025). Temporal processing and non-invasive brain stimulation techniques. In *Neural Bases of Timing and Time Perception, G. Mioni & S. Grondin*. Routledge. In press.

Betti, S., Fedele, M., Castiello, U., Sartori, L., & Budisavljević, S. (2022). Corticospinal excitability and conductivity are related to the anatomy of the corticospinal tract. *Brain Structure and Function*, *227*(3), 1155–1164. https://doi.org/10.1007/s00429-021-02410-9

Bevan, S., & Szolcsányi, J. (1990). Sensory neuron-specific actions of capsaicin: mechanisms and applications. *Trends in Pharmacological Sciences*, *11*(8), 331–333. https://doi.org/10.1016/0165-6147(90)90237-3

Biggs, E. E., Timmers, I., Meulders, A., Vlaeyen, J. W. S., Goebel, R., & Kaas, A. L. (2020). The neural correlates of pain-related fear: A meta-analysis comparing fear conditioning studies using painful and non-painful stimuli. *Neuroscience and Biobehavioral Reviews*, *119*(August), 52–65. https://doi.org/10.1016/j.neubiorev.2020.09.016

Blasini, M., Corsi, N., Klinger, R., & Colloca, L. (2017). Inaugural Review Series Translational Pain Research Nocebo and pain: an overview of the psychoneurobiological mechanisms. *PAIN Reports*, *2*, 1–9. http://dx.doi.org/10.1097/PR9.0000000000000585

Bolles, R. C., Hayward, L., & Crandall, C. (1981). Conditioned taste preferences based on caloric density. *Journal of Experimental Psychology: Animal Behavior Processes*, *7*(1), 59–69. https://doi.org/10.1037/0097-7403.7.1.59

Borgomaneri, S., Vitale, F., Battaglia, S., de Vega, M., & Avenanti, A. (2024). Task-related modulation of motor response to emotional bodies: A TMS motor-evoked potential study. *Cortex*, *171*, 235–246. https://doi.org/10.1016/j.cortex.2023.10.013

Boucsein, W., Fowles, D. C., Grimnes, S., Ben-Shakhar, G., Roth, W. T., Dawson, M. E., & Filion, D. L. (2012). Publication recommendations for electrodermal measurements. *Psychophysiology*, *49*(8), 1017–1034. https://doi.org/10.1111/j.1469-8986.2012.01384.x

Bower, G. H. (1994). A Turning Point in Mathematical Learning Theory. *Psychological Review*, *101*(2), 290–300. https://doi.org/10.1037/0033-295X.101.2.290

Brasil-Neto, J. P., Pascual-Leone, A., Valls-Sole, J., Cohen, L. G., & Hallett, M. (1992). Focal transcranial magnetic stimulation and response bias in a forced-choice task. *Journal of Neurology, Neurosurgery and Psychiatry*, *55*(10), 964–966. https://doi.org/10.1136/jnnp.55.10.964

Brinjikji, W. c, Luetmer, P. H., Comstock, B., Bresnahan, B. W., Chen, L. E., Deyo, R. A., Halabi, S., Turner, J. A., Avins, A. L., James, K., Wald, J. T., Kallmes, D. F., & Jarvik, J. G. (2015). Systematic literature review of imaging features of spinal degeneration in asymptomatic populations. *AJNR. American Journal of Neuroradiology*, *36*(4), 811–816. https://doi.org/10.3174/AJNR.A4173

Campbell, J. I. D., & Thompson, V. A. (2012). MorePower 6.0 for ANOVA with relational confidence intervals and Bayesian analysis. *Behavior Research Methods*, *44*(4), 1255–1265. https://doi.org/10.3758/S13428-012-0186-0/FIGURES/3

Canevaro S., & Bonicalzi V. (1995). Neurosurgical forum Cortical Stimulation for Central Pain. *J Neurosurg*, *91*, 715–716.

Carlsson, K., Andersson, J., Petrovic, P., Petersson, K. M., Öhman, A., & Ingvar, M. (2006). Predictability modulates the affective and sensory-discriminative neural processing of pain. *NeuroImage*, *32*(4), 1804–1814. https://doi.org/10.1016/j.neuroimage.2006.05.027

Carlsson, K., Petrovic, P., Skare, S., Petersson, K. M., & Ingvar, M. (2000). Tickling expectations: Neural processing in anticipation of a sensory stimulus. *Journal of Cognitive Neuroscience*, *12*(4), 691–703. https://doi.org/10.1162/089892900562318

Casey, K. L. (2023). The introduction and current status of the multidimensional model of pain neurobiology. *Frontiers in Pain Research*, *4*(April), 1–7. https://doi.org/10.3389/fpain.2023.1161877

Casey, K. L., Minoshima, S., Morrow, T. J., & Koeppe, R. A. (1996). Comparison of human cerebral activation patterns during cutaneous warmth, heat pain, and deep cold pain. *Journal of Neurophysiology*, *76*(1), 571–581. https://doi.org/10.1152/jn.1996.76.1.571

Castegnetti, G., Tzovara, A., Staib, M., Gerster, S., & Bach, D. R. (2017). Assessing fear learning via conditioned respiratory amplitude responses. *Psychophysiology*, *54*(2), 215–223. https://doi.org/10.1111/psyp.12778

Castegnetti, G., Tzovara, A., Staib, M., Paulus, P. C., Hofer, N., & Bach, D. R. (2016). Modeling fear-conditioned bradycardia in humans. *Psychophysiology*, *53*(6), 930–939. https://doi.org/10.1111/psyp.12637

Charlton, E. (1995). Ethical guidelines for pain research in humans. Committee on Ethical Issues of the International Association for the Study of Pain. *Pain*, *63*(3), 277–278. https://doi.org/10.1016/0304-3959(95)90040-3

Chen, R., Classen, J., Gerloff, C., Celnik, P., Wassermann, E. M., Hallett, M., & Cohen, L. G. (1997). Depression of motor cortex excitability by low-frequency transcranial magnetic stimulation. *Neurology*, *48*(5), 1398–1403. https://doi.org/10.1212/WNL.48.5.1398

Chen, Z. S., & Wang, J. (2023). Pain, from perception to action: A computational perspective. *IScience*, *26*(1), 105707. https://doi.org/10.1016/j.isci.2022.105707

Cho, J. H., Deisseroth, K., & Bolshakov, V. Y. (2013). Synaptic encoding of fear extinction in mPFC-amygdala circuits. *Neuron*, *80*(6), 1491–1507. https://doi.org/10.1016/j.neuron.2013.09.025

Chowdhury, N. S., Chang, W. J., Millard, S. K., Skippen, P., Bilska, K., Seminowicz, D. A., & Schabrun, S. M. (2022). The Effect of Acute and Sustained Pain on Corticomotor Excitability: A Systematic Review and Meta-Analysis of Group and Individual Level Data. *Journal of Pain*, *23*(10), 1680–1696. https://doi.org/10.1016/j.jpain.2022.04.012

Christe, G., Crombez, G., Edd, S., Opsommer, E., Jolles, B. M., & Favre, J. (2021). Relationship between psychological factors and spinal motor behaviour in low back pain: a systematic review and meta-analysis. *Pain*, *162*(3), 672–686. https://doi.org/10.1097/j.pain.0000000000002065

Cisek, P. (2021). *Evolution of behavioural control from chordates to primates*.

Clouston, P. D., Kiers, L., Menkes, D., Sander, H., Chiappa, K., & Cros, D. (1995). Modulation of motor activity by cutaneous input: inhibition of the magnetic motor evoked potential by digital electrical stimulation. *Electroencephalography and Clinical Neurophysiology/ Electromyography*, *97*(2), 114–125. https://doi.org/10.1016/0924-980X(94)00310-4

Coghill, R. C., Gilron, I., & Iadarola, M. J. (2001). Hemispheric lateralization of somatosensory processing. *Journal of Neurophysiology*, *85*(6), 2602–2612. https://doi.org/10.1152/JN.2001.85.6.2602

Colloca, L., Benedetti, F., & Pollo, A. (2006). Repeatability of autonomic responses to pain anticipation and pain stimulation. *European Journal of Pain*, *10*(7), 659. https://doi.org/10.1016/j.ejpain.2005.10.009

Cook, A. J., Woolf, C. J., & Wall, P. D. (1986). Prolonged C-fibre mediated facilitation of the flexion reflex in the rat is not due to changes in afferent terminal or motoneurone excitability. *Neuroscience Letters*, *70*(1), 91–96. https://doi.org/10.1016/0304-3940(86)90443-X

Cooper, S. E., van Dis, E. A. M., Hagenaars, M. A., Krypotos, A. M., Nemeroff, C. B., Lissek, S., Engelhard, I. M., & Dunsmoor, J. E. (2022). A meta-analysis of conditioned fear generalization in anxiety-related disorders. *Neuropsychopharmacology*, *47*(9), 1652–1661. https://doi.org/10.1038/s41386-022-01332-2

Cornsweet, T. N. (1962). The staircrase-method in psychophysics. *The American Journal of Psychology*, *75*(3), 485–491. https://doi.org/10.2307/1419876

Correa, C. M. C., Noorman, S., Jiang, J., Palminteri, S., Cohen, M. X., Lebreton, M., & van Gaal, S. (2018). How the level of reward awareness changes the computational and electrophysiological signatures of reinforcement learning. *Journal of Neuroscience*, *38*(48), 10338–10348. https://doi.org/10.1523/JNEUROSCI.0457-18.2018

Cote, J. N., & Hoeger Bement, M. K. (2010). Update on the relation between pain and movement: Consequences for clinical practice. *Clinical Journal of Pain*, *26*(9), 754–762. https://doi.org/10.1097/AJP.0b013e3181e0174f

Coull, J. T., & Nobre, A. C. (1998). *Where and When to Pay Attention: The Neural Systems for Directing Attention to Spatial Locations and to Time Intervals as Revealed by Both PET and fMRI*.

Coull, J. T., & Nobre, A. C. (2008). Dissociating explicit timing from temporal expectation with fMRI. *Current Opinion in Neurobiology*, *18*(2), 137–144. https://doi.org/10.1016/J.CONB.2008.07.011

Craig, A. D. (2002). How do you feel? Interoception: the sense of the physiological condition of the body. *Nature Reviews Neuroscience*, *3*(August), 655–666.

Critchley, H. D., Mathias, C. J., & Dolan, R. J. (2001). Neural activity in the human brain relating to uncertainty and arousal during anticipation. *Neuron*, *29*(2), 537–545. https://doi.org/10.1016/S0896-6273(01)00225-2

Crombez, G., Eccleston, C., Baeyens, F., & Elen, P. (1998). Attentional disruption is enhanced by the threat of pain. *Behaviour Research and Therapy*, *36*, 195–204. https://pubmed.ncbi.nlm.nih.gov/9613025/

Dalbagno, D., Betti, S., Garofalo, S., Mannari, V., Pellegrino, G. di, & Starita, F. (2025). Learning the time of pain in the human motor system. *Pain*, *00*(00), 1–17. https://doi.org/10.1097/j.pain.0000000000003730

Davis, K. D., Taylor, S. J., Crawley, A. P., Wood, M. L., & Mikulis, D. J. (1997). Functional MRI of pain- and attention-related activations in the human cingulate cortex. *Journal of Neurophysiology*, *77*(6), 3370–3380. https://doi.org/10.1152/jn.1997.77.6.3370

De Ruddere, L., Goubert, L., Stevens, M., Amanda, A. C., & Crombez, G. (2013). Discounting pain in the absence of medical evidence is explained by negative evaluation of the patient. *Pain*, *154*(5), 669–676. https://doi.org/10.1016/j.pain.2012.12.018

Delgado, M. R., Jou, R. L., LeDoux, J. E., & Phelps, E. A. (2009). Avoiding negative outcomes: Tracking the mechanisms of avoidance learning in humans during fear conditioning. *Frontiers in Behavioral Neuroscience*, *3*(NOV). https://doi.org/10.3389/neuro.08.033.2009

Derbyshire, S. W. G., Whalley, M. G., Stenger, V. A., & Oakley, D. A. (2004). Cerebral activation during hypnotically induced and imagined pain. *NeuroImage*, *23*(1), 392–401. https://doi.org/10.1016/j.neuroimage.2004.04.033

Derosiere, G., Vassiliadis, P., & Duque, J. (2020). Advanced TMS approaches to probe corticospinal excitability during action preparation. *NeuroImage*, *213*(November 2019), 116746. https://doi.org/10.1016/j.neuroimage.2020.116746

Deutsch, R., Smith, K. J. M., Kordts-Freudinger, R., & Reichardt, R. (2015). How absent negativity relates to affect and motivation: An integrative relief model. *Frontiers in Psychology*, *6*(MAR), 1–23. https://doi.org/10.3389/fpsyg.2015.00152

Di Lazzaro, V., Oliviero, A., Pilato, F., Saturno, E., Dileone, M., Mazzone, P., Insola, A., Tonali, P. A., & Rothwell, J. C. (2004). The physiological basis of transcranial motor cortex stimulation in conscious humans. *Clinical Neurophysiology*, *115*(2), 255–266. https://doi.org/10.1016/j.clinph.2003.10.009

Dickinson, A., & Balleine, B. (1990). Motivational Control of Instrumental Performance following a Shift from Thirst to Hunger: *Https://Doi.Org/10.1080/14640749008401892*, *42*(4), 413–431. https://doi.org/10.1080/14640749008401892

Dickinson, & Balleine. (2002). The Role of Learning in the Operation of Motivational Systems. In *Stevens' Handbook of Experimental Psychology* (pp. 497–533). John Wiley & Sons, Inc. https://doi.org/10.1002/0471214426.pas0312

Downing, B. D. (1968). Salience and learning rate in concept identification. *Psychonomic Science*, *10*(2), 73–74. https://doi.org/10.3758/BF03331413

Dubé, J. A., & Mercier, C. (2011a). Effect of pain and pain expectation on primary motor cortex excitability. *Clinical Neurophysiology*, *122*(11), 2318–2323. https://doi.org/10.1016/j.clinph.2011.03.026

Dubé, J. A., & Mercier, C. (2011b). Effect of pain and pain expectation on primary motor cortex excitability. *Clinical Neurophysiology*, *122*(11), 2318–2323. https://doi.org/10.1016/j.clinph.2011.03.026

Duits, P., Cath, D. C., Lissek, S., Hox, J. J., Hamm, A. O., Engelhard, I. M., Van Den Hout, M. A., & Baas, J. M. P. (2015). Updated meta-analysis of classical fear conditioning in the anxiety disorders. *Depression and Anxiety*, *32*(4), 239–253. https://doi.org/10.1002/da.22353

Dunsmoor, J. E., Kroes, M. C. W., Braren, S. H., & Elizabeth, A. (2017). *Threat intensity widens fear generalization gradients*. *131*(2), 168–175. https://doi.org/10.1037/bne0000186.Threat

Dunsmoor, J. E., Otto, A. R., & Phelps, E. A. (2017). Stress promotes generalization of older but not recent threat memories. *Proceedings of the National Academy of Sciences of the United States of America*, *114*(34), 9218–9223. https://doi.org/10.1073/pnas.1704428114

Dunsmoor, J. E., & Paz, R. (2015). Fear Generalization and Anxiety: Behavioral and Neural Mechanisms. *Biological Psychiatry*, *78*(5), 336–343. https://doi.org/10.1016/j.biopsych.2015.04.010

Duque, J., & Ivry, R. B. (2009). Role of corticospinal suppression during motor preparation. *Cerebral Cortex*, *19*(9), 2013–2024. https://doi.org/10.1093/cercor/bhn230

Duque, J., Lew, D., Mazzocchio, R., Olivier, E., & Ivry, R. B. (2010). Evidence for two concurrent inhibitory mechanisms during response preparation. *Journal of Neuroscience*, *30*(10), 3793–3802. https://doi.org/10.1523/JNEUROSCI.5722-09.2010

Eisenberger, N. I., Lieberman, M. D., & Williams, K. D. (2003). Does rejection hurt? An FMRI study of social exclusion. *Science (New York, N.Y.)*, *302*(5643), 290–292. https://doi.org/10.1126/SCIENCE.1089134

Elman, I., & Borsook, D. (2018). Threat response system: Parallel brain processes in pain vis-à-vis fear and anxiety. *Frontiers in Psychiatry*, *9*(FEB), 1–11. https://doi.org/10.3389/fpsyt.2018.00029

Emadi Andani, M., Braga, M., Da Dalt, F., Piedimonte, A., Carlino, E., & Fiorio, M. (2025). Premovement activity in the corticospinal tract is amplified by the placebo effect: an active inference account. *Social Cognitive and Affective Neuroscience*, *20*(1), 14. https://doi.org/10.1093/SCAN/NSAF014

Fanselow, M., Angeles, L., & Lester, L. S. (1988). A Functional Behavioristic Approach to Aversively Motivated Behavior: Predatory Imminence as a Determinantof the Topography of Defensive Behavior. *Evolution and Learning*, (January 1988), 197–224. https://doi.org/10.4324/9780203781647-14

Fanselow, M. S. (1994). Neural organization of the defensive behavior system responsible for fear. *Psychonomic Bulletin & Review*, *1*(4), 429–438. https://doi.org/10.3758/BF03210947

Farina, D., Arendt-Nielsen, L., & Graven-Nielsen, T. (2005). Experimental muscle pain reduces initial motor unit discharge rates during sustained submaximal contractions. *Journal of Applied Physiology*, *98*(3), 999–1005. https://doi.org/10.1152/japplphysiol.01059.2004

Farina, S., Tinazzi, M., Le Pera, D., & Valeriani, M. (2003). Pain-related modulation of the human motor cortex. *Neurological Research*, *25*(2), 130–142. https://doi.org/10.1179/016164103101201283

Farina, S., Valeriani, M., Rosso, T., Aglioti, S., Tamburin, S., Fiaschi, A., & Tinazzi, M. (2001). Transient inhibition of the human motor cortex by capsaicin-induced pain. A study with transcranial magnetic stimulation. *Neuroscience Letters*, *314*(1–2), 97–101. https://doi.org/10.1016/S0304-3940(01)02297-2

Foa, E. B., Steketee, G., & Rothbaum, B. O. (1989). Behavioral/cognitive conceptualizations of post-traumatic stress disorder. *Behavior Therapy*, *20*(2), 155–176. https://doi.org/10.1016/S0005-7894(89)80067-X

Fossataro, C., Bucchioni, G., D'Agata, F., Bruno, V., Morese, R., Krystkowiak, P., & Garbarini, F. (2018). Anxiety-dependent modulation of motor responses to pain expectancy. *Social Cognitive and Affective Neuroscience*, *13*(3), 321–330. https://doi.org/10.1093/scan/nsx146

Fossataro, C., Burin, D., Ronga, I., Galigani, M., Rossi Sebastiano, A., Pia, L., & Garbarini, F. (2020). Agent-dependent modulation of corticospinal excitability during painful transcutaneous electrical stimulation. *NeuroImage*, *217*(May 2019), 116897. https://doi.org/10.1016/j.neuroimage.2020.116897

Friston, K. (2010). The free-energy principle: A unified brain theory? *Nature Reviews Neuroscience*, *11*(2), 127–138. https://doi.org/10.1038/NRN2787;SUBJMETA

Fullana, M. A., Harrison, B. J., Soriano-Mas, C., Vervliet, B., Cardoner, N., Àvila-Parcet, A., & Radua, J. (2016). Neural signatures of human fear conditioning: An updated and extended meta-analysis of fMRI studies. *Molecular Psychiatry*, *21*(4), 500–508. https://doi.org/10.1038/mp.2015.88

Garofalo, S., Finotti, G., Orsoni, M., Giovagnoli, S., & Benassi, M. (2023). *Testing Bayesian Informative Hypotheses in 5 steps with R and JASP*. https://doi.org/10.1177/25152459241260259

Garofalo, S., Giovagnoli, S., Orsoni, M., Starita, F., & Benassi, M. (2022). Interaction effect: Are you doing the right thing? *PLoS ONE*, *17*(7 July), 1–19. https://doi.org/10.1371/journal.pone.0271668

Gershman, S. J. (2016). Empirical priors for reinforcement learning models. *Journal of Mathematical Psychology*, *71*, 1–6. https://doi.org/10.1016/j.jmp.2016.01.006

Gizzi, L., Röhrle, O., Petzke, F., & Falla, D. (2019). People with low back pain show reduced movement complexity during their most active daily tasks. *European Journal of Pain (United Kingdom)*, *23*(2), 410–418. https://doi.org/10.1002/ejp.1318

Golkar, A., Selbing, I., Flygare, O., Öhman, A., & Olsson, A. (2013). Other People as Means to a Safe End: Vicarious Extinction Blocks the Return of Learned Fear. *Psychological Science*, *24*(11), 2182–2190. https://doi.org/10.1177/0956797613489890

Grandjean, J., Derosiere, G., Vassiliadis, P., Quemener, L., Wilde, Y. de, & Duque, J. (2018). Towards assessing corticospinal excitability bilaterally: Validation of a double-coil TMS method. *Journal of Neuroscience Methods*, *293*, 162–168. https://doi.org/10.1016/J.JNEUMETH.2017.09.016

Granovsky, Y., Sprecher, E., & Sinai, A. (2019). Motor corticospinal excitability. *PAIN Reports*, *4*(2), e725.

Graven-Nielsen, T., Lund, H., Arendt-Nielsen, L., Danneskiold-Samsøe, B., & Bliddal, H. (2002). Inhibition of maximal voluntary contraction force by experimental muscle pain: A centrally mediated mechanism. *Muscle & Nerve*, *26*(5), 708–712. https://doi.org/10.1002/MUS.10225

Graven-Nielsen, T., Svensson, P., & Arendt-Nielsen, L. (1997). Effects of experimental muscle pain on muscle activity and co-ordination during static and dynamic motor function. *Electroencephalography and Clinical Neurophysiology - Electromyography and Motor Control*, *105*(2), 156–164. https://doi.org/10.1016/S0924-980X(96)96554-6

Green, S. R., Kragel, P. A., Fecteau, M. E., & LaBar, K. S. (2014a). Development and validation of an unsupervised scoring system (Autonomate) for skin conductance response analysis. *International Journal of Psychophysiology : Official Journal of the International Organization of Psychophysiology*, *91*(3), 186–193. https://doi.org/10.1016/J.IJPSYCHO.2013.10.015

Green, S. R., Kragel, P. A., Fecteau, M. E., & LaBar, K. S. (2014b). Development and validation of an unsupervised scoring system (Autonomate) for skin conductance response analysis. *International Journal of Psychophysiology*. https://doi.org/10.1016/j.ijpsycho.2013.10.015

Grönroos, M., & Pertovaara, A. (1993). Capsaicin-induced central facilitation of a nociceptive flexion reflex in humans. *Neuroscience Letters*, *159*(1–2), 215–218. https://doi.org/10.1016/0304-3940(93)90837-B

Groppa, S., Oliviero, A., Eisen, A., Quartarone, A., Cohen, L. G., Mall, V., Kaelin-Lang, A., Mima, T., Rossi, S., Thickbroom, G. W., Rossini, P. M., Ziemann, U., Valls-Solé, J., & Siebner, H. R. (2012). A practical guide to diagnostic transcranial magnetic stimulation: Report of an IFCN committee. *Clinical Neurophysiology*, *123*(5), 858–882. https://doi.org/10.1016/j.clinph.2012.01.010

Gu, X., Hoijtink, H., Mulder, J., & Rosseel, Y. (2019). Bain: a program for Bayesian testing of order constrained hypotheses in structural equation models. *Https://Doi.Org/10.1080/00949655.2019.1590574*, *89*(8), 1526–1553. https://doi.org/10.1080/00949655.2019.1590574

Gu, X., Mulder, J., Deković, M., & Hoijtink, H. (2014). Bayesian evaluation of inequality constrained hypotheses. *Psychological Methods*, *19*(4), 511–527. https://doi.org/10.1037/met0000017

Gu, X., Mulder, J., & Hoijtink, H. (2018). Approximated adjusted fractional Bayes factors: A general method for testing informative hypotheses. *British Journal of Mathematical and Statistical Psychology*, *71*(2), 229–261. https://doi.org/10.1111/BMSP.12110

Haaker, J., Golkar, A., Hermans, D., & Lonsdorf, T. B. (2014). A review on human reinstatement studies: An overview and methodological challenges. In *Learning and Memory*. https://doi.org/10.1101/lm.036053.114

Hagenaars, M. A., Oitzl, M., & Roelofs, K. (2014). Updating freeze: Aligning animal and human research. *Neuroscience & Biobehavioral Reviews*, *47*, 165–176. https://doi.org/10.1016/J.NEUBIOREV.2014.07.021

Hall, G., & Rodríguez, G. (2017). Habituation and conditioning: Salience change in associative learning. *Journal of Experimental Psychology: Animal Learning and Cognition*, *43*(1), 48–61. https://doi.org/10.1037/xan0000129

Hallett, M. (2007). Transcranial Magnetic Stimulation: A Primer. *Neuron*, *55*(2), 187–199. https://doi.org/10.1016/j.neuron.2007.06.026

Halsband, U., Ito, N., Tanji, J., & Freund, H.-J. (1993). *The role of premotor cortex and the supplementary motor area in the temporal control of movement in man* (pp. 243–266). Brain, Volume 116, Issue 1.

Hamm, A. O., & Vaitl, D. (1996). Affective learning: awareness and aversion. *Psychophysiology*, *33*, 698–710.

Hassanzahraee, M., Zoghi, M., & Jaberzadeh, S. (2019). Longer Transcranial Magnetic Stimulation Intertrial Interval Increases Size, Reduces Variability, and Improves the Reliability of Motor Evoked Potentials. *Brain Connectivity*, *9*(10), 770–776. https://doi.org/10.1089/brain.2019.0714

Henson, R. (2006). Forward inference using functional neuroimaging: Dissociations versus associations. *Trends in Cognitive Sciences*, *10*(2), 64–69. https://doi.org/10.1016/j.tics.2005.12.005

Hodges, P. W., Moseley, G. L., Gabrielsson, A., & Gandevia, S. C. (2003). Experimental muscle pain changes feedforward postural responses of the trunk muscles. *Experimental Brain Research*, *151*(2), 262–271. https://doi.org/10.1007/s00221-003-1457-x

Hodges, P. W., & Smeets, R. J. (2015). Interaction between pain, movement, and physical activity: Short-term benefits, long-term consequences, and targets for treatment. *Clinical Journal of Pain*, *31*(2), 97–107. https://doi.org/10.1097/AJP.0000000000000098

Hodges, P. W., & Tucker, K. (2011). Moving differently in pain: A new theory to explain the adaptation to pain. *Pain*, *152*(SUPPL.3), S90–S98. https://doi.org/10.1016/j.pain.2010.10.020

Hoijtink, H., Gu, X., & Mulder, J. (2019). Bayesian evaluation of informative hypotheses for multiple populations. *British Journal of Mathematical and Statistical Psychology*, *72*(2), 219–243. https://doi.org/10.1111/bmsp.12145

Hoijtink, H., Mulder, J., van Lissa, C., & Gu, X. (2019). A Tutorial on Testing Hypotheses Using the Bayes Factor. *Psychological Methods*. https://doi.org/10.1037/met0000201

Hoijtink, H., van Kooten, P., & Hulsker, K. (2016a). Why Bayesian Psychologists Should Change the Way They Use the Bayes Factor. *Multivariate Behavioral Research*, *51*(1), 2–10. https://doi.org/10.1080/00273171.2014.969364

Hoijtink, H., van Kooten, P., & Hulsker, K. (2016b). Why Bayesian Psychologists Should Change the Way They Use the Bayes Factor. *Multivariate Behavioral Research*, *51*(1), 2–10. https://doi.org/10.1080/00273171.2014.969364

Hollander, M. Den, De Jong, J. R., Volders, S., Goossens, M. E., Smeets, R. J., & Vlaeyen, J. W. (2010). Fear reduction in patients with chronic pain: A learning theory perspective. *Expert Review of Neurotherapeutics*, *10*(11), 1733–1745. https://doi.org/10.1586/ern.10.115

Homan, P., Levy, I., Feltham, E., Gordon, C., Hu, J., Li, J., Pietrzak, R. H., Southwick, S., Krystal, J. H., Harpaz-Rotem, I., & Schiller, D. (2019). Neural computations of threat in the aftermath of combat trauma. *Nature Neuroscience*, *22*(3), 470–476. https://doi.org/10.1038/s41593-018-0315-x

Hsieh, J. C., Stone-Elander, S., & Ingvar, M. (1999). Anticipatory coping of pain expressed in the human anterior cingulate cortex: A positron emission tomography study. *Neuroscience Letters*, *262*(1), 61–64. https://doi.org/10.1016/S0304-3940(99)00060-9

IASP, (Int. Assoc. Study Pain). (1979). *Pain terms: a list with definitions and notes on usage. Recommended by the IASP Subcommittee on Taxonomy - PubMed*. PAIN. https://pubmed.ncbi.nlm.nih.gov/460932/

Ingvar, M. (1999). Pain and functional imaging. *Philosophical Transactions of the Royal Society B: Biological Sciences*, *354*(1387), 1347–1358. https://doi.org/10.1098/rstb.1999.0483

Jentsch, V. L., Wolf, O. T., & Merz, C. J. (2020). Temporal dynamics of conditioned skin conductance and pupillary responses during fear acquisition and extinction. *International Journal of Psychophysiology*, *147*, 93–99. https://doi.org/10.1016/j.ijpsycho.2019.11.006

Jiang, X., Burleigh, L., & Greening, S. G. (2021). Complete the triangulation: Quantifying differential fear conditioning with a noninterfering and sensitive behavioral measure along with self-report and physiological measures. *Psychophysiology*, *58*(8), 1–12. https://doi.org/10.1111/psyp.13831

Johansen, J. P., Fields, H. L., & Manning, B. H. (2001). The affective component of pain in rodents: Direct evidence for a contribution of the anterior cingulate cortex. *Proceedings of the National Academy of Sciences of the United States of America*, *98*(14), 8077–8082. https://doi.org/10.1073/pnas.141218998

Johansson, H., & Sojka, P. (1991). Pathophysiological mechanisms involved in genesis and spread of muscular tension in occupational muscle pain and in chronic musculoskeletal pain syndromes: A hypothesis. *Medical Hypotheses*, *35*(3), 196–203. https://doi.org/10.1016/0306-9877(91)90233-O

Julkunen, P., Säisänen, L., Hukkanen, T., Danner, N., & Könönen, M. (2012). Does second-scale intertrial interval affect motor evoked potentials induced by single-pulse transcranial magnetic stimulation? *Brain Stimulation*, *5*(4), 526–532. https://doi.org/10.1016/j.brs.2011.07.006

Kaneko, K., Kawai, S., Taguchi, T., Fuchigami, Y., Yonemura, H., & Fujimoto, H. (1998). Cortical motor neuron excitability during cutaneous silent period. *Electroencephalography and Clinical Neurophysiology - Electromyography and Motor Control*, *109*(4), 364–368. https://doi.org/10.1016/S0924-980X(98)00031-9

Kangas, B. D., Ang, Y. S., Short, A. K., Baram, T. Z., & Pizzagalli, D. A. (2024). Computational Modeling Differentiates Learning Rate From Reward Sensitivity Deficits Produced by Early-Life Adversity in a Rodent

Touchscreen Probabilistic Reward Task. *Biological Psychiatry Global Open Science*, *4*(6), 100362. https://doi.org/10.1016/j.bpsgos.2024.100362

Karos, K., Meulders, A., Gatzounis, R., Seelen, H. A. M., Geers, R. P. G., & Vlaeyen, J. W. S. (2017). Fear of pain changes movement: Motor behaviour following the acquisition of pain-related fear. *European Journal of Pain (United Kingdom)*. https://doi.org/10.1002/ejp.1044

Katayama, Y., Tsubokawa, T., & Yamamoto, T. (1994). Chronic motor cortex stimulation for central deafferentation pain: experience with bulbar pain secondary to Wallenberg syndrome. *Stereotact Funct Neurosurg*, *62*, 295–199.

Kenins, P. (1982). Responses of single nerve fibres to capsaicin applied to the skin. *Neuroscience Letters*, *29*(1), 83–88. https://doi.org/10.1016/0304-3940(82)90369-X

Khera, T., & Rangasamy, V. (2021). Cognition and Pain: A Review. *Frontiers in Psychology*, *12*(May), 1–11. https://doi.org/10.3389/fpsyg.2021.673962

Kirkpatrick, K., & Balsam, P. D. (2016). Associative learning and timing. *Current Opinion in Behavioral Sciences*, *8*, 181–185. https://doi.org/10.1016/J.COBEHA.2016.02.023

Klein, S. A. (2001). Measuring, estimating, and understanding the psychometric function: A commentary. *Perception & Psychophysics 2001 63:8*, *63*(8), 1421–1455. https://doi.org/10.3758/BF03194552

Kluytmans, A., van de Schoot, R., Mulder, J., & Hoijtink, H. (2012). Illustrating Bayesian evaluation of informative hypotheses for regression models. *Frontiers in Psychology*, *3*(JAN), 1–11. https://doi.org/10.3389/fpsyg.2012.00002

Knechtle, D., Schmid, S., Suter, M., Riner, F., Moschini, G., Senteler, M., Schweinhardt, P., & Meier, M. L. (2021). Fear-Avoidance beliefs are associated with reduced lumbar spine flexion during object lifting in pain-free adults. *Pain*, *162*(6), 1621–1631. https://doi.org/10.1097/j.pain.0000000000002170

Knight, D. C., Nguyen, H. T., & Bandettini, P. A. (2005). The role of the human amygdala in the production of conditioned fear responses. *NeuroImage*, *26*(4), 1193–1200. https://doi.org/10.1016/J.NEUROIMAGE.2005.03.020

Kofler, M., Fuhr, P., Leis, A. A., Glocker, F. X., Kronenberg, M. F., Wissel, J., & Stetkarova, I. (2001a). Modulation of upper extremity motor evoked potentials by cutaneous afferents in humans. *Clinical Neurophysiology*, *112*(6), 1053–1063. https://doi.org/10.1016/S1388-2457(01)00540-5

Kofler, M., Fuhr, P., Leis, A. A., Glocker, F. X., Kronenberg, M. F., Wissel, J., & Stetkarova, I. (2001b). Modulation of upper extremity motor evoked potentials by cutaneous afferents in humans. *Clinical Neurophysiology*, *112*(6), 1053–1063. https://doi.org/10.1016/S1388-2457(01)00540-5

Kofler, M., Glocker, F. X., Leis, A. A., Seifert, C., Wissel, J., Kronenberg, M. F., & Fuhr, P. (1998a). Modulation of upper extremity motoneurone excitability following noxious finger tip stimulation in man. *Neuroscience Letters*, *246*(2), 97–100. https://doi.org/10.1016/S0304-3940(98)00243-2

Kofler, M., Glocker, F. X., Leis, A. A., Seifert, C., Wissel, J., Kronenberg, M. F., & Fuhr, P. (1998b). Modulation of upper extremity motoneurone excitability following noxious finger tip stimulation in man: A study with transcranial magnetic stimulation. *Neuroscience Letters*, *246*(2), 97–100. https://doi.org/10.1016/S0304-3940(98)00243-2

Kohoutová, L., Atlas, L. Y., Büchel, C., Buhle, J. T., Geuter, S., Jepma, M., Koban, L., Krishnan, A., Lee, D. H., Lee, S., Roy, M., Schafer, S. M., Schmidt, L., Wager, T. D., & Woo, C. W. (2022). Individual variability in brain

representations of pain. *Nature Neuroscience*, *25*(6), 749–759. https://doi.org/10.1038/s41593-022-01081-x

Körding, K. P., & Wolpert, D. M. (2004). Bayesian integration in sensorimotor learning. *Nature*, *427*(6971), 244–247. https://doi.org/10.1038/nature02169

Korn, C. W., Staib, M., Tzovara, A., Castegnetti, G., & Bach, D. R. (2016). *A pupil size response model to assess fear learning*. https://doi.org/10.1111/psyp.12801

Koyama, T., Kato, K., & Mikami, A. (2000). During pain-avoidance neurons activated in the macaque anterior cingulate and caudate. *Neuroscience Letters*, *283*(1), 17–20. https://doi.org/10.1016/S0304-3940(00)00894-6

Koyama, T., Kato, K., Tanaka, Y. Z., & Mikami, A. (2001). Anterior cingulate activity during pain-avoidance and reward tasks in monkeys. *Neuroscience Research*, *39*(4), 421–430. https://doi.org/10.1016/S0168-0102(01)00197-3

Kruschke, J. K. (2021). Bayesian Analysis Reporting Guidelines. *Nature Human Behaviour*, *5*(10), 1282–1291. https://doi.org/10.1038/s41562-021-01177-7

Krypotos, A. M., Arnaudova, I., Effting, M., Kindt, M., & Beckers, T. (2015). Effects of Approach-Avoidance Training on the Extinction and Return of Fear Responses. *PLOS ONE*, *10*(7), e0131581. https://doi.org/10.1371/JOURNAL.PONE.0131581

Krypotos, A. M., Effting, M., Kindt, M., & Beckers, T. (2015). Avoidance learning: a review of theoretical models and recent developments. *Frontiers in Behavioral Neuroscience | Www.Frontiersin.Org*, *1*, 189. https://doi.org/10.3389/fnbeh.2015.00189

Kulkarni, B., Bentley, D. E., Elliott, R., Youell, P., Watson, A., Derbyshire, S. W. G., Frackowiak, R. S. J., Friston, K. J., & Jones, A. K. P. (2005). Attention to pain localization and unpleasantness discriminates the functions of the medial and lateral pain systems. *European Journal of Neuroscience*, *21*(11), 3133–3142. https://doi.org/10.1111/j.1460-9568.2005.04098.x

Kwan, C. L., Crawley, A. P., Mikulis, D. J., & Davis, K. D. (2000). An fMRI study of the anterior cingulate cortex and surrounding medial wall activations evoked by noxious cutaneous heat and cold stimuli. *Pain*, *85*(3), 359–374. https://doi.org/10.1016/S0304-3959(99)00287-0

Laird, R. A., Gilbert, J., Kent, P., & Keating, J. L. (2014). Comparing lumbo-pelvic movement in people with and without back pain: a systematic review. *BMC Musculoskeletal Disorders*, *15*, 1–13.

Laird, R. A., Keating, J. L., & Kent, P. (2018). Subgroups of lumbo-pelvic flexion kinematics are present in people with and without persistent low back pain. *BMC Musculoskeletal Disorders*, *19*(1), 1–13. https://doi.org/10.1186/s12891-018-2233-1

Lakens, D. (2013). Calculating and reporting effect sizes to facilitate cumulative science: A practical primer for t-tests and ANOVAs. *Frontiers in Psychology*, *4*(NOV), 863. https://doi.org/10.3389/FPSYG.2013.00863/ABSTRACT

Lang, P. J., & Bradley, M. M. (2010). Emotion and the motivational brain. *Biological Psychology*, *84*(3), 437–450. https://doi.org/10.1016/j.biopsycho.2009.10.007

Lang, P. J., Davis, M., & Öhman, A. (2000). Fear and anxiety: Animal models and human cognitive psychophysiology. *Journal of Affective Disorders*, *61*(3), 137–159. https://doi.org/10.1016/S0165-0327(00)00343-8

Laxmi, T. R., Stork, O., & Pape, H. C. (2003). Generalisation of conditioned fear and its behavioural expression in mice. *Behavioural Brain Research*, *145*(1–2), 89–98. https://doi.org/10.1016/S0166-4328(03)00101-3

Le Pelley, M. E. (2004). The role of associative history in models of associative learning: A selective review and a hybrid model. *Quarterly Journal of Experimental Psychology Section B: Comparative and Physiological Psychology*, *57*(3), 193–243. https://doi.org/10.1080/02724990344000141

Le Pera, D., Graven-Nielsen, T., Valeriani, M., Oliviero, A., Di Lazzaro, V., Tonali, P. A., & Arendt-Nielsen, L. (2001). Inhibition of motor system excitability at cortical and spinal level by tonic muscle pain. *Clinical Neurophysiology*, *112*(9), 1633–1641. https://doi.org/10.1016/S1388-2457(01)00631-9

LeDoux, J., & Daw, N. D. (2018). Surviving threats: neural circuit and computational implications of a new taxonomy of defensive behaviour. *Nature Reviews Neuroscience 2018 19:5*, *19*(5), 269–282. https://doi.org/10.1038/nrn.2018.22

LeDoux, J. E. (2014). Emotion Circuits in the Brain. *FOCUS*. https://doi.org/10.1176/foc.7.2.foc274

Leeuw, M., Goossens, M. E. J. B., Linton, S. J., Crombez, G., Boersma, K., & Vlaeyen, J. W. S. (2007). The fear-avoidance model of musculoskeletal pain: Current state of scientific evidence. *Journal of Behavioral Medicine*, *30*(1), 77–94. https://doi.org/10.1007/s10865-006-9085-0

Lefaucheur, J. P., Aleman, A., Baeken, C., Benninger, D. H., Brunelin, J., Di Lazzaro, V., Filipović, S. R., Grefkes, C., Hasan, A., Hummel, F. C., Jääskeläinen, S. K., Langguth, B., Leocani, L., Londero, A., Nardone, R., Nguyen, J. P., Nyffeler, T., Oliveira-Maia, A. J., Oliviero, A., … Ziemann, U. (2020). Evidence-based guidelines on the therapeutic use of repetitive transcranial magnetic stimulation (rTMS): An update (2014–2018). *Clinical Neurophysiology*, *131*(2), 474–528. https://doi.org/10.1016/j.clinph.2019.11.002

Leuchs, L., Schneider, M., Czisch, M., & Spoormaker, V. I. (2017). Neural correlates of pupil dilation during human fear learning. *NeuroImage*, *147*(November 2016), 186–197. https://doi.org/10.1016/j.neuroimage.2016.11.072

Levine, A. J., Lewallen, K. A., & Pfaff, S. L. (2012). Spatial organization of cortical and spinal neurons controlling motor behavior. *Current Opinion in Neurobiology*, *22*(5), 812–821. https://doi.org/10.1016/j.conb.2012.07.002

Li, F., & Jackson, T. (2022). Psychophysiological correlates of pain resilience in anticipating, experiencing, and recovering from pain. *Psychophysiology*, *59*(2). https://doi.org/10.1111/PSYP.13962

Li, J., Schiller, D., Schoenbaum, G., Phelps, E. A., & Daw, N. D. (2011). Differential roles of human striatum and amygdala in associative learning. *Nature Neuroscience*, *14*(10), 1250–1252. https://doi.org/10.1038/nn.2904

Li, X., Liu, Z., Hu, Y., Jin, R., Lou, W., & Peng, W. (2024). Analgesic effects of high-frequency rTMS on pain anticipation and perception. *Communications Biology*, *7*(1), 1–12. https://doi.org/10.1038/s42003-024-07129-x

Lipp, O. V., Sheridan, J., & Siddle, D. A. T. (1994). Human Blink Startle During Aversive and Nonaversive Pavlovian Conditioning. *Journal of Experimental Psychology: Animal Behavior Processes*, *20*(4), 380–389. https://doi.org/10.1037/0097-7403.20.4.380

Lonsdorf, T. B., Menz, M. M., Andreatta, M., Fullana, M. A., Golkar, A., Haaker, J., Heitland, I., Hermann, A., Kuhn, M., Kruse, O., Meir Drexler, S., Meulders, A., Nees, F., Pittig, A., Richter, J., Römer, S., Shiban, Y., Schmitz, A., Straube, B., … Merz, C. J. (2017). Don't fear 'fear conditioning': Methodological considerations for the design and analysis of studies on human fear acquisition, extinction, and return of fear. In *Neuroscience and Biobehavioral Reviews*. 10.1016/j.neubiorev.2017.02.026

Lorenz, J., Minoshima, S., & Casey, K. L. (2003). Keeping pain out of mind: the role of the dorsolateral prefrontal cortex in pain modulation. *Brain : A Journal of Neurology*, *126*(Pt 5), 1079–1091. https://doi.org/10.1093/BRAIN/AWG102

Love, J., Selker, R., Marsman, M., Jamil, T., Dropmann, D., Verhagen, J., Ly, A., Gronau, Q. F., Šmíra, M., Epskamp, S., Matzke, D., Wild, A., Knight, P., Rouder, J. N., Morey, R. D., & Wagenmakers, E. J. (2019). JASP: Graphical Statistical Software for Common Statistical Designs. *Journal of Statistical Software*, *88*(1), 1–17. https://doi.org/10.18637/JSS.V088.I02

Löw, A., Weymar, M., & Hamm, A. O. (2015). When Threat Is Near, Get Out of Here: Dynamics of Defensive Behavior During Freezing and Active Avoidance. *Psychological Science*, *26*(11), 1706–1716. https://doi.org/10.1177/0956797615597332

Lucchetti, C., Ulrici, A., & Bon, L. (2005). Dorsal premotor areas of nonhuman primate: Functional flexibility in time domain. *European Journal of Applied Physiology*, *95*(2–3), 121–130. https://doi.org/10.1007/s00421-005-1360-1

Lund, J. P., Donga, R., Widmer, C. G., & Stohler, C. S. (1991). The pain-adaptation model: A discussion of the relationship between chronic musculoskeletal pain and motor activity. *Canadian Journal of Physiology and Pharmacology*, *69*(5), 683–694. https://doi.org/10.1139/y91-102

Luyten, L., Vansteenwegen, D., van Kuyck, K., & Nuttin, B. (2011). Towards chronic contextual conditioning in rats: The effects of different numbers of unpaired tone-shock presentations on freezing time and startle. *Acta Neurobiologiae Experimentalis*, *71*(3), 331–338. https://doi.org/10.55782/ane-2011-1855

Lykken, D. T., & Venables, P. H. (1971). Direct measurement of skin conductance: A proposal for standardization. *Psychophysiology*, *8*(5), 656–672. https://doi.org/10.1111/j.1469-8986.1971.tb00501

Mackintosh, N. J. (1975). A theory of attention: Variations in the associability of stimuli with reinforcement. *Psychological Review*, *82*(4), 276–298. https://doi.org/10.1037/h0076778

MacLean, P. D. (1949). Psychosomatic disease and the visceral brain; recent developments bearing on the Papez theory of emotion. *Psychosomatic Medicine*, *11*(6), 338–353. https://doi.org/10.1097/00006842-194911000-00003

Mano, H., & Seymour, B. (2015). Pain: A Distributed Brain Information Network? *PLoS Biology*, *13*(1). https://doi.org/10.1371/journal.pbio.1002037

Martin, P. G., Weerakkody, N., Gandevia, S. C., & Taylor, J. L. (2008). Group III and IV muscle afferents differentially affect the motor cortex and motoneurones in humans. *Journal of Physiology*, *586*(5), 1277–1289. https://doi.org/10.1113/jphysiol.2007.140426

Martin-Fernandez, M., Menegolla, A. P., Lopez-Fernandez, G., Winke, N., Jercog, D., Kim, H. R., Girard, D., Dejean, C., & Herry, C. (2023). Prefrontal circuits encode both general danger and specific threat representations. *Nature Neuroscience*, *26*(12), 2147–2157. https://doi.org/10.1038/s41593-023-01472-8

Mathôt, S., Schreij, D., & Theeuwes, J. (2012). OpenSesame: An open-source, graphical experiment builder for the social sciences. *Behavior Research Methods*, *44*(2), 314–324. https://doi.org/10.3758/S13428-011-0168-7/FIGURES/4

McGregor, T., Purves, K. L., Barry, T., Constantinou, E., Craske, M. G., Breen, G., Young, K. S., & Eley, T. C. (2022). Introducing the Fear Learning and Anxiety Response (FLARe) app and web portal for the remote delivery of fear conditioning experiments. *Behavior Research Methods*. https://doi.org/10.3758/s13428-022-01952-y

McLaren, I. P. L., & Mackintosh, N. J. (2002). Associative learning and elemental representation: II. Generalization and discrimination. *Animal Learning and Behavior*, *30*(3), 177–200. https://doi.org/10.3758/BF03192828

Melzack, R. (2001). Pain and the Neuromatrix in the Brain. *Journal of Dental Education*, *65*(12), 1378–1382. https://doi.org/10.1007/978-94-009-7907-9_16

Melzack, R., & Casey, K. L. (1968). Sensory, Motivational, and Central Control Determinants of Pain. In *The skin senses* (Number April, pp. 423–439). CHARLES C THOMAS.

Mense S. (1993). Nociception from skeletal muscle in relation to clinical muscle pain. *Pain*, *54*(6221), 241–289.

Merchant, H., & Yarrow, K. (2016). How the motor system both encodes and influences our sense of time. *Current Opinion in Behavioral Sciences*, *8*, 22–27. https://doi.org/10.1016/j.cobeha.2016.01.006

Mertens, G., & Engelhard, I. M. (2020). A systematic review and meta-analysis of the evidence for unaware fear conditioning. *Neuroscience and Biobehavioral Reviews*, *108*(April 2019), 254–268. https://doi.org/10.1016/j.neubiorev.2019.11.012

Mills, K. R., Boniface, S. J., & Schubert, M. (1992). Magnetic brain stimulation with a double coil: the importance of coil orientation. *Electroencephalography and Clinical Neurophysiology*, *85*(1), 17–21. https://doi.org/10.1016/0168-5597(92)90096-T

Mioni, G., Stablum, F., McClintock, S. M., & Grondin, S. (2014). Different methods for reproducing time, different results. *Attention, Perception, and Psychophysics*, *76*(3), 675–681. https://doi.org/10.3758/s13414-014-0625-3

Mobbs, D., Headley, D. B., Ding, W., & Dayan, P. (2020). Space, Time, and Fear: Survival Computations along Defensive Circuits. *Trends in Cognitive Sciences*, *24*(3), 228–241. https://doi.org/10.1016/j.tics.2019.12.016

Mohammadi, M., Bergado-Acosta, J. R., & Fendt, M. (2014). Relief learning is distinguished from safety learning by the requirement of the nucleus accumbens. *Behavioural Brain Research*, *272*, 40–45. https://doi.org/10.1016/j.bbr.2014.06.053

Mohammadi, M., & Fendt, M. (2015). Relief learning is dependent on NMDA receptor activation in the nucleus accumbens. *British Journal of Pharmacology*, *172*(9), 2419–2426. https://doi.org/10.1111/bph.13070

Mollet, G. A., & Harrison, D. W. (2006). Emotion and pain: A functional cerebral systems integration. *Neuropsychology Review*, *16*(3), 99–121. https://doi.org/10.1007/s11065-006-9009-3

Morris, R. W., & Bouton, M. E. (2006). Effect of unconditioned stimulus magnitude on the emergence of conditioned responding. *Journal of Experimental Psychology: Animal Behavior Processes*, *32*(4), 371–385. https://doi.org/10.1037/0097-7403.32.4.371

Moseley, G. L., Nicholas, M. K., & Hodges, P. W. (2004). Does anticipation of back pain predispose to back trouble? *Brain : A Journal of Neurology*, *127*(Pt 10), 2339–2347. https://doi.org/10.1093/BRAIN/AWH248

Mouraux, A., Diukova, A., Lee, M. C., Wise, R. G., & Iannetti, G. D. (2011). A multisensory investigation of the functional significance of the "pain matrix." *NeuroImage*, *54*(3), 2237–2249. https://doi.org/10.1016/j.neuroimage.2010.09.084

Narayanan, N. S., Horst, N. K., & Laubach, M. (2006). Reversible inactivations of rat medial prefrontal cortex impair the ability to wait for a stimulus. *Neuroscience*, *139*(3), 865–876. https://doi.org/10.1016/j.neuroscience.2005.11.072

Narayanan, N. S., & Laubach, M. (2006). Top-Down Control of Motor Cortex Ensembles by Dorsomedial Prefrontal Cortex. *Neuron*, *52*(5), 921–931. https://doi.org/10.1016/j.neuron.2006.10.021

Nasser, H. M., & Delamater, A. R. (2016). *The determining conditions for Pavlovian learning: Psychological and neurobiological considerations* (pp. 7–46). The Wiley handbook on the cognitive neuroscience of learning. https://doi.org/10.1002/9781118650813

Neige, C., Lebon, F., Mercier, C., Gaveau, J., Papaxanthis, C., & Ruffino, C. (2022). Pain, No Gain: Acute Pain Interrupts Motor Imagery Processes and Affects Mental Training-Induced Plasticity. *Cerebral Cortex*, *32*(3), 640–651. https://doi.org/10.1093/cercor/bhab246

Neige, C., Mavromatis, N., Gagné, M., Bouyer, L. J., & Mercier, C. (2018). Effect of movement-related pain on behaviour and corticospinal excitability changes associated with arm movement preparation. *Journal of Physiology*, *596*(14), 2917–2929. https://doi.org/10.1113/JP276011

Ney, L. J., O'Donohue, M., Wang, Y., Richardson, M., Vasarhelyi, A., & Lipp, O. V. (2023). The next frontier: Moving human fear conditioning research online. *Biological Psychology*, *184*(June), 108715. https://doi.org/10.1016/j.biopsycho.2023.108715

Niv, X. Y., Daniel, X. R., Geana, A., Gershman, S. J., Leong, Y. C., Radulescu, A., & Wilson, R. C. (2015). *Reinforcement Learning in Multidimensional Environments Relies on Attention Mechanisms*. *35*(21), 8145–8157. https://doi.org/10.1523/JNEUROSCI.2978-14.2015

Niv, Y., Edlund, J. A., Dayan, P., & O'Doherty, J. P. (2012). Neural prediction errors reveal a risk-sensitive reinforcement-learning process in the human brain. *Journal of Neuroscience*, *32*(2), 551–562. https://doi.org/10.1523/JNEUROSCI.5498-10.2012

Niv, Y., & Schoenbaum, G. (2008). Dialogues on prediction errors. *Trends in Cognitive Sciences*, *12*(7), 265–272. https://doi.org/10.1016/j.tics.2008.03.006

Öhman, A., & Mineka, S. (2001). Fears, phobias, and preparedness: toward an evolved module of fear and fear learning. *Psychological Review*, *108*(3), 483–522. https://doi.org/10.1037/0033-295X.108.3.483

Ojala, K. E., & Bach, D. R. (2020). Measuring learning in human classical threat conditioning: Translational, cognitive and methodological considerations. In *Neuroscience and Biobehavioral Reviews*. https://doi.org/10.1016/j.neubiorev.2020.04.019

Oldfield, R. C. (1971). THE ASSESSMENT AND ANALYSIS OF HANDEDNESS: THE EDINBURGH INVENTORY. In *Neuropsychologia* (Vol. 9). Pergamon Press.

Ouyang, L., & Dunsmoor, J. E. (2024). Emotional intensity produces a linear relationship on conditioned learning but an inverted U-shaped effect on episodic memory. *Learning and Memory*, *31*(12), 1–13. https://doi.org/10.1101/lm.053982.124

Palminteri, S., Wyart, V., & Koechlin, E. (2017). The Importance of Falsification in Computational Cognitive Modeling. *Trends in Cognitive Sciences*, *21*(6), 425–433. https://doi.org/10.1016/j.tics.2017.03.011

Pearce, J. M., & Hall, G. (1980). A model for Pavlovian learning: Variations in the effectiveness of conditioned but not of unconditioned stimuli. *Psychological Review*, *87*(6), 532–552. https://doi.org/10.1037/0033-295X.87.6.532

Peck, C. C., Murray, G. M., & Gerzina, T. M. (2008). How does pain affect jaw muscle activity? The integrated pain adaptation model. *Australian Dental Journal*, *53*(3), 201–207. https://doi.org/10.1111/j.1834-7819.2008.00050.x

Peng, W., Huang, X., Liu, Y., & Cui, F. (2019). Predictability modulates the anticipation and perception of pain in both self and others. *Social Cognitive and Affective Neuroscience*, *14*(7), 747–757. https://doi.org/10.1093/SCAN/NSZ047

Peng, W., Peng, H., Lu, J., Fan, B., & Cui, F. (2019). Others' Pain Appraisals Modulate the Anticipation and Experience of Subsequent Pain. *Neuroscience*, *410*, 16–28. https://doi.org/10.1016/j.neuroscience.2019.04.055

Peyron, R., García-Larrea, L., Grégoire, M. C., Costes, N., Convers, P., Lavenne, F., Mauguière, F., Michel, D., & Laurent, B. (1999). Haemodynamic brain responses to acute pain in humans. Sensory and attentional networks. *Brain*, *122*(9), 1765–1779. https://doi.org/10.1093/brain/122.9.1765

Peyron, R., Laurent, B., & Garcia-Larrea, L. (2000). Functional imaging of brain responses to pain. *Clinical Neurophysiology*, *30*(5), 263–288. papers://40c68295-5659-4035-8dff-71162e06882b/Paper/p420

Phillips, R. G., & LeDoux, J. E. (1992). Differential Contribution of Amygdala and Hippocampus to Cued and Contextual Fear Conditioning. *Behavioral Neuroscience*, *106*(2), 274–285. https://doi.org/10.1037/0735-7044.106.2.274

Pirazzini, G., Starita, F., Ricci, G., Garofalo, S., di Pellegrino, G., Magosso, E., & Ursino, M. (2023). Changes in brain rhythms and connectivity tracking fear acquisition and reversal. *Brain Structure and Function*, *228*(5), 1259–1281. https://doi.org/10.1007/s00429-023-02646-7

Pittig, A., Wong, A. H. K., Glück, V. M., & Boschet, J. M. (2020). Avoidance and its bi-directional relationship with conditioned fear: Mechanisms, moderators, and clinical implications. *Behaviour Research and Therapy*, *126*(August 2019), 103550. https://doi.org/10.1016/j.brat.2020.103550

Ploghaus, A., Tracey, I., Gati, J. S., Clare, S., Menon, R. S., Matthews, P. M., Rawlins, J. N. P., Ploghaus, A., Tracey, I., Gati, J. S., Clare, S., Menon, R. S., Matthews, P. M., & Rawlins, J. N. P. (2016). Dissociating Pain from Its Anticipation in the Human Brain. *Science*, *284*(5422), 1979–1981.

Poldrack, R. A. (2006). Can cognitive processes be inferred from neuroimaging data? *Trends in Cognitive Sciences*, *10*(2), 59–63. https://doi.org/10.1016/j.tics.2005.12.004

Pool, E. R., Pauli, W. M., Cross, L., & O'Doherty, J. P. (2023). Neural substrates of parallel devaluation-sensitive and devaluation-insensitive Pavlovian learning in humans. *Nature Communications*, *14*(1), 1–17. https://doi.org/10.1038/s41467-023-43747-5

Pool, E. R., Pauli, W. M., Kress, C. S., & O'Doherty, J. P. (2019). Behavioural evidence for parallel outcome-sensitive and outcome-insensitive Pavlovian learning systems in humans. *Nature Human Behaviour*, *3*(3), 284–296. https://doi.org/10.1038/s41562-018-0527-9

Porro, C. A., Baraldi, P., Pagnoni, G., Serafini, M., Facchin, P., Maieron, M., & Nichelli, P. (2002). *Does Anticipation of Pain Affect Cortical Nociceptive Systems?*

Poulos, C. X., Furedy, J. J., & Heslegrave, R. J. (1979). Effects of US habituation following skin-conductance response conditioning: Support for a Pavlovian S-S position and a habituation account of nonmonotonic acquisition functions. *Physiological Psychology*. https://doi.org/10.3758/BF03326640

R Core Team (2022) R A Language and Environment for Statistical Computing. R Foundation for Statistical Computing, Vienna. - References - Scientific Research Publishing. (n.d.). Retrieved October 27, 2023, from https://www.scirp.org/(S(lz5mqp453ed%20snp55rrgjct55))/reference/referencespapers.aspx?referenceid=3456808

Raij, T. T., Numminen, J., Närvänen, S., Hiltunen, J., & Hari, R. (2005). Brain correlates of subjective reality of physically and psychologically induced pain. *Proceedings of the National Academy of Sciences of the United States of America*, *102*(6), 2147–2151. https://doi.org/10.1073/PNAS.0409542102

Rainville, P. (2002). Brain mechanisms of pain affect and pain modulation. *Current Opinion in Neurobiology*, *12*(2), 195–204. https://doi.org/10.1016/S0959-4388(02)00313-6

Raja, S., Carr, D. B., Cohen, M., Finnerup, N. B., Herta, F., Gibson, S., Keefe, F., Mogil, J. S., Ringkamp, M., Sluka, K. A., Song, X.-J., Stevens, B., Sullivan, M., Tutelman, P., Ushida, T., & Vader, K. (2021). The Revised IASP definition of pain: concepts, challenges, and compromises. *Pain*, *161*(9), 1976–1982. https://doi.org/10.1097/j.pain.0000000000001939.The

Rangel, A., Camerer, C., & Montague, P. R. (2008). Neuroeconomics: The neurobiology of value-based decision-making. *Nat Rev Neurosci*, *9*(7), 545–556. https://doi.org/10.1038/nrn2357.Neuroeconomics

Reinhard, G., & Lachnit, H. (2002). Differential conditioning of anticipatory pupillary dilation responses in humans. *Biological Psychology*. https://doi.org/10.1016/S0301-0511(02)00011-X

Rescorla, R., & Wagner, A. (1972). A theory of Pavlovian conditioning: The effectiveness of reinforcement and non-reinforcement. *Classical Conditioning: Current Research and Theory*, (March), 64–99. https://www.researchgate.net/publication/239030972

Roelofs, K. (2017). Freeze for action: Neurobiological mechanisms in animal and human freezing. In *Philosophical Transactions of the Royal Society B: Biological Sciences*. https://doi.org/10.1098/rstb.2016.0206

Rokyta, R., & Fricovà, J. (2012). Neurostimulation methods in the treatment of chronic pain. *Physiological Research*, *61*(4), S23–S31. https://doi.org/10.1007/s00702-019-02092-y

Roland, M. O. (1986). Review Paper A critical review of the evidence for a pain-spasm-pain cycle in spinal disorders was palpated. *Spine*, 102–109.

Romaniello, A., Cruccu, G., McMillan, A. S., Arendt-Nielsen, L., & Svensson, P. (2000). Effect of experimental pain from trigeminal muscle and skin on motor cortex excitability in humans. *Brain Research*, *882*(1–2), 120–127. https://doi.org/10.1016/S0006-8993(00)02856-0

Rossi, S., Antal, A., Bestmann, S., Bikson, M., Brewer, C., Brockmöller, J., Carpenter, L. L., Cincotta, M., Chen, R., Daskalakis, J. D., Di Lazzaro, V., Fox, M. D., George, M. S., Gilbert, D., Kimiskidis, V. K., Koch, G., Ilmoniemi, R. J., Pascal Lefaucheur, J., Leocani, L., … Hallett, M. (2021). Safety and recommendations for TMS use in healthy subjects and patient populations, with updates on training, ethical and regulatory issues: Expert Guidelines. *Clinical Neurophysiology*, *132*(1), 269–306. https://doi.org/10.1016/j.clinph.2020.10.003

Rossi, S., Hallett, M., Rossini, P. M., Pascual-Leone, A., Avanzini, G., Bestmann, S., Berardelli, A., Brewer, C., Canli, T., Cantello, R., Chen, R., Classen, J., Demitrack, M., Di Lazzaro, V., Epstein, C. M., George, M. S., Fregni, F., Ilmoniemi, R., Jalinous, R., … Ziemann, U. (2009). Safety, ethical considerations, and application guidelines for the use of transcranial magnetic stimulation in clinical practice and research. In *Clinical Neurophysiology* (Vol. 120, Number 12, pp. 2008–2039). https://doi.org/10.1016/j.clinph.2009.08.016

Rossini, P. M., Barker, A. T., Berardelli, A., Caramia, M. D., Caruso, G., Cracco, R. Q., Dimitrijević, M. R., Hallett, M., Katayama, Y., Lücking, C. H., Maertens de Noordhout, A. L., Marsden, C. D., Murray, N. M. F., Rothwell, J. C., Swash, M., & Tomberg, C. (1994). Non-invasive electrical and magnetic stimulation of the brain, spinal cord and roots: basic principles and procedures for routine clinical application. Report of an IFCN committee. *Electroencephalography and Clinical Neurophysiology*, *91*(2), 79–92. https://doi.org/10.1016/0013-4694(94)90029-9

Rossini, P. M., Burke, D., Chen, R., Cohen, L. G., Daskalakis, Z., Di Iorio, R., Di Lazzaro, V., Ferreri, F., Fitzgerald, P. B., George, M. S., Hallett, M., Lefaucheur, J. P., Langguth, B., Matsumoto, H., Miniussi, C., Nitsche, M. A., Pascual-Leone, A., Paulus, W., Rossi, S., … Ziemann, U. (2015). Non-invasive electrical and magnetic stimulation of the brain, spinal cord, roots and peripheral nerves: Basic principles and procedures for routine clinical and research application. An updated report from an I.F.C.N. Committee. *Clinical Neurophysiology : Official Journal of the International Federation of Clinical Neurophysiology*, *126*(6), 1071–1107. https://doi.org/10.1016/J.CLINPH.2015.02.001

Rothwell, J. C. (1997). Techniques and mechanisms of action of transcranial stimulation of the human motor cortex. *Journal of Neuroscience Methods*, *74*(2), 113–122. https://doi.org/10.1016/S0165-0270(97)02242-5

Roux, S., Coulmance, M., & Riehle, A. (2003). Context-related representation of timing processes in monkey motor cortex. *European Journal of Neuroscience*, *18*(4), 1011–1016. https://doi.org/10.1046/j.1460-9568.2003.02792.x

Salomoni, S. E., & Graven-Nielsen, T. (2012). Experimental muscle pain increases normalized variability of multidirectional forces during isometric contractions. *European Journal of Applied Physiology*, *112*(10), 3607–3617. https://doi.org/10.1007/S00421-012-2343-7/METRICS

Sandrini, G., Serrao, M., Rossi, P., Romaniello, A., Cruccu, G., & Willer, J. C. (2005). The lower limb flexion reflex in humans. *Progress in Neurobiology*, *77*(6), 353–395. https://doi.org/10.1016/j.pneurobio.2005.11.003

Sassenhagen, J., & Draschkow, D. (2019). Cluster-based permutation tests of MEG/EEG data do not establish significance of effect latency or location. *Psychophysiology*, *56*(6), 1–8. https://doi.org/10.1111/psyp.13335

Schieber, M. H. (2001). Constraints on somatotopic organization in the primary motor cortex. *Journal of Neurophysiology*, *86*(5), 2125–2143. https://doi.org/10.1152/jn.2001.86.5.2125

Schiller, D., Levy, I., Niv, Y., LeDoux, J. E., & Phelps, E. A. (2008). From fear to safety and back: Reversal of fear in the human brain. *Journal of Neuroscience*, *28*(45), 11517–11525. https://doi.org/10.1523/JNEUROSCI.2265-08.2008

Schultz, W., Dayan, P., & Montague, P. R. (1997). A neural substrate of prediction and reward. *Science*. https://doi.org/10.1126/science.275.5306.1593

Schutter, D. J. L. G., Hofman, D., & Van Honk, J. (2008). Fearful faces selectively increase corticospinal motor tract excitability: A transcranial magnetic stimulation study. *Psychophysiology*, *45*(3), 345–348. https://doi.org/10.1111/j.1469-8986.2007.00635.x

Schwarz, G. (2007). Estimating the Dimension of a Model. *The Annals of Statistics*, *6*(2), 461–464. https://doi.org/10.1214/aos/1176344136

Seifert, F., Schuberth, N., De Col, R., Peltz, E., Nickel, F. T., & Maihöfner, C. (2013). Brain activity during sympathetic response in anticipation and experience of pain. *Human Brain Mapping*, *34*(8), 1768–1782. https://doi.org/10.1002/hbm.22035

Seminowicz, D. A., & Moayedi, M. (2017). The Dorsolateral Prefrontal Cortex in Acute and Chronic Pain. *Journal of Pain*, *18*(9), 1027–1035. https://doi.org/10.1016/j.jpain.2017.03.008

Sevenster, D., Beckers, T., & Kindt, M. (2012). Instructed extinction differentially affects the emotional and cognitive expression of associative fear memory. *Psychophysiology*, *49*(10), 1426–1435. https://doi.org/10.1111/j.1469-8986.2012.01450.x

Seymour, B. (2019). Pain: A Precision Signal for Reinforcement Learning and Control. *Neuron*, *101*(6), 1029–1041. https://doi.org/10.1016/j.neuron.2019.01.055

Seymour, B., & Dolan, R. (2013). Emotion, Motivation, and Pain. In *Textbook of Pain* (pp. 248–255).

Seymour, B., & Mancini, F. (2020). Hierarchical models of pain: Inference, information-seeking, and adaptive control. *NeuroImage*, *222*(May), 117212. https://doi.org/10.1016/j.neuroimage.2020.117212

Shanahan, C. J., Hodges, P. W., Wrigley, T. V., Bennell, K. L., & Farrell, M. J. (2015). Organisation of the motor cortex differs between people with and without knee osteoarthritis. *Arthritis Research and Therapy*, *17*(1), 1–11. https://doi.org/10.1186/s13075-015-0676-4

Smith, J. C., & Sclafani, A. (2002). Saccharin as a sugar surrogate revisited. *Appetite*, *38*(2), 155–160. https://doi.org/10.1006/appe.2001.0467

Smith, M. C. (1968). CS-US interval and US intensity in classical conditioning of the rabbit's nictitating membrane response. *Journal of Comparative and Physiological Psychology*, *66*(3 PART 1), 679–687. https://doi.org/10.1037/h0026550

Song, Y., Yao, M., Kemprecos, H., Byrne, A., Xiao, Z., Zhang, Q., Singh, A., Wang, J., & Chen, Z. S. (2021). Predictive coding models for pain perception. In *Journal of Computational Neuroscience* (Vol. 49, Number 2). https://doi.org/10.1007/s10827-021-00780-x

Spampinato, D. A., Ibanez, J., Rocchi, L., & Rothwell, J. (2023). Motor potentials evoked by transcranial magnetic stimulation: interpreting a simple measure of a complex system. *Journal of Physiology*, *601*(14), 2827–2851. https://doi.org/10.1113/JP281885

Spoormaker, V. I., Andrade, K. C., Schröter, M. S., Sturm, A., Goya-Maldonado, R., Sämann, P. G., & Czisch, M. (2011). The neural correlates of negative prediction error signaling in human fear conditioning. *NeuroImage*, *54*(3), 2250–2256. https://doi.org/10.1016/j.neuroimage.2010.09.042

Spoormaker, V. I., Blechert, J., Goya-Maldonado, R., Sämann, P. G., Wilhelm, F. H., & Czisch, M. (2012). Additional support for the existence of skin conductance responses at unconditioned stimulus omission. *NeuroImage*, *63*(3), 1404–1407. https://doi.org/10.1016/j.neuroimage.2012.08.050

Spratling, M. W. (2012). Predictive coding accounts for V1 response properties recorded using reverse correlation. *Biological Cybernetics*, *106*(1), 37–49. https://doi.org/10.1007/s00422-012-0477-7

Starita, F., Garofalo, S., Dalbagno, D., Degni, L. A. E., & di Pellegrino, G. (2022). Pavlovian threat learning shapes the kinematics of action. *Frontiers in Psychology*, *13*(October), 1–15. https://doi.org/10.3389/fpsyg.2022.1005656

Starita, F., Kroes, M. C. W., Davachi, L., Phelps, E. A., & Dunsmoor, J. E. (2019). Threat learning promotes generalization of episodic memory. *Journal of Experimental Psychology: General*, *148*(8), 1426–1434. https://doi.org/10.1037/XGE0000551

Starita, F., Pirazzini, G., Ricci, G., Garofalo, S., Dalbagno, D., Degni, L. A. E., Di Pellegrino, G., Magosso, E., & Ursino, M. (2023a). Theta and alpha power track the acquisition and reversal of threat predictions and correlate with skin conductance response. *Psychophysiology*. https://doi.org/10.1111/psyp.14247

Starita, F., Pirazzini, G., Ricci, G., Garofalo, S., Dalbagno, D., Degni, L. A. E., Magosso, E., Ursino, M., & di Pellegrino, G. (2023b). Theta and alpha power track the acquisition and reversal of threat learning and correlate with autonomic arousal. *International Journal of Psychophysiology*, *188*, 33. https://doi.org/10.1016/j.ijpsycho.2023.05.083

Starita, F., Stussi, Y., Garofalo, S., & di Pellegrino, G. (2023). Threat learning in space: how stimulus-outcome spatial compatibility modulates conditioned skin conductance response. *International Journal of Psychophysiology*, *190*(January), 30–41. https://doi.org/10.1016/j.ijpsycho.2023.06.003

Stemerding, L. E., van Ast, V. A., Gerlicher, A. M. V., & Kindt, M. (2022). Pupil dilation and skin conductance as measures of prediction error in aversive learning. *Behaviour Research and Therapy*, *157*(December 2021), 104164. https://doi.org/10.1016/j.brat.2022.104164

Stohler, C. S. (1999). Craniofacial pain and motor function: Pathogenesis, clinical correlates, and implications. *Critical Reviews in Oral Biology and Medicine*, *10*(4), 504–518. https://doi.org/10.1177/10454411990100040601

Storm, H., Fremming, A., Édegaard, S., Martinsen, É. G., & Mùrkrid, L. (2001). The development of a software program for analyzing skin conductance changes in preterm infants. *Clinical Neurophysiology*, *112*(8), 1562–1568. https://doi.org/10.1016/S1388-2457(01)00573-9

Strube, A., Horing, B., Rose, M., & Büchel, C. (2023). Agency affects pain inference through prior shift as opposed to likelihood precision modulation in a Bayesian pain model. *Neuron*, *111*(7), 1136-1151.e7. https://doi.org/10.1016/j.neuron.2023.01.002

Stussi, Y. (2025). Affective and computational determinants of threat extinction biases. *Behaviour Research and Therapy*, *192*(November 2024), 104804. https://doi.org/10.1016/j.brat.2025.104804

Stussi, Y., & Coppin, G. (2024). Letter to the Editor: Stimulus intensities and sensory modalities constitute two major challenges for online threat conditioning research. *Biological Psychology*, *190*(April). https://doi.org/10.1016/j.biopsycho.2024.108805

Stussi, Y., Pourtois, G., Olsson, A., & Sander, D. (2021). Learning biases to angry and happy faces during Pavlovian aversive conditioning. *Emotion*, *21*(4), 742–756. https://doi.org/10.1037/EMO0000733

Stussi, Y., Pourtois, G., & Sander, D. (2018a). Enhanced Pavlovian aversive conditioning to positive emotional stimuli. *Journal of Experimental Psychology: General*, *147*(6), 905–923. https://doi.org/10.1037/XGE0000424

Stussi, Y., Pourtois, G., & Sander, D. (2018b). Enhanced Pavlovian aversive conditioning to positive emotional stimuli. *Journal of Experimental Psychology: General*, *147*(6), 905–923. https://doi.org/10.1037/xge0000424

Sugiyama, T., Uehara, S., & Izawa, J. (2024). Meta-learning of human motor adaptation via the dorsal premotor cortex. *Proceedings of the National Academy of Sciences*, *121*(44), e2417543121. https://doi.org/10.1073/PNAS.2417543121

Sullivan, M. J. L. (2008). Toward a biopsychomotor conceptualization of pain: Implications for research and intervention. *Clinical Journal of Pain*, *24*(4), 281–290. https://doi.org/10.1097/AJP.0b013e318164bb15

Summerfield, C., Egner, T., Greene, M., Koechlin, E., Mangels, J., & Hirsch, J. (2018). Predictive Codes for Forthcoming Perception in the Frontal Cortex Linked references are available on JSTOR for this article : Predictive Codes for Forthcoming Perception in the Frontal Cortex. *Science*, *314*(5803), 1311–1314.

Sutton, R. S., & Barto, A. G. (2014). An introduction to reinforcement learning. In *The MIT Press Cambridge, Massachusetts London, England*. https://doi.org/10.4018/978-1-60960-165-2.ch004

Suzuki, M., Kirimoto, H., Onishi, H., Yamada, S., Tamaki, H., Maruyama, A., & Yamamoto, J. I. (2012). Reciprocal changes in input–output curves of motor evoked potentials while learning motor skills. *Brain Research*, *1473*, 114–123. https://doi.org/10.1016/J.BRAINRES.2012.07.043

Svensson, P., Houe, L., & Arendt-Nielsen, L. (1997). Bilateral experimental muscle pain changes electromyographic activity of human jaw-closing muscles during mastication. *Experimental Brain Research*, *116*(1), 182–185. https://doi.org/10.1007/PL00005738/METRICS

Svensson, P., Johannsen, P., Jensen, T. S., Arendt-Nielsen, L., Nielsen, J., Stødkilde-Jørgensen, H., Gee, A. D., Baarsgaard Hansen, S., & Gjedde, A. (1998). Cerebral blood-flow changes evoked by two levels of painful heat stimulation: A positron emission tomography study in humans. *European Journal of Pain*, *2*(2), 95–106. https://doi.org/10.1016/S1090-3801(98)90001-5

Svensson, P., Minoshima, S., Beydoun, A., Morrow, T. J., & Casey, K. L. (1997). Cerebral processing of acute skin and muscle pain in humans. *Journal of Neurophysiology*, *78*(1), 450–460. https://doi.org/10.1152/jn.1997.78.1.450

Tabor, A., & Burr, C. (2019). Bayesian Learning Models of Pain: A Call to Action. *Current Opinion in Behavioral Sciences*, *26*, 54–61. https://doi.org/10.1016/j.cobeha.2018.10.006

Tabor, A., Thacker, M. A., Moseley, G. L., & Körding, K. P. (2017). Pain: A Statistical Account. *PLoS Computational Biology*, *13*(1), 1–13. https://doi.org/10.1371/journal.pcbi.1005142

Tallot, L., & Doyère, V. (2020). Neural encoding of time in the animal brain. In *Neuroscience and Biobehavioral Reviews* (Vol. 115, pp. 146–163). Elsevier Ltd. https://doi.org/10.1016/j.neubiorev.2019.12.033

Tamburin, S., Manganotti, P., Zanette, G., & Fiaschi, A. (2001). Cutaneomotor integration in human hand motor areas: Somatotopic effect and interaction of afferents. *Experimental Brain Research*, *141*(2), 232–241. https://doi.org/10.1007/s002210100859

Tan, L. L., & Kuner, R. (2021). Neocortical circuits in pain and pain relief. In *Nature Reviews Neuroscience* (Vol. 22, Number 8, pp. 458–471). Nature Research. https://doi.org/10.1038/s41583-021-00468-2

Touge, T., Taylor, J. L., & Rothwell, J. C. (1998). Reduced excitability of the cortico-spinal system during the warning period of a reaction time task. *Electroencephalography and Clinical Neurophysiology/Electromyography and Motor Control*, *109*(6), 489–495. https://doi.org/10.1016/S0924-980X(98)00050-2

Tracey, I., & Mantyh, P. W. (2007). The Cerebral Signature for Pain Perception and Its Modulation. *Neuron*, *55*(3), 377–391. https://doi.org/10.1016/j.neuron.2007.07.012

Treede, R. D., Kenshalo, D. R., Gracely, R. H., & Jones, A. K. P. (1999). The cortical representation of pain. *Pain*, *79*(2–3), 105–111. https://doi.org/10.1016/S0304-3959(98)00184-5

Treister, R., Kliger, M., Zuckerman, G., Aryeh, I. G., & Eisenberg, E. (2012). Differentiating between heat pain intensities: The combined effect of multiple autonomic parameters. *Pain*, *153*(9), 1807–1814. https://doi.org/10.1016/j.pain.2012.04.008

Trujillo-Ortiz, A. (2005). *Cookdist, MATLAB Central File Exchange*. MathWorks. https://it.mathworks.com/help/stats/cooks-distance.html

Tucker, K., Larsson, A. K., Oknelid, S., & Hodges, P. (2012). Similar alteration of motor unit recruitment strategies during the anticipation and experience of pain. *Pain*, *153*(3), 636–643. https://doi.org/10.1016/j.pain.2011.11.024

Tursky, B. (1974). Physical, Physiological, and Psychological Factors That Affect Pain Reaction to Electric Shock. *Psychophysiology*, *11*(2), 95–112. https://doi.org/10.1111/j.1469-8986.1974.tb00830

Tyng, C. M., Amin, H. U., Saad, M. N. M., & Malik, A. S. (2017). The influences of emotion on learning and memory. *Frontiers in Psychology*, *8*(AUG). https://doi.org/10.3389/fpsyg.2017.01454

Urban, P. P., Solinski, M., Best, C., Rolke, R., Hopf, H. C., & Dieterich, M. (2004). Different short-term modulation of cortical motor output to distal and proximal upper-limb muscles during painful sensory nerve stimulation. *Muscle and Nerve*. https://doi.org/10.1002/mus.20011

Uzuneser, T. C., & Fendt, M. (2020). Individual expression of conditioned safety but not of conditioned relief is correlated with contextual fear. *Behavioural Brain Research*, *393*(June), 112799. https://doi.org/10.1016/j.bbr.2020.112799

Valeriani, M., Restuccia, D., Di Lazzaro, V., Oliviero, A., Le Pera, D., Profice, P., Saturno, E., & Tonali, P. (2001). Inhibition of biceps brachii muscle motor area by painful heat stimulation of the skin. *Experimental Brain Research*, *139*(2), 168–172. https://doi.org/10.1007/s002210100753

Valeriani, M., Restuccia, D., Di Lazzaro, V., Oliviero, A., Profice, P., Le Pera, D., Saturno, E., & Tonali, P. (1999a). Inhibition of the human primary motor area by painful heat stimulation of the skin. *Clinical Neurophysiology*, *110*(8), 1475–1480. https://doi.org/10.1016/S1388-2457(99)00075-9

Valeriani, M., Restuccia, D., Di Lazzaro, V., Oliviero, A., Profice, P., Le Pera, D., Saturno, E., & Tonali, P. (1999b). Inhibition of the human primary motor area by painful heat stimulation of the skin. *Clinical Neurophysiology*, *110*(8), 1475–1480. https://doi.org/10.1016/S1388-2457(99)00075-9

Van Diest, I., Bradley, M. M., Guerra, P., Van den Bergh, O., & Lang, P. J. (2009). Fear-conditioned respiration and its association to cardiac reactivity. *Biological Psychology*, *80*(2), 212–217. https://doi.org/10.1016/j.biopsycho.2008.09.006

Van Elswijk, G., Kleine, B. U., Overeem, S., & Stegeman, D. F. (2007). Expectancy induces dynamic modulation of corticospinal excitability. *Journal of Cognitive Neuroscience*, *19*(1), 121–131. https://doi.org/10.1162/jocn.2007.19.1.121

van Meurs, B., Wiggert, N., Wicker, I., & Lissek, S. (2014). Maladaptive behavioral consequences of conditioned fear-generalization: A pronounced, yet sparsely studied, feature of anxiety pathology. *Behaviour Research and Therapy*, *57*(1), 29–37. https://doi.org/10.1016/J.BRAT.2014.03.009

Vervliet, B., Lange, I., & Milad, M. R. (2017). Temporal dynamics of relief in avoidance conditioning and fear extinction: Experimental validation and clinical relevance. *Behaviour Research and Therapy*, *96*, 66–78. https://doi.org/10.1016/j.brat.2017.04.011

Vlaeyen, J. W. S., & Crombez, G. (2020). Behavioral Conceptualization and Treatment of Chronic Pain. *Annual Review of Clinical Psychology*, *16*, 187–212. https://doi.org/10.1146/annurev-clinpsy-050718-095744

Vlaeyen, J. W. S., & Linton, S. J. (2000). Fear-avoidance and its consequences in chronic musculoskeletal pain: A state of the art. *Pain*, *85*(3), 317–332. https://doi.org/10.1016/S0304-3959(99)00242-0

Waddell, G., & Richardson, J. (1992). Observation of overt pain behaviour by physicians during routine clinical examination of patients with low back pain. *Journal of Psychosomatic Research*, *36*(1), 77–87. https://doi.org/10.1016/0022-3999(92)90116-J

Wager, T. D., Rilling, J. K., Smith, E. E., Sokolik, A., Kenneth, L., Davidson, R. J., Kosslyn, S. M., Rose, R. M., & Cohen, J. D. (1881). American Association for the Advancement of Science. *Science*, *os-2*(57), 341–342. https://doi.org/10.1126/science.os-2.57.341-a

Wagner, A. R. (1981). SOP: A Model of Automatic Memory Processing in Animal Behavior. In N. E. S. & R. R. Miller (Ed.), *Information Processing in Animals: Memory Mechanisms* (Number April, pp. 5–47). Erlbaum (Lawrence Erlbaum Associates).

Wall, P. D., & Woolf, C. J. (1985). Muscle but not cutaneous C-afferent input produces prolonged increases in the excitability of the flexion reflex in the rat. *Pain*, *22*(2), 206–207. https://doi.org/10.1016/0304-3959(85)90186-1

Wallwork, S. B., Grabherr, L., O'Connell, N. E., Catley, M. J., & Moseley, G. L. (2017). Defensive reflexes in people with pain - A biomarker of the need to protect? A meta-analytical systematic review. *Reviews in the Neurosciences*, *28*(4), 381–396. https://doi.org/10.1515/REVNEURO-2016-0057/MACHINEREADABLECITATION/RIS

Wen, Z., Pace-Schott, E. F., Lazar, S. W., Rosén, J., Åhs, F., Phelps, E. A., Ledoux, J. E., & Milad, M. R. (2024). *Distributed neural representations of conditioned threat in the human brain*. (April 2023), 1–14. https://doi.org/10.1038/s41467-024-46508-0

Wendt, J., Löw, A., Weymar, M., Lotze, M., & Hamm, A. O. (2017). Active avoidance and attentive freezing in the face of approaching threat. *NeuroImage*. https://doi.org/10.1016/j.neuroimage.2017.06.054

Wiech, K., & Tracey, I. (2013). Pain, decisions, and actions: A motivational perspective. *Frontiers in Neuroscience*, *7*(7 APR), 1–12. https://doi.org/10.3389/fnins.2013.00046

Willems, A. L., & Vervliet, B. (2021a). When nothing matters: Assessing markers of expectancy violation during omissions of threat. *Behaviour Research and Therapy*, *136*(November 2020), 103764. https://doi.org/10.1016/j.brat.2020.103764

Willems, A. L., & Vervliet, B. (2021b). When nothing matters: Assessing markers of expectancy violation during omissions of threat. *Behaviour Research and Therapy*, *136*(April 2020), 103764. https://doi.org/10.1016/j.brat.2020.103764

Willer, J. C. (1975). The influence of anticipation of pain on heart and respiratory rates and on the pain reflex in man. *Physiology and Behavior*, *15*(4), 411–415. https://doi.org/10.1016/0031-9384(75)90251-6

Wilson, R. C., & Collins, A. G. E. (2019). Ten simple rules for the computational modeling of behavioral data. *ELife*, *8*, 1–33. https://doi.org/10.7554/eLife.49547

Wood, K. H., Ver Hoef, L. W., & Knight, D. C. (2014). The amygdala mediates the emotional modulation of threat-elicited skin conductance response. *Emotion*, *14*(4), 693–700. https://doi.org/10.1037/a0036636

Woolf, C. J., & McMahon, S. B. (1985). Injury-induced plasticity of the flexor reflex in chronic decerebrate rats. *Neuroscience*, *16*(2), 395–404. https://doi.org/10.1016/0306-4522(85)90011-9

Wu, X., Wang, T., Liu, C., Wu, T., Jiang, J., Zhou, D., & Zhou, J. (2017). Functions of learning rate in adaptive reward learning. *Frontiers in Human Neuroscience*, *11*(December), 1–15. https://doi.org/10.3389/fnhum.2017.00592

Xu, A., Larsen, B., Baller, E. B., Scott, J. C., Sharma, V., Adebimpe, A., Basbaum, A. I., Dworkin, R. H., Edwards, R. R., Woolf, C. J., Eickhoff, S. B., Eickhoff, C. R., & Satterthwaite, T. D. (2020). Convergent neural representations of experimentally-induced acute pain in healthy volunteers: A large-scale fMRI meta-analysis. *Neuroscience and Biobehavioral Reviews*, *112*(September 2019), 300–323. https://doi.org/10.1016/j.neubiorev.2020.01.004

Xu, X., Fukuyama, H., Yazawa, S., Mima, T., Hanakawa, T., Magata, Y., Kanda, M., Fujiwara, N., Shindo, K., Nagamine, T., & Shibasaki, H. (1997). Functional localization of pain perception in the human brain studied by PET. *NeuroReport*, *8*(2), 555–559. https://doi.org/10.1097/00001756-199701200-00035

Yang, S., & Chang, M. C. (2020). Effect of Repetitive Transcranial Magnetic Stimulation on Pain Management: A Systematic Narrative Review. *Frontiers in Neurology*, *11*, 114. https://doi.org/10.3389/FNEUR.2020.00114

Zale, E. L., Lange, K. L., Fields, S. A., & Ditre, J. W. (2013). The relation between pain-related fear and disability: A meta-analysis. *Journal of Pain*, *14*(10), 1019–1030. https://doi.org/10.1016/j.jpain.2013.05.005

Zhang, S., Mano, H., Ganesh, G., Robbins, T., & Seymour, B. (2016). Dissociable Learning Processes Underlie Human Pain Conditioning. *Current Biology*, *26*(1), 52–58. https://doi.org/10.1016/J.CUB.2015.10.066